Mario Pagliaro, Giovanni Palmisano,
and Rosaria Ciriminna

WILEY-VCH

Flexible Solar Cells

Mario Pagliaro, Giovanni Palmisano, and Rosaria Ciriminna
Flexible Solar Cells

Related Titles

Brabec, C., Scherf, U., Dyakonov, V. (eds.)

Organic Photovoltaics

Materials, Device Physics, and Manufacturing Technologies

2008
ISBN: 978-3-527-31675-5

Poortmans, J., Arkhipov, V. (eds.)

Thin Film Solar Cells

Fabrication, Characterization and Applications

2006
ISBN: 978-0-470-09126-5

Klauk, H. (ed.)

Organic Electronics

Materials, Manufacturing and Applications

2006
ISBN: 978-3-527-31264-1

Würfel, P.

Physics of Solar Cells

From Principles to New Concepts

2005
ISBN: 978-3-527-40428-5

Luque, A. Hegedus, S. (eds.)

Handbook of Photovoltaic Science and Engineering

2003
ISBN: 978-0-471-49196-5

Mario Pagliaro, Giovanni Palmisano,
and Rosaria Ciriminna

Flexible Solar Cells

WILEY-VCH Verlag GmbH & Co. KGaA

The Authors

Prof. Mario Pagliaro
CNR
Institute for Nanostructured Materials
via Ugo La Malfa 153
90146 Palermo
Italy

Giovanni Palmisano
CNR
Institute for Nanostructured Materials
via Ugo La Malfa 153
90146 Palermo
Italy

Dr. Rosaria Ciriminna
CNR
Institute for Nanostructured Materials
via Ugo La Malfa 153
90146 Palermo
Italy

Cover
Cover image was kindly supplied by Solar Integrated Technologies Inc. and was reproduced with permission.

Library of Congress Card No.: applied for

British Library Cataloguing-in-Publication Data
A catalogue record for this book is available from the British Library.

Bibliographic information published by the Deutsche Nationalbibliothek
Die Deutsche Nationalbibliothek lists this publication in the Deutsche Nationalbibliografie; detailed bibliographic data are available on the Internet at http://dnb.d-nb.de.

Composition Thomson Digital, Noida, India
Printing Strauss GmbH, Mörlenbach
Bookbinding Litges & Dopf GmbH, Heppenheim

Printed in the Federal Republic of Germany
Printed on acid-free paper

ISBN: 978-3-527-32375-3

To Bob Pirsig.
For the luminous light shed
on the concept of quality for all of us.

Contents

Flexible Solar Cells. M. Pagliaro, G. Palmisano, and R. Ciriminna

ISBN: 978-3-527-32375-3

Preface

Nordhuas and Shellenberger are right [1]. The Internet was not invented by taxing the telegraph. Similarly, cheap and abundant electricity from the sun will not be obtained by adding taxation on carbon dioxide emissions, but rather by inventing new, cheap solar modules capable of performing the light to electric power conversion with >50% efficiency instead of the current 22%.

These modules, furthermore, will have to be flexible and lightweight in order to produce electricity reliably with little maintenance while being integrated into existing buildings, fabrics, tents, sails, glass and all sorts of surfaces. By so doing, the price of solar energy will be reduced to the level of coal-generated electricity (the cheapest electricity) so that people living in huge emerging countries will also rapidly adopt solar energy for their economic development.

The good news is that the first generation of such commercial modules – the topic of this book – is now ready, having entered the global energy market in the last two years. Their 5–15% efficiency is still too low and, despite a considerably lower price than that of traditional silicon-based panels, much higher conversion efficiency will have to be achieved. However, there is no doubt that these long awaited advances will take place.

Three years of high oil prices and the first ubiquitous signs of climate change have been enough to assist to the market a number of photovoltaic technologies based on thin films of photoactive material that have lain dormant in industrial laboratories for many years.

The 12 billion dollar photovoltaics industry with, for the last five years, an impressive 35% annual growth rate, is rapidly switching to thin film photovoltaics. Ironically, the inventor of the silicon solar cell had already in 1954 clearly forecast that thin film would be the configuration of forthcoming industrial cells.

From a scientific viewpoint, new flexible solar cells are the result of nanotechnology advances and in particular of nanochemistry. Indeed, it has been our chemical ability to manipulate matter on the nanoscale for industrial applications that has recently made possible the synthesis of the photoactive layers needed to carry out the photovoltaic conversion with the necessary stability required for practical applications.

Flexible Solar Cells. M. Pagliaro, G. Palmisano, and R. Ciriminna

ISBN: 978-3-527-32375-3

Almost silent among more glamorous scientific disciplines, chemistry in the last 20 years has extended its powerful synthetic methodology to make materials where size and shape are as important as structure. In other words, we have learned how to make nanoscale building blocks of different size and shape, composition and surface structure, that can be useful in their own right or in a self-assembled structure [2], such as in the case of the "nano ink" developed by Nanosolar (Chapter 3) to make its CIGS panels, producing power at less than 1$/W (i.e., the price of coal electricity).

This book offers a treatment of its topic which includes both inorganic and organic photovoltaics over thin films with an emphasis on the (nano)chemistry approach by which these devices were conceived and eventually manufactured.

However, the solar energy revolution which is unveiling requires leadership engagement at the highest corporate and political levels. Readers of this book therefore will include policy makers and those from the top levels of management and management consultancy, as well as science and energy communicators.

As the world's population is rapidly learning, climate change due to human activities is not an opinion: it is a reality that in America has already hit entire cities (New Orleans), and in Southern Europe hurt not only people but the whole ecosystem with temperatures close to 50 °C in mid-June 2007.

We need to curb CO_2 emissions soon; thus, we need to use on a massive scale renewable materials and renewable energy.

In striking contrast, to fulfill our energy needs, we are still dependent on energy sources and conversion and storage technologies that are 100 to 150 years old, while virtually every other sector of the economy has transformed itself. To get an idea of the obsolescence of our energy devices, just think how often you need to recharge your mobile phone; and how cumbersome and polluting are batteries.

The whole energy industry has been particularly resistant to innovation thanks to its huge profits ensured by hydrocarbon extraction and refining. Put simply, companies had *no* reason to invest in changing this idyllic situation, and virtually every alternative energy source we have – solar, wind, nuclear, fuel cells – has resulted from taxpayer funded innovation.

All that, however, has changed for ever.

Today, not only has the price of oil reached and surpassed the threshold of 100 dollar per barrel, but the energy return on energy invested (EROI) is falling rapidly. Considering the US, for instance, the EROI has dwindled to 15 joules per joule invested, whereas in the 1930s the figure was 100 joules per joule [3].

By the same token, Italy's oil company Eni is, along with Shell, Total and ExxonMobil among the companies which own the rights to exploit the newly discovered huge oil field of Kashagan in Kazakhstan.Unfortunately, this oil lies underneath such a large amount of hydrogen sulfide that, even if the companies can solve the technical problems and start to drill it, the price of the solutions implemented will inevitably be reflected in significantly lower EROI and higher costs.

It is exactly this decreasing trend in EROI that, along with climate change due to increasing carbon levels in the atmosphere, is forcing society globally to switch from fossil to renewable fuels, until the day when cheap and abundant solar energy becomes a reality.

Along with the interest of citizens, companies and governments, private and public investments in solar energy are eventually booming. Numerous start-up photovoltaic companies are attracting financial investment from the world's leading venture capitalists and even from oil companies. Google, for example, largely funded Nanosolar in the US; whereas investors in Konarka, a manufacturer of plastic solar cells, include some of the world's largest oil companies.

Similarly, we think that Islamic finance will play a crucial role in making abundant, cheap and clean solar electricity a reality for mankind. Those same investors, politicians and their advisors will find in this book plenty of information on which to base their choices.

Two billion people lacking access to the electric grid will benefit immensely from the advances that are being made, as will companies and citizens in the developed world where the electricity bill has become a serious economic problem.

This book addresses the need to provide updated, exhaustive information on different thin film PV technologies that will rapidly find widespread use. However, there are entire volumes on *each* of the seven chapters of the present book.

Using therefore a concise style and numerous illustrations, the nanochemistry of thin film photovoltaics is discussed, along with relevant industrial/market information that is generally difficult to retrieve. An effort has been made to focus on the practical aspects of flexible solar cells, discussing their application in some detail. As we think in words, we have tried to "look after commas [4]" and use correct language to enable readers to think carefully about an important topic.

Our web site (qualitas1998.net) complementing the book has additional supplemental materials online. Readers will tell whether we have succeeded in producing a book that, as is our intention, should act as a lasting reference of scientific and practical usefulness in the field of solar energy.

Palermo, September 2008

Mario Pagliaro
Giovanni Palmisano
Rosaria Ciriminna

References

1 Nordhuas, T. and Shellenberger, M. (2007) *Break Through: From The Death of Environmentalism to the Politics of Possibility*, Houghton Mifflin, New York.

2 Ozin, G. and Arsenault, A. (2006) *Nanochemistry: A Chemical Approach to Nanomaterials*, Royal Society of Chemistry Publishing, Cambridge.

3 Cleveland, C. *et al.* (2006) Energy Returns on Ethanol Production. *Science*, **312**, 1746.

4 Myers, B.R. (April 2008) Keeping a Civil Tongue. *The Atlantic Monthly.*

1
Towards a Solar Energy Revolution

1.1
Flexible Solar Cells

> Topic: Thin film solar company seeking partners
>
> Started By: Paul Norrish Sep 4, 2007 04 : 17 a.m.
>
> G24 Innovations is a UK based manufacturer of Dye sensitised solar cells. We are interested in partnering with an LED manufacturer and distribution partners to launch a Solar powered light in Africa/Asia.
>
> If this is of interest please respond to Paul.Norrish@g24i.com
>
> Regards
> Paul

Needless to say, this post on the Lighting Africa Business Forums [1] received a large response and the company has formed a number of partnerships in Africa with which to commercialize its photovoltaic (PV) flexible technology, one of the main topics of this book.

In general, flexible electronic devices that are ready to enter the market will shortly become predominant in the market (Figure 1.1). For example, the production of flexible displays using organic light-emitting diodes (OLEDs) started in 2008 with an initial capacity of more than a million display modules per year. Used in displays, these organic materials applied in thin layers over flexible plastic make electronic viewing more convenient and ubiquitous.

The thinness, lightness and robustness enabled by the flexibility of OLED-based displays will enable the manufacture of electronic reader products that are as comfortable and natural to read as paper, whether at the beach or on a train. Thus far, in fact, people have been reluctant to read on laptops, phones and PDAs, even in this age of pervasive digital content. The first manufacturing facility targeted at flexible active-matrix display modules has been built by Plastic Logic in Dresden, Germany [2]. Wireless connectivity will allow users to purchase and

Flexible Solar Cells. M. Pagliaro, G. Palmisano, and R. Ciriminna

ISBN: 978-3-527-32375-3

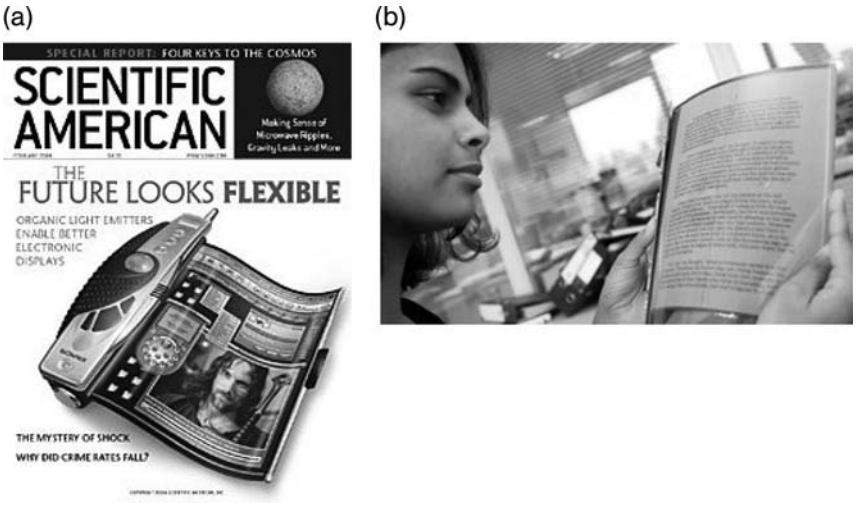

Figure 1.1 Long awaited flexible electronics ((a) shows the cover of *Scientific American* for February 2004) is now a reality with OLED displays (b) enabling ubiquitous, comfortable reading (Photo courtesy: Plastic Logic).

download a book or pick up the latest edition of a newspaper wherever and whenever they desire.

In its turn, a flexible plastic solar module (Figure 1.2) of the types described in the following chapters, might easily power the OLED device enabling unlimited access to thousands of pages.

The vision is that of the so-called *plastic electronics*, namely to print circuits and devices on flexible substrates, at room temperature (low energy) and with roll-to-roll

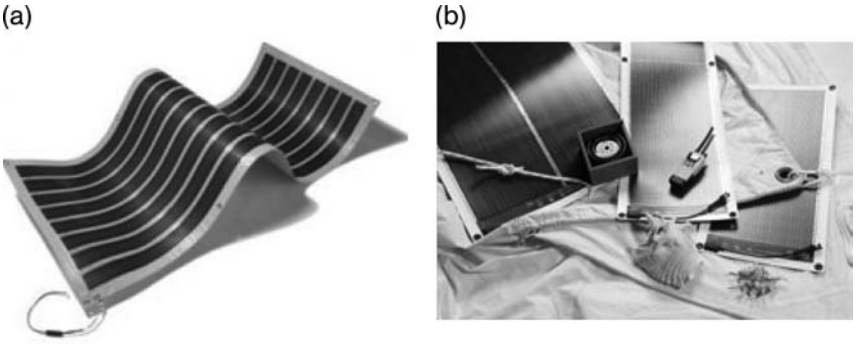

Figure 1.2 Plastic solar cells such as (a) that entirely organic (Photo courtesy: Konarka) or (b) that using amorphous Si (Photo courtesy: Flexcell) are lightweight (25–50 g m^{-2}), and ideally suited for customized integrated solutions.

processes (high throughput). Flexible solar PV devices offer an alternative energy source at low cost, ample surface area, flexible, light, silent and clean energy for indoor and outdoor applications.

In general, their advantages over existing technologies are clear [3].

highly flexible
The true mechanical flexibility of flexible solar PV modules allows for the integration with elements of various shapes and sizes and the design of innovative solar products.

customised & integratable
The roll-to-roll manufacturing processes allow for the production of PV modules of various lengths and widths, thus rendering the technology very attractive for customised integrated solutions.

thin & lightweight
The lightness of flexible solar PV foil makes it suitable for applications where weight is important.
Such very thin PV foil enables the aesthetic integration with various different materials.

unbreakable
Unlike conventional crystalline silicon PV modules, which are based on bulky and brittle glass substrates, flexible solar PV modules are made of thin and flexible polymers, which are tough, durable and safe to use.

environmentally friendly
In addition to these unique properties, flexible solar PV foil is environmentally friendly. The electricity produced is clean and the manufacturing processes is based on abundant, recyclable materials. The energy payback of flexible products is 3-5 times faster than products based on conventional PV technologies.

The photovoltaic material is printed on a roll of conductive plastic [4] using fast newspaper printing technology. Printing enables one to achieve high materials utilization of the photoactive material. As a result, this simple, highest-yield technique in plain air is capital-efficient and eliminates the need for costly vacuum deposition techniques such as conventionally used to fabricate thin-film solar cells (Figure 1.3).

These chemistry-based cells are lightweight, flexible and more versatile than previous generations of products. The result is a new breed of coatable, plastic, flexible photovoltaics that can be used in many applications where traditional photovoltaics cannot compete. The photovoltaic functionality is integrated at low cost into existing structures, printing rolls of the stuff anywhere, from windows to

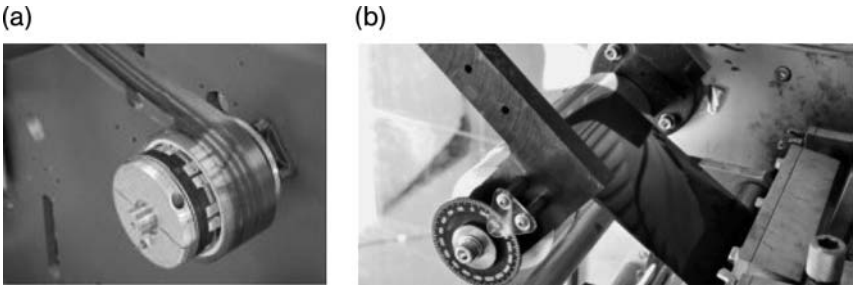

Figure 1.3 (a) Roll-to-roll manufacturing of photovoltaic Plastic Power (photo courtesy: Konarka) is analogous to (b) ink printing of semiconductor CIGS on aluminum foil (photo courtesy: Nanosolar).

roofs, through external and internal walls. Flexible solar cells, indeed, replace the traditional installation approach with an *integration* strategy (Figure 1.4).

In general, man is eventually learning how to efficiently harness the immense amount of solar energy that reaches the Earth every second by mimicking Nature and by operating at the nanoscale. In other words, we are learning how to deliver cost-efficient solar electricity.

The average price for a PV module, excluding installation and other system costs, has dropped from almost $100 per watt in 1975 to about $4 per watt at the end of 2007 (Figure 1.5).

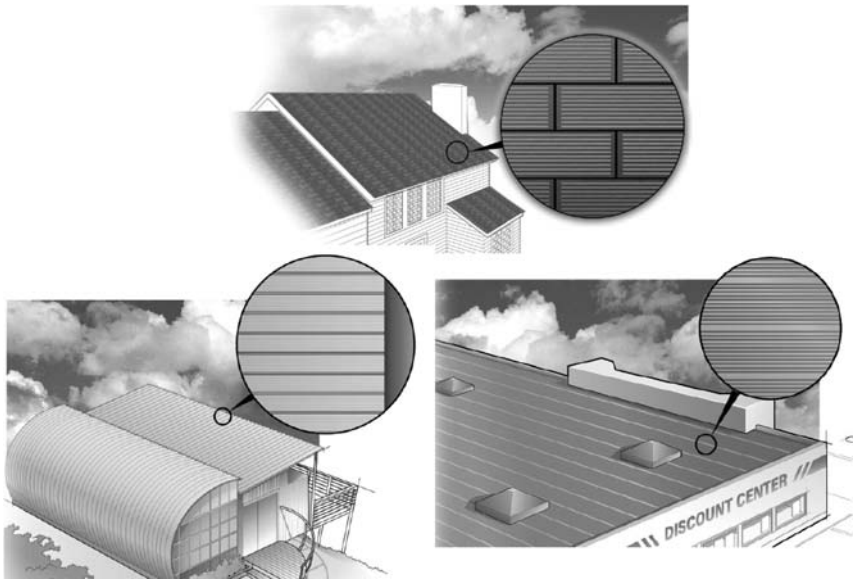

Figure 1.4 New flexible solar modules are integrated, rather than installed, into existing or new buildings (adapted from Konarka).

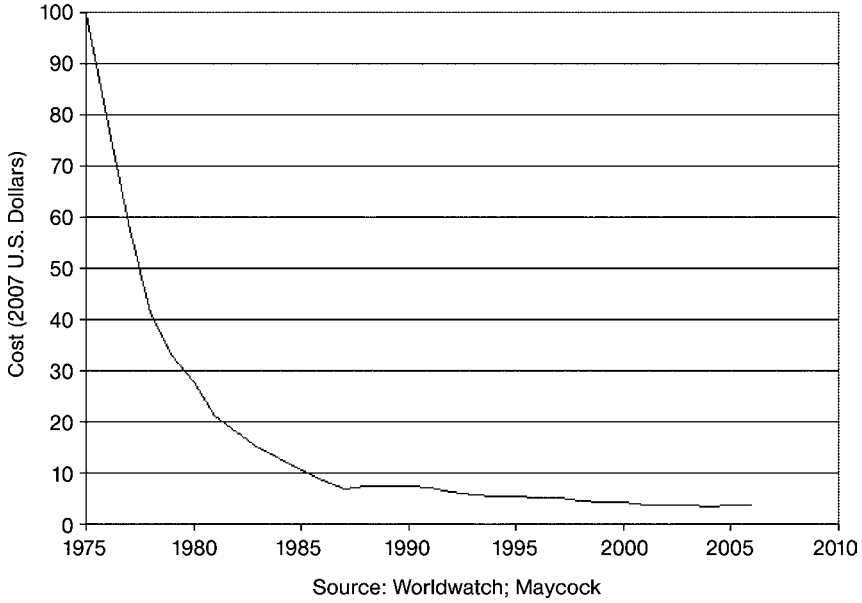

Figure 1.5 Average cost per watt of PV module 1975–2006. (Source: Earth Policy Institute, 2007).

In 2004, a prediction of an industry's practitioner concluded that for "thin-film PV alone, production costs are expected to reach $1 per watt in 2010" [5], a cost that makes solar PV competitive with coal-fired electricity.

Adding relevance to this book's arguments, however, the first flexible thin-film solar modules profitably generating electricity for 99 cents a watt (i.e., the price of coal-fired electricity) were commercialized in late 2007, concomitant with the commercial launch of the first plastic solar cells.

These high-performance wafer-thin solar cells are mass-produced printing on aluminum foil with an ink made of inorganic semiconductor CIGS (Chapter 3).

1.2 Why We are Entering the Solar Age

With concerns about rising oil prices and climate change spawning political momentum for renewable energy, solar electricity is poised to take a prominent position in the global energy economy (Figure 1.6).

However, claiming that we are ready to enter the solar age, when the global consumption of oil is steadily on the rise may sound as a green-minded false prophecy. All predictions of an oil peak made in the 1960s were wrong [6]: We never experienced lack of oil as was doomed inevitable after the 1973 oil shock, and the exhaustion of world oil reserves is a hotly debated topic. For example, an oil industry geologist tackling the mathematics of Hubbert's method suggests that the oil peak occurred at the end of 2005 [7].

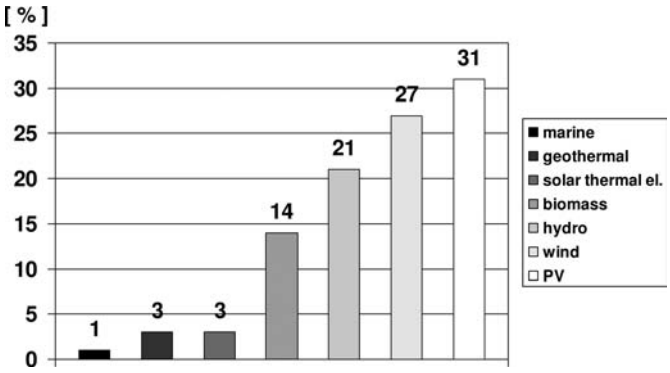

Figure 1.6 Predicted scenario by 2040. Out of a total electricity consumption of 36.346 TWh (from 15.578 TWh in 2001, IEA) renewable energy sources will cover 29.808 TWh, with solar energy becoming largely predominant. (Source: EREC).

On the other hand, the price of oil has multiplied by a factor of 10 in the last few years, whereas in the US, for example, domestic petroleum now returns as little as 15 joules for every joule invested compared to the 1930s when the energy return on energy invested (EROI) ratio was 100 [8].

The demand for oil has boomed in concomitance with globalization and rising demand from China and India. In China and India, governments are managing the entrance to the industry job market of some 700 million farmers, that is about twice the overall amount of workers in the European Union.

Global energy demand will more than double by 2050 and will triple by the end of the century. At the same time, an estimated 1.64 billion people, mostly in developing countries, are not yet connected to an electric grid.

Finally, the world's population is rapidly learning that climate change due to human activities is not an opinion: it is a reality that in the US has already hit entire cities (New Orleans, 2005), and in southern Europe hurt people and the whole ecosystem with temperatures close to 50 °C in mid-June 2007.

Overall, these economic, environmental and societal critical factors require us to curb CO_2 emissions soon, and switch to a massive scale use of renewable materials and renewable energy (RE) until the day when cheap and abundant solar energy becomes a reality.

Access to affordable solar energy on a large scale, admittedly, is an enormous challenge given that presently only 0.2% of global energy is of solar origin. The low price of oil in the 1990s ($10–$20 a barrel) put a dampener on scientific ingenuity for the whole decade, since many developments were put on the shelf until a day in the future when their use would become "economically viable."

All is rapidly changing with booming oil prices. Solar electricity generation is now the fastest-growing electricity source, doubling its output every two years (Figure 1.7) [9]. The solar energy market has grown at a rate of about 50% for two years, growing to 3800 MW in 2007 from 2521 MW in 2006.

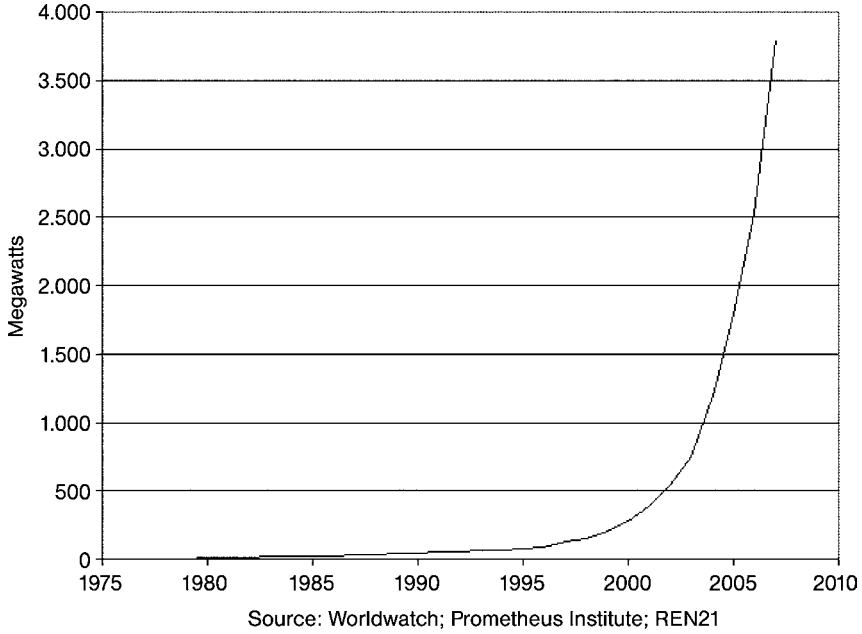

Figure 1.7 World annual PV production, 1975–2007: 3.8 GW by the end of 2007, is doubling every two years. (Source: Earth Policy Institute, 2007).

Competitiveness that was already proven in industrial off-grid, consumer and rural electrification application, is rapidly expanding to in-grid systems, first in local replacement of peak tariff electricity kWh in liberalized southern European countries and in some US states, and soon afterwards in the rest of the world.

Figure 1.8, for example, clearly shows that the electrical energy fed into the grid from an office in Spain reaches its maximum in the high tariff time range whereas the electricity supplied by the utility is drawn at periods of low tariff [10].

This competitiveness explains why the sector is now attracting government and venture capital investments on an unprecedented scale, with some 71 billion dollars of new investment in 2006 alone, amounting to a 43% increase relative to the previous year [9].

Yet, even at this large pace of growth, in order to make solar energy a significant contributor to the global energy production, we need to go through a revolutionary process.

In place of the 11 billion dollars photovoltaic global industry, largely based on silicon panels introduced in the early 1970s, which currently contributes <0.1% to the global energy industry (15 terawatt, which adds every 10 years the equivalent of the current US yearly consumption), we need a new photovoltaic technology of distinctly superior efficiency, versatility, and availability, compared to traditional silicon-wafer-based photovoltaic devices.

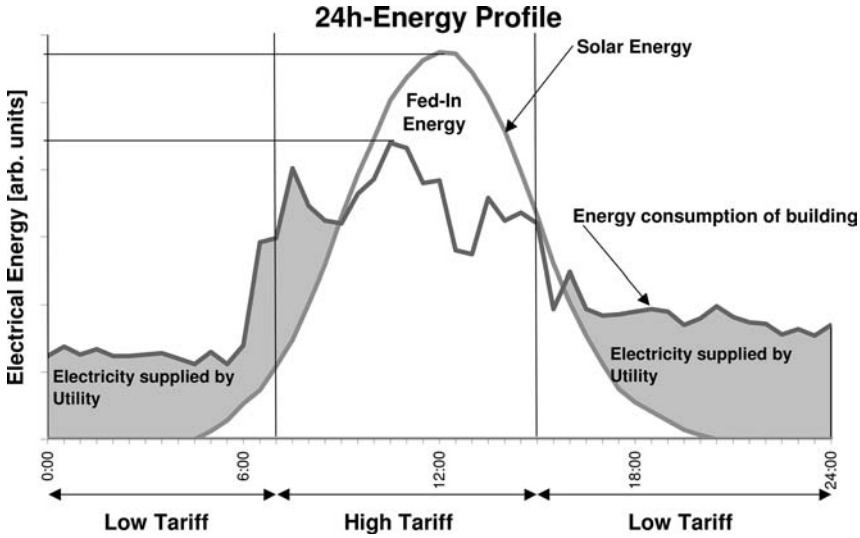

Figure 1.8 Correlation between daily PV power production and energy consumption of an office building in Spain. (Source: EPIA, 2004).

And even if it still an open question as to which photovoltaic material will be used, this technology evolution (Figure 1.9) will first go through massive adoption of thin films of inorganic and organic materials; and then likely though new quantum technologies employing multiple cells and newly synthesized materials such as epitaxial GaAs and graphene (Chapter 6).

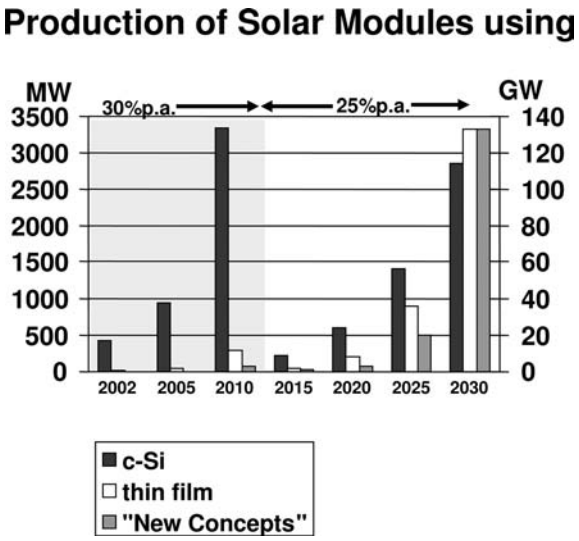

Figure 1.9 PV Technology evolution. (Source: EPIA, 2004).

1.3
Capturing Solar Light and Transferring Energy Efficiently

Whether an electron is powering a cell phone or a cellular organism makes little difference to the electron; it is the ultimate currency of modern society and biology, and electricity is the most versatile and relevant energy available to man.

The ability to capture light and then to transfer that energy to do work are the two main steps in a photovoltaic system. In Nature, such steps happen too fast for energy to be wasted as heat and in green plants (Figure 1.10) the light energy is captured by highly effective photosynthetic complexes and then transferred with almost 100% efficiency to reaction centers, where long term energy storage is initiated.

Traditional silicon-based solar PV systems, however, do not follow Nature's model.

In Nature, the energy transfer process involves electronic quantum coherence (Figure 1.11). Indeed, this wavelike characteristic of the energy transfer within the photosynthetic complex can explain its extreme efficiency, as it allows the complexes to sample vast areas of phase space to find the most efficient path.

Two-dimensional electronic spectroscopy investigation [11] of the bacteriochlorophyll complex has, in fact, shown direct evidence for remarkably long-lived electronic quantum coherence. The lowest-energy exciton (a bound electron–hole pair formed when an incoming photon boosts an electron out of the valence energy band into the conduction band) gives rise to a diagonal peak that clearly oscillates. Surprisingly, this quantum beating lasted the entire 660 femtoseconds, contrary to the older assumption that the electronic coherences responsible for such oscillations are rapidly destroyed.

It may therefore come as no surprise that the first plastic solar cells are largely based on biomimetics, that is, on artificial photosynthesis based on human ability to gather and organize complex materials and organic molecules to replicate photosynthesis in a practical way.

Figure 1.10 Green plants harvest light's energy with almost 100% efficiency.

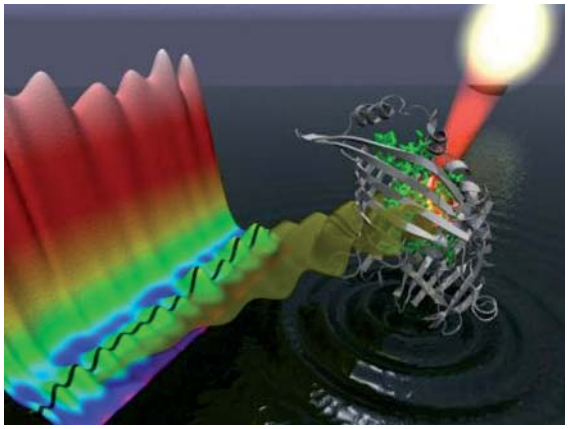

Figure 1.11 Sunlight absorbed by bacteriochlorophyll (green) within the FMO protein (gray) generates a wavelike motion of excitation energy whose quantum mechanical properties can be mapped through the use of two-dimensional electronic spectroscopy. (Image courtesy of Greg Engel, Lawrence Berkeley National Laboratory).

A typical cell contains a porous film of nanostructured titania formed on a transparent electrically conducting substrate and photosensitized by a monolayer of a ruthenium dye. The dye ensures complete visible light absorption thanks to efficient electron transfer from the excited chromophore into the conduction band of the semiconductor oxide (which requires a high electronic coupling between the dye and the semiconductor for efficient charge injection).

An electrolyte, based on an $I_2 - I_3^-$ redox system is placed between the layer of photosensitized titania and a second electrically conducting catalytic substrate (Figure 1.12).

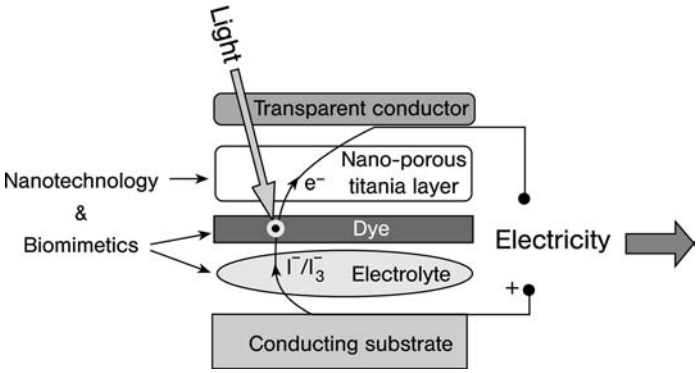

Figure 1.12 State-of-the-art dye-sensitized solar cells show greater than 11% light-conversion efficiency.

Like plants that are effective at capturing energy over a wide range of light conditions, dye-sensitized solar cells work in lower light levels than traditional PV. Thus, the outdoor environments of hospitals, airports, station windows and surfaces become energy sources at low cost.

The first full-size production cells achieve close to 10% efficiency, whereas a technology roadmap aims to reach 20% in the next ten years. This breakthrough puts the materials on a par with, or in some cases exceeding, second-generation materials, but at lower cost and with more options in the product form factor.

The environment on the nanoscale largely influences the photoelectric effect and the electron transfer process on which photovoltaics is based. Hence, through better chemical control of the properties of the photoactive material on the nanoscale – namely through nanochemistry [12] – we are learning how to build more efficient means of collecting, storing, and transporting solar energy.

For example, in dye-sensitized solar cells (DSC) structural organization of the material improves the performance. Thus, organized mesoporous TiO_2 films exhibit solar conversion efficiency about 50% greater than films of the same thickness made from randomly oriented anatase crystals (Figure 1.13) [13].

Improvement here results from a remarkable enhancement of the short circuit photocurrent which in turn is due to fivefold enhanced roughness of a 1-μm-thick film and thus to an accessible huge surface area.

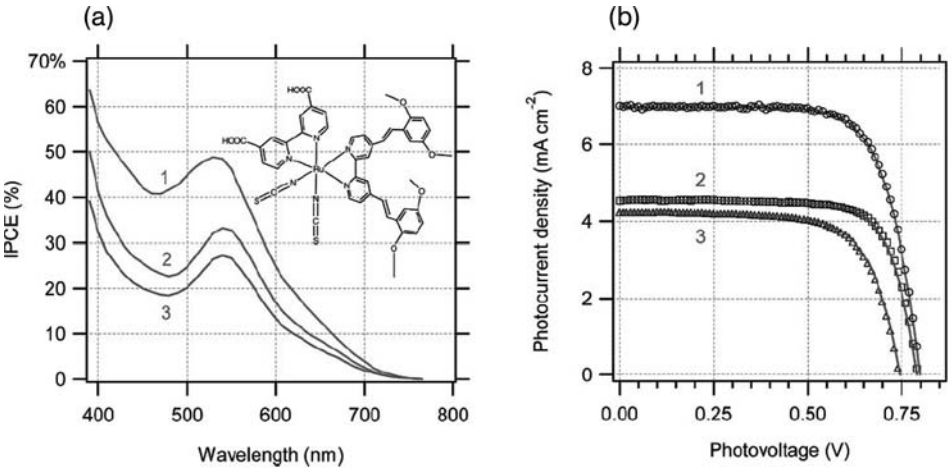

Figure 1.13 Efficiency (a) and photocurrent–voltage characteristics (b) of a solar cell based on TiO_2 films sensitized by N945 (inset shows its chemical formula). Pluronic-templated three-layer film (1); nonorganized anatase treated with $TiCl_4$ (2); nonorganized anatase not treated with $TiCl_4$ (3). (Reproduced from Ref. [11], with permission).

1.4 Three Waves of Innovation

In the early 2000s, the improvements in efficiency targeted by industry for 2020 were clear [9].

- For monocrystalline silicon cells from 16.5 to 22%
- For polysilicon from 14.5 to 20%
- For thin film (a-Si/mc-Si, CIS, GIGS and CdTe) up to 10–15%.

Architectonic integration was highly recommended to reduce the price of PV adoption in real estate; and advancements in organic cells and the use of advanced materials such as GaAs were recommended.

Remarkably, major advancements indeed took place shortly after these recommendations, and many of them are discussed in the following. In general, solar power technology evolved in three waves of innovation (Table 1.1).

The *First Wave* started with the introduction of silicon-wafer based solar cells over three decades ago. While ground-breaking, it is clear until today that this technology came out of a market environment with little concern for cost, capital efficiency, and the product cost/performance ratio.

Despite continued incremental improvements, silicon-wafer cells (Figure 1.14) have a built-in disadvantage of fundamentally high materials cost and poor capital efficiency. Because silicon does not absorb light very strongly, silicon wafer cells have to be very thick. And because wafers are fragile, their intricate handling complicates processing all the way up to the panel product.

Table 1.1 The evolution from wafer cells through thin film on glass and then on foil has led to a reduction in payback from 3 years to less than 1 month. (Source: Nanosolar).

Technology wave	I. Wafer cells	II. Vacuum-based thin film on glass	III. Roll-printed thin film on foil
Process:	Silicon wafer processing	Sputtering, evaporation in a vacuum chamber	Printing in plain air
Process control:	Fragile wafers	Expensive metrology	Built-in bottom-up reproducibility
Process yield:	Robust	Fragile	Robust
Materials utilization:	30%	30–50%	Over 95%
Substrate:	Wafer	Glass	Conductive Foil
Continuous processing:	No–wafer handling	No–glass handling	Yes
Cell matching:	Yes	No	Yes
Panel current:	High	Low	High
Energy payback:	3 years	1.7 years	<1 month
Throughput/Cap.Ex.	1	2–5	10–25

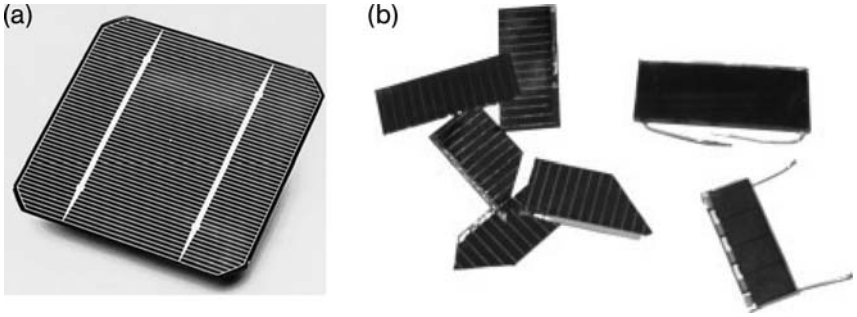

Figure 1.14 (a) A solar cell, made from a monocrystalline silicon wafer and (b) polycrystalline silicon PV cells deposited as thin films. (Photo courtesy: Wikipedia).

The *Second Wave* came about a decade ago with the arrival of the first commercial thin-film solar cells. This established that new solar cells based on a stack of layers 100 times thinner than silicon wafers can make a solar cell that is just as good. However, the first thin-film approaches were handicapped by two issues:

1. The cell's semiconductor was deposited using slow and expensive high-vacuum based processes because it was not known how to employ much simpler and higher yield printing processes.
2. The thin films were deposited directly onto glass as a substrate, eliminating the opportunity of using a conductive substrate directly as the electrode (and thus avoiding bottom-electrode deposition cost).

Indeed, the prediction of greatly reduced costs for thin film solar cells made by thin epitaxial deposits of semiconductors on lattice-matched wafers (Figure 1.14) has yet to be achieved.

The *Third Wave* of solar power combines the materials-cost advantage of thin films and of organic photovoltaics (OPV) with the process cost advantage of faster process technology.

Inorganic thin solar films are more than 100 times thinner than silicon-wafer cells, and thus have correspondingly lower materials cost, but are printed in plain air using a stable, nanostructured ink of photoactive material. The result is the world's most cost-efficient solar modules (Figure 1.15)

By testing the products under much harsher conditions than mandated by official certification standards, including harsh outdoor environments such as the Arizona desert and the Antarctic (Figure 1.16), modules have been developed that are supplied with the 25-year durability and longevity warranty of conventional rooftop PV solar cells (which improves on the low performance of thin-film amorphous silicon solar cells which revealed unexpected degradation rates that were not identified in the laboratory).

Organic-inorganic solar cells also show excellent durability, ranging from 13 to 22 years depending on whether they are employed in Central or Southern European climates (Figure 1.17).

Figure 1.15 The first solar panels based on CIGS printed on aluminum foil yielding electricity at 1$/W were delivered on December 2007. (Photo courtesy: Nanosolar).

Placing this in a Green context, the path to a sustainable energy future based on the sun's energy is a technological challenge that can be met [14]; and the new generation PV technologies that are being discovered and commercialized at increasing pace will assist in ensuring that change will indeed take place "on a reasonable timescale."

Figure 1.16 Testing of thin-film solar panels in the Antarctic. (Photo Courtesy: Nanosolar).

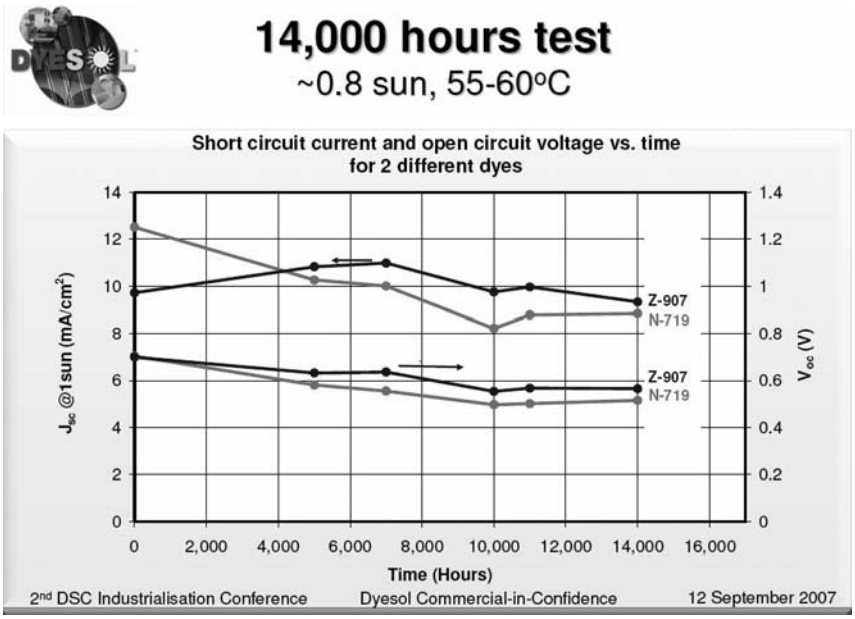

Figure 1.17 Real PV modules based on DSC last 13 or 22 years depending on whether they are in a Southern or Central European climate, respectively. (Source: Dyesol).

1.5 Solar Design

From energy saving and architecturally inelegant, shiny black panels mounted awkwardly on the roof of remote buildings, photovoltaic architecture has created elegant PV elements that are increasingly conceived as building-integrated (BI) components. Clearly, the improved esthetic impact of PV systems increases their acceptance and diffusion, especially in wealthy regions where immaterial values increasingly drive consumer's choice.

Panels installed recently in New York City (Figure 1.18), for example, were "a deep indigo blue framed with a border of white stone ballast that keeps them earth-bound" [15]. Clearly, a crucial aspect as innovative modules are characterized by a significant upgrading of their value, and thus price, by extra (cost-relevant) production steps in comparison to standard modules.

Dye solar cells, for example, can be processed in different colors and adapted to different and demanding esthetic requirements actually expanding, rather than limiting, the design possibilities, as shown by the Toyota exhibition pavilion at the Aichi's 2005 Expo (Figure 1.19).

By incorporating color and design in solar power products, designers will be able to use the cells not only on the roof or out of sight locations, but also as a primary element of housing and environment design.

Figure 1.18 Solar panels on the garage roof of this apartment building in New York City Washington Heights gather sunlight from dawn to dusk. Here, the streets were bathed in orange hues from streetlights. (Photo courtesy: The New York Times).

Just like newspapers can include text, images and a variety of colors, new generation solar cells can include a vast range of colors and drawings. It becomes possible to design entire networks of PV polymer without adding weight to the structure.

Cost-effective thin-layer technology is used increasingly for large façades and large roofs. Thin-layer modules, indeed, are installed directly onto the roofing, without frames, without covers and without assembly frameworks. Hence, their integration prevents problems of statics. For example, the PV roof on a factory store in the Belgian town of Halle consists of thin film modules in amorphous silicon achieving a total output of 330 kWp (kilowatt peak performance). The modules are each over 5 m in

Figure 1.19 DSC-based modules coating the windows of the pavilion house of Toyota at Aichi's 2005 Expo. (Photo courtesy: Toyota).

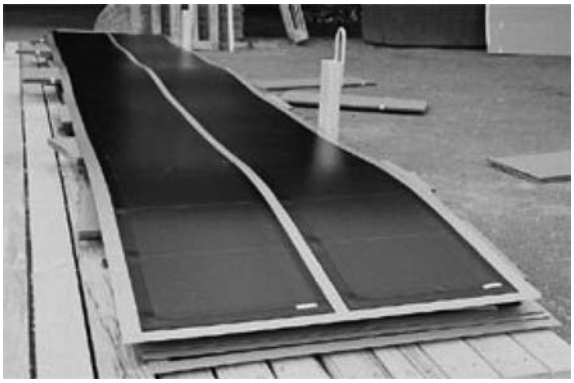

Figure 1.20 Large plate system module achieving an output of 2×136 Wp, primarily aimed at the agricultural and industrial sectors. (Photo courtesy: Biohaus).

length and weigh only 50 kg (Figure 1.20), so they can be stuck directly onto the roof. With the triple-junction technology used, these modules achieve excellent output, even if the pitch of the roof is minimal – in the present case the pitch is a mere 3° – and regardless of whether the buildings are facing to the East or the West.

Transparent PV facades establish contact with the outside world and allow impressive lighting effects in the inside of buildings. Even from an economical point of view, the replacement of conventional façade elements may be of interest, because solar systems not only supply solar energy but also fulfill the tasks of building shells. Thus a photovoltaic façade can replace expensive natural stone tiles or stainless steel elements and can also represent a high prestige value.

For example, the façade-integrated CIS modules with their uniform matt black surface at a silo tower in Ulm, Germany (Figure 1.21a), reaching a height of 102 m, are made up of 1300 CIS modules with a total nominal output of 98 kWp. Every year this produces about 70 000 kWh of solar power and thus avoids approximately 50 000 kg of CO_2 emissions. The prominent position of the building at the entrance to the city led to construction and planning companies paying particular attention to the visual appearance of the tower.

Similarly, the $8 \times 80\,m^2$ shining black solar façade integrated in 2007 at Berlin's Ferdinand-Braun Institute (Figure 1.21b) is made of 730 elegantly shaped anthracite-colored CIS modules achieving 39 kWp.

In general, new thin film PV modules provide architects with better ways of integrating PV into new and existing buildings, well beyond the employment of solar tiles (Figure 1.22) that use the strength of a glass laminate to form a framing system for solar panels [16].

For example, the 120 m tall and 40 years old skyscraper in Manchester has recently been covered with over 7000 photovoltaic panels (Figure 1.23) on each of three sides of its 25 stories. These modules now freely supply 30% of the power needs for the building; the panels replace the original facade of the building and also weatherproof

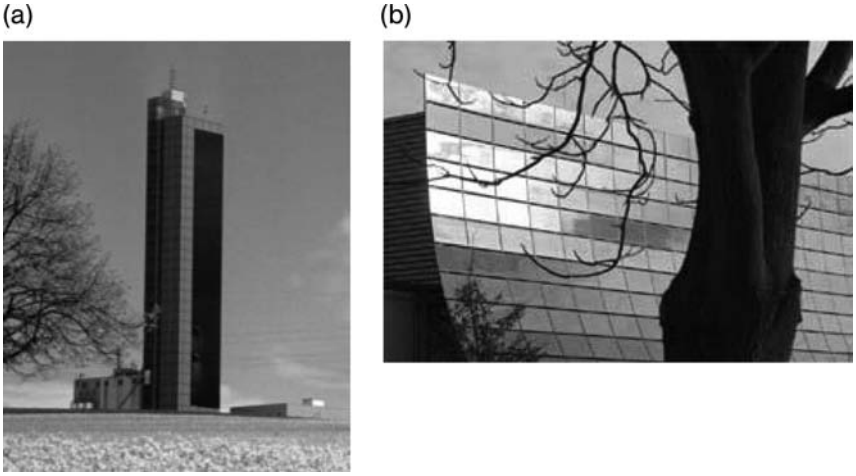

Figure 1.21 (a) The façade of Ulm's wheat silo that consists of 1300 CIS photovoltaic modules with a total output of 98 kWp (Photo courtesy: Solarserver.de). (b) The solar wall of 640 m^2 at Berlin's Braun Institute. (Photo courtesy: Forschungsverbund Berlin).

Figure 1.22 Tiles are a better option for building traditional Si-based PV roofs. (Photo courtesy: PV Tiles Inc.).

its core as the original facade of the tower was composed of small mosaic tiles which over time had begun to fall off, exposing the concrete structure to the weather.

The first 38 guidelines for an esthetically pleasant integration of solar power plants into old buildings, monuments, existing urban districts and landscapes have been available since 2006 in the book *Solar Design* (Figure 1.24), originating from an EU-financed seminal project [17] aimed at improving the esthetics, and thus the market potential, of photovoltaic modules through innovative design.

The same project resulted in the creation of a range of PV prototype panels, based on CIS thin-film technology, harmonized with the scale, color, materials and decorative elements of four demonstration sites in Italy and in Germany, including old buildings, historical sites, the urban space and landscapes.

Figure 1.23 Dark blue solar panels in thin film Si undergoing integration on the façade of a 120 m tall skyscraper in Manchester. (Photo courtesy: Inhabitat.com).

Today architects are involved in PV projects as early as possible to avoid conflicts between esthetics and solar technology; and solar power modules are now deliberately used as design elements. The homogeneous black color and pinstriped appearance of the CIS modules, for instance, give an additional advantage in comparison to other PV material products, whereas a variety of design options like semitransparency, with a wide range of transparency values and designs, provides unprecedented design opportunities. For example, when planning a glass administrative building the design team developed a combined shading and photovoltaic system (Figure 1.25).

The high level of incident energy as a consequence of the high proportion of glass facade clearly had to be limited in the summer months to avoid the need for additional

Figure 1.24 The first book with 38 guidelines for designing building integrated PV was published in 2005. (Photo courtesy: Jovis Verlag).

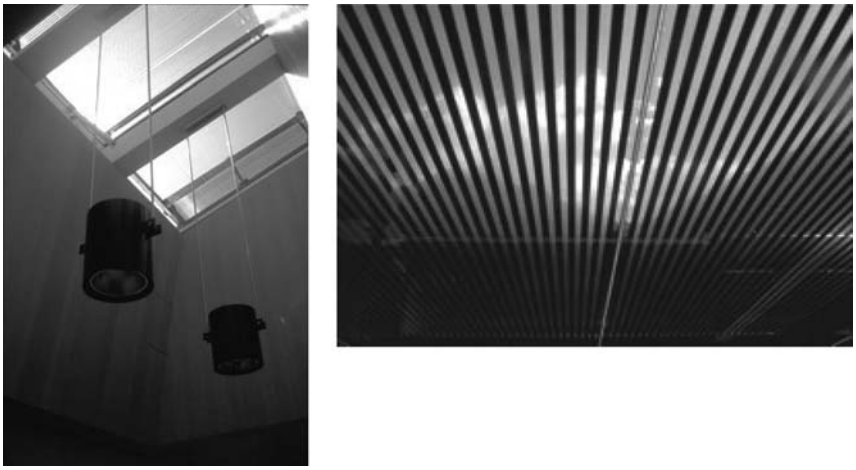

Figure 1.25 New seminstransparent PV modules using CIS as photoactive material create a combined shading and photovoltaic system. (Photo courtesy: Würth Solar).

cooling loads. At the same time, it was necessary to ensure that sufficient daylight enters the atrium, such that it is possible to avoid artificial lighting during the daytime. These requirements were smoothly met by using ten rows of skylights in the building, each 12 m long on average, that were equipped on the outside with a motor-powered, adjustable blanking system alternating with fixed, partially transparent CIS photovoltaic modules.

This configuration led to an optically appealing chessboard pattern for the entire skylight area. All CIS shading elements include ventilation. This avoids permeation of the radiant heat energy into the building. As part of a coordinated energy concept, adjustable glass plates were installed on the facade to complement the skylight solution. The overall strategy applied made it possible to regulate the lighting and incident radiation conditions within the atrium, to effectively block the penetration of incident sunlight and, at the same time, to generate power.

Similarly, new semitransparent CIS modules can be integrated sensitively on cultural heritage sites, as shown by a wall-integration in the medieval town of Marbach am Neckar (Figure 1.26). A square photovoltaic plant in front of the southern city wall welcomes visitors, thereby promoting the town as Schiller's birthplace, and as a clean energy user. The electricity gained is fed into the grid via an inverter and taken from the grid to illuminate the plate at night.

A different solution was conceived for lighting the inner courtyard of the listed monument Castello Doria in Porto Venere (Figure 1.27). Here three "solar flags" hang on steel wires, in each of six wall arches. Intervention in the historical walls was minimized by using existing holes to fix the wires. The modules are transparent, slightly curved acrylic glass components with imbedded semitransparent gray solar cells integrated with light emitting diodes (LED). The power generated by the 18 solar flags is stored in a battery and used to power the LED at night and thus light up the modules.

Figure 1.26 Semintransparent CIS solar panels coating the entrance of Schiller's home in Marbach am Neckar. (Photo courtesy: EU Commission).

Both the modules and the integrated lighting may also be produced in different colors and since any number of them can be added and mounted in various ways and on various sub-structures, they are just as suited for the – also temporary – design of public squares as for use in solar trees.

The positive results of the life cycle analysis for these PV modules indicate a clear reduction in the overall environmental impact, which contributes positively to the energy balance of our urban environments and opens a bright future for architecturally-integrated applications of advanced PV technology.

Finally, a comparison of the three thin film technologies (silicon, CIS and CdTe; Figure 1.28) clearly shows that the payback time for thin-film modules is largely shorter than conventional silicon-based panels which shows, also in the case of

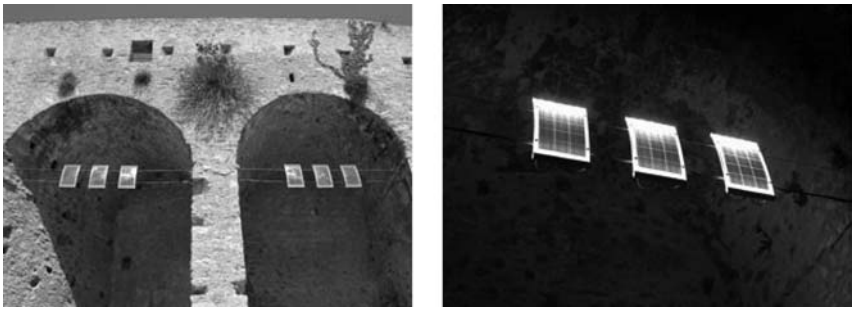

Figure 1.27 Solar flags equipped with LED lights collect solar energy by day and use it by night to light a monument in Porto Venere (Italy). (Photo courtesy: EU Commission).

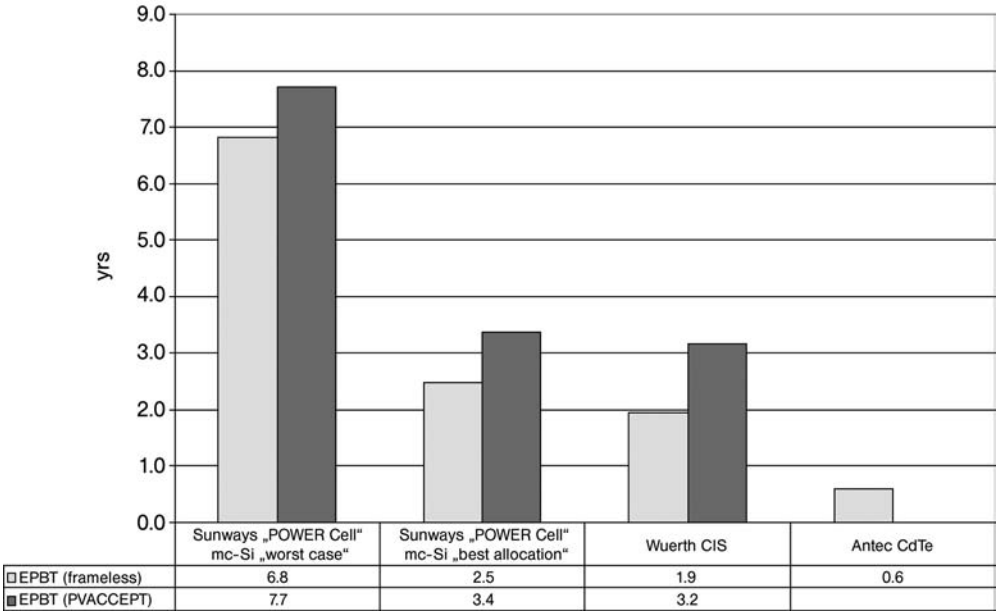

Figure 1.28 Payback time for three different PV technologies shows considerable reduction in payback time for thin-film modules. Results for the Si-based systems are given in two separate columns, one for the worst case scenario, essentially representative of older-generation PV systems, and one for the best case scenario. (Reproduced from Ref. [16], with permission).

elegantly designed modules, that thin-films are indeed the photovoltaic technology of the near future [18] .

1.6 New Solar Companies

A number of solar firms and companies manufacture, sell and develop solar modules that do not use crystalline silicon as the photovoltaic material. Most were founded in the last five years. All use thin-film PV technologies, and in the following chapters we shall refer extensively to the leading representatives of each technology segment. Here, we focus on the strategic factors that made possible such rapid industrial evolution which will have a profound impact on the future of the PV industry as well as, in general, on future energy generation.

Many analysts considered 2006 the “year of the solar IPO,” as solar PV companies continued to make up the largest portion of existing and additional companies in the top 140 publicly traded renewable energy companies worldwide. Several renewable energy companies went through high profile initial public offerings (IPOs), generating market capitalization above or near $1 billion during 2006/2007. These

Figure 1.29 Honda's Kumamoto CIGS-based cells production factory. (Source: Honda Soltec).

included the solar PV companies First Solar (USA), Trina Solar (USA), Centrosolar (Germany), and Renesola (UK). First Solar was the largest IPO, with market value in excess of $4 billion by 2007. Several Chinese PV companies also went public in 2006 and early 2007.

Large companies which were entirely absent from the PV market entered into the solar cell business. For example, in 2006 the motor manufacturer Honda established a wholly-owned subsidiary, Honda Soltec, to produce 27.5 MW thin film solar modules annually using copper, indium, gallium and selenium (CIGS) semiconductor (Figure 1.29) [19]. The company achieves a major reduction (approximately 50%) in the amount of energy consumed during the manufacturing process compared to what is required to produce conventional crystal silicon solar cells. This makes the new solar cell more environmentally friendly by even reducing the amount of CO_2 generated in the production stage.

Similarly, the Würth Group created Würth Solar (Figure 1.30) and built a production plant, the Schwäbisch Hall plant in Germany, where it manufactures CIS-based solar modules. The investment of some 55 million € is the highest single investment in the company history.

In general, all these technologies offer major development opportunities in terms of product properties and production technologies.

According to some analysts, photovoltaics would not be an arena where private energy companies were likely to make the required technology breakthrough [20]. However, major advances realized in academic laboratories are currently in the

Figure 1.30 Würth Solar's trademark.(Source: Würth Solar).

process of being commercialized by start-up companies financed by venture capital funds and led by the inventor scientists.

Human ingenuity is opening new paths in practically every respect, by greatly improving existing PV technology and creating entirely new technologies such as those described in Chapter 6.

For example, Global Warming Solutions has developed a new hybrid photovoltaic/thermal (PV-T) solar energy conversion technology which makes possible the year-round production of thermal and electric energy by increasing the electric power 1.5–2 times as compared to traditional Si cells, and the thermal output by 170% [21]. This technology allows the storage of energy and solves the problem of solar power traditionally being hampered by a lack of storage capability.

Dispatchability of energy supply indeed has great value, because it means that the energy supply is guaranteed or predictable. The more predictable it is, the higher its value. Fossil fuel driven power plants and nuclear power are dispatchable. Renewable energy sources alone are generally not. Therefore, the renewable energy sources must be configured with a means of "energy storage" (that is, batteries or hybrid systems (renewable energy and another energy source)) to provide customers with an experience analogous to that enjoyed using grid electricity of fossil origin.

The light electric and thermal generator (LETG) technology uses a solar collector combined with photovoltaic cells that have been coated with a liquid luminophor (a novel organic polymer) which works in the Stokes spectrum area effectively cooling the silicon photocell.

In practice, the module has a shell where liquid luminophor circulates (Figure 1.31). Solar irradiation passes through the layer of this luminophor and is transferred to a longer-wavelength area of the spectrum near a maximum of solar cell sensitiveness on the basis of c-Si, covered by a special dielectric optical layer. Thus, a part of the luminescence energy is expended on luminophor heating. In addition, the layer of liquid luminophor actively absorbs solar radiation in the infrared range of the spectrum. This collateral heat can be used for domestic needs or transformed into electricity.

Critical to all this is the fact that in these hybrid PV cells not only can all types of silicon (monocrystalline, c-Si, polycrystalline (poly-Si) and amorphous silicon, a-Si) be used, but also all new semiconductor materials with even greater potential for transforming light into electricity.

Additional expenses associated with the production of hybrid modules based on luminophors are small in comparison with those of the ordinary cells that are its component part. The increase in electric power compensates these expenses and results in reduction in the price of the modules, calculated per unit of generated power (Table 1.2).

Thus, by coupling thermal and photovoltaic energy generation, the integrated LETG technology greatly extends what solar power can deliver, providing solar power in winter when days are short or by night (when there is no sunlight).

In an industry constantly striving to reduce costs and increase efficiency in an effort to make solar power more affordable and accessible, the new coating and the manufacturing process will be beneficial to the whole solar industry.

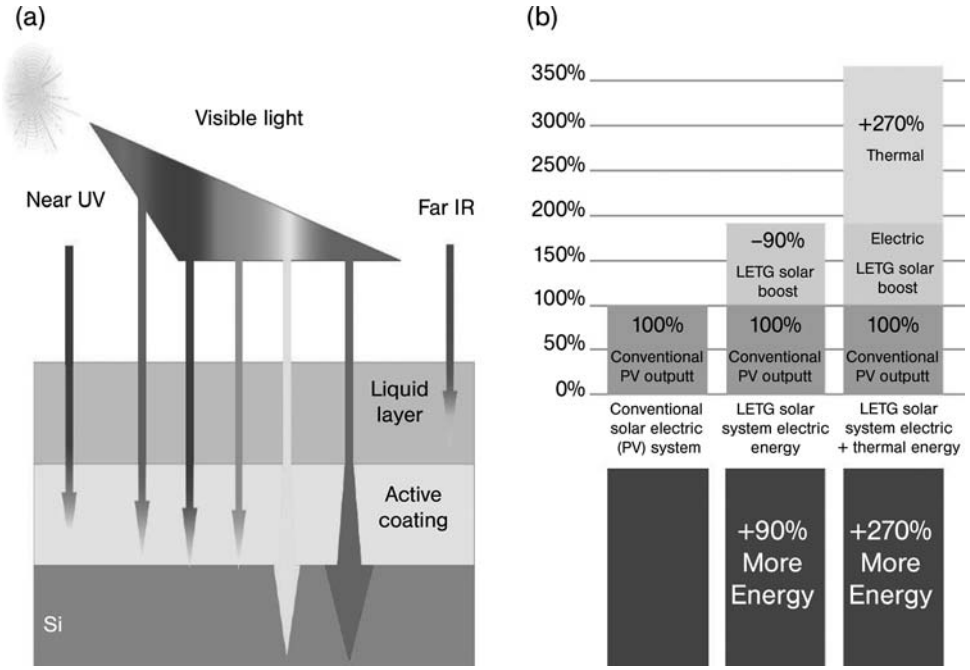

Figure 1.31 (a) Structure of a hybrid PV thermal cell covered by a liquid and an active luminophore layer. (b) The resulting enhancements results in electricity and heat generation. (Source. Global Warming Solutions).

In another development that aims to make alternative energy generation more efficient and more affordable, the Finnish company Braggone has discovered a method of capturing more light in a solar cell.

The shiny nature of silicon (Figure 1.32) means that about 30% of sunlight is reflected back into the sky. To help trap as much photo energy and convert it into as much electricity as possible an anti-reflective coating is used. This is prepared by hydrogenation and chemical vapor deposition (CVD) processes that are costly for manufacturers.

The new technology reduces the optical loss in the cell or module in addition to improving the efficiency of electrical conversion within the cell. The product is

Table 1.2 Solar module index retail price per watt (peak).

System	USD/Wp	Notes
Standard silicon PVC module	4.9	Solarbuzz.com
The hybrid PVC module (prototype)	3.65	With a two-sided silicon photocell
The hybrid PVC module	2.55	With a two-sided silicon photocell and reflecting surfaces

Source: Global Warming Solutions.

Figure 1.32 The efficiency of traditional silicon panels is significantly increased by spraying an anti-reflecting coating. (Source: Braggone).

used by spray coating it onto the solar cell, or glass, then curing it at an elevated temperature. A pre-coat (LUX-MH10) enables the passivation of the surface of a single crystal or of the bulk in multi-crystalline Si cells. Coupled with an anti-reflective coating (LUX-ME), it increases the efficiency and replaces the costly hydrogenation and CVD anti-reflective process with increased throughput with a simple spray coat process [22].

The innovative new product line is a breakthrough for crystalline silicon makers, but can also be used in thin film photovoltaics as well as in solar module manufacturing to further improve their power output.

While interest in alternative energy is increasing across the United States, interest in solar power, especially, is increasing in California. Eight of more than a dozen of the US companies developing photovoltaic cells are based in California, and seven of those are in Silicon Valley [23]. California, is poised to be both the world's next big solar market and its entrepreneurial center. Three-quarters of the nation's demand for solar power comes from residents and companies in California, where the State has earmarked $3.2 billion to subsidize solar installation, with the goal of putting solar cells on one million rooftops.

The subsidies have prompted a surge in private investment, led by venture capitalists. California received roughly half of all solar power venture investments made in 2007 in the United States, with $654 million in 33 solar-related deals in California, up from $253 million in 16 deals in 2006 [24].

San Jose-based SunPower, manufacturer of silicon-based cells, reported 2007 revenue of more than $775 million, more than triple its 2006 revenue, while its stock price grew 251% in 2007. In the same city, Nanosolar recently started making CIGS photovoltaic cells in a large factory, making it one of the biggest producers in the world. The company uses the newspaper printing roll-to-roll technology by spraying

Figure 1.33 Easy installation by Solar Integrated of a lightweight white single-ply roofing membrane, and thin-film photovoltaic membrane transforms commercial and industrial roofs in clean energy generators. (Source. Solar Integrated).

the CIGS material onto giant rolls of aluminum foil and then cutting it into pieces the size of solar panels, as described in Chapter 3.

Another company, Solar Integrated, based in Los Angeles, has developed a low-cost approach to integrating flexible photovoltaic modules made of a-Si directly into the roofs of commercial buildings (Figure 1.33).

All of these companies have the chance to be billion-dollar operators [25]. Yet, to ensure that solar PV is not just for a green elite, and to make it the basis for the economy, we should start from the fact that solar energy represents less than one-tenth of 1% of the $3 trillion global energy market.

There are two intrinsic major differences from the unfulfilled promises of the 1970s, and two external drivers – the skyrocketing oil price and global warming – that will profoundly affect the evolution of solar energy (Chapter 7).

Considering the main two factors: first, through innovation and volume, prices are coming down to such an extent that Nanosolar claims electricity generated through its panels has the same price as electricity from coal. Second, there is a wide consensus that large scale electricity generation will take place through systems

Figure 1.34 Flat reflectors move following the position of the sun and reflect the energy of the sunlight to the fixed pipe receiver above, where water is heated and becomes the steam needed to power a turbine. (Source: Ausra).

that concentrate sunlight from reflecting mirrors to ensure we reach the scale we need to really solve the planet's problems given that, in the meantime, coal-burning power plants, the main source of CO_2 emissions linked to global warming, are being built around the world at a rate of more than one a week.

One such solar thermal plant is the 177-megawatt plant that Ausra, a Palo Alto start-up backed by the investor Vinod Khosla and his former venture capital firm, is building in central California to generate power for more than 120 000 homes beginning in 2010. Its core technology is the compact linear Fresnel reflector (CLFR) solar collector and steam generation system, originally conceived in the early 1990s at Sydney University, that is now being refined and built at large scale by Ausra around the world (Figure 1.34) [26].

The company develops large-scale power projects incorporating CLFR solar fields, and helps utilities generate clean energy for millions of customers. Remarkably, the system uses water as the thermal liquid, eliminating any toxic, corrosive and expensive fluids. Within a year, the company claims it will match the price of natural gas plants, which generate electricity at about 9.2 cents per kilowatt hour; and within three years, it will match the cost of coal-fired plants, which is about 6–8 cents per kilowatt hour.

Another example is that of eSolar, a company in Pasadena (co-financed by Google.org, the philanthropic division of the Internet company) that builds heliostats designed from the ground up to minimize every possible cost [27]. eSolar has designed a solar field layout (Figure 1.35) made of small size heliostats (for higher reliability in all wind conditions and more power plant up-time) that minimizes installation time and cost. By employing a repeating frame structure and a new calibration system, the company has eliminated the need for high-precision surveying, delicate installation,

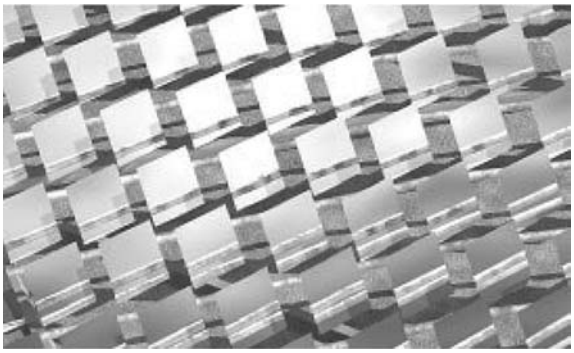

Figure 1.35 New heliostats are designed to fit efficiently into shipping containers to keep transportation costs low, and are pre-assembled at the factory to minimize on-site labor. (Source: eSolar).

and individual alignment of mirrors. Minimal skilled labor is needed to build the solar field, allowing mirror deployment efficiencies that scale with project size and deadlines.

References

1 See the whole thread at: http://lightingafrica.org/index.cfm?Page=Forums&ap=thread&ConfID=1473&MessageID=1546.

2 http://www.plasticlogic.com.

3 see for instance Flexcell's products at http://www.flexcell.ch.

4 For an account of the discovery of conductive polymers, see: http://nobelprize.org/nobel_prizes/chemistry/laureates/2000/heeger-lecture.html.

5 Hoffmann, W. A Vision for PV Technology up to 2030 and beyond – An Industry View, European Photovoltaic Industry Association, Brussels: September 28th, 2004.

6 Maugeri, L. (2006) *The Age of Oil – The Mythology, History, and Future of the World's Most Controversial Resource*, Praeger Publishers, New York.

7 Deffeyes, K.S. (2005) *Beyond Oil: The View from Hubbert's Peak*, Hill and Wang, New York.

8 Cleveland, C.J., Hall, C.A.S. and Herendeen, R. (2006) Energy returns on ethanol production. *Science*, **312**, 1746.

9 Dorn, J.G. *Solar Cell Production Jumps 50 Percent in 2007*, Earth Policy Institute, Washington: December 27, 2007. Available at: http://www.earth-policy.org/Indicators/Solar/2007.htm.

10 The report of the European Photovoltaic Industry Association, *EPIA roadmap*, June 2004. Available at: http://www.epia.org/fileadmin/EPIA_docs/publications/epia/EPIAroadmap.PDF.

11 Engel, G.S., Calhoun, T.R., Read, E.L., Ahn, T.-K., Mancal, T., Cheng, Y.-C., Blankenship, R.E. and Fleming, G.R. (2007) Evidence for wavelike energy transfer through quantum coherence in photosynthetic systems. *Nature*, **446**, 782.

12 Ozin, G. and Arsenault, A. (2006) *Nanochemistry*, RSC Publishing, Cambridge.

13 Zukalova, M., Zukal, A., Kavan, L., Nazeeruddin, M.K., Liska, P. and Gratzel, M. (2005) Organized Mesoporous TiO_2 Films Exhibiting Greatly Enhanced Performance in Dye-Sensitized Solar Cells. *Nano Letters*, **9**, 1789.

14 Green, M.A. Cited on the occasion of the honorary award of the 2002 The Right Livelihood Award, http://www.rightlivelihood.org/green.html.

15 Dwyer, J. (Solar) Power to the People Is Not So Easily Achieved, *The New York Times*, January 23, 2008. http://www.nytimes.com/2008/01/23/nyregion/23about.html?ref=nyregion.

16 www.pvsolartiles.com.

17 The research and demonstration project PVACCEPT funded by the European Commission from 2001 to 2004. A complete account on the project is at: http://www.pvaccept.de.

18 The data are reported in: *PVACCEPT Final Report*, (eds I. Hermannsdörfer, C. Rüb), 2005.

19 http://world.honda.com/HondaSoltec/.

20 Revkin, A.C. and Wald, M.L. (2007) Solar Power Wins Enthusiasts but Not Money, *The New York Times*, July 16.

21 www.globalwarmingsolutions.com.

22 http://www.braggone.com/index.php?option=content&task=view&id=28.

23 Richtel, M. and Markoff, J. A Green Energy Industry Takes Root in California, *The New York Times*, February 1, 2008.

24 Data from The Cleantech Group, which tracks investments in alternative energy. http://www.cleantech.com/.

25 See for instance the analyses of the University of California's Professor D. Kammen at: http://socrates.berkeley.edu/~kammen/.

26 http://ausra.com/news/releases/071105.html.

27 The technology is discussed in detail at: http://www.esolar.com.

2
Photovoltaics

2.1
How a Solar Cell Works

The term photovoltaic is derived by combining the Greek word for light, photos, with voltaic, named after Alessandro Volta. A solar photovoltaic (PV) cell converts sunlight to electricity. In the photoelectric effect at a metal surface, electrons are freed once the energy exceeds the bond energy. In a solar cell, an asymmetry is established by contacting two semiconductors of opposite polarity which drives electrons that are freed by the incident light in a circuit (Figure 2.1) [1].

A conventional solar cell (Figure 2.2) consists of two layers of semiconductor, one positive (p-type) and the other negative (n-type), sandwiched together to form a p/n junction.

When the semiconductor is exposed to light, the energy $h\nu$ of incident photons exceeding the threshold bandgap is absorbed by the semiconductor's electrons that access the conduction band starting to conduct electricity. Electrons in semiconductors, in fact, are weakly bonded to the atomic nucleus and occupy the valence energy band.

For each negatively charged electron, a corresponding mobile positive charge, a hole, is created.The electrons and holes near the p/n junction are swept across in opposite directions by the action of the electric field, where a contact drives such electrons to an external circuit where they lose energy doing work such as powering a light source and then return to the material's valence band through a second selective contact closing the circuit (Figure 2.3).

Only photons whose energy is greater than the enery bandagap (E_G) are able to create an electron–hole pair (Figure 2.4) and thus contribute to the energy conversion process. Therefore, the spectral nature of sunlight is a fundamental aspect affecting the design of efficient solar cells (Figure 2.5).

The solar cell is the photovoltaics building block. Usually, it is made of a 100 cm^2 silicon wafer whose surface has been treated to maximize light absorption and thus appears dark blue or black. Such a cell hit by radiation from the sun generates a tens of milliamps per cm^2 current caused by a 0.5–1 V potential, which is too low for most applications.

Flexible Solar Cells. M. Pagliaro, G. Palmisano, and R. Ciriminna

ISBN: 978-3-527-32375-3

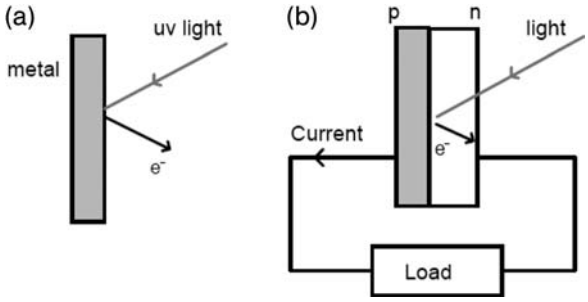

Figure 2.1 Asymmetry in a solar cell (b) drives electrons that are freed by the incident light in the circuit. In the photoelectric effect at a metal surface (a), electrons are freed once the energy exceeds the bond energy. (Reproduced from Ref. [1], with permission).

Cells are thus connected in series in a module (using a blocking to avoid complete failure in case of a single cell failure) which typically contains 28–36 cells to generate an output voltage of 12 V in standard illumination conditions. Modules are further arranged in parallel in arrays ("panels") that are those marketed.

To power alternating current (AC) devices and to connect to the grid, the array is connected to an inverter. A solar cell can thus replace a battery in a circuit (Figure 2.6).

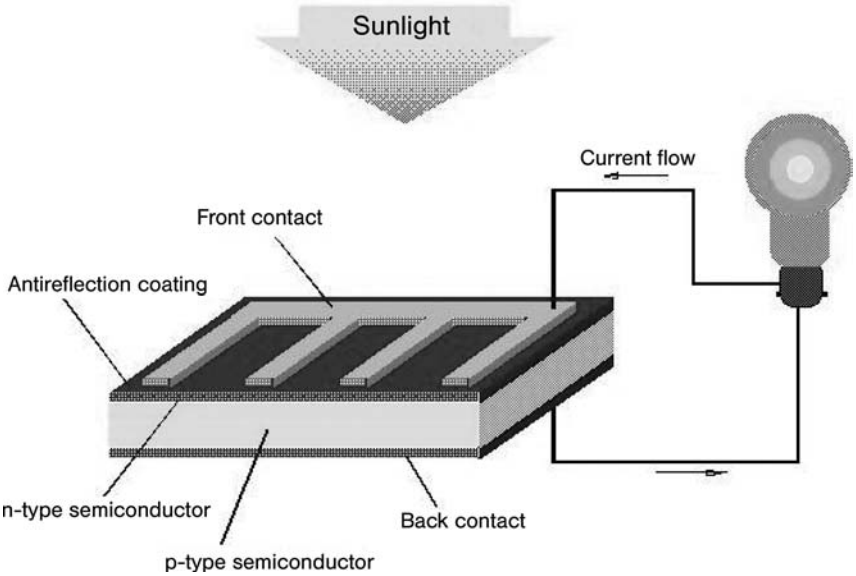

Figure 2.2 A photovoltaic cell under illumination generates electricity as electrons move to the conduction band leaving holes behind in the material. (Reproduced from Ref. [2], with permission).

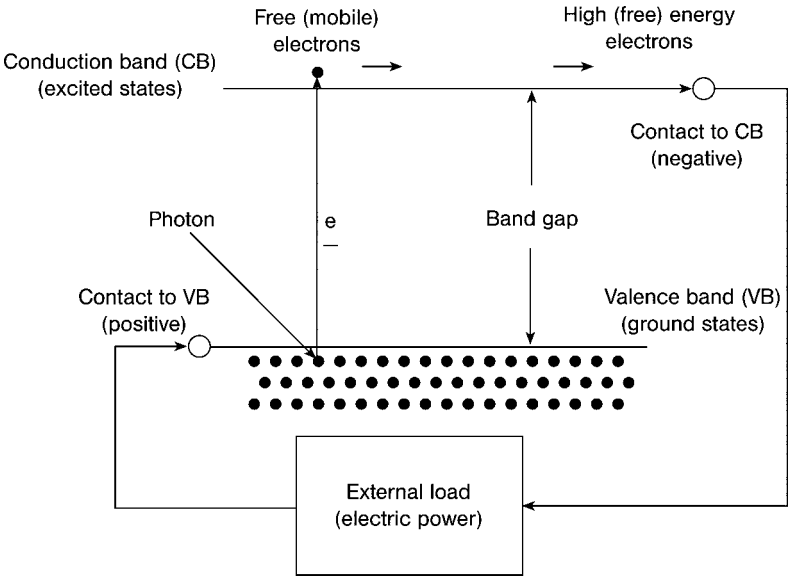

Figure 2.3 Relation between the energy and the spatial boundaries in a solar cell. (Reproduced from Ref. [1], with permission).

The voltage V_{OC} developed when the terminals are isolated is the *open circuit voltage*. The current I_{SC} flowing when the terminals are connected is the *short circuit current*. For any intermediate load resistance R_L, the circuit develops a voltage between 0 and V_{OC} and delivers a current I such that $V = IR_L$ and $I(V)$ is determined by the *current–voltage characteristic* of the cell.

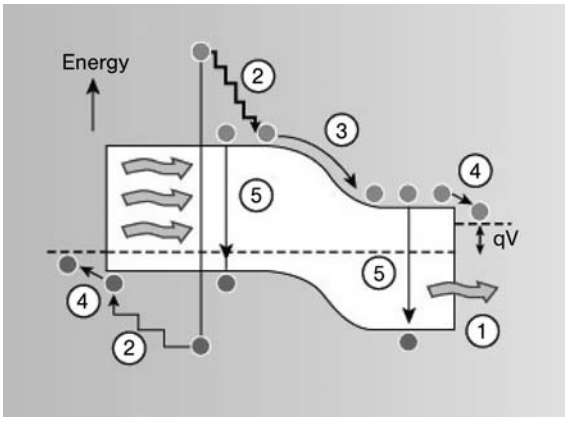

Figure 2.4 Loss processes in a standard solar cell: (1) non-absorption of below bandgap photons; (2) lattice thermalization loss; (3) and (4) junction and contact voltage losses; (5) recombination loss. (Reproduced from Ref. [3], with permission).

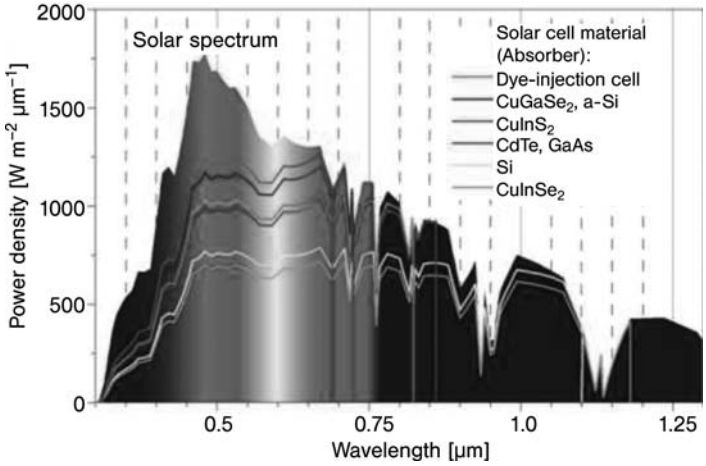

Figure 2.5 The solar spectrum of sunlight together with the quantum efficiency profile of semiconductors commonly employed in solar cells. (Image courtesy: Hahn-Meitner-Institut Berlin).

Since the current is roughly proportional to the illuminated area, the relevant parameter for comparison is the *current intensity* J_{SC}. The power delivered to a load by a battery is relatively constant, whereas the power delivered by a solar cell is dependent on the incident light intensity and not on the load (Figure 2.7).

The e.m.f derives in fact from a temporary change in the electrochemical potential induced by the light. The current density is related to the incident spectrum through the cell's *quantum efficiency* $QE(E)$, that is the probability that a photon of energy $E = h\nu$ induces electron transition to the external circuit. Then

$$J_{SC} = q \int b_S(E) QE(E) \mathrm{d}E \tag{2.1}$$

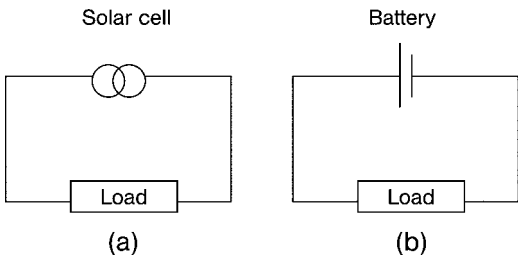

Figure 2.6 A solar cell can thus replace a battery in a circuit. (Reproduced from Ref. [1], with permission).

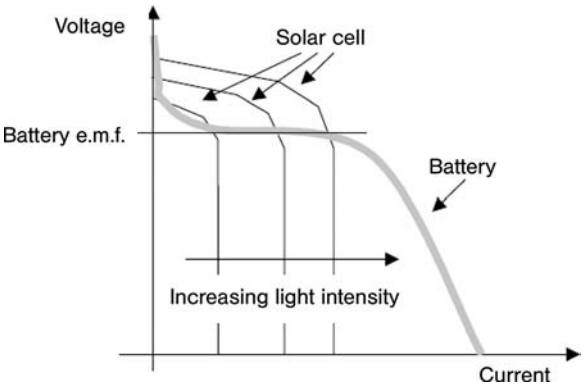

Figure 2.7 A battery is essentially a voltage source whereas a solar cell is a current source. Whereas a battery delivers a constant voltage at practically any current (until it becomes exhausted on discharge), the solar cell delivers a constant current for any given illumination level and the voltage is largely determined by the resistance of the load. (Reproduced from Ref. [1], with permission).

Where q is the electron charge, and $b_S(E)$ is the flux density of the incident photons, namely the number of photons of energy $E + dE$ which are incident on unit area in unit time.

Thus, as J_{SC} is obtained by integrating the product of the photon density and QE over the photon energy, it is desirable to have a high quantum efficiency at the energy where the photon density is high. The QE of a cell's material (Figure 2.5) in turn depends on (i) the efficiency of charge *separation*; (ii) the *absorption* capacity of the material; and, (iii) the efficiency of charge *collection* in the device.

The operating regime of the solar cell is in the range of bias, between $V = 0$ and V_{OC}, in which the cell delivers power. And the cell power density P is

$$P = JV \tag{2.2}$$

P reaches a maximum at the cell's operating point or maximum power point. This occurs at the voltage V_m with a corresponding current density J_m as shown in Figure 2.8.

The *fill factor FF* is thus defined as the ratio

$$FF = \frac{J_m V_m}{J_{OC} V_{OC}} \tag{2.3}$$

The FF thus describes the "squareness" of the J–V curve.

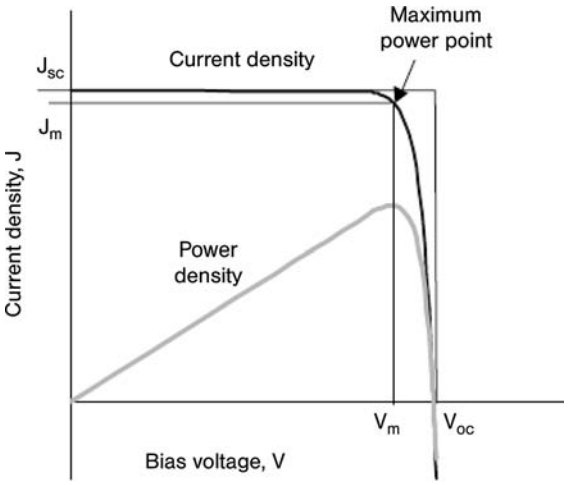

Figure 2.8 The current voltage (black) and power voltage (gray) chracteristics of an ideal solar cell. Power voltage reaches a maximum at a bias voltage, V_m, close to V_{OC}. The maximum power density $J_m \times V_m$ is given by the area of the inner rectangle. The outer rectangle has area $J_{SC} \times V_{OC}$. If the fill factor is equal to 1, the current voltage curve follows the outer rectangle. (Reproduced from Ref. [1], with permission).

The efficiency of a cell is the power density delivered at the operating point as a fraction of the power density of the incident light, P_S,

$$\eta = \frac{J_m V_m}{P_S} \tag{2.4}$$

Efficiency η is related to J_{SC} and to V_{OC} through the fill factor,

$$\eta = \frac{J_{SC} V_{OC} FF}{P_S} \tag{2.5}$$

These four quantities J_{SC}, V_{OC}, FF and η define the performance of a solar cell, and are thus its key characteristics.

For effective comparison, all must thus be expressed under standard illumination conditions. The standard test condition (STC) for solar cells, regardless of design and active material, is the Air Mass 1.5 spectrum (AM 1.5G), an incident power density of $1000\,W\,m^{-2}$, which is defined as the standard "1 sun" value, at an ambient temperature of 25 °C (Figure 2.9).

It must be emphasized that the average sun power density on Earth is $170\,W\,m^{-2}$, namely one sixth of the standard density chosen to compare the efficiency of solar cells. As the manager of a manufacturer of dye-sensitized solar cells put it, "there is no such a thing as 1 Sun at 25 °C except on the Jungfrau (a 4158 m high mountain in Switzerland) in summer."

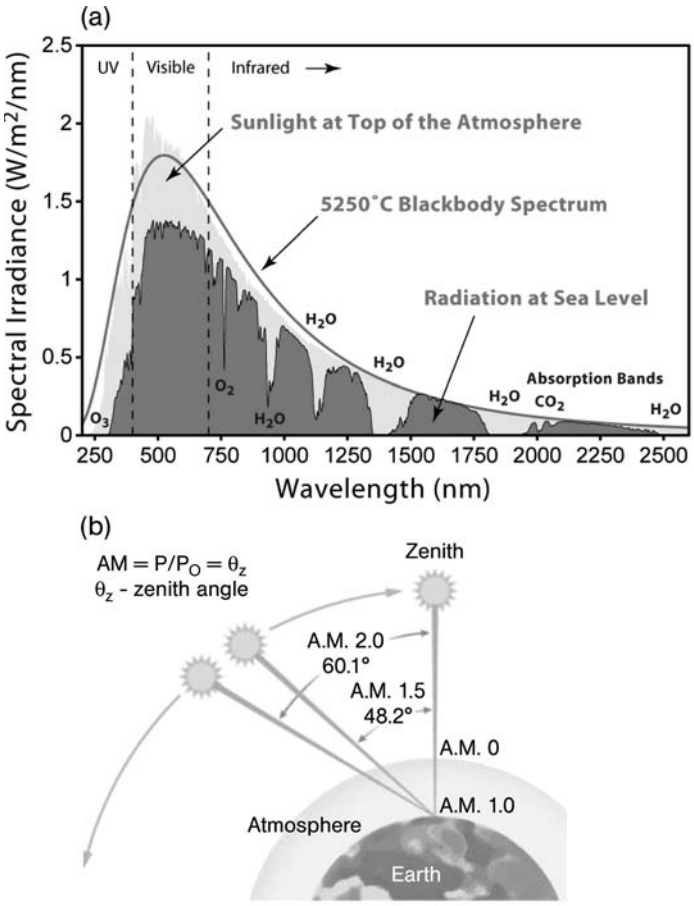

Figure 2.9 Solar irradiance spectrum above atmosphere and at surface (a). The air-mass value AM 0 (b) equates to insolation at sea level with the Sun at its zenith. AM 1.0 represents sunlight with the Sun at its zenith above the Earth's atmosphere and absorbing oxygen and nitrogen gases. AM 1.5 is the same, but with the Sun at an oblique angle of 48.2°, which simulates a longer optical path through the Earth's atmosphere; AM 2.0 extends that oblique angle to 60.1°. (Image courtesy of LaserFocusWorld).

This must be always taken into consideration in all practical applications as the efficiency of conventional cells rapidly decreases at lower power densities, and cells with lower nominal efficiency can deliver significantly larger energy output than their counterparts due to better performance at lower light intensity and higher temperature.

Figure 2.10 illustrates the correlation between J_{SC} and V_{OC} together with the relationship for a cell of maximum efficiency. The values in Table 2.1 for the main solar cells, show that cells with higher J_{SC} tend to have lower V_{OC}. This is a consequence of the material's semiconductor band gap. In general, in practical photovoltaic applications, a compromise is made between the photocurrent and the voltage.

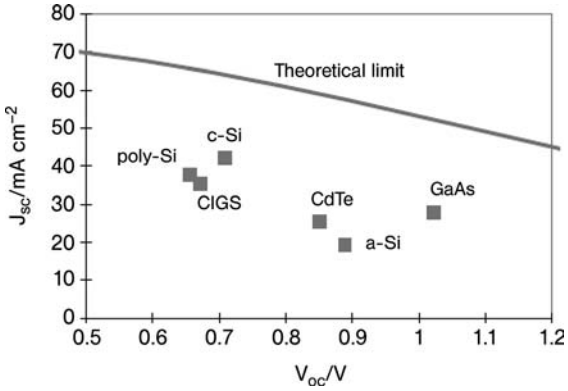

Figure 2.10 Plot of the J_{SC} vs. V_{OC} for the cells listed in Table 2.1. Due to the bandgap, materials with high V_{OC} tend to have lower J_{SC}. (Reproduced from Ref. [1], with permission).

Table 2.1 Performance of some types of PV cell [Green *et al.*, 2001].

Cell type	Area (cm^2)	V_{oc} (V)	J_{sc} (mA cm^{-2})	FF	Efficiency (%)
crystalline Si	4.0	0.706	42.2	82.8	24.7
crystalline GaAs	3.9	1.022	28.2	87.1	25.1
poly-Si	1.1	0.654	38.1	79.5	19.8
a-Si	1.0	0.887	19.4	74.1	12.7
$CuInGaSe_2$	1.0	0.669	35.7	77.0	18.4
CdTe	1.1	0.848	25.9	74.5	16.4

2.2 The Solar Cell: A Current Generator

In practice, when a load is present a potential difference develops between the terminals of the cell. This potential generates a current which acts in the opposite direction to the photocurrent, and the net current is reduced from its short circuit value. This reverse current is called the *dark current*, in analogy with the current $I_{\text{dark}}(V)$ which flows across the device under an applied voltage, or *bias*, V, in the dark.

Most solar cells behave as a diode in the dark, admitting a much larger current under forward bias ($V>0$) than under reverse bias ($V<0$). For an ideal diode, the *dark current density* varies like

$$J_{\text{dark}} = J_{\text{o}}(\text{e}^{qV/k_{\text{B}}T}-1) \tag{2.6}$$

Where k_{B} is Boltzmann's constant, T is the temperature and J_{o} is a constant. Thus the net current flowing in a circuit powered by a solar cell is

$$J(V) = J_{\text{sc}}-J_{\text{dark}} \tag{2.7}$$

$$J(V) = J_{\text{sc}}-J_{\text{o}}(\text{e}^{qV/k_{\text{B}}T}-1) \tag{2.8}$$

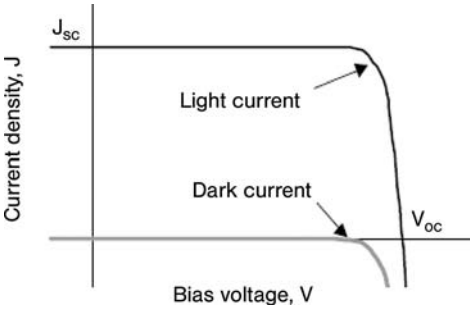

Figure 2.11 Current–voltage curve for an ideal diode in the dark and under light. (Reproduced from Ref. [1], with permission).

When the contacts are isolated the potential difference has its maximum value, V_{OC}, which is equivalent to the condition when the short circuit current and the dark current exactly cancel out. It thus follows that, for an ideal diode,

$$V_{OC} = \frac{k_B T}{q} \frac{\ln(J_{SC}+1)}{J_o} \tag{2.9}$$

In other words, the V_{OC} increases logarithmically (and thus very slowly) with light intensity.

Figure 2.11 shows that the cell generates power when the voltage is between 0 and V_{OC}. At $V<0$ the cell acts as a photodetector, consuming power to generate a photocurrent. In certain cases, in this diode regime, the dark current in solar cells is accompanied by emission of light.

Electrically, therefore, the solar cell is equivalent to a current generator in parallel to a resistive diode (Figure 2.12). It is this diode that establishes a photovoltage enabling the photocurrent through the load.

When illuminated, the solar cell produces a photocurrent proportional to the light intensity. This photocurrent is divided by the load and the diode, in a ratio that depends on the light intensity and on the load resistance.

In real cells, power is dissipated through the contact resistance and through leakage currents around the sides of the device. Electrically, these effects are equivalent to two parasitic resistances in series (R_s) and one in parallel (R_{sh}), as shown in Figure 2.13.

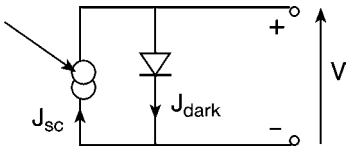

Figure 2.12 The solar cell is equivalent to a current generator in parallel to a resistive diode. (Reproduced from Ref. [1], with permission).

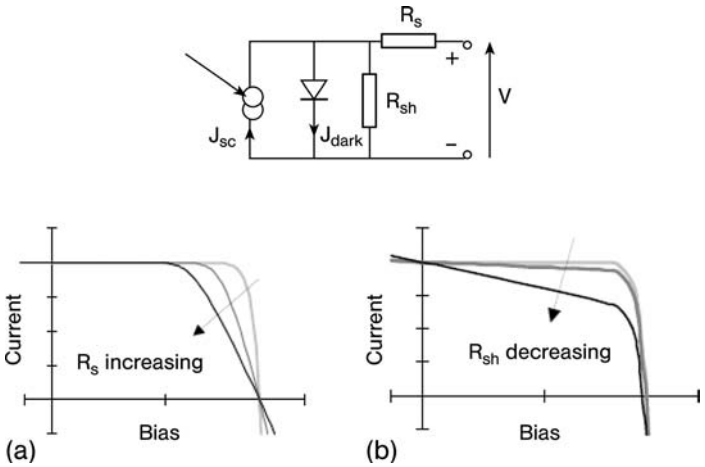

Figure 2.13 Effect of (a) increasing series resistance and (b) reducing parallel resistance on the current–voltage curve. In both cases, the outer curve has $R_s = 0$ and $R_{sh} = \infty$. In practice, the effect of deviating from this ideal behavior is to reduce the fill factor of the cell. (Reproduced from Ref. [1], with permission).

Series and parallel resistances reduce the fill factor. Hence, for an efficient cell one desires to have R_s as small and R_{sh} (or R_p) as large as possible. The series resistance arises from the cell's material resistance to the current flow, particularly through the front surface to the contacts (and it is a serious problem at high current densities under concentrated light). The parallel, or shunt, resistance is a problem of poorly rectifying devices (and it arises from leakage of current through the cell).

Thus, the Shockley diode equation corrected for real inorganic devices with series and shunt resistance is

$$j_L = j_0\left(\exp\left(\frac{q(V-jR_s)}{nkT}\right)-1\right)-\frac{V-jR_s}{R_p}-j_{ph} \tag{2.10}$$

where an optional (constant) photocurrent j_{ph} is included by a parallel shift of the current–voltage curve down the current axis.

In summary, a positive bias leads to the injection of charge carriers into the solar cell, and the current increases exponentially, diode-like behavior (in the ideal case). In real solar cells, however, there are losses, considered in the second equation above by two resistors.

This equation works nicely for silicon solar cells, but in organic solar cells (Chapter 4) the "parallel resistance" now seems to depend on the voltage and illumination intensity and the "series resistance" also changes with voltage.

Thus, the $j(V)$ curve for a typical organic solar cells has a strongly field-dependent photocurrent. There is for example a crossing point of dark and illuminated curve at approx. 700 mV which cannot be explained by the Shockley equation (Figure 2.14).

The reason is that the Coulomb bound electron–hole pairs have to be split by the externally applied electric field. At 700 mV (in this instance), however, the internal

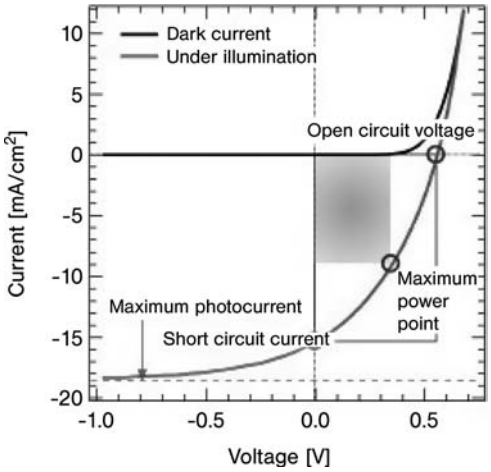

Figure 2.14 *J–V* curve for an organic solar cell shows a strongly field-dependent photocurrent. (Image courtesy of Dr. Carsten Deibel, from http://blog.disorderedmatter.eu).

electric field, which is the contact potential difference minus the external electric field, is zero. This means flat band conditions, and therefore there is not enough driving force for the polaron pairs to be separated: there has to be a crossing point.

As one can see from the upper part of the figure, the maximum photocurrent is not reached at 0 V, that is, under short circuit conditions, but only at more negative bias, corresponding to a higher internal field. This happens in organic solar cells where the polaron pair dissociation is more difficult, for example, if the active layer is thicker, and therefore at the same (external) voltage, the (internal) field at zero bias is lower.

Indeed, there is no analytic equation yet to properly describe the peculiarities of organic solar cells. Actually, even in inorganic compound semiconductors such as $CuInSe_2$ there are similar crossing points.

2.3
Efficiency Limits of the Photovoltaic Conversion

In principle, sunlight can be converted to electricity at an efficiency close to the Carnot 95% limit for the sun modeled as a black-body at $T_1 = 6000$ K (the temperature of the sun surface), and a cell operating at room temperature ($T_2 = 300$ K) [4].

$$\eta = 1-(T_2/T_1) = 1-(300/6000) = 0.95 \tag{2.11}$$

Indeed, the maximum theoretical yield of 93.3% is only slightly different [5].

This means that large improvements are potentially within reach, on moving from the theoretical 31% conversion efficiency limit calculated for a single-junction solar cell in 1961 (see below), to such as those based on silicon wafer and thin films presently commercialized [6].

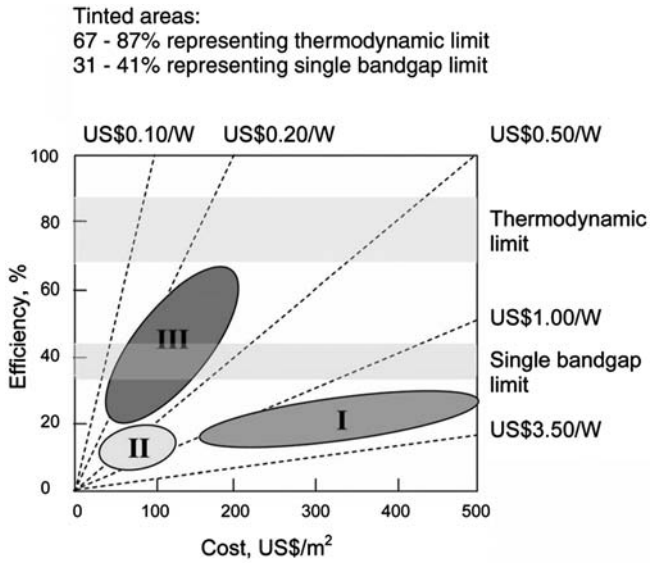

Figure 2.15 Efficient cost trade-off for the three generations of solar cell technologies: wafer, thin-films, advanced thin-films. (Reproduced from Ref. [3], with permission).

Since the early days of terrestrial photovoltaics, a common perception has been that first generation silicon wafer-based solar cells eventually would be replaced by a second generation of lower cost thin-film technology, probably also involving a different semiconductor.

First generation solar cells (Figure 2.15) had high production costs with moderate efficiency (15–20%); second generation cells offer much lower overall production cost but efficiencies are even lower (5–10%). Third generation cells have high efficiency and slightly higher production costs, which is largely paid back by the increase in efficiency resulting from the low unit cost of electricity (Table 2.2).

Historically, cadmium sulfide, amorphous silicon, copper indium diselenide, cadmium telluride and now thin-film polycrystalline silicon have been regarded as key thin-film candidates. Indeed, these inorganic materials show excellent promise in terms of efficiency [7] (Figure 2.16) and thin films can be molded as lightweight modules onto existing constructions.

Table 2.2 The three waves of evolution of PV technologies.

Generation	Efficiency	Cost €/watt
I	0.15	1
II	0.15	0.50
III	0.8	0.20

(Reproduced from Ref. [2], with permission).

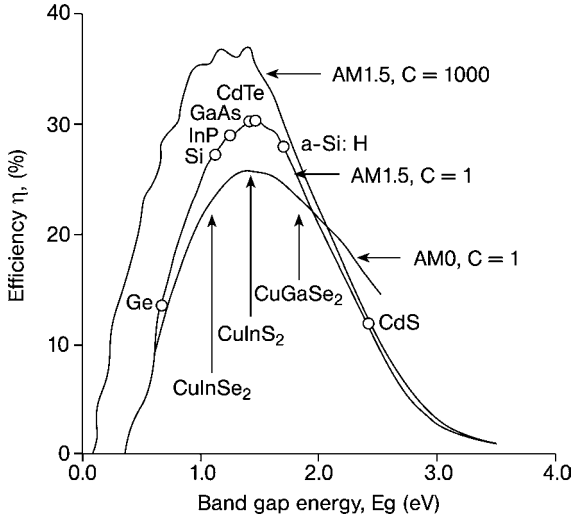

Figure 2.16 Predicted efficiency versus bandgap for thin film photovoltaic materials for solar spectra in space (AM0) and on earth (AM1.5) at 300 K compared with other photovoltaic materials with concentrated and unconcentrated (1) sunlight. (Reproduced from Ref. [6], with permission).

Any mature solar cell technology seems likely to evolve to the stage where costs are dominated by those of the constituent materials, be they silicon wafers or glass sheet.

Photovoltaics is likely to evolve, in its most mature form, to a third generation of high-efficiency thin-film technology. By high efficiency is meant energy conversion values double or triple the 15–20% range presently targeted, closer to the thermodynamic limit of 93%.

Third generation concepts are based on devices that can exceed the theoretical solar conversion efficiency limit for a single energy threshold material. This was calculated in 1961 by Shockley and Queisser as 31% under 1 sun illumination and 40.8% under maximal concentration of sunlight (46 200 suns), for an optimized bandgap of 1.3 eV and 1.1 eV, respectively [8]. According to this elegant analysis, the number of electrons flowing from an ideal solar cell through an external circuit is equal to the difference between the number of photons absorbed over the energy range E_l to E_h and the number of photons the device emits over the same energy range. The formulation is not detailed here but uses the Planck equation for the spectrum of light received from the sun and a modified Planck equation for the light emitted by the cell, the latter exponentially enhanced by the forward bias of the cell, just as for a light-emitting diode.

For Si and GaAs bandgaps of 1.12 and 1.45 eV, respectively, the limiting efficiencies are both about 29% for unconcentrated light. Thus, the record efficiencies in each case of 24.7 and 25.1% at one-sun illumination indicate devices approaching the radiative limit.

The routes to exceeding the Shockley–Queisser limit address the band gap and the thermalization loss mechanisms. Three types of approach have been proposed for applying multiple energy levels:

- increasing the number of energy levels
- multiple carrier pair generation per high energy photon
- capturing carriers before thermalization.

To increase efficiency, we need to use the whole solar spectrum. One possibility resides in using double (tandem) cells which split the solar spectrum into narrow frequency bands that are converted by the best suited cell maximizing efficiency. The process is similar to that that takes place in "rectennas", that is rectifying antennas that transmit solar radiation in tunnel diodes. The quantum phenomena therein produce variable currents, whose energy is equivalent to that of the incident radiation – whereas the tension generated in the circuit rises linearly with the frequency of the incident photon. As 44% of solar radiation has wavelengths between 0.4 and 0.7 μm, to absorb it entirely the rectenna should function at up to 600 THz.

2.4 Multiple Junction Cells

Multijunction solar cells are one high-efficiency approach aiming to design a device that absorbs the sun's broadband spectrum emission over the entire visible range (from about 350 to 800 nm) [3]. Efficiency here is increased by adding more cells of different bandgap to a cell stack, at the expense of increased complexity and spectral sensitivity. Some of the losses due to the bandgap limitations are avoided by cascading semiconductors of different bandgaps (Figure 2.17).

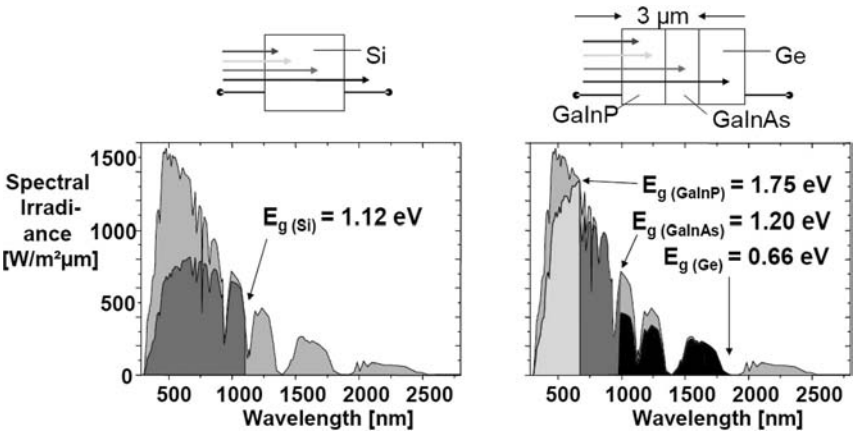

Figure 2.17 Better utilization of the solar spectrum through the multijunction approach.

The tandem or multicolor cell uses the strategy of increasing the number of energy levels. Solar cells consisting of p–n junctions in different semiconductor materials of increasing bandgap are placed on top of each other, such that the highest bandgap intercepts the sunlight first. The elegance of the approach – first suggested by Jackson in 1955 – is that both spectrum splitting and photon selectivity are automatically achieved by the stacking arrangement.

The particle balance limiting efficiency depends on the number of subcells in the device. For 1, 2, 3, 4, and ∞ subcells, the efficiency η is 31.0, 42.5, 48.6, 52.5, and 68.2% for unconcentrated light, and 40.8, 55.5, 63.2, 67.9, and 86.8% for maximally concentrated light. Hence, the efficiency increases with the number of subcells in both cases, but the efficiency gain decreases with each subsequent subcell [3].

To achieve the highest efficiency from the overall tandem device, the power from each cell in the stack must be optimized. This is done by choosing appropriate bandgaps, thicknesses, junction depths, and doping characteristics, such that the incident solar spectrum is split between the cells most effectively. The next requirement is to extract electrical power from the device most effectively.

For a real, variable spectrum, the mechanically stacked design gives greater flexibility because of the ability to optimize the *I–V* curve of each cell externally and then connect them in an external circuit. The reduced flexibility of just optimizing the *I–V* curve for the whole stack, because the same current must flow through each cell, makes the in-series design more sensitive to spectral variations. Furthermore, the cells become increasingly spectrally sensitive as the number of bandgaps increases. This is particularly the case at the beginning and end of the day when the spectrum is significantly red-shifted by the thickness of the atmosphere.

The highest efficiency tandem devices are made using single-crystal III–V materials. These are grown monolithically by very expensive epitaxial processes such as metal organic vapor phase epitaxy and are indeed used in space applications.

An alternative approach to reducing the cost per watt makes use of cheaper materials of lesser quality (higher defect density and lower efficiency), but that can be produced by much cheaper, low-energy intensity deposition methods such as amorphous silicon (a-Si); thus meeting the two requirements of third-generation devices (low cost per watt and the use of nontoxic and abundant materials).

Hence, for example, 8% efficient modules in a-Si are made by vacuum deposition of triple junction cells constructed of three separate p-i-n type a-Si sub-cells, each with a different spectral response characteristics.

Despite STC efficiency around 8%, Figure 2.18 showing the influence of irradiance in outdoor, real conditions (the test was carried out in the Netherlands) [9] indicates that such cells perform significantly better than crystalline Si PV technologies at low light conditions (40–100 $W\,m^{-2}$) with up to 20% increase in the kWh energy output per Wp installed either in cold climates, where low and diffuse light conditions prevail, or in warm climates where better performance dependence on temperature also contributes to higher output .

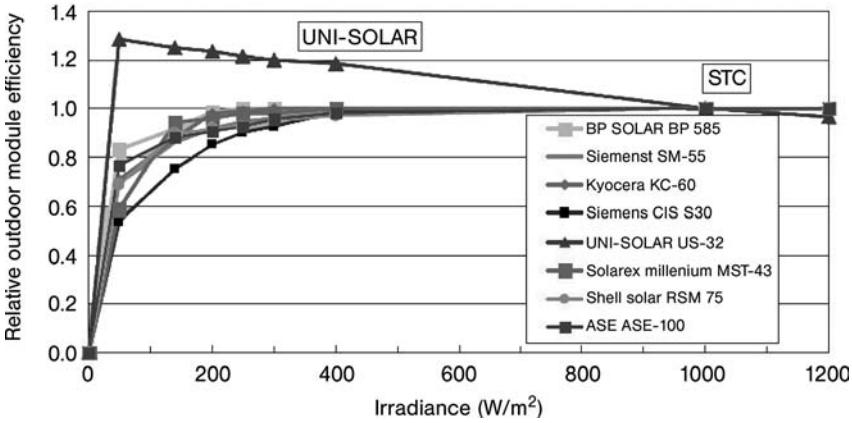

Figure 2.18 Dependence of the efficiency of a-Si triple junction modules points to significantly better performance of these multijunction cells at low irradiation compared to crystalline Si modules. (Image courtesy of Unisolar).

2.5 Solar Cell Applications

The first practical application of solar cells was developed for space applications. Starting with the US satellite "Vanguard" – which was equipped with a dual power system of chemical batteries and silicon solar cells, of which the batteries failed after a week while the silicon solar cells kept the satellite communicating with Earth for years – spacecraft have all been powered by solar cells.

Thus, solar energy has played a crucial role in society's technological progress over the past forty years because it powers the satellites that made possible the telecommunication revolution.

The advantages and disadvantages of photovoltaics are summarized in Table 2.3.

The increasing demand for solar cells in space opened an increasing and relatively large business for those manufacturing solar cells. The first mass market developed in the early 1970s when Elliot Berman, financed by the Exxon Corporation, designed a significantly less costly solar cell by using a poorer grade of silicon

Table 2.3 Advantages and disadvantages of photovoltaics.

Advantages	Disadvantages
Infinite, free energy source	Energy source is diffuse (unconcentrated)
Zero emissions	Lack of economic energy storage systems
No noise	High installation costs
Safe	Higher costs compared to traditional fuels
Versatility (modular and integrable in existing structures)	

Figure 2.19 Aids to Navigation: Honolulu, HI – Coast Guard Cutter Walnut (WLB 205) deck crew paints the 18 000-lb. Hotel buoy. (Photo courtesy of Sarah Foster-Snell).

and packaging the cells with cheaper materials, bringing the price down from $100 per watt to $20 per watt. Hence photovoltaics first became competitive in contexts where conventional electricity supply is expensive or simply not possible, such as navigation, rural areas, telecommunications and for enhancement of supply in grid-connected loads at peak use [10].

Solar cells could now compete in situations where people needed electricity distant from power lines. Off-shore oil rigs, for example, required warning lights and horns to prevent ships from running into them (Figure 2.19). Furthermore, microwave and high frequency repeaters for telecommunication (including telephone and television) systems are generally powered by locally generated solar electricity.

Compared to cumbersome, short-lived batteries solar modules proved a bargain. Many gas and oil fields on land but far away from power lines needed small amounts of electricity to combat corrosion in well heads and piping. Major purchases of solar modules by the gas and oil industry gave the fledgling terrestrial solar cell industry the needed capital to persevere.

Stand-alone photovoltaic applications, whether for remote buildings (Figure 2.20), service applications or island power supplies, represent about 90% of installed PV power today. They provide power when and where it is needed, without the need for a utility grid. Batteries are included to provide energy storage to operate loads during the night and during cloudy weather. The solar module(s) recharge the batteries when average or good weather returns.

On the other hand, direct connected systems get the job done without the need for batteries. Solar modules produce DC current that is immediately used by a DC motor load. As sunlight rises and falls, current and voltage rise and fall, and the motor speeds up and slows down proportionately. There is no storage, the motor does not operate at night, and operates slowly during cloudy or stormy weather. Solar water

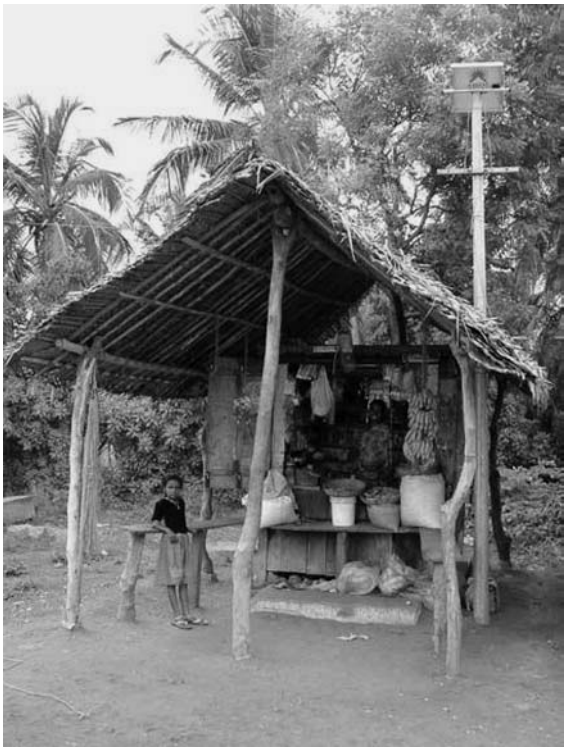

Figure 2.20 A small, road-side shop in Karnataka (Africa) uses a household solar power system. (Photo courtesy: UNEP/Riso).

pumps used in the Sahara are an example of this type of application. The importance of water pump systems, clearly, cannot be overestimated.[1)]

A number of national governments are developing financial incentives to encourage homeowners to place modules on their rooftops. Indeed, for most stand-alone applications, a PV system is the most cost-effective alternative for providing power. For example, tens of thousands of households today in Africa, Asia, Mexico, Central America and India, that is, in all those places that lack access to the electric grid, rely on solar-generated power. More recently, a $1.5 million United Nations programme has helped 16 600 Indians living in the southern state of Karnataka to buy solar power systems for their homes and small businesses. This has created a thriving market for household solar panels in India, and the project is being extended to Tunisia, China, Indonesia, Egypt, Mexico, Ghana, Morocco and Algeria [11].

1) Dominique Campana, a graduate student in Paris in the 1970s, came up with the idea of applying solar water pumping. French physicist Jean Roger translated her concept into a working prototype on the island of Corsica. After viewing the Corsican installation, Verspieren, starting in the late 1970s, initiated a solar water pumping program that has become the template for success in the developing world.

Overall, by 2007 more than 2.5 million households in developing countries were receiving electricity from solar home systems [12]. Most growth has been occurring in a few specific Asian countries (Bangladesh, China, India, Nepal, Sri Lanka and Thailand), where the affordability problem has been overcome either with micro-credit or by selling small systems for cash, and where government and international donor programs have supported markets. In each of these countries, monthly additions in the hundreds or thousands of new household installations have occurred in recent years. China has been by far the largest market, with over 400 000 systems added. In Bangladesh, there are now over 150 000 households with solar home systems, and 7000 are being added monthly. Outside Asia, other large markets include Kenya, Mexico, and Morocco.

The plans of a number of Latin American countries may shift solar home system growth toward that region if promising approaches to affordability, including government subsidies and/or fee-for-service models, continue to be followed. Along with growing solar electricity for rural schools, health clinics, and community buildings, solar street lighting is another growing application, with 55 000 solar streetlights now in India (Figure 2.21).

Africa, with its very low rural-electrification rates and low per capita income, has experienced slower growth in solar home systems, with the exception of a few countries. Still, there have been at least half a million systems installed in Africa. Kenya has 200 000 systems and continuing market growth, driven by cash sales of small modules to households in rural and peri-urban areas. South Africa has 150 000 systems, and smaller numbers exist in several other countries. Uganda has a 10-year program that targets solar home systems and other productive uses in small industry, education, and health care. Other countries like Mali, Senegal, and Tanzania are trying to provide limited subsidies for rural renewables like solar home systems. In Morocco, solar PV programs by the national utility and fee-for-service concessions

Figure 2.21 Street lighting installed in 2006 in the roads of Maharashtra, India, uses PV to power LED lamps at night. (Photo courtesy of Grameen Surya Bijlee Foundation, www.suryabijlee.com).

have achieved more than 37 000 systems in thousands of villages, with a program for another 80 000 systems under way and a target of 150 000 by 2010 as part of their rural electrification planning.

Instead ofrelying on costly and dangerous solutions to light their homes and power their appliances, such as kerosene lamps, automobile batteries and generators, these people now rely on clean solar power to obtain quality lighting and a reliable supply of electricity.

Similarly, effective marketing of PV in developing countries has been clearly demonstrated by the Punjab State (India) solar-powered pumping program for farmers, previously relying heavily on subsidies, that has been able to establish a market for PV devices where there was none before [13]. An ESCO (energy service company) providing an integrated energy service was key to this success: in exchange for a periodic payment from users, it installed the solar-powered pump, and trained users how to properly use and maintain it. As a result, 98% of the installed power was in place after one year and farmers switched to efficient crop irrigation growing high-value plantation crops instead of field crops.

During the 1990s silicon-based solar cells established a market as decentralized power sources and the market expanded at a 15–20% annual rate, with relevant economies of scale that were reflected in lower prices. In recent years, the main global market has become urban grid-connected modules, led by regions with solar-friendly policies like Japan, Germany, Spain and some US States. Those who elect to place solar cells on their roof can sell electricity to their local utility during the day when the sun is shining and buy it back at night when it is not; which explains the boom in the market in Europe, and particularly in Germany.

Grid-tied PV systems (Figure 2.22) wired into buildings connected to the utility grid are currently finding application all over the world. Energy produced by the PV system is used directly in the building, or if there is an excess, flows out through a meter, providing power to neighbors. In many nations, one receives a credit for this excess power, to be used later, at night for example, when power is drawn from the grid (Net Metering arrangement).

Overall, grid-connected solar photovoltaics is the fastest-growing power generation technology in the world, with 50% annual increases in cumulative installed capacity in both 2006 and 2007, to an estimated 7.8 GW by the end of 2007 (Figure 2.23).

This capacity translates into an estimated 1.5 million homes with rooftop solar PV feeding into the grid worldwide. Germany accounted for half the global market in 2006, with about of 850–1000 MW added. Grid-connected solar PV increased by about 300 MW in Japan, 100 MW in the United States, and 100 MW in Spain in 2006. The Spanish solar PV market grew the fastest of any country during 2007, in part due to new and revised policies, and an estimated 400 MW was added in 2007, a fourfold increase over 2006 additions.

Emerging strong growth in other European countries, especially Italy and Greece with the recent introductions of policies, is also changing the balance. France's recently revised feed-in policies are beginning to accelerate what had been slow growth. Italy looked set to install 20 MW in 2007 and France 15 MW, both double the

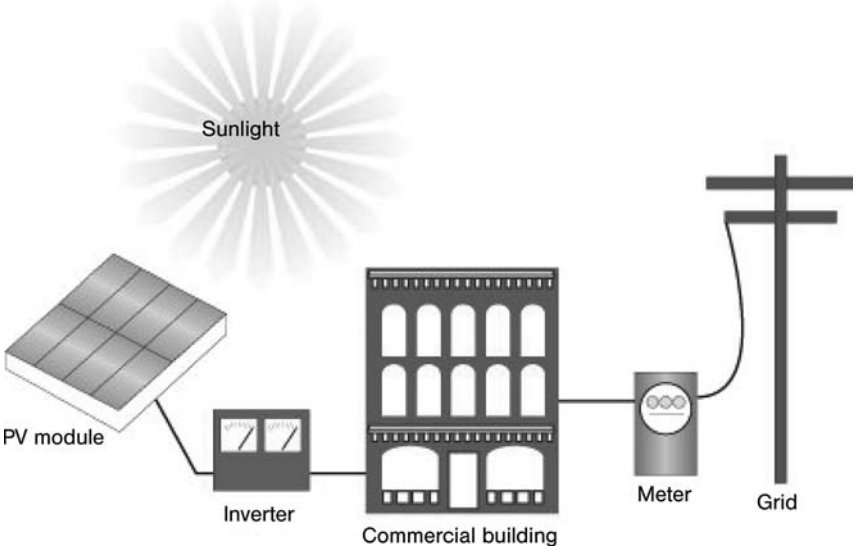

Figure 2.22 A grid-connected PV system generates usable AC current after passing through the inverter, is connected to the conventional electricity grid, offsets energy that would normally come in through the conventional grid with clean solar energy, and can send (and sell) power back to the grid if it is generating more than the home requires since the local power company accepts cogeneration. (Photo courtesy: Southface Energy Institute, USA).

2006 installation amounts. In the United States, California remains the clear leader, after capturing 70% of the US market in 2006. New Jersey is second, with other emerging markets in several southwestern and eastern states. Korea is also emerging as a strong market.

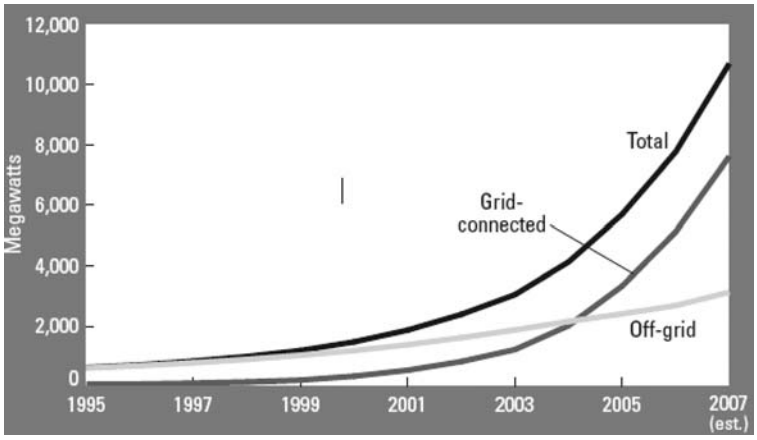

Figure 2.23 Solar PV, existing world capacity (1995–2007, source: Worldwatch Institute).

2.6
Brief History of Modern Photovoltaics

The story of photovoltaics, started in 1839 when Becquerel discovered the photovoltaic effect from a silver-coated platinum electrode immersed in an electrolyte irradiated with light, has been brilliantly told [14]. What is emphasized here is that a number of early thin film cells had already been developed in the 1930s, based on the Schottky barrier device, using a semitransparent metal layer deposited on top of selenium that provided the asymmetric junction.

At that time, scientists were interested in the photoconductive current which, being proportional to the frequency of the incident light, could function as a reliable photographic light meter.

As early as 1967, the first thin film CdS cell deposited on plastic was ready; while soon after a number of new photovoltaic materials were discovered, stimulated by theoretical work, including GaAs, InAs and CdTe, indicating that these materials would offer higher efficiency. The strategies for higher energy of multiple bandgap designs and tandem cells were also established at that time.

Adding to the surprise, the use of thin films that is nowadays changing the PV industry on a global scale was conceived by Chapin (co-discoverer of the silicon cell at ATT Bell Laboratories in 1953, Figure 2.24), at the very beginning of the modern solar PV.

Then, in the 1970s, scientists taking part in the US PV Research and Development Program developed thin films of crystalline Si and a whole range of new semiconductor materials (CIS, CdTe, InP, Zn_3P_2, Cu_2Se, WSe_2, GaAs, ZnSiAs), that is, almost all the alternative materials used by today's new PV industry, including polycrystalline and amorphous silicon, and organic semiconductors.

Finally, in the early 1980s, Barnett developed the polycrystalline silicon thin film cell; while Martin Green replaced the silicon serigraphy with a silicon solar cell with

Figure 2.24 Gerald Pearson, Daryl Chapin, and Calvin Fuller (left-to-right), the principle discoverers of the silicon solar cell at ATT Bell Labs in 1953. (Reproduced from Californiasolarcenter.org, with permission).

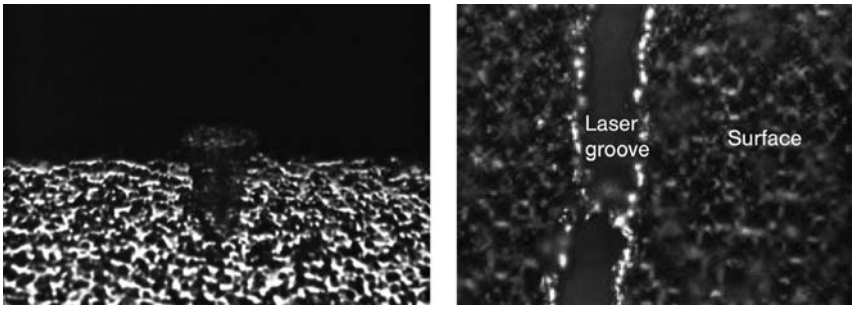

Figure 2.25 The buried contact is formed by using a laser to make a groove in the cell's surface and then filling it with copper. The enlarged cross-section shows the buried contact. It is a strip of copper imbedded in the silicon of the cell. (Photo courtesy: Center for Photovoltaic Devices and Systems, UNSW).

greater surface area to catch the sun's rays with tiny, laser-etched grooves in which the wires (contacts) that carry the electric current are buried, leading to 20% efficient cells (Figure 2.25).

In 1997 the first modules using a triple junction amorphous silicon cell were commercialized by Sharp and also in 2007 Sanyo achieved an efficiency of 22% at the research level with its HIT solar cells. The HIT (heterojunction with intrinsic thin layer) solar cell is composed of a single thin crystalline silicon wafer surrounded by ultra-thin amorphous silicon layers. The structure of the HIT cell enables an improvement in the overall output by reducing recombination loss by surrounding the energy generation layer of single thin crystalline silicon with high quality ultra-thin amorphous silicon layers. In the meanwhile, highly efficient GaAs cells were developed to power spacecraft that now, exploiting the recent discovery of the near perfect growth of GaAs crystals as well as quantum-well solar cells based on the same material, are likely to open the way to third generation solar cells (see Chapter 6).

References

1 Nelson, J. (2003) *The Physics of Solar Cell*, Imperial College Press, London.

2 The website of the University of New South Wales School of Photovoltaic Engineering: http://www.pv.unsw.edu.au.

3 Conibeer, G. (2007) Third-generation photovoltaics. *Materials Today*, **10**, 42.

4 Luque, A. and Hegedus, S. (eds) (2003) *Handbook of Photovoltaic Science and Engineering*, John Wiley & Sons, New York.

5 Landsberg, P.T. and Baruch, P. (1989) The thermodynamics of the conversion of radiation energy for photovoltaics. *Journal of Physics A-Mathematical and General*, **22**, 1911.

6 Green, M.A. (2005) *Third Generation Photovoltaics*, Springer, New York.

7 Hepp, A.F., Bailey, S.G. and Raffaelle, R.P. (2005) Inorganic Photovoltaic Materials and Devices: Past, Present and Future, in

Organic Photovoltaics. Mechanisms, Materials and Devices (eds S.S. Sun and N.S. Sariciftici), Taylor and Francis.

8 Shockley, W. and Queisser, H.J. (1961) Detailed balance limit of efficiency of p-n junction solar cells. *Journal of Applied Physics*, **32**, 510.

9 Uni-solar, *Technical Report*, October 2006. Freely available at: http://www.uni-solar.com/uploadedFiles/AA53606-02Technical%20Report120706small.pdf.

10 Anderson, D. (2001) *Clean Electricity from Photovoltaics* (eds M.D. Archer and R.D. Hill), Imperial College Press, London.

11 Brahic, C. Affordable solar power brings light to India, *NewScientist.com*, 29 April 2007, http://environment.newscientist.com/article/dn11740-affordable-solar-power-brings-light-to-india.html.

12 REN21. (2008) "Renewables 2007 Global Status Report" (Paris: REN21 Secretariat and Washington, DC: Worldwatch Institute).

13 Hegde, G. and Nayer, C.V. (2007) Marketing Photovoltaic Technologies in Developing Countries, in *Renewable Resources and Renewable Energy – A Global Challenge* (eds M. Graziani and P. Fornasiero), CRC Press/Taylor & Francis Group, Boca Raton FL.

14 Perlin, J. (1999) *From Space to Earth – The Story of Solar Electricity*, aatec Publications, Ann Arbor MI.

3
Inorganic Thin Films

3.1
Thin Film PV: Technology for the Future

Customers buying photovoltaic modules are interested in high energy yields per purchased watt peak-power over a certain time period of a PV system in true outdoor conditions. This is especially relevant in countries where there are high feed-in tariffs per kWh produced available, such as Germany or Spain.

Modules are usually sold with their peak power performance (Wp) tested under laboratory conditions (STC): that is, under a very high and direct irradiation ($1000\,W\,m^{-2}$), module temperature of 25 °C, and only one type of solar spectrum (AM1.5: mainly direct irradiation).

Under real outdoor conditions, this peak power is seldom achieved, since module temperature is usually more in the range of 40–60 °C under illumination (especially true for modules that are building integrated), the hours of $1000\,W\,m^{-2}$ irradiation is only about 1% of the total sun-hours and the spectral and specular content of the solar spectrum change continuously with varying climatic conditions. Diffuse light for instance dominates when the sky is clouded or during mornings and evenings. In Northern and Central Europe, the majority of solar irradiation comes from diffuse light (more than 50% of all solar irradiation) and even in Madrid the diffuse part is still 33%.

In order therefore to predict what will be the energy output of a PV module or a PV system with a certain nominal power, it is necessary to evaluate the behavior of the modules under various climatic conditions [1].

Thin film (TF) PV modules consistently outperform conventional silicon-based panels in this crucial aspect. Moreover, since the cost per unit power output largely determines the competitiveness of a PV panel, thin films will dominate the future of photovoltaics as they have the greatest potential for low cost production.

Worldwide, silicon-based PV technologies continue to dominate at more than 94% of the market share, with the share of TFPV at less than 6% in 2007. However, this is expected to grow to 20% by 2010 and beyond 30% in the long term [2].

Flexible Solar Cells. M. Pagliaro, G. Palmisano, and R. Ciriminna

ISBN: 978-3-527-32375-3

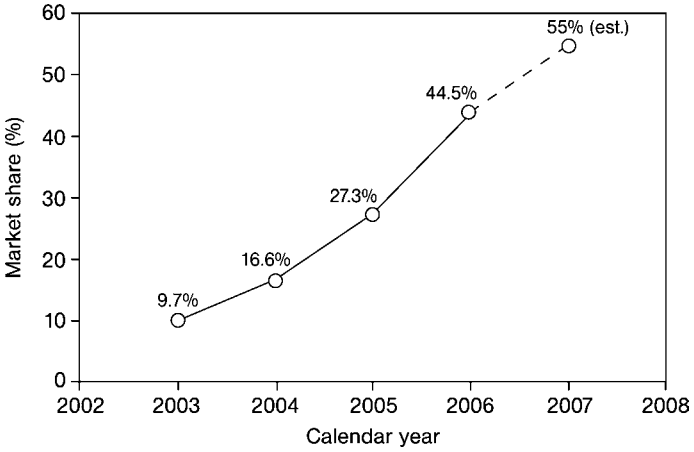

Figure 3.1 Evolution of thin film PV market share in the US. (Reproduced from Ref. [3], with permission).

For example, the market share for TFPV in the United States has grown rapidly over the past several years and in 2007, the TFPV market share is expected to surpass that of Si technology in the US (Figure 3.1).

Compared to traditional wafer-based crystalline silicon technologies, thin film technologies yield products of comparable performance but with significant advantages in manufacturing:

- Lower consumption of direct and indirect materials.
- Independence from shortages of silicon supplies.
- Fewer and automated processing steps.
- Integrated, monolithic circuit design – no assembly of individual solar cells into final products.

These advantages will translate into substantially reduced cost of product manufacture. As shown in Figure 3.2, the complete traditional process involves more than two dozen separate steps to prepare and process silicon ingots, wafers, cells, and circuit assemblies before a module is complete. Thin film module production, on the other hand, requires only half as many process steps as crystalline silicon with simplified materials handling.

Thin film PV circuits require deposition of three layers: a base electrode layer, a semiconductor layer, and a transparent conductor window layer. Three patterning steps, one after each of the three layers, create the integrated series connection from cell to cell on the circuit. Lastly, a front cover glass is simply laminated to the circuit glass for final module assembly (Figure 3.3).

A key force driving the advancement of thin film technologies has been a polysilicon shortage that began in 2004. In 2006, for the first time, more than half of polysilicon production went into PV instead of computer chips. Polysilicon supply is expected to match demand by 2010, but not before thin TFPV grabs 20% of the

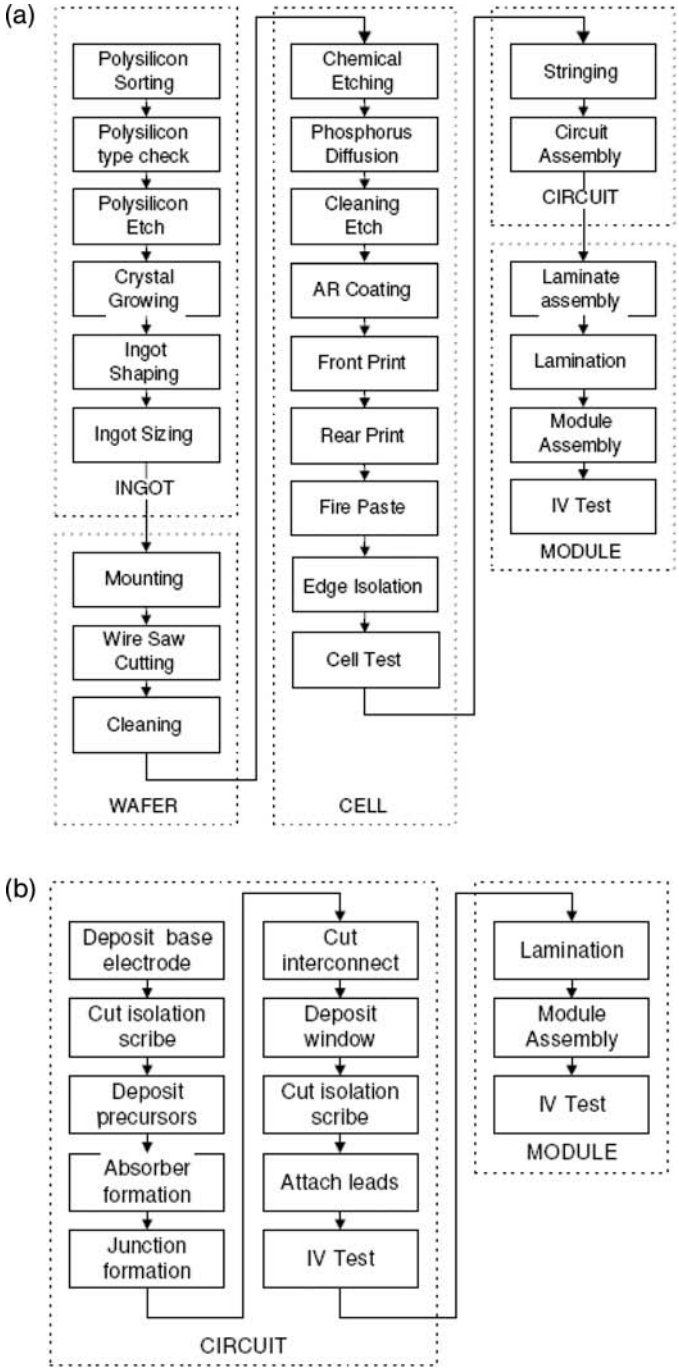

Figure 3.2 Process sequence for manufacturing crystalline silicon modules (a) and process sequence for manufacturing thin film modules (b). (Reproduced from Ref. [4], with permission).

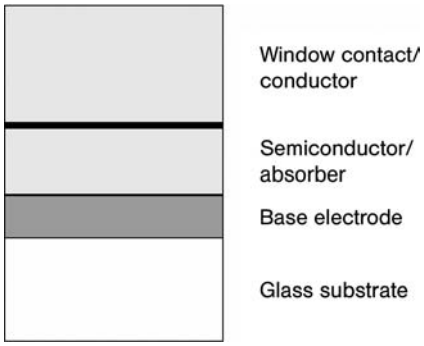

Figure 3.3 Common elements of most thin film photovoltaic cells.

market. With increasing polysilicon supplies, in turn, average PV prices are projected to drop to $2 per watt in 2010.

Worldwide estimated projections for 2010 are that thin film PV production capacity will be more than 3700 MW, with production capacity estimated at 1127 MW in the US, 1312 MW in Japan, 793 MW in Europe and 472 MW in Asia (Table 3.1).

In general, TFPV is expected to account for 35% of the photovoltaics market by 2015, at $7.2 billion compared to just over $1.0 billion today [5]. Of this, the value of printed TFPV is expected to reach over $3.0 billion as printing PV has the potential for lowering capital costs by as much as 75%, reducing waste and increasing throughput.

The market is being driven by the inherent advantages of TFPV including low cost, low weight, and the ability to manufacture them on flexible substrates and embed solar power capabilities into walls, roofs and even windows that double as PV panels. The fact that TFPV is much lighter than conventional PV means that it can be added to a roof without the need to reinforce the roof.

The US company Solar Integrated manufactures laminated PV coating made of thin film amorphous Si cells integrated into heavy-duty fabrics. The result is a fused fabric and flexible solar panel product weighing just 3.66 kg m^{-2} that can literally be rolled on for fast installation to virtually any flat surface.

Similarly, the Swiss company Flexcell manufactures flexible a-Si-based modules that are elegantly integrated into buildings. The installation starts with the existing roof top surface and adds rigid insulation and gypsum board that provides resistance against punctures and fire, topping the roof with a durable white finish (Figure 3.4). These three components provide customers with an energy efficient, weather-tight roof that significantly improves the thermal performance of the roof and reduces energy consumption by lowering the rooftop temperatures. This is accomplished by reflecting solar radiance rather than absorbing it, a feature that actually improves the productivity of the photovoltaic cells once they are added.

The company, which trades on the London Stock Exchange, actually tripled its production from 8.5 MW in 2007 to 24 MW in 2008, with revenues going from 38 million $ in 2006 to 145 million by the end of 2008.

Table 3.1 Thin film PV capacity (2007–2010).

	Group	Material	Present (MW)	Additional (MW)	Total (MW)	Group	Material	Present (MW)	Additional (MW)	Total (MW)	Totals	Grand Total
USA	First Solar	CdTe	90	–	90	Nanosolar	CIS	–	430	430	1127	3704
	Uni-Solar	a-Si	60	240	300	AVA Solar	CdTe	3	20	3		
	MiaSole	CIS	5	50	55	Nano PV	a-Si	–	4	4		
	Global Solar	CIS	3	60	63	OptiSolar	a-Si	–	40	40		
	EPV	a-Si	2	25	27	Primestar Solar	CdTe	–	20	20		
	Daystar Technologies	CIS	1	10	11	SoloPower	CIS	–	20	20		
	Power Film	a-Si	1	10	11	ISET	CIS	–	3	3		
	Ascent Solar	CIS	2	25	27	MWDE Solar	a-Si	–	3	3		
						Heliovolt	CIS	–	20	20		
JAPAN	Kaneka	a-Si	20	50	70	MH1	a-Si	14	56	70	1312	
	Showa Shell	CIS	20	60	80	Kanto Sanyo	a-Si	7	–	7		
	Sharp	a-Si	15	1000	15	Honda	CIS	3	27	30		
	Fuji	a-Si	15	25	40							
EUROPE	First Solar	CdTe	120	100	120	AMI	a-Si	–	160	160	793	
	CSG Solar	Thin-Si	10	15	25	Johanna Solar Tech	CIS	–	30	30		
	Wurth Solar	CIS	3	15	18	Brilliant	a-Si	–	25	25		
	Antec Solar	CdTe	10	–	10	Solisbro	CIS	–	30	30		
	Schott Solar	a-Si	3	27	30	Global Solar	CIS	–	30	30		
	ICP Solar Tech	a-Si	3	–	3	Helio Grid	a-Si	–	50	50		
	Solar Cells	a-Si	1	–	1	SunFilm	a-Si	–	60	60		
	Free Energy	a-Si	1	–	1	T.J. Solar	a-Si	–	40	40		
	Solar Plus	a-Si	–	5	5	Signet Solar	a-Si	–	20	20		
	Sulfur Cells	CIS	5	–	5	Clyxco	CdTe	–	25	25		
	Aleo Solar	CIS	–	30	30	Avancis	CIS	–	20	20		
	Ersol	a-Si	–	40	40	Odersun	CIS	–	5	5		
						Scheuten Solar	CIS	–	10	10		
ASIA	First Solar	CdTe	–	220	220	GET	a-Si	–	40	40	472	
	Bangkok Solar	a-Si	7	–	7	Nanowin Tech	a-Si	–	35	35		
	Sinonar	a-Si	3	–	3	Mosen Baer	a-Si	–	20	20		
	T.J. Solar Cell	a-Si	2	–	2	Solar Morph	a-Si	–	20	20		
	Soltech	a-Si	15	–	15	Topray Solar	a-Si	20	–	20		
	Suntech Power	a-Si	–	50	50	CMC	a-Si	–	40	40		

(Reproduced from Ref. [3], with permission).

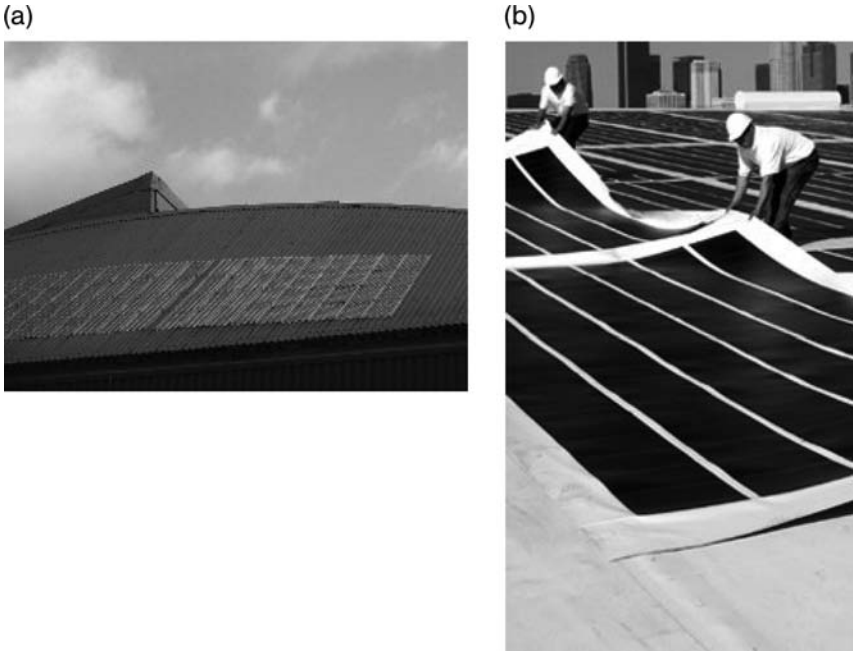

Figure 3.4 Flexible PV modules made with a-Si are produced in Europe (a) and in the US (b). Light weight, ease of installation and low cost are causing rapid market success. (Photo courtesy: Solar Integrated and Flexcell).

The stock graph for one company (First Solar) shows the immense interest in the market for TFPV (Figure 3.5). As a result of this general trend, most manufacturers are ramping up production capacity and several – including First Solar, Fuji Electric, Nanosolar, Sanyo, Uni-Solar and G24i – are building plants with more than 100 MW capacity.

Investors and industry players agree in recognizing that PV is entering a phase of commoditization. But unlike any other mature commodity industry, it will not consolidate into a single winning "technology" based on lowest cost, as different customers will demand different products.

Ultimately, competitive advantages in the market will be determined by a combination of cost structure and product attributes that locally drive the customer's choice. In other words, the new PV industry will exhibit multiple commodity categories with suppliers exploiting diversified product designs for different applications (Figure 3.6) [6].

Whatever the technology of choice, however, to retain the economic advantages of TFPV, manufacturing progress needs to achieve moisture barrier levels of 10^{-6} g m^{-2} per day or better (Figure 3.7).

Figure 3.5 This stock graph reporting the 2007 and early 2008 performance for a thin film CdTe manufacturer, shows that thin film solar is an explosive technology. (Image courtesy: Edgar Online).

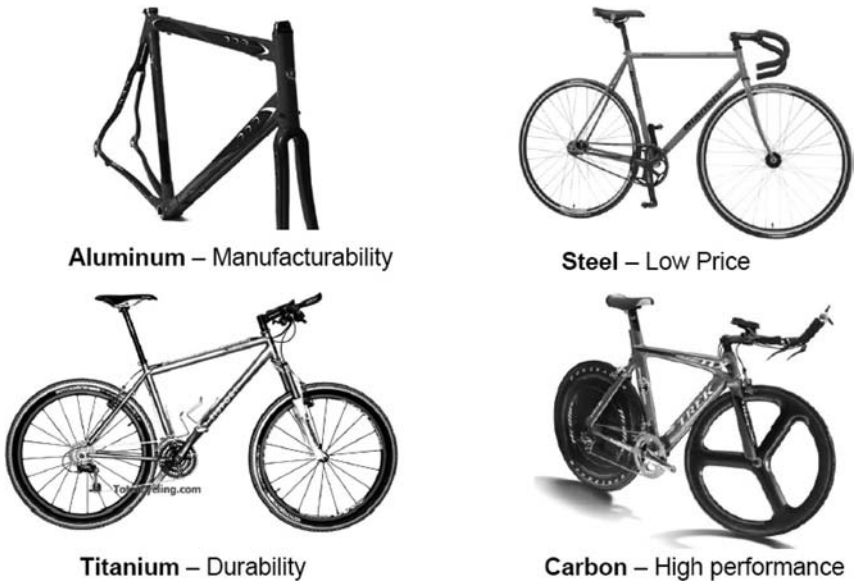

Figure 3.6 Just as different bicycle materials serve different needs, commoditization of PV will lead to a similar variety in the technology offered. (Reproduced from Ref. [6], with permission).

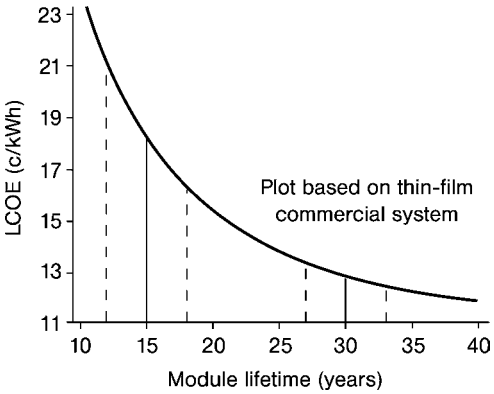

Figure 3.7 Lifetimes of thin film module. Nearly all benefits of flexibility will be negated unless a lifetime greater than 20 years is achieved. (Source: DOE, US).

3.2
Amorphous Si Thin Films

Wafer-based crystalline silicon has dominated the photovoltaic industry since the dawn of the solar PV era. It is widely available, has a convincing track record in reliability and its physical characteristics are well understood. The price of the technology has decreased by 20% for each doubling of cumulative installed capacity due to a cycle of policy-driven demand creation, capital investment, and production growth (Figure 3.8).

Wafers are increasingly becoming thinner and larger. For example, they have decreased in thickness from 400 μm in 1990 to 200 μm in 2006 and have increased in area from 100 to 240 cm^2; modules have increased in efficiency from about 10% in 1990 to typically 15.5% today.

Amorphous silicon (a-Si) alloy thin film technology offers an interesting opportunity to reduce the materials cost of the solar cells. Because a-Si alloy absorbs light more efficiently than its crystalline counterpart, the a-Si solar cell thickness can be up to 300 times less than that of conventional cells, thereby significantly reducing materials cost. A significant step in this development was the introduction in 1997 of the triple junction modules that provide relatively high levels of efficiency and stability (stabilized aperture area cell efficiency of 8.0–8.5%) [7].

In a triple junction cell (Figure 3.9) cells of different bandgaps are stacked together. The top cell, which captures the blue photons, uses a-Si alloy with an optical gap of ∼1.8 eV for the intrinsic (i) layer. The i layer for the middle cell is an amorphous silicongermanium (a-SiGe) alloy with about 10–15% Ge and optical gap of ∼1.6 eV, which is ideally suited for absorbing the green photons. The bottom cell captures the red and infrared photons and uses an i layer of a-SiGe alloy with about 40–50% Ge, corresponding to an optical gap of ∼1.4 eV.

Light that is not absorbed in the cells gets reflected from the aluminum/zinc oxide (Al/ZnO) back reflector, which is usually textured to facilitate light trapping.

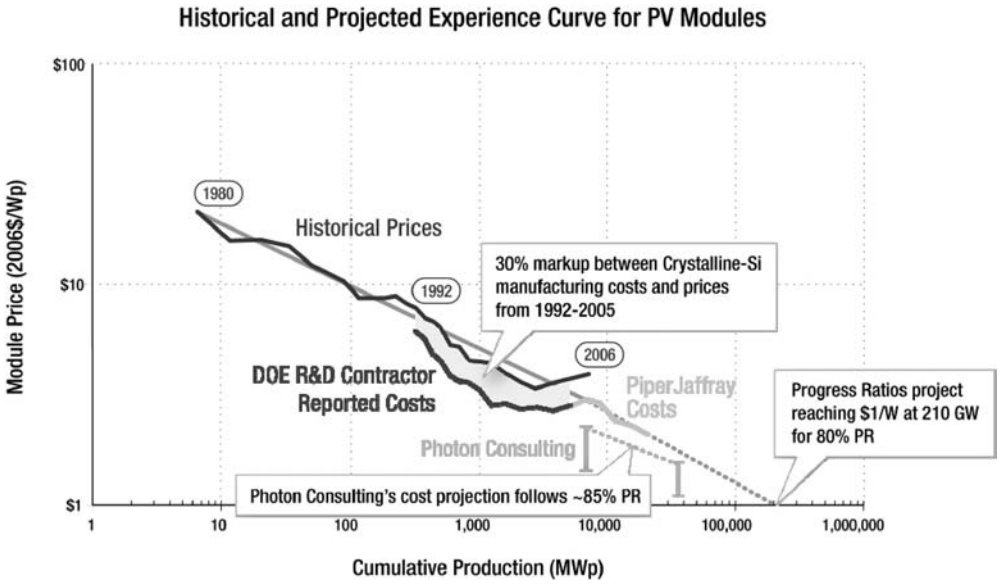

Figure 3.8 The PV industry is approaching grid parity across OECD, due to a cycle of policy-driven demand creation, capital investment, and production growth. (Reproduced from Ref. [6], with permission).

The resulting thin film photovoltaic product has the ability to capture a greater percentage of the incident light energy which is one of the keys to higher efficiencies and higher energy output, especially at lower irradiation levels and under diffused light.

The cell is deposited using a vapor deposition process at low temperatures; the energy payback time is therefore much smaller than that for the conventional

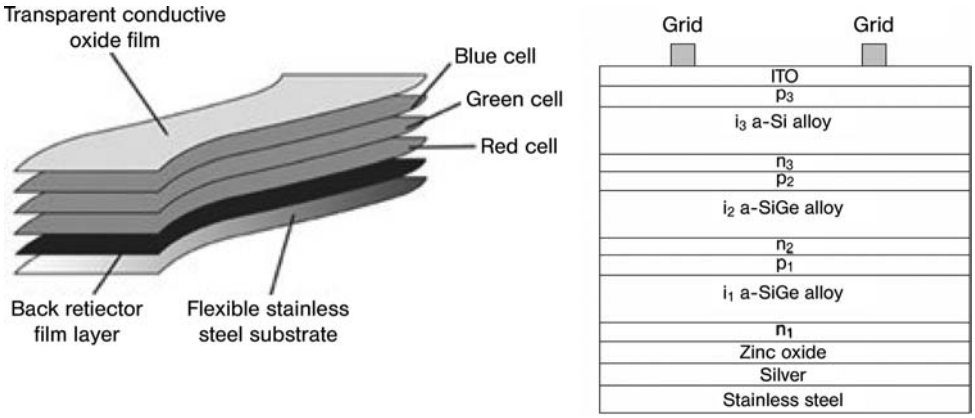

Figure 3.9 Amorphous silicon schematic of a triple-junction structure. (Reproduced from Uni-solar.com, with permission).

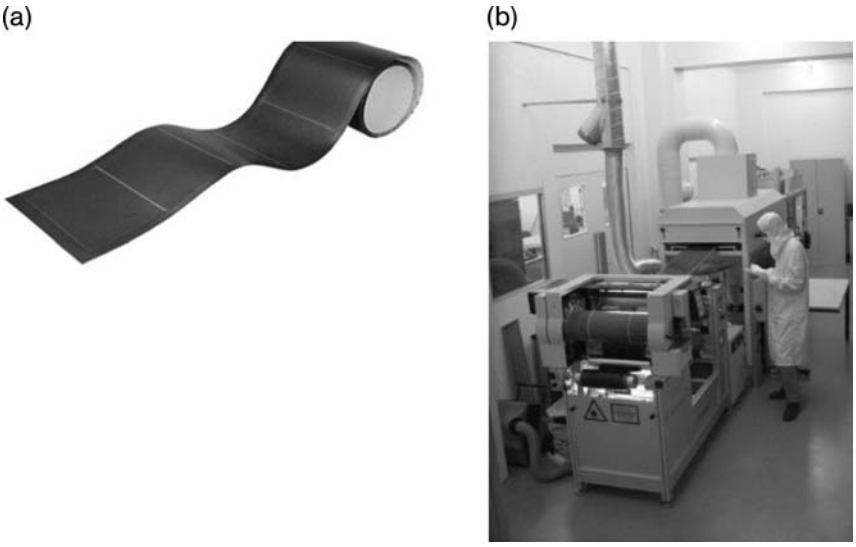

Figure 3.10 United Solar Ovonic flexible PV laminate is made of a-Si triple deposited over steel (a) while thin films of Flexcell are roll-to-roll deposited over plastic substrates (b). (Reproduced from www.uni-solar.com and www.flexcell.ch, with permission).

technology. The roll-to-roll process utilizes a flexible, stainless steel substrate (Figure 3.10).

Once the solar cell material has been provided with suitable electrodes, the cells are encapsulated in UV-stabilized, weather-defying polymers. This laminating process incorporates a fluoropolymer on the top side. The bottom side of the finished product is a polyester material suitable for adhesives. The inherent flexibility of the resulting laminate as well as the durable encapsulate, results in a lightweight, photovoltaic module that has a broad range of applications ranging from battery charging to large-scale grid-connected systems.

In a high-volume manufacturing plant in Michigan (USA) solar cells are deposited on rolls of stainless steel that are a mile-and-a half long using automated manufacturing machines. Rolls of stainless steel, 2500 m long, 36 cm wide, and 125 μm thick, move in a continuous manner through four machines to complete the solar cell fabrication. The four machines are the wash machine that washes the web one roll at a time; a back reflector machine that deposits the back reflector by sputtering Al and ZnO onto the washed rolls; an amorphous silicon alloy processor that deposits the layers of a-Si and a-SiGe alloy; and, finally, an anti-reflection coating machine that deposits indium tin oxide (ITO) on top of the rolls. The coated web is next processed to make a variety of lightweight, flexible and rugged products.

Flexcell, in Switzerland, uses a four-step roll-to-roll manufacturing process in which metal coating of a plastic roll (thickness 50 μm) is followed by chemical vapor

deposition of a-Si layers and TCO through layer structuring and module encapsulation with plastic foils (Figure 3.10).

Under actual environmental conditions, the triple-junction, amorphous silicon technology shows consistent performance over time. The results of prolonged, independent testing verify indeed less than 1% degradation, approximately the same as for crystalline silicon PV panels (Figure 3.11).

Hence, whereas the thermal coefficient for crystalline photovoltaic cells is a negative constant of approximately −0.5% per °C, the thermal coefficient for triple-junction photovoltaic cells is −0.21% per °C. This means that at a normal cell temperature of 60 °C, the relative power output of a crystalline module would be reduced by about 17% from the STC rating while the triple junction module output would be reduced by about 4–6%. The effect of this characteristic is a higher level of energy output at normal to high cell temperatures.

For example, comparison of amorphous and monocrystalline silicon-based PV modules connected to the residential grid in Thailand clearly shows that the amorphous modules outperform the crystalline module by about 15% in terms of annual final yield and average performance ratio (Figure 3.12) [8].

Such performance enhancement is due to better performance in the hot season, and under diffuse light conditions that are typical of Thailand's rainy season. Similarly, in Japan single junction a-Si modules of another large manufacturer (Kaneka) yield a larger annual output than either poly- or mono-crystalline silicon panels.

Adding relevance to the technology, in Northern and Central European climates, where low light conditions and diffuse light prevails, this enhanced low light sensitivity results in higher yearly energy output when normalised to Wp purchased power. Triple junction PV modules, in fact, perform more than 40% better in low light conditions (50–100 $W\,m^{-2}$), than most current crystalline technologies.

Whereas for all c-Si modules and other thin film technologies the outdoor efficiency rapidly decreases below 300 $W\,m^{-2}$, the efficiency of triple-junction modules shows a constant increase up to values as low as 50 $W\,m^{-2}$. The outdoor efficiency at 100 $W\,m^{-2}$ is more than 25% higher than the STC efficiency.

The world's leading companies in the a-Si TFPV field are undergoing rapid expansion from an annual production capacity of about 30 MW to 300 MW by 2010, to apply this technology as widely as possible and drive the expansion of its market share, applying its products to free-land, roof and building-façade applications.

For the triple-junction technology, the power conversion efficiency level of 12% is currently the world's highest, and such highly efficient cells have been commercialized since 2001 by Kaneka.

An interlayer ensures efficient light trapping and thus a 19% increase in short circuit current in the thin film Si stacked module. An initial aperture efficiency of 13.1% has been achieved for this module (Figure 3.13) that under stabilized efficiency reduces to 12% [9] .

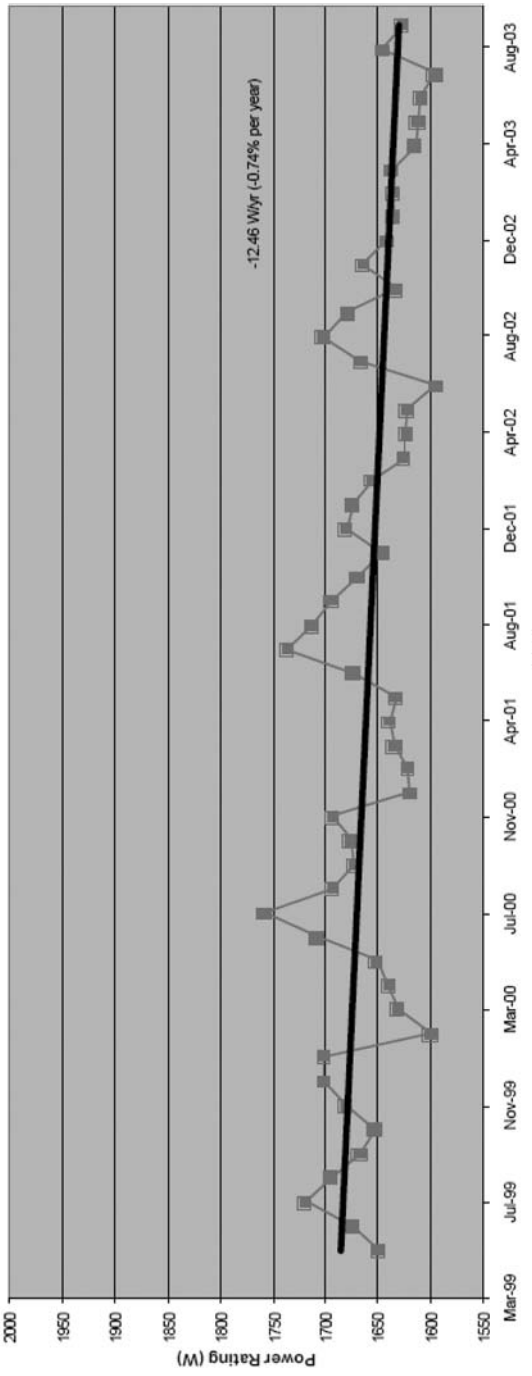

Figure 3.11 Uni-solar modules based on triple junction cells have stable efficiency with an average degradation not higher than 0.74%. (Reproduced from Ref. [1], with permission).

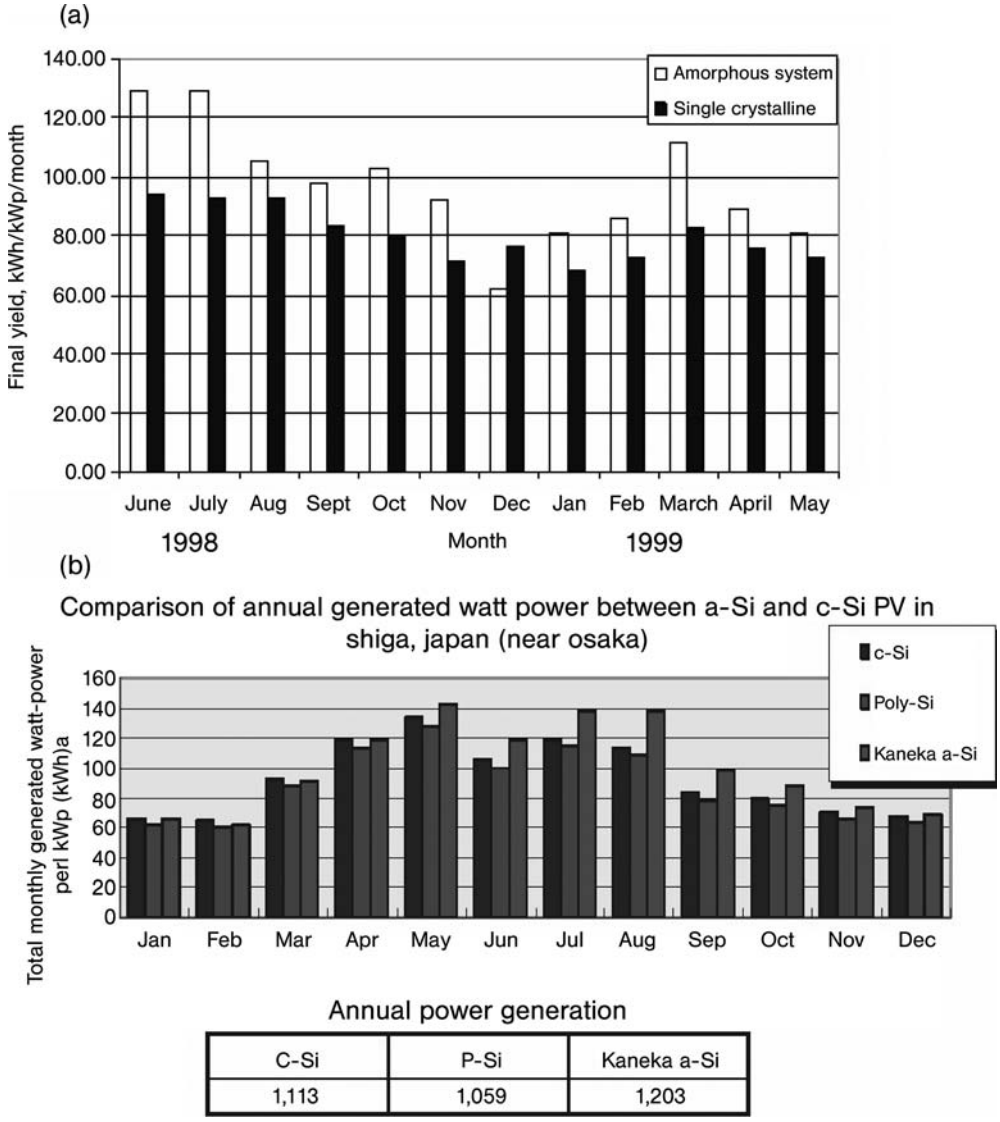

C-Si	P-Si	Kaneka a-Si
1,113	1,059	1,203

Figure 3.12 Monthly final yield trends over a year for a-Si and c-Si modules in Thailand (a) and in Japan (b), clearly show that a-Si modules consistently yield more energy. (Reproduced from Ref. [8], with permission).

3.3
CIGS Thin Films on Metal Foil

From the very beginning of research in the mid 1970s, copper indium gallium diselenide (CIGS) moved to the forefront of thin film materials with respect to solar

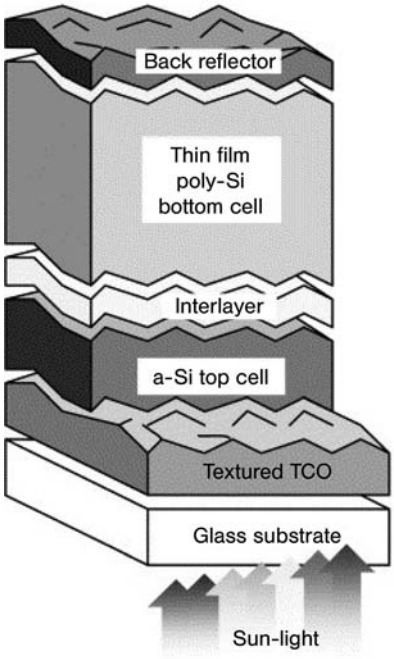

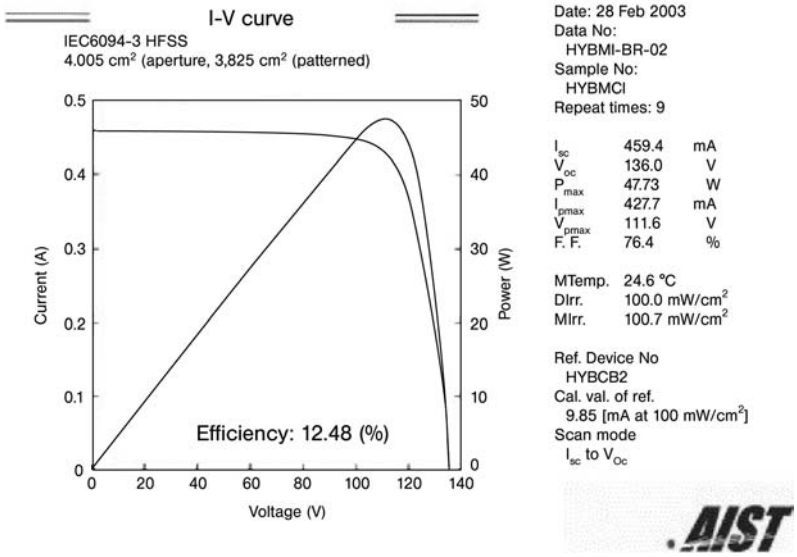

Figure 3.13 The performance of a HYBRID module confirmed by AIST. (Reproduced from Ref. [9], with permission).

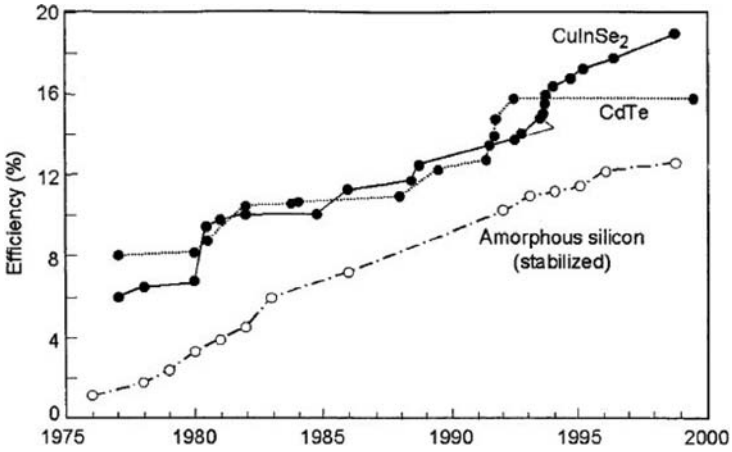

Figure 3.14 Efficiency evolution for different TFPV technologies. (Reproduced from Ref. [13], with permission).

cell efficiencies (Figure 3.14). Indeed, thin film solar cells based on CdTe and Cu(In,Ga)Se_2 show the highest performance among thin film solar cells in terms of efficiency and on the module level. CIGS solar cells and modules have achieved 19.5 and 13% efficiencies, respectively. Likewise, CdTe cells and modules have reached 16.5 and 10.2% efficiencies, respectively [10].

The CIGS thin film belongs to the Cu-chalcopyrite compounds whose bandgap can be modified by varying the Group III cations among In, Ga, and Al and the anions between Se and S [11]. A wide range of bandgaps can be obtained using combinations of different compositions, and since the bandgap range of interest for this technology is between 1 and 1.7 eV, CIGS-based solar cells offer the required versatility.

With 19.5% efficiency under standard test conditions at laboratory scale, the best CIGS cell is about as efficient as the best polycrystalline-silicon cell. Table 3.2 compares the efficiency and power of different commercial-sized CIGS, CIGSS, and CdTe modules and shows that the performance of the CIGS and CdTe modules are now approaching that of polycrystalline silicon PV.

Table 3.2 Polycrystalline thin film PV modules.

Company	Device	Aperture area (cm^2)	Efficiency (%)	Power (W)	Date
Global Solar	CIGS	8390	10.2	88.9	05/05
Shell Solar	CIGSS	7376	11.7	86.1	10/05
Würth Solar	CIGS	6500	13.0	84.6	06/04
First Solar	CdTe	6623	10.2	67.5	02/04
Shell Solar GmbH	CIGSS	4938	13.1	64.8	05/03
Antec Solar	CdTe	6633	7.3	52.3	06/04
Shell Solar	CIGSS	3626	12.8	46.5	03/03
Showa Shell	CIGS	3600	12.8	44.15	05/03

(Reproduced from Ref. [10], with permission).

Companies that seek to produce CIGS modules commercially initially aim for the 12–15% range as a target that optimally trades off cost and performance. In this range, CIGS modules are still as efficient as the bulk of the silicon modules on the market today. For comparison, the best alternative thin film module on the market today, Unisolar's, is 6.2–6.4% efficient, so CIGS modules are essentially twice as efficient.

Furthermore, as there is no intrinsic mechanism that damages cell performance, these modules are extremely stable and are delivered to customers with a 25-year warranty. In fact, cells often improve during actual operation as a self-healing mechanism due to defect relaxation with the help of mobile copper actually leads to performance enhancement with time [12].

CIGS thin film modules are available also on a flexible substrate, manufactured by Global Solar Energy in the US.

Monolithic integration of thin film solar cells leads to significant manufacturing cost reduction compared to crystalline Si technology and, since the CdTe and CIGS modules share common structural elements and similar manufacturing cost per unit area, the module efficiency will eventually be the discriminating factor that determines the cost per watt.

In fact, these two thin film technologies have a common device/module structure: substrate, base electrode, absorber, junction layer, top electrode, patterning steps for monolithic integration, as shown in Figure 3.15 where cross sections of scanning electron micrographs provide true physical perspectives of the structures.

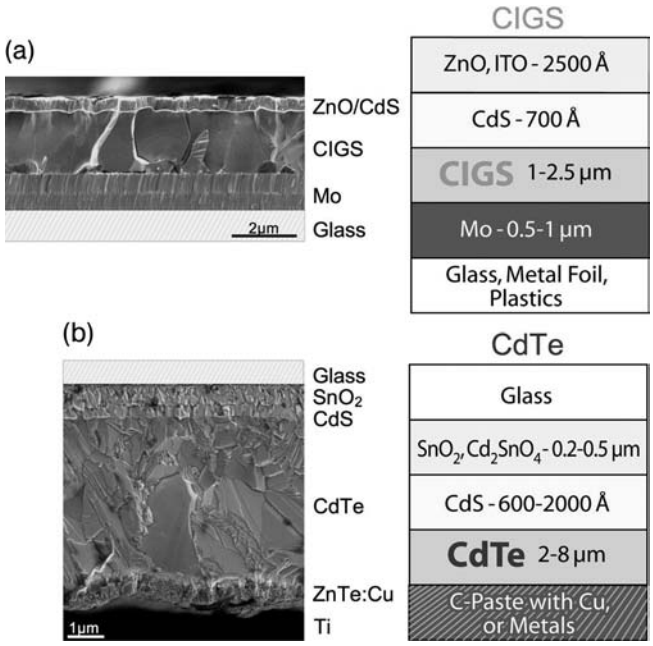

Figure 3.15 (a) CIGS and (b) CdTe device structures. (Reproduced from Ref. [1], with permission).

Figure 3.16 Nanosolar's nanostructure CIGS ink. (Photo courtesy: Nanosolar).

As early as 2000 a comprehensive report [13] on CIGS thin film solar cells concluded that the obstacles to large-scale production and commercialization of Cu(In,Ga)Se_2-based modules were "the complexity of the material and the manufacturing processes;" and that it was important to further improve performance "by increasing the bandgap to achieve individual cells with high voltage."

This is exactly what the company, Nanosolar, which delivered at the end of 2007 the first CIGS-based batch of panels product has done [14]. Its major advance has been the development of a nanostructured CIGS ink that makes it possible to simply print the semiconductor of a high-performance solar cell (Figure 3.16).

Clearly, to fabricate low-cost CIGS PV modules, it is desirable to reduce the amount of materials used and, in particular, to reduce the use of In, which is a relatively less abundant and more expensive element. The high absorption coefficient of $10^5\ cm^{-1}$ for light energy greater than the bandgap ensures that all the light is absorbed in a film that is less than 1 μm thick.

Printed CIGS technology based on semiconductor ink approaches was developed in the mid-1990s as only fast printing-on-roll technology can ensure the high 1 module per minute productivity of a manufacturing facility designed to produce 10 MW of photovoltaics in a year.

At that time, the state of the art process yielded the highest efficiency CIGS modules (over 12%) made by ink methods [15]. Not surprisingly, therefore, Nanosolar acquired the complete IP assets of Unisun Corporation, a pioneer in printing CIGS with the earliest filing date of any printed-CIGS patent.

This new ink is made of a homogeneous mix of CIGS nanoparticles stabilized by an organic dispersion. Chemical stability ensures that the atomic ratios of the four elements are retained when the ink is printed, even across large areas of deposition. This is crucial for delivering a semiconductor of high electronic quality and contrasts with vacuum deposition processes where, due to the four-element nature of CIGS, one effectively has to "atomically" synchronize various materials sources.

Rolls that are meters wide and miles long are thus processed efficiently with very high throughput (Figure 3.17). A key advantage of roll-to-roll processing over processing wafers or glass plates is that, after the first few meters of initializing a new roll, the whole process hits a steady state which can then be maintained for the entire rest of the roll, resulting in a very uniform deposition process applied to essentially the entire foil substrate.

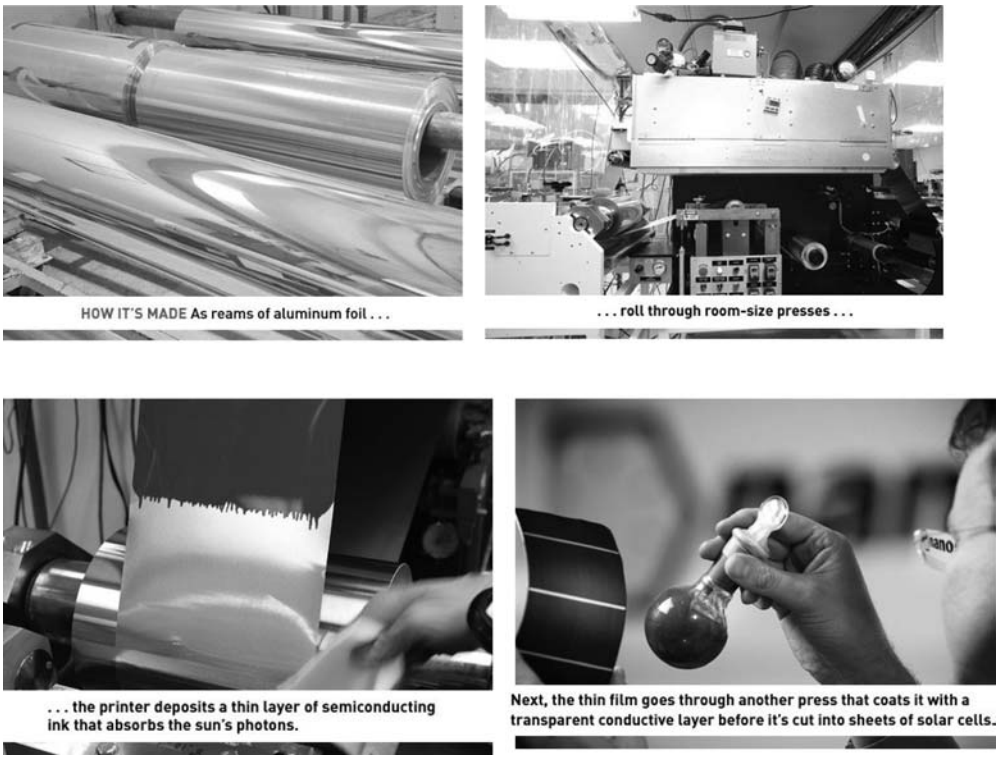

Figure 3.17 Roll-to-roll production of CIGS-based solar cells. (Photo courtesy of PopSci.com).

Wafers or glass plates, on the other hand, have to be moved in and out of each process station individually, introducing undesirable variability in the process and consequent quality problems (and thus cost).

Solar modules are thus produced with printing-press-style machines that set down a layer of solar-absorbing nano-ink onto metal sheets as thin as aluminum foil (Figure 3.18).

An aluminum base layer (A) supports the first molybdenum electrode (B). Light hitting the CIGS semiconductor (C) induces the photoelectron effect The p/n junction layer of CdS (D) passes the electrons to the transparent zinc oxide electrode (E, the window material) through which electrons reach the powering circuit before coming back to the first electrode.

The company is currently building the world's largest CIGS-based solar cell factory in California. In fact, another fundamental reason for the reduced cost of solar electricity resides in the capability of delivering high-power solar panels with 5–10 times higher current than other thin film solar panels on the market today, thus dramatically reducing the balance-of-system cost involved in deploying solar electricity systems.

HOW IT WORKS A solar cell is basically a sandwich of semiconductor—which converts the sun's photons to electrons—surrounded by layers of electrodes. In Nanosolar's PowerSheet, an aluminum base layer [A] supports the first of these electrodes, a coating of molybdenum [B]. Light hits the semiconductor [C], kicking electrons loose. The P/N junction layer [D] passes the electrons onto the clear zinc oxide electrode [E], which sends them off to power your Xbox before they come back to the first electrode, completing the circuit. Nanosolar created the perfect recipe for the semiconducting ink, a mix of copper, indium, gallium and selenium nanoparticles that, when printed, self-assemble onto the foil in a uniform layer that is one hundredth the thickness of the absorber layer in traditional cells.

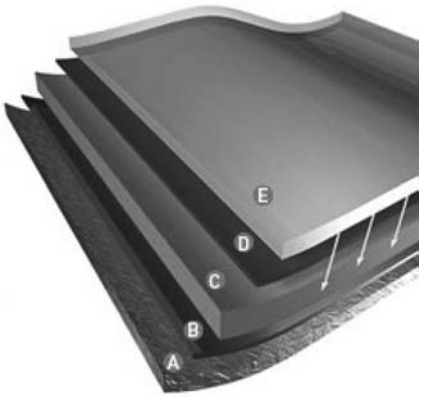

Figure 3.18 The PowerSheet solar cell is a sandwich of semiconductor surrounded by electrodes. (Photo courtesy of Nanosolar).

The amount of current that a panel can support is important because current capacity limitations negatively impact balance-of-system cost and thus power economics.

The aluminum foil substrate is both low cost and highly conductive (more than 20 times higher than the conductivity of the stainless steel), and thus enables major cost

reduction on the solar cell's thin film bottom electrode, by avoiding the need to deposit separately an expensive bottom electrode layer (as required for a non-conductive substrate such as glass). Furthermore, the metal foil allows assembly of cells by individually matched electrical characteristics.

3.4 CdTe Thin Films

The energy bandgap of CdTe, at 1.45 eV is a good match to the solar spectrum and thus it enables conversion of more energy from the solar spectrum than the lower energy bandgap silicon (1.20 eV) used historically. As a result, CdTe is capable of converting solar energy into electricity at an efficiency rate comparable to silicon-based technologies with about 1% of the semiconductor material requirement.

In the real solar cell device (Figure 3.19), this bandgap may vary somewhat as a result of its interaction with the CdS (~2.4 eV bandgap) heterojunction partner during processing [16]. CdTe/CdS PV modules appear to be more environmentally friendly than all other current uses of Cd. First, both cadmium and tellurium in CdTe are derived as byproducts of mining processes (Cd from zinc smelting waste and Te from copper refining), thus preventing potentially dangerous elemental cadmium

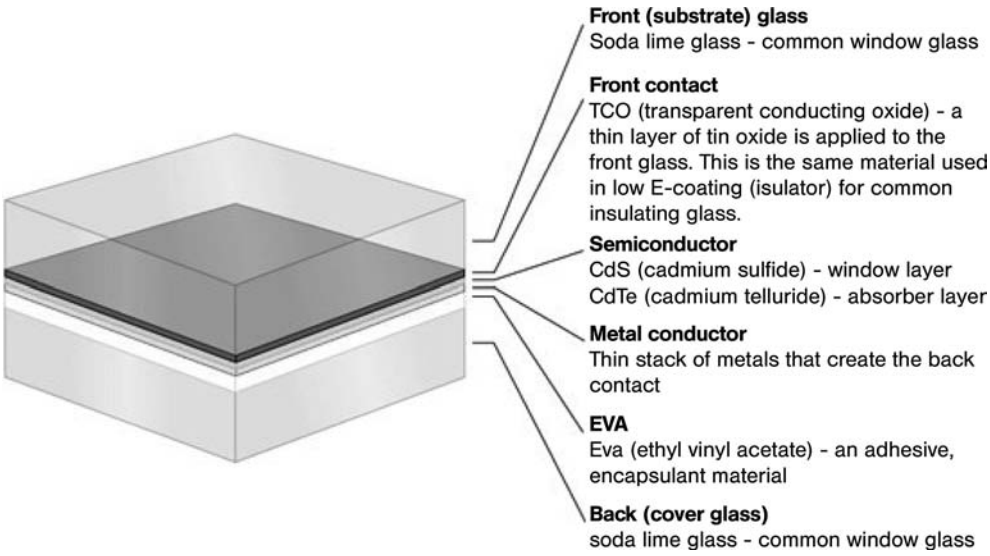

Figure 3.19 The semiconductor materials (CdTe and CdS) in a typical module are sourced from the byproducts of mining operations and are incorporated at 1% of the semiconductor material used in typical crystalline silicon solar modules. (Image courtesy: First Solar).

from entering the environment. Moreover, during operation the modules do not produce any pollutants, and thus do not present any risks to health and the environment. Full recycling of the modules at the end of their useful life resolves any environmental concerns while, by displacing fossil fuels, CdTe-based PV modules offer a net environmental benefit [17].

The typical structure is glass/SnO_2/CdS/CdTe/contacts. The absorber layer for commercial products uses either co-evaporation or a two-stage process such as the deposition of the precursors by sputtering. The most common deposition methods for the CdTe device involve acquiring commercial SnO_2-coated glass, followed by chemical-bath deposition of CdS. The CdTe thin film absorber is usually applied by close-spaced sublimation, vapor-transport deposition, or electrodeposition, followed by $CdCl_2$ treatment.

The back contact is then applied after etching the back surface of CdTe. The nature of the back contact varies – from a carbon paste containing Cu_xTe and HgTe, to a combination of other metals with Cu.

Traditional solar modules become less efficient at converting solar energy into electricity as their cell temperatures increase. However, the efficiency of CdTe is less susceptible to cell temperature increases, enabling CdTe solar modules to generate relatively more electricity under high ambient (and therefore high cell) temperatures.

CdTe also absorbs low and diffuse light and thus converts such light more efficiently to electricity under cloudy weather and dawn and dusk conditions where conventional cells operate less efficiently. As a result, under real world conditions CdTe will generally produce more electricity than a conventional solar module with similar power ratings.

In manufacturing terms (Figure 3.20), First Solar achieved substantial progress by being able to increase their power ratings of a 60 cm × 120 cm module from 50 and

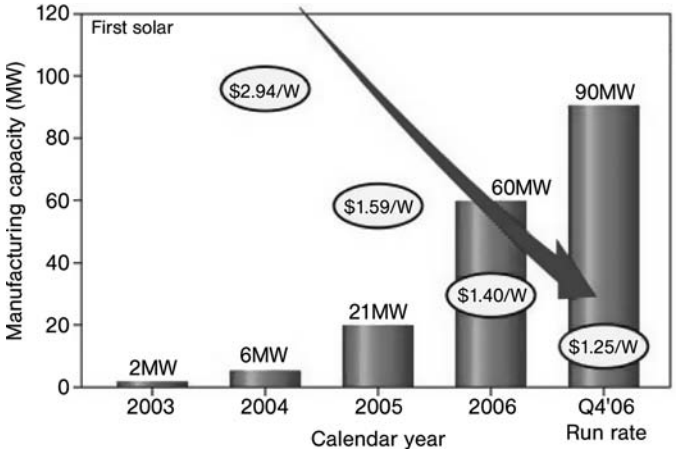

Figure 3.20 Thin film CdTe manufacturing capacity and cost reduction versus calendar year. (Reproduced from Ref. [3], with permission).

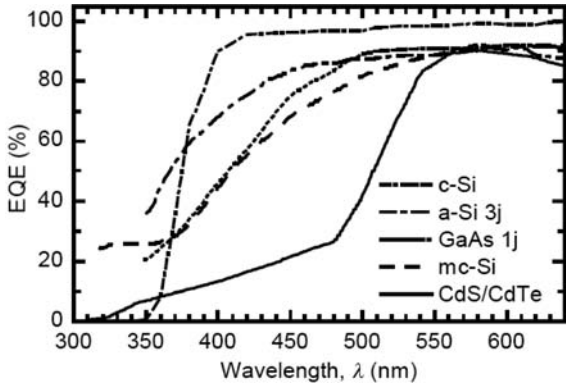

Figure 3.21 External quantum efficiency (EQE) of different types of commercially produced PV modules. (Reproduced from Ref. [18], with permission).

55 Wp to 55 to 65 Wp within 2006 alone. Both Cd and Te elements are present in abundant quantities to support multi-GWs of annual production. With economies of scale, the manufacturing cost has dropped substantially from \$2.94/W (6 MW) in 2004 to \$1.25/W (90 MW) in 2006. The target manufacturing cost is \$0.70/W by 2012 with improvements in productivity, module efficiency and yield, thus making it competitive with grid-parity electricity.

Areas of research include nonuniformity of CdTe films and its impact on device performance, thin CdTe absorber layers, interdiffusion at the CdS/CdTe interface, where S diffuses into the CdTe film, and the role of Cu doping that is usually used for back-contacting procedures.

For example, in CdTe/CdS TF cells, the direct bandgap semiconductor CdS with $E = 2.4$ eV strongly absorbs the majority of short-wavelength (violet to blue-green) light before it can be usefully absorbed in the CdTe material. As a result, commercial PV modules exhibit poor external quantum efficiency (EQE) at short wavelengths (Figure 3.21), thereby reducing the amount of photocurrent that can be generated from this part of the solar spectrum.

However, the addition of a mixture of up to four fluorescent organic dyes, which are cheap and photostable, significantly enhances the short-circuit current density (J_{sc}) of CdS/CdTe solar cells by $\Delta J_{sc} = 3.1$ mA cm^{-2}, corresponding to an increase in conversion efficiency (η) from 9.6 to 11.2% under air-mass 1.5 global (AM1.5G) solar radiation [18].

The dyes layer acts as a luminescent down-shifting (LDS) agent absorbing the short wavelength photons that would not have contributed towards electron–hole pair generation in the solar cell, and re-emitting them at longer wavelength where the PV device possesses a much higher EQE. Significantly, the application of LDS layers does not require any alteration to the structure of the solar cell.

3.5
CIS Thin Films

Copper indium selenide (CIS) modules consist of multilayer CIS solar cells connected in series. These absorb a broad spectrum of light energy and ensure a maximum power output, even during unfavorable weather conditions. By virtue of their high reliability and durability, CIS solar modules are suitable for almost all fields of application and magnitudes of solar power systems. Commercial module development activities are being actively pursued by more than a dozen companies. A typical cell has the structure shown in Figure 3.22 [19].

After a first, short optimization phase, the first modules were fabricated and measured already at above 8% efficiency in 2001. The average module efficiencies have since increased to 9–10% in 2002, 10–11% in 2003, and 11.0–11.5% in 2004 and 2005. Maximum values of 13% have already been achieved, which correspond to about 85 W for the standard module at standard test conditions (STC).The development of CIS module quality and the estimated progress until 2010 are shown in Figure 3.23.

Assuming realistic further improvements, it is expected that the existing equipment and processes are capable of reaching an average module efficiency of at least 12.5% within the next two years. Adding modifications of the CIS process that have already been proven in the laboratory and further optimizing the contact layers Mo and ZnO, together with minimization of patterning losses, it is realistic to fabricate CIS modules at a level of 14–15% within the next decade.

One major aspect is the reduction of material costs. Hence, the ZnO deposition process is being improved, aiming at a higher material yield and the use of Zn in a reactive sputtering environment; whilst efforts are directed at using lower-purity input materials and reducing the film thickness for all deposition processes.

A detailed cost study [20] estimated, some ten years ago, that CIS has the potential of production costs at about 0.7 Eur/Wp at a production volume of 50 MWp/a, while an average efficiency of 12% and an overall process yield of 85% are realistic and achievable.

Again, since the standard test conditions of 1000 W m^{-2} irradiance at 25 °C do not represent real outdoor operation conditions, the CIS modules characterized under

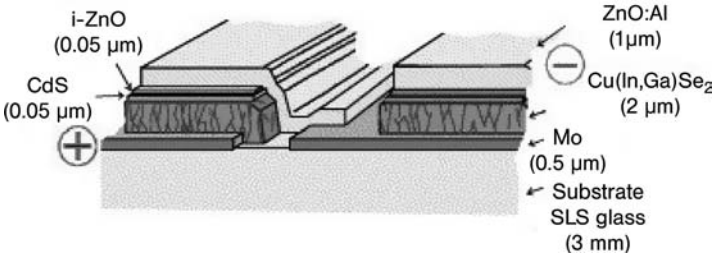

Figure 3.22 Design of the CIS cell and interconnect of two cells applied in CIS module production. (Reproduced from Ref. [19], with permission).

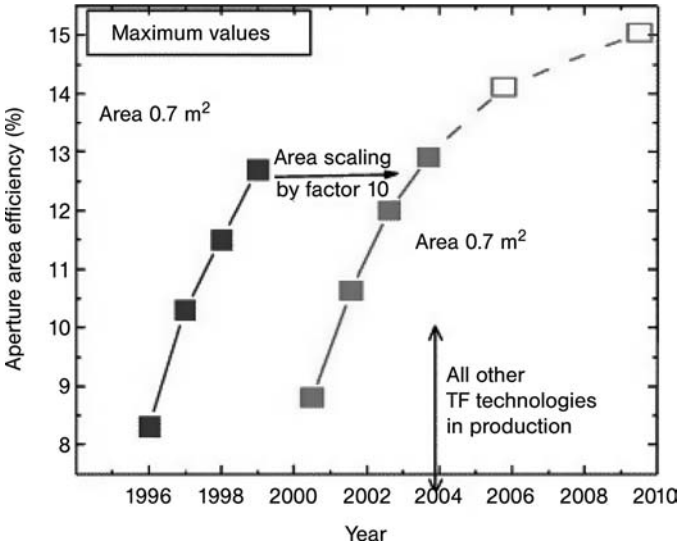

Figure 3.23 Development of CIS module quality and estimated progress until 2010. (Reproduced from Ref. [19], with permission).

realistic illumination/temperature conditions show (Figure 3.24), as expected, that the module has a lower open-circuit voltage at higher temperature, but the current remains at the same level and the curve maintains a good shape.

The curve measured at $200\,W\,m^{-2}$ and $25\,^{\circ}C$ in Figure 3.24 represents cloudy sky at lower temperatures. At one-fifth of the irradiance, the module still produces

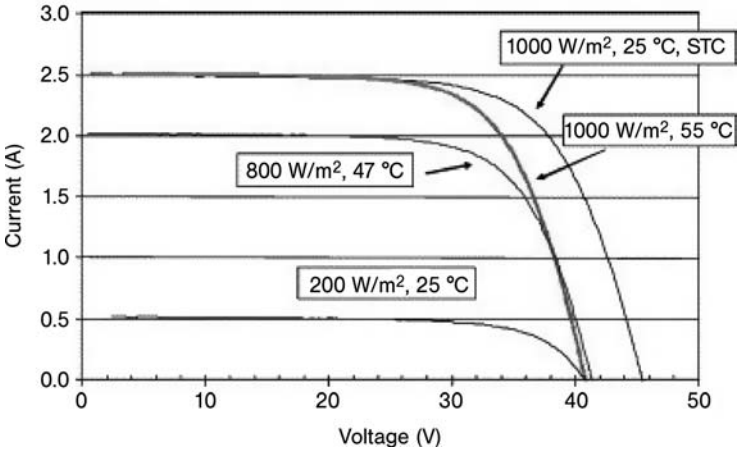

Figure 3.24 *I–V* characteristics of a typical CIS module at realistic illumination/temperature conditions. The characteristic at standard testing conditions is included for comparison. (Reproduced from Ref. [19], with permission).

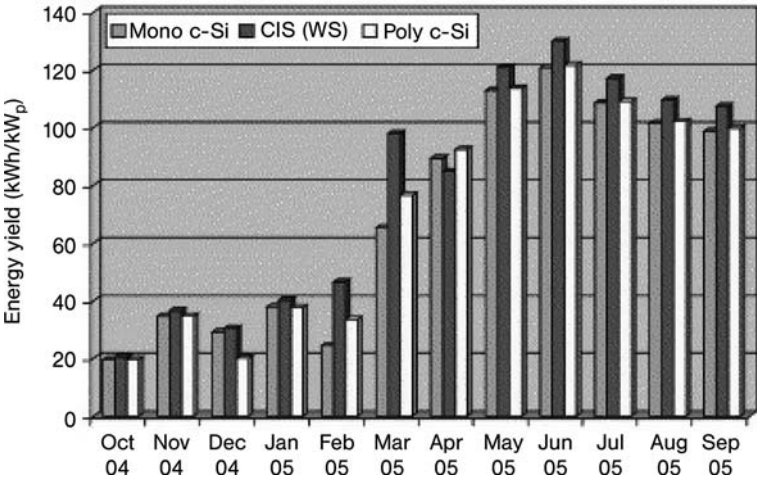

Figure 3.25 Energy yield per kWp of a CIS installation in Germany compared to a c-Si installation. (Source: Wurth Solar).

one-fifth of the current. Due to the lower temperature, the open-circuit voltage is at the same 40 V as for a sunny day. The curve at 800 W m^{-2} and 47 °C gives reasonable intermediate results.

Finally, comparison of the CIS technology with crystalline and polycrystalline silicon modules under real conditions in Germany indicates very good energy yields with the CIS technology (Figure 3.24). The kWh/kWp yield of the CIS installation is the highest, even in comparison with the high-quality monocrystalline Si installation, due to good performance under lower illumination conditions (compare Figure 3.25) and better (i.e., lower) temperature coefficient.

In general, the esthetic matt black appearance of the new modules and their flexibility as regards size and shape make them ideal construction and design elements. Besides integration in buildings (Chapter 1), thanks to their esthetic appearance and flexibility in size, CIS modules are especially well suited for customized integration in products used in daily life (Figure 3.26). The special production technique allows the technical properties to be matched for the required system solution even during production.

A future aspect is to replace the glass substrate and/or front glass by other materials, for example, flexible materials like metal or plastic foils. The processing needs to be modified partially to fulfill the requirements of these materials. Results are not yet good enough to transfer to manufacturing.

Second generation CIS modules are also produced in Torgau, Germany, at a plant with annual capacity of 20 MWp, by a joint venture, Avancis, between Shell and Saint-Gobain. The average efficiency of large, 1 foot × 4 foot, modules in pilot production is nearly 13%. This performance is comparable to many modules based on crystalline silicon, and is substantially better than the performance reported for any series-produced thin film modules based on competing technologies.

Figure 3.26 Solar powered roller blinds. These modules generate a nominal power of 2 Wp and each module has the dimensions $53 \times 600\,mm^2$. (Reproduced from Wurthsolar.de, with permission).

3.6
Environmental and Economic Concerns

These new PV technologies use the toxic heavy metal cadmium (CdSe, CdS, CdTe), whereas CIGS (copper indium gallium selenide) PV cells use indium, a metal in relatively short supply (Figure 3.27) [21]. Indium is used in ITO, and tin is used in both ITO and fluorine-doped tin oxide. Both are used as transparent conductive

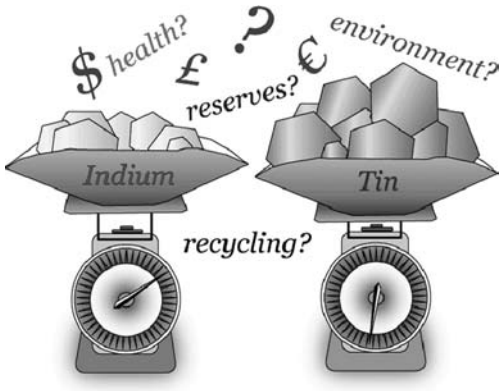

Figure 3.27 Indium and tin, and also cadmium, in new PV technologies pose economic and environmental problems that must be addressed. (Reproduced from Ref. [21], with permission).

oxides (TCOs) that are widely employed both for new solar cell designs and for flat screen displays.

A simple economic geology analysis based on the United States Geological Survey (USGS) suggests that, only in the US, indium use grew by 10% over 2006 (and 15% over 2005) [22]. The country imports the majority of indium from China, Canada, and Japan. Moreover, manufacturing processes in the electronics industry such as processing of reel-to-reel polymer coatings for plasma screens and LCD laptop screens are so wasteful that only 15% of all ITO goes into actual products; the rest of the unused ITO being scrapped and not recycled.

Considering the USGS estimate for the global primary reserve base of indium (about 6000 metric tons) and current rate of consumption of indium for technology (global refining of 480–500 metric tons per annum), even mining all the indium in the world, we are facing a worst case scenario of only 12–13 years of indium remaining. Then recycling will be the only option to access indium.

As demand for In has risen at a steady pace of 40% each year since 2002 (exceeding supply), the price of the metal has risen dramatically (Figure 3.28). This means that future production of innovative modules such as CIS and CIGS could be dramatically affected by shortage of the metal to a far greater extent than has occurred in the traditional PV industry since the shortage of polysilicon began in the early 2000s.

In the epoch of hypercompetition, basing future cost estimates upon historical costs leads to wrong predictions. Overall, to capture the inherent cost advantages of thin film technology, manufacturing companies of innovative TFPV based on these rare metals will implement a service strategy for which, rather than selling PV modules, they will sell energy produced by these modules, retaining ownership of the modules and implementing a maintenance, recovery and full recycle global service throughout the years of service of the contract. This, as has been demonstrated in several industries [24], will mitigate supply risks, enhance productivity and act as an incentive for innnovation.

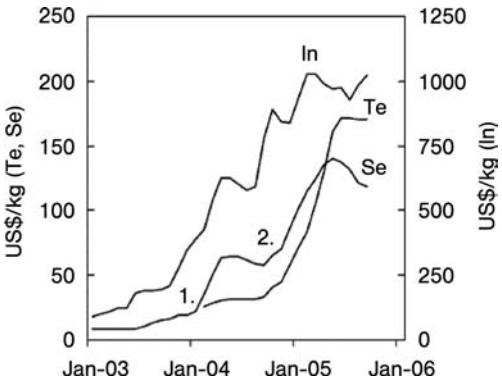

Figure 3.28 Prices for In (99.99%), Se (99.5%) and Te (99.95%) over the 2003–2006 timeframe. (Reproduced from Ref. [23], with permission).

References

1 van Cleef, M., Lippens, P. and Call, J. Superior Energy Yields of UNI-SOLAR® Triple Junction Thin Film Silicon Solar Cells compared to Crystalline Silicon Solar Cells under Real Outdoor Conditions in *Western Europe, 17th European Photovoltaic Solar Energy Conference and Exhibition*, 22–26 October, 2001, Munich (Germany).

2 The European Photovoltaic Technology Platform, *Strategic Research Agenda (SRA) for Photovoltaic Technology*, June 2007. http://www.eupvplatform.org/fileadmin/Documents/PVPT_SRA_Complete_070604.pdf.

3 Ullal, H.S. and von Roedern, B. *Thin Film CIGS and CdTe Photovoltaic Technologies: Commercialization, Critical Issues, and Applications*, paper presented at the 22nd European Photovoltaic Solar Energy Conference and Exhibition, Milan, September 3–7, 2007.

4 Avancis, Why Thin Film Technology for Photovoltaics? See at the URL: http://www.avancis.de/fileadmin/user_upload/Why_ThinFilmPV_01-07.pdf.

5 NanoMarkets, *Materials Markets for Thin film and Organic Photovoltaics*, February 2008. Additional details are available at the URL: www.nanomarkets.net.

6 Cornelius, C. Venture Investing in Solar - 2007/2008. Investment Theses, Market Gaps, and Opportunities, 2008. http://www.eere.energy.gov/solar/solar_america/.

7 Gregg, A., Blieden, R., Chang, A. and Ng H. Performance Analysis of Large Scale, Amorphous Silicon Photovoltaic Power Systems, *31st Institute of Electrical and Electronics Engineers, Photovoltaic Specialist Conference and Exhibition*, January 3–7, 2005, Lake Buena Vista, Florida USA.

8 Adhikaria, S., Kumara, S. and Siripuekpongb, P. Comparison of Amorphous and Single Crystal Silicon Based Residential Grid Connected PV Systems: Case of Thailand, *Technical Digest of the International PVSEC-14*, Bangkok, Thailand, 2004 8–5.

9 Yamamoto, K., Nakajima, A., Yoshimi, M., Sawada, T., Fukuda, S., Suezaki, T., Ichikawa, M., Koi, Y., Goto, M., Meguro, T., Matsuda, T., Kondo, M., Sasaki, T. and Tawada, Y. (2004) A high efficiency thin film silicon solar cell and module. *Solar Energy*, **77**, 939.

10 Noufi, R. and Zweibel, K. (2006) High-Efficiency CdTe and CIGS Thin film Solar Cells: Highlights and Challenges, Conference Paper, WPEC4, Hawaii.

11 Rau, U. and Schock, H.W. (1999) Electronic properties of $Cu(In,Ga)Se_2$ heterojunction solar cells-recent achievements, current understanding, and future challenges. *Applied Physics*, **69**, 131.

12 Rau, U., Jasenek, A., Herberholz, R., Schock, H.W., Guillemoles, J.F., Lincot, D. and Kronik, L. (1998) The inherent stability of $Cu(In,Ga)Se_2$. Proceedings 2nd World Conference on Photovoltaic Energy Conversion (eds J. Schmid, H.A. Ossenbrink, P. Helm, H. Ehmann and E.D. Dunlop), EU Joint Research Centre, Luxembourg, p. 428.

13 Schock, H.-W. and Noufi, R. (2000) CIGS-based solar cells for the next millennium. *Progress in Photovoltaics: Research and Applications*, **8**, 151.

14 Wolfe, J. Solar Power Heats Up With Nanotechnology, *Forbes*, July 9, 2007. Available at the URL: http://www.forbes.com/2007/07/09/nanotech-roscheisen-solar-pf-guru-in_jw_0709adviserqa_inl.html.

15 Shafarman, W.N., Basol, B.M., Britt, J.S., Hall, R.B. and Rocheleau, R.E. (1997) Semiconductor processing and manufacturing. *Progress in Photovoltaics: Research and Applications*, **5**, 359.

16 McCandless, B. and Sites, J.R. (2003) *Handbook of Photovoltaic Science and Engineering* (eds A. Luque and S. Hegedus), Wiley, West Sussex, England, p. 637.

17 Fthenakis, V.M. (2004) Life Cycle Impact Analysis of Cadmium in CdTe PV Production. *Renewable and Sustainable Energy Reviews*, **8**, 303.

18 Richards, B.S. and McIntosh, K.R. (2006) Enhancing the Efficiency of Production of CdS/CdTe PV Modules by Overcoming Poor Spectral Response at Short Wavelengths Via Luminescence Down-Shifting, Photovoltaic Energy Conversion, Conference Record of the 2006 IEEE 4th World Conference on 1, 213.

19 Dimmlera, B. and Wächter, R. (2007) Manufacturing and application of CIS solar modules. *Thin Solid Films*, **515**, 5973.

20 Woodcock, M., Schade, H., Maurus, H., Dimmler, B., Springer, J. and Ricaud, A. (1997) Proceedings of the 14th European Photovoltaic Solar Energy Conference, Stephens & Associates, Bedford, UK, p. 857.

21 Brownson, J.R.S. Nanomech in Photovoltaics, Blog on third generation photovoltaics. This analysis can be found at the URL: http://network.nature.com/blogs/user/U289513E8/2007/05/23/environmentally-aware-materials-science-case-study.

22 Indium 2007 Mineral Commodities Summary.

23 Green, M.A. (2006) Consolidation of Thin film Photovoltaic Technology: The Coming Decade of Opportunity. *Progress in Photovoltaics: Research and Applications*, **14**, 383.

24 Hawken, P., Lovins, A. and Lovins, L. Hunter (2000) *Natural Capitalism: Creating the Next Industrial Revolution*, Back Bay Books, New York.

4
Organic Thin Film Solar Cells

4.1
Organic Solar Cells

In a classical inorganic solar cell, weakly Coulomb bound pairs of charge carrier (an electron and a hole) are generated by the absorbed sunlight. In organic semiconductors, the screening of opposite charges is much weaker as the dielectric constant is lower. This leads to a much stronger interaction of the photogenerated positive and negative charges. Therefore, the primary optical excitation in organic materials is a singlet exciton, that is, a strongly bound electron–hole pair. As this binding is more difficult to overcome than that in inorganic systems, the concept of organic solar cells has to be different.

Another significant difference between organic and inorganic solar cells is that organic semiconductors are amorphous and thus charge transport is more difficult than in crystals.

An advantage, however, is the ability to synthesize tailor-made organic substances, which allows fine tuning of the absorption range and the charge transport properties, and self-assembly through nanochemistry techniques. Moreover, very thin (100 nm) organic films can absorb all the light shone on them (within their absorption range), which should be compared to an absorption length around 300 μm for thick standard crystalline silicon wafers, and 1 μm for thin films of polycrystalline $CuInSe_2$.

Invented in the mid 1980s, the first organic solar cells with enough current output were based on an active *bilayer* made of donor and acceptor materials [1]. Light is usually absorbed mainly in the so-called donor material, a hole-conducting small molecule or conjugated polymer. The photogenerated singlet excitons diffuse within the donor towards the interface to the second material, the acceptor, which is usually strongly electronegative. A prominent example of an electron acceptor material is the buckminsterfullerene (C_{60}).

The exciton moves by diffusion towards the donor–acceptor heterojunction, where the transfer of the electron to the acceptor molecule is energetically favorable (Figure 4.1). This charge transfer is very fast (it can be faster than 100 fs in polymer–fullerene systems) and very efficient, as the alternative loss mechanisms are much slower [2].

Flexible Solar Cells. M. Pagliaro, G. Palmisano, and R. Ciriminna

ISBN: 978-3-527-32375-3

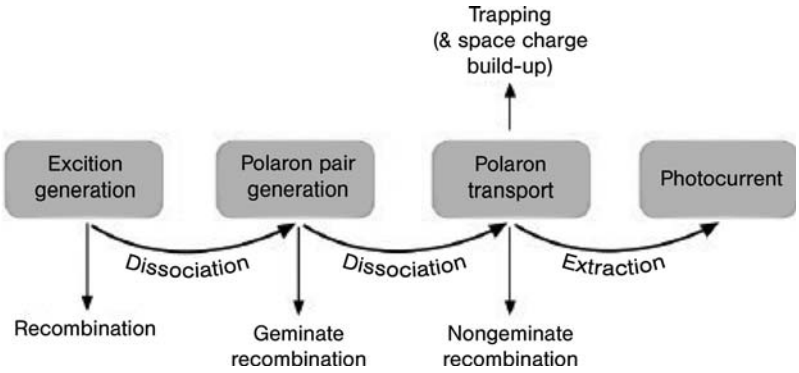

Figure 4.1 Steps from exciton generation to photocurrent in organic solar cells. (Image courtesy of Dr. C. Deibel, http://blog.disorderedmatter.eu).

The exciton is now dissociated because the hole stays on the polymer. Even though now residing on two separate materials, the electron and hole are still Coulomb bound, even though the recombination rate is clearly lowered (lifetime: micro- to milli-seconds) as compared to the singlet exciton (lifetime: nanoseconds).

For the final charge pair dissociation and to avoid monomolecular recombination, an electric field is needed to overcome the Coulomb attraction, and this dependence becomes manifest in the typical, strongly field-dependent photocurrent of organic solar cells. Such a field is an internal field, which is influenced by the built-in potential due to the work function difference between the electrodes.

In practice, the photoactive organic layer is placed between two different electrodes, the upper being transparent (Figure 4.2). Charge separation takes place in the organic phase, the anode and cathode being chosen to have largely different (asymmetric) work functions, and thus to enhance modest charge separation.

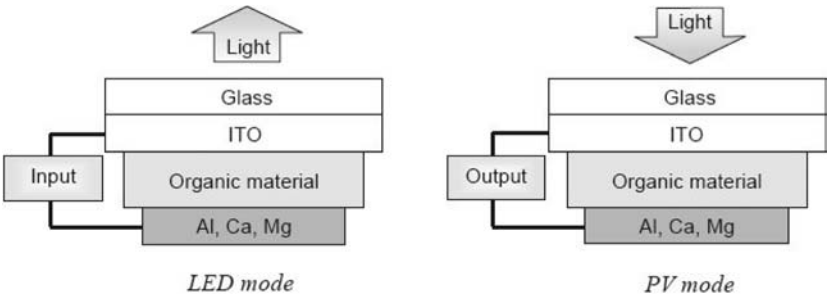

Figure 4.2 Organic materials sandwiched between two electrodes can work as photovoltaic or light emitting diode devices. In the former case electrons are collected at the metal electrode and holes at the ITO electrode. (Reproduced from Ref. [3], with permission).

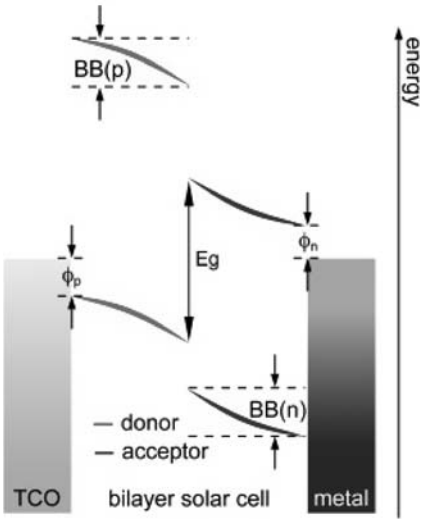

Figure 4.3 Schematic energy level diagram of a bilayer solar cell (ϕ: workfunction, E_g: bandgap: BB(n): depletion width). (Image courtesy of Dr. C. Deibel, http://blog.disorderedmatter.eu).

Figure 4.3 shows the schematic energy level diagram of a bilayer solar cell. The anode is made of TCO (transparent conductive oxide), then follow the donor and acceptor, and finally the metal cathode. The exciton is photogenerated in the donor, which can diffuse to and dissociate at the interface to the acceptor. The resulting polaron pair is then energetically separated by the effective band gap of the organic solar cell, for example.

The first organic bilayer solar cell made of two conjugated small molecules, achieved a power conversion efficiency (PCE) of about 1% [1]. A fruitful technique to obtain a more efficient charge separation is the formation of two-layer polymer diodes through lamination followed by controlled annealing, yielding a cell with almost double (1.9%) PCE [4].

The limiting factor in this concept is that, for full absorption of the incident light, a layer thickness of the absorbing material has to be of the order of the absorption length, approximately 100 nm. This is much more than the 10 nm diffusion length of the excitons. As, in general, the exciton diffusion length is much shorter than the absorption length, the potential of the bilayer solar cell is difficult to exploit.

In the beginning of the 1990s, the novel bulk heterojunction (BHJ) solar cell concept was introduced, taking into account the low exciton diffusion length in disordered organic semiconductors, as well as the required thickness for a sufficient light absorption [5].

This approach features a distributed junction between the donor and acceptor materials: both components interpenetrate one another, so that the interface between them is no longer planar but is spatially distributed. It is implemented by spincoating a polymer–fullerene blend, or by co-evaporation of conjugated molecules.

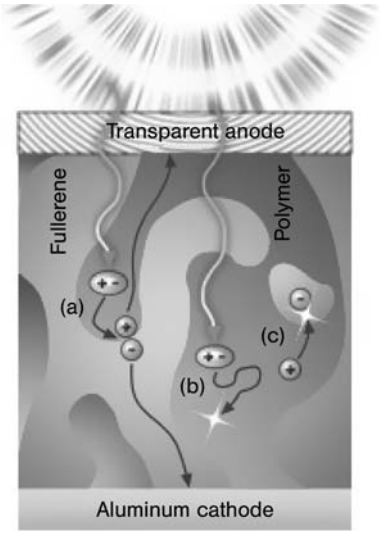

Figure 4.4 Processes of generation and recombination in disordered organic solar cells. (Image courtesy of Dr. C. Deibel, http://blog.disorderedmatter.eu).

Bulk heterojunctions have the advantage of being able to dissociate excitons very efficiently over the whole extent of the solar cell, and thus can generate polaron pairs anywhere in the film. The disadvantage is that it is somewhat more difficult to separate these polaron pairs due to the increased disorder; also, it is more likely that trapped charge carriers will recombine with mobile ones.

The most important processes of generation and recombination in disordered BHJ organic solar cells are shown in Figure 4.4. In the linear heterojunction only the geometrical interface between the conjugated polymer and fullerene layers is the area where donors and acceptors interact but in the bulk heterojunction the entire volume of the composite layer is involved. This is why such a configuration is attractive, giving rise to short circuit currents orders of magnitude higher than the previously described devices.

Excitons are photogenerated, diffuse to a donor–acceptor junction and dissociate to polaron pairs (a) or recombine radiatively (b). If polaron pairs *are* generated, then they can also be separated with the help of an external electric field; the free polarons can then hop to the corresponding electrodes to generate a photocurrent (a) or recombine with other mobile or trapped charges (c).

4.2
Bulk Heterojunction Solar Cells

In general, the bulk heterojunction ensures a high interfacial area and thus an optimal donor–acceptor contact. This is usually made by fast solvent

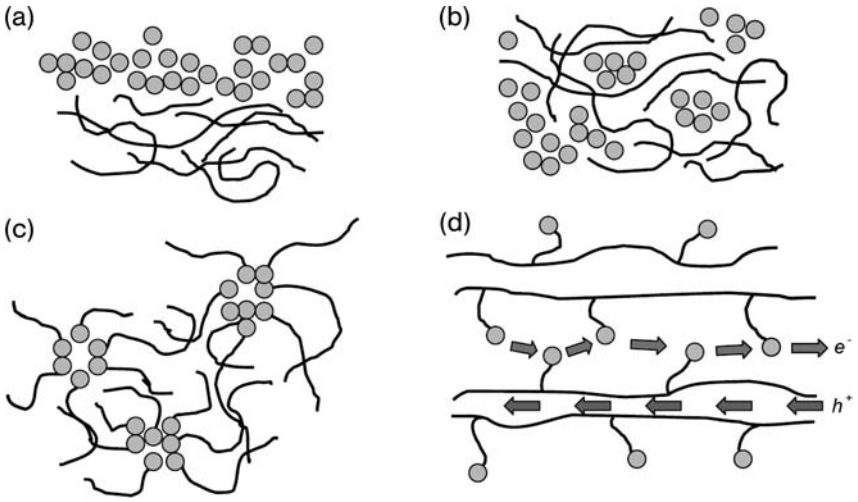

Figure 4.5 Representation of different morphologies of heterojunctions (a) two-layer heterojunction, (b) bulk heterojunction, (c) molecular heterojunction, (d) double-cable polymers. (Reproduced from Ref. [3], with permission).

evaporation, thus preventing equilibrium conditions that favor phase segregation. Four major modes (Figure 4.5) of realizing the heterojunction have been developed thus far, namely: (a) two-layer, (b) bulk, (c) molecular and (d) double-cable polymers.

Most conjugated polymers in their undoped state are electron donors when photoexcited. Moreover, their use as PV tools originates from the stability of the photo-induced polarons on this kind of polymer's backbone [6].

Conjugated polymers soluble in common solvents are particularly attractive for the production of large area PV cells because then wet printing techniques can be applied to the production of thin films made of such polymers, with the employment of reduced amounts of expensive photoactive material. Among the candidates, there are poly(*p*-phenylene vinylene) (PPV, Figure 4.6) and poly(alkyl-thiophenes) (PATs), poly(3-hexylthiophene) (P3HT), poly[2-methoxy-5-(2′-ethylhexoxy)-1,4-phenylenevinylene] (MEH-PPV), and poly[2-methoxy-5-(3′,7′-dimethyloctyloxy)-*p*-phenylenevinylene] (OC_1C_{10}-PPV).

Molecular heterojunction cells are among the material systems with the highest PCEs [7]. The bulk heterojunction here is based on blends of polymer donors and highly soluble fullerene-derivative acceptors. Konarka Technologies, for example, demonstrated a 5.21% efficient plastic solar cell with an active area of 1.024 cm^2 showing the potential of the technology. Finally, conjugated block copolymers show good potential for further improvements due to reduced exciton, photon and carrier loss, via three-dimensional space and energy level optimizations [8].

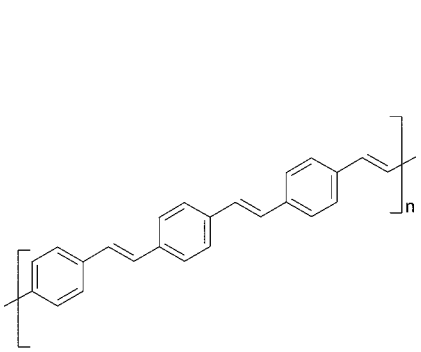

poly(*p*-phenylene vinylene) (PPV)

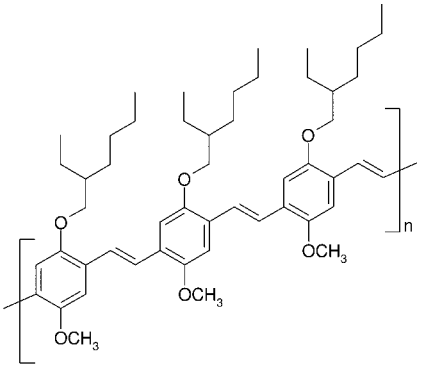

poly((2-methoxy-5-(2'-ethylhexoxy)-*p*-phenylene)vinylene) (MEH-PPV)

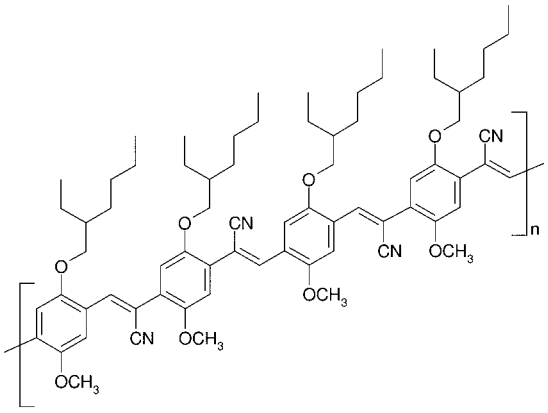

poly(2-methoxy-5-(2'-ethylhexoxy)-1,4-(1-cyanovinylene)phenylene) (MEH-CN-PPV)

Figure 4.6 Chemical structures of some representative conjugated poly(*p*-phenylene vinylenes).

4.3 Optimization of Organic Solar Cells

Following the discovery of the BHJ cells, a number of methods of optimization have been successfully developed. The choice of solvent as well as the annealing of the solution processed polymer–fullerene solar cells, both lead to a more favorable inner structure with regard to polaron pair dissociation and charge transport. Thus, the power conversion efficiency was increased manyfold, in the case of annealing from a bare half percent to above 3% [9]. Clearly, optimization by novel routes is a continuing process and recently solution processed polythiophene–fullerene cells with 5.8% PCE were reported, which make use of low bandgap polymers processed with alkane dithiols [10].

In general, in order to improve the power conversion efficiency of organic solar cells, novel donor and acceptor materials will have to be synthesized. Two main properties are being targeted:

- the ability to self-organize (enhancing order and thus charge transport)
- an absorption spectrum as wide as possible.

An absorbing acceptor has a large potential for increasing the photocurrent as, in most cases, only the donor material absorbs light efficiently. Additionally, by variation of the relative energy levels of the donor and acceptor materials, the energy loss due to electron transfer can be minimized. For inorganic solar cells, the detailed balance calculation of Shockley and Queisser, power conversion efficiency vs. band gap, is shown as a black solid line in Figure 4.7.

For organic solar cells, on the other hand, there is no complete analytic theory to describe all parameters proportional to the properties. A recent estimate based on the following (reasonable) assumptions, however, shows the potential of plastic solar cells [11]

- quantum efficiency 100% (within absorption band of 200 nm (blue) and 400 nm (red) width)
- fill factor 80%
- thickness 200 nm
- open circuit voltage with recombination strength, γ, either $10^{-15}\,m^3\,s^{-1}$ or a reduced value of $10^{-18}\,m^3\,s^{-1}$ (green)
- E_g is set to an "energy gap" minus exciton binding energy E_b of 0.3 eV.

The maximum power conversion that can be reached is clearly lower than for inorganic Si-based solar cells and to reach the maximum power conversion efficiencies new donor and acceptor materials with wider absorption ranges will have to be synthesized. However, disordered organic solar cells have a lot of potential in view of

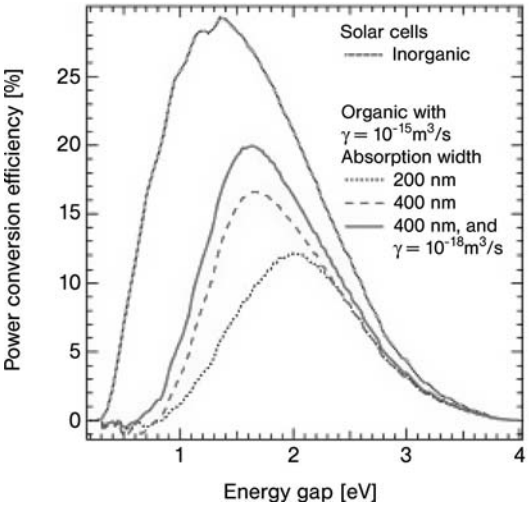

Figure 4.7 Power conversion efficiency for silicon (black solid line) and organic solar cells with absorption band of 200 nm (blue) or 400 nm (red). (Image courtesy of Dr. C. Deibel, http://blog.disorderedmatter.eu).

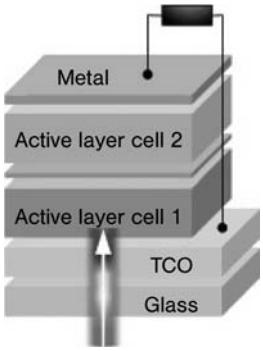

Figure 4.8 A tandem organic solar cell. (Image courtesy of Dr. C. Deibel, http://blog.disorderedmatter.eu).

manufacturing by roll-to-roll printing (see below), low cost, flexibility and light weight.

Higher intrinsic absorption is not the only route for higher organic photovoltaic performances. Another possibility to cover a broader range of the solar spectrum, including both UV–visible and IR fractions, is solution-processed multijunction solar cells combining different absorption ranges of already existing materials.

One example is the tandem solar cell, made from the connection in series of two subcells with complementary absorption ranges (Figure 4.8) [12]. Both subcells generate their own photocurrent by absorbing light and generating charges, and have their own open circuit voltage.

The two cells connected in series influence each other. The photogenerated holes of cell 1 are extracted by the intermediate ITO recombination layer, and recombine with photogenerated holes from cell 2. The open circuit voltage is approximately equal to the sum of the open circuit voltages of each cell. So, approximately, in a tandem solar cell of subcells 1 and 2:

- open circuit voltage $Voc = Voc_1 + Voc_2$
- short circuit current $Isc = \min(Isc_1, Isc_2)$.

Based on this approach, a 6.5% efficient organic tandem solar cell was recently reported [13]. The subcells are made of of polymer–fullerene blends. The anode is ITO on a glass substrate. The top cell is PCPDTBT–PC60BM, the recombination layer is made fromTiO_x and a special PEDOT–PSS, and the bottom cell is P3HT:PC70M. The cathode is made of TiO_x and aluminum. By adjusting the thickness of the two subcells, the photocurrent was balanced in order to get a high resulting photocurrent.

4.4 Printed Plastic Solar Cells

Once developed, efficient and stable polymeric solar cells will rapidly find widespread application [14]. Indeed compared to Si-based solar cells, efficient solar cells

Figure 4.9 Rolls of commercial grade solar photovoltaics printed with an inkjet printer. (Image courtesy: Konarka Technologies, Inc.).

employing organic semiconductors would be less expensive and more easily manufactured, whereas being lightweight and flexible they will be rapidly integrated into existing estate.

Molecular heterojunction cells can be efficiently printed using the inkjet printing technology, opening the route to large scale production of organic solar cells.

As recently as March 2008, Konarka Technologies successfully conducted the first ever demonstration of manufacturing solar cells by highly efficient inkjet printing [15]. The demonstration (Figure 4.9) confirms that organic solar cells can be processed with printing technologies with little or no loss compared to "clean room" semiconductor technologies such as spin coating.

As in the case of the printed CIGS-based solar cells manufactured by Nanosolar (Chapter 3), the continuous roll-to-roll printing technology provides easy and fast deposition of polymer films over large area substrates. The process is significantly less expensive and capital intensive than the multi-step assembly of traditional solar cells.

Finally, the polymer devices are compatibile with various substrates and do not need additional patterning, whereas inkjet printing enables manufacturing of solar cells with multiple colors and patterns for lower power requirement products, like indoor or sensor applications.

The morphological and interfacial properties of the inkjet printed polymer–fullerene blend photoactive layer are favorably determined by a suitable solvent formulation [15]. In detail, a mixture of high and low boiling solvents, (68% *ortho*-dichlorobenzene and 32% 1,3,5-trimethylbenzene), allows the production of inkjet printed organic solar cells with power conversion efficiency in the range of 3%.

Figure 4.10a shows a schematic representation of organic film formation by inkjet printing. The spreading and wetting of the liquid on the substrate and the drying behavior of the printed film are controlled by the solvent formulation and the temperature of the inkjet printing table. During the drying process and subsequent annealing, the suggested oDCB–mesitylene solvent mixture leads to an optimum phase separation network of the polymer donor and fullerene acceptor and therefore strongly enhances the performance.

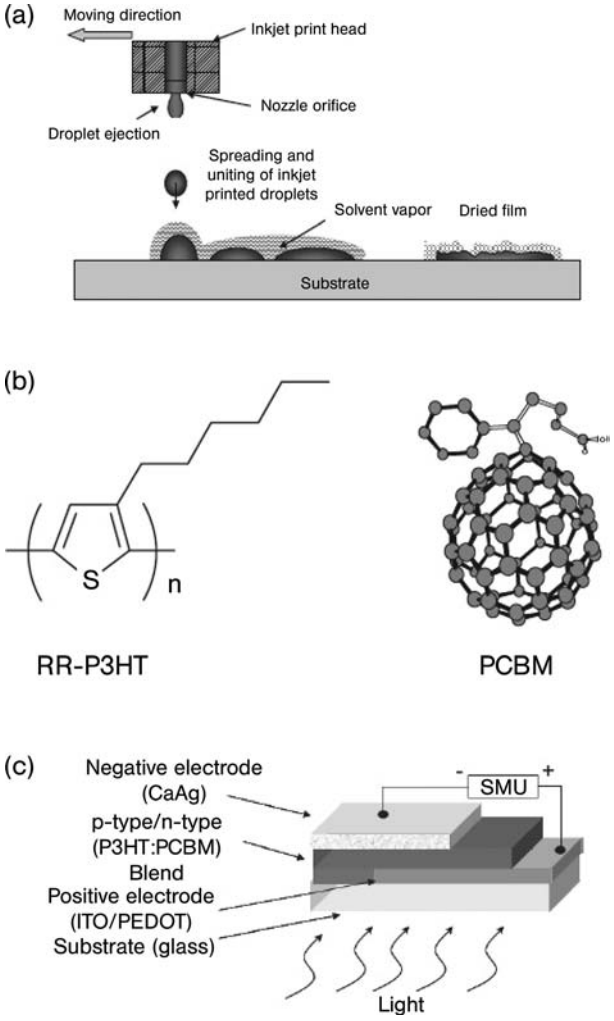

Figure 4.10 (a) Schematic of organic film formation by inkjet printing. (b) Chemical structure of the regioregular P3HT polymer donor and PCBM acceptor used to print the photoactive layer. (c) The device structure of the Glass/ITO/PEDOT:PSS/P3HT:PCBM/CaAg solar cells. (Reproduced from Ref. [15], with permission).

In this case, the photoactive layer consists of regioregular poly(3-hexylthiophene) (P3HT) blended with fullerene [6,6]-phenyl C61 butyric acid methyl ester (PCBM) and dissolved in a tetralene and oDCB–mesitylene solvent mixture. An inkjet platen temperature of 40 °C results in a uniform film and reliable printing with respect to the spreading and film formation.

The combination of oDCB–mesitylene, a higher/lower boiling solvent mixture, serves two purposes: (i) the first component of the solvent mixture (oDCB with b.p. = 180 °C) can be used to prevent nozzle clogging and provide a reliable jetting of the printhead; (ii) the second component (mesitylene) of the solvent mixture, with a lower surface tension, is used to achieve optimum wetting and spreading of the solution on the substrate. Furthermore, mesitylene has a higher vapor pressure of 1.86 mm Hg at 20 °C and a lower boiling point of 165 °C compared to oDCB and tetralene. Therefore, it increases the drying rate of the solvent mixture, which is a critical parameter for the morphology. For an efficient bulk heterojunction solar cell, good control of the morphology is essential [16].

The resulting morphology is dependent on the fabrication tool chosen for the deposition of the active layer. The AFM images of the P3HT–PCBM blend films inkjet printed using either tetralene (Figure 4.11a) or the mixture of oDCB and mesitylene (Figure 4.11b) indeed show significant distinction in the grain size and surface roughness between the inkjet printed layers. The larger grain size of the P3HT–PCBM inkjet printed layer for the tetralene formulation indicates morphological limitations, due to the slow drying rate leading to demixing of the polymer and fullerene within the inkjet printed blend.

The tetralene formulation displays significantly rough surfaces for the inkjet printed active region (mean roughness 21 nm), while the mean roughness for the oDCB–mesitylene mixture inkjet printed active layer is only 2.6 nm. Again, non-uniform surface roughness affects the interfaces of the photoactive layer and therefore the performance of the inkjet printed device.

In contrast, the devices with an inkjet printed active layer based on the oDCB–mesitylene solvent mixture formulation have a significantly higher J_{SC} of 8.4 mA cm^{-2}, a V_{OC} of 0.54 V and a FF of 64% yielding an overall PCE of 2.9%. Enhanced values that are directly related to improved morphology and the smoother surface roughness profiles (Figure 4.12).

Konarka has pursued large-scale commercialization with the German firm Leonhard Kurz to devise a high-speed press capable of producing Power Plastic cells. The process is simple, energy efficient, environmentally friendly, replicable and scalable.

The semiconducting conjugated polymers that make up the photosensitive layers of the cell are created in batches of several liters each. Their final form is that of a fluffy powder. When manufacturers are ready to use the material, they combine it with standard industrial solvents, common in printing, to create an ink or coatable liquid. The semiconducting polymers are thus applied through inkjet printing.

The roll-to-roll line (Figure 4.13) contains five stands. Each stand corresponds to a layer of the solar cell. The coating technology used is analogous to that of a slot die (extrusion) or slide coater. The first coat to go on the substrate is a semitransparent electrode, typically a transparent conductive oxide layer. Next is a patterning step that

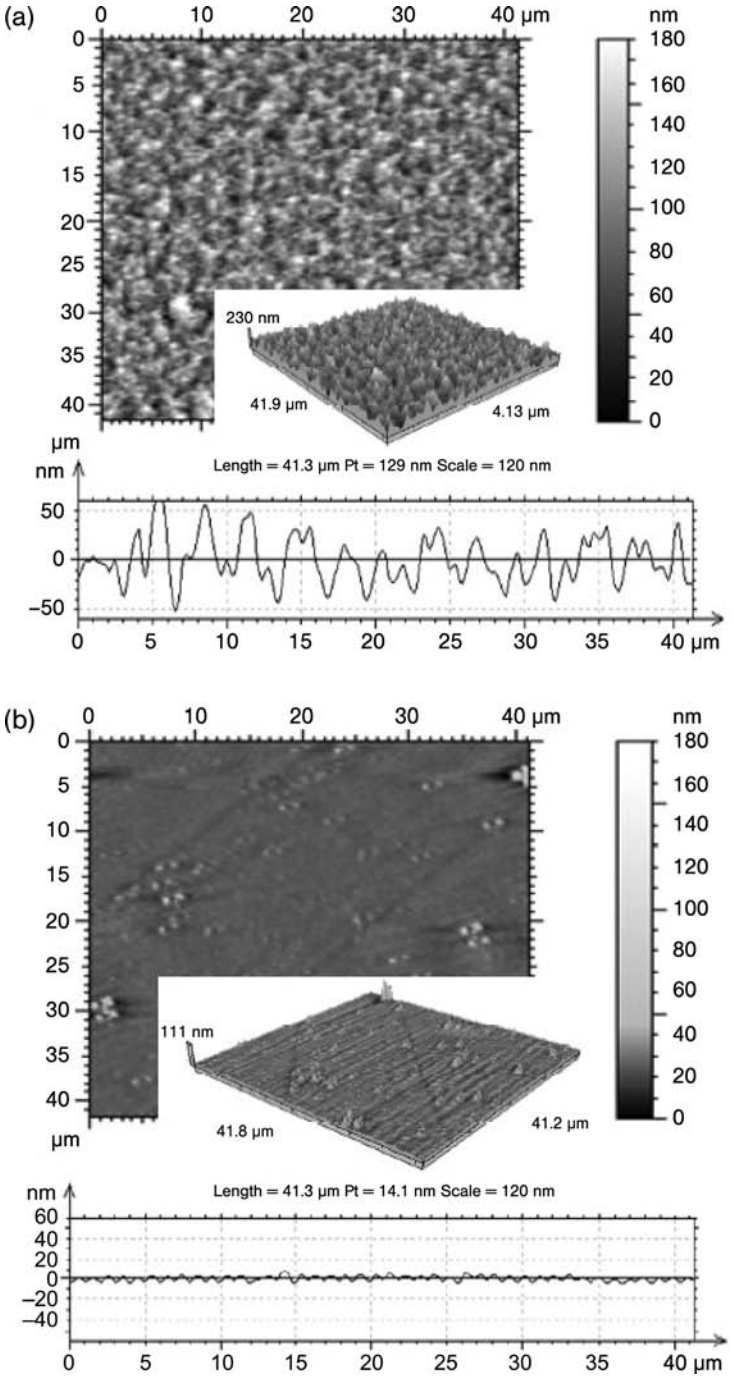

Figure 4.11 AFM images of P3HT–PCBM blend solution. (a) Deposited from tetralene formulation. (b) Deposited from oDCB–mesitylene formulation by inkjet printing. (Reproduced from Ref. [15], with permission).

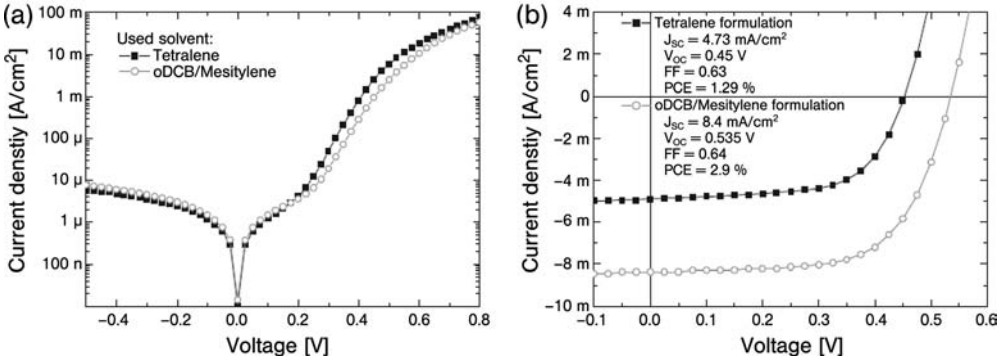

Figure 4.12 *J–V* curves for the inkjet printed solar cells processed using as solvent tetralene (solid squares) and oDCB-mesitylene (open circles). (a) In the dark in a semi-logarithmic representation. (b) Under light in a linear representation. (Reproduced from Ref. [15], with permission).

separates the cells from each other so they can later be connected in series. Active layers are deposited next, followed by a top electrode to complete the active stack. The completed cells are cut apart and laminated to produce the voltage outputs dictated by the customer.

All of these layers are remarkably thin. The base TCO layer, for example is about 100 nm thick. Some of the active layers of semiconducting polymers are only tens of nanometers deep. Such shallow layers dry quickly and thus promote the use of fast web speeds.

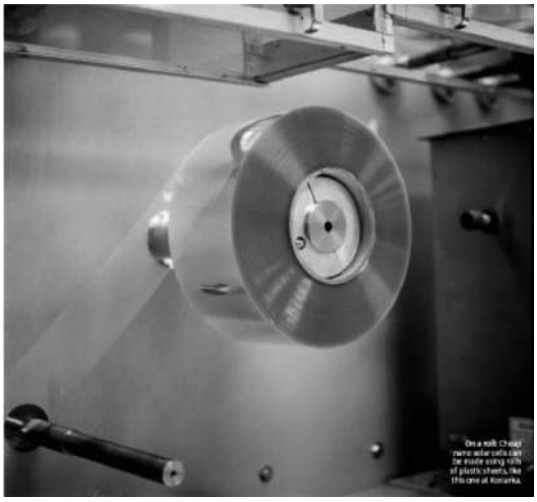

Figure 4.13 A plastic solar cell production line, where solar cells are printed as newspapers are, roll-to-roll. (Photo courtesy of Konarka).

The key to making the process practical is in the quality of the application process. Pinholes in the applied material, for example, introduce shorts between layers. Konarka has tweaked its printing methodologies to ensure the critical middle layers are pinhole-free.

Another strategic step in fabrication consists of heating that creates islands of crystals within an otherwise amorphous polymer. This annealing process to get the right nanostructure is carried out at about 110 °C and takes just a few seconds.

Cleanliness during deposition is important but rather than encase the whole production line in a clean room to keep out dust, only the coating stations are sealed off. This lets the entire line reside in an ordinary factory environment.

The cells coming off Konarka's roll-to-roll line today are about 3% efficient. The company has devised a new cell structure that is over 5% efficient and intends to use it for future products.

4.5 Brushing Plastic Solar Cells

Figure 4.14 shows the brushing production schematic and the resulting *I–V* curves for two BHJ solar cells made by brushing or by traditional spin-coating the polymers. Clearly, the brush-painting process greatly enhances the performance of the plastic solar cells [17].

The brush painting was performed on a poly(3,4-ethylenedioxythiophene) (PEDOT):poly(styrene sulfonate) (PSS)-coated indium tin oxide (ITO) substrate on a hot plate at a temperature of 50 °C. A fast brush-painting process with a blend-soaked brush can induce the rapid solidification of the active layer and allows critical control of the thickness. Here, the thickness of the active layers could be controlled uniformly and is 90 nm.

Other printing processes such as doctor blading and slot extrusion, which are more compatible with the roll-to-roll system than spin-coating, usually show variations in efficiency resulting from nonuniform thicknesses.

In the fabrication of solar cells, a uniform film thickness is an important factor because of the strong dependence of efficiency on the film thickness. Using the brush painting technique, remarkably reproducible and uniform thickness control was possible because of the effective control of the undesirable flow of free surfaces.

The improved ordering of the polymer, which is responsible for the enhanced efficiency, results from the more effective application of shear stress to the polymer chains across the entire depth of the polymer solution during the brushing process. In the case of a Newtonian type of polymer solution, the shear stress (τ), which causes the organization of polymer chains, is proportional to the viscosity (ν) and the velocity gradient ($\Delta\nu$) of the solution [$\tau \approx \nu \times \Delta\nu$].

Instead of the free surface with zero shear stress, there are two boundaries, the polymer solution–ITO substrate and the polymer solution–brush interfaces, as shown in Figure 4.14a. Thus, the brushing process can induce a higher degree of ordering in the polymer across the depth, compared to spin-coating or dip-coating.

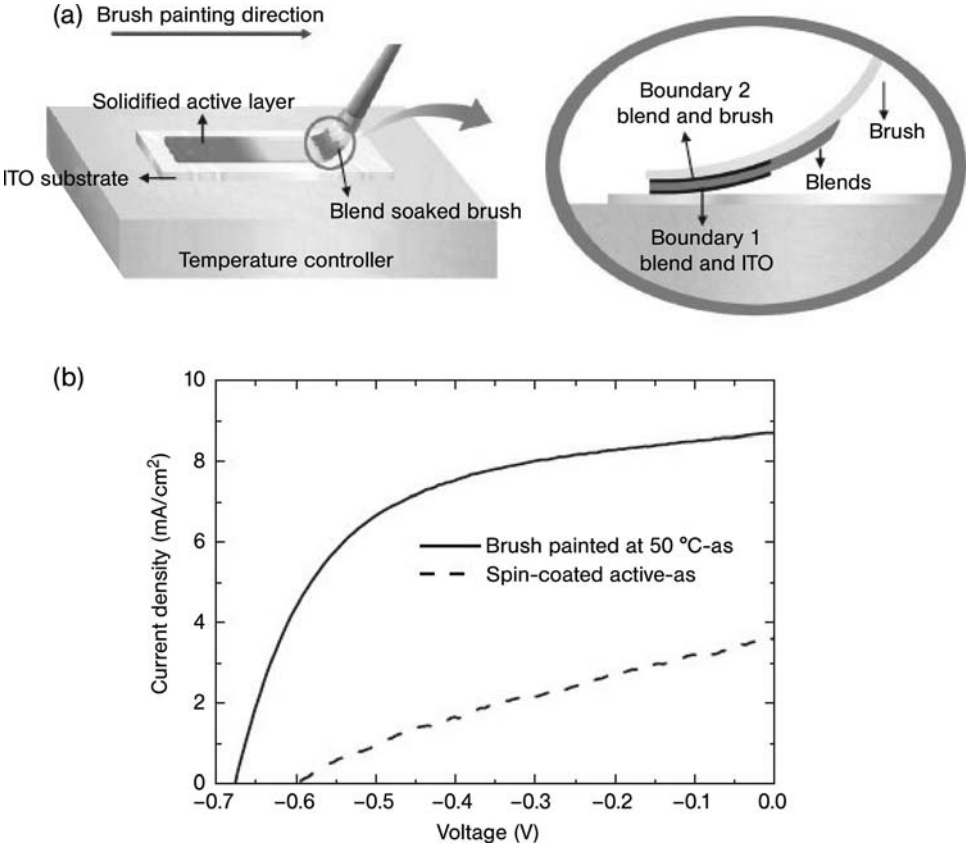

Figure 4.14 (a) Schematic of the brush-painting process. (b) *I–V* curves of solar cells fabricated by spin-coating (dashed line) and brush painting (solid line) at 50 °C without any pre- or post-treatment. (Reproduced from Ref. [17], with permission).

When brush-painting is used, a constant shear stress ($\Delta v = \text{constant}$) develops across the entire depth of the polymer solution, because an effective contact between the brush and the polymer solution is maintained. When spin-coating or dip-coating is used, the presence of a free surface at the top (polymer solution–air boundary) induces a zero stress at the top (τ surface $= 0$, $\Delta v = 0$). Thus, the shear stress across the depth profile is maximal at the bottom (substrate–polymer solution boundary) and decreases linearly along the height, becoming zero at the top.

The morphology of the active layer, has a critical influence on the charge separation and transport within the donor and acceptor networks. A similar morphology consisting of bicontinuous interpenetrating networks of donors and acceptors on a nanoscale was observed in the TEM images of both the spin-coated and brush-painted at 50 °C active layers, as shown in the inset of Figure 4.15a and b.

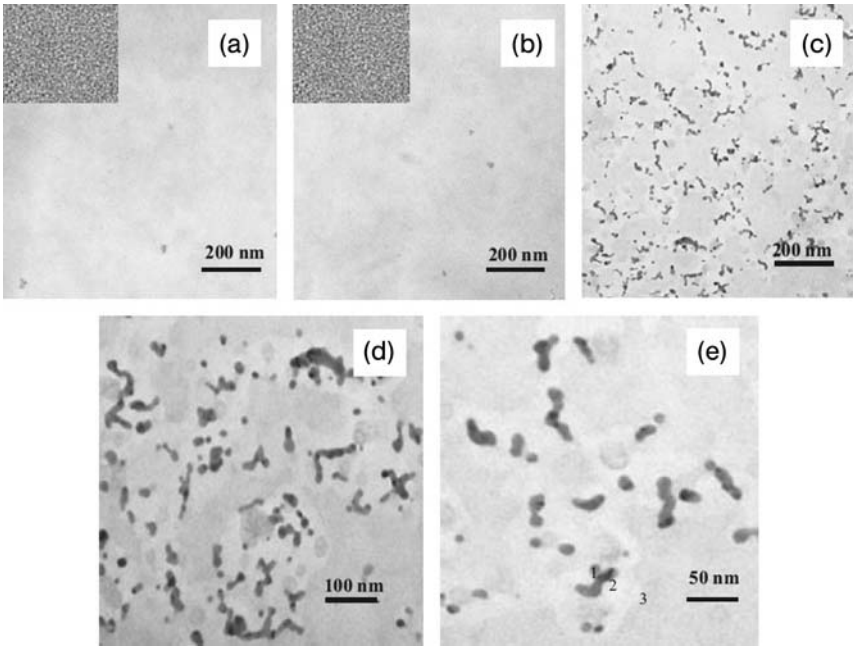

Figure 4.15 TEM images of (a) a spin-coated active layer, (b) brush-painted at 50 °C active layer, and (c) brush-painted at 130 °C active layer. (d–e) enlarged TEM images of a brush-painted active layer at 130 °C followed by annealing at 110 °C for 7 min. (Reproduced from Ref. [17], with permission).

In contrast to the TEM images of the spin-coated layer and the brush-painted at 50 °C layer, severe aggregation was observed in the TEM images of the brush-painted at 130 °C layer (Figure 4.15c).

The low FF and efficiency can be attributed to the formation of large aggregates during the brush painting process at high temperature (130 °C), which limits the efficient charge separation and transport. In other words, even though enough ordering of the polymer chains could be achieved when painting at high temperature (closer to the boiling point), optimized nanoscale morphology for efficient plastic solar cells was not found at this temperature.

The brush painting process must be carried out at temperatures above 50 °C to make a smooth and uniform active layer with a high degree of ordering. This temperature requirement is related to the evaporation rate of the solvent chlorobenzene that must be rapid enough to yield good-quality films.

On the other hand, after thermal annealing of the spin-coated active layer at 110 °C for 7 min, an improved performance with $V_{OC} = 0.65$ V, $I_{SC} = 10.61$ mA cm^{-2}, FF 56.3%, and $\eta_e = 3.9\%$ is obtained that derives from a more efficient charge transport because of the improved degree of ordering (Figure 4.16). The relatively clearer XRD peak at $2\theta \approx 5.3^\circ$ confirms an increased crystallinity, resulting in a higher mobility of

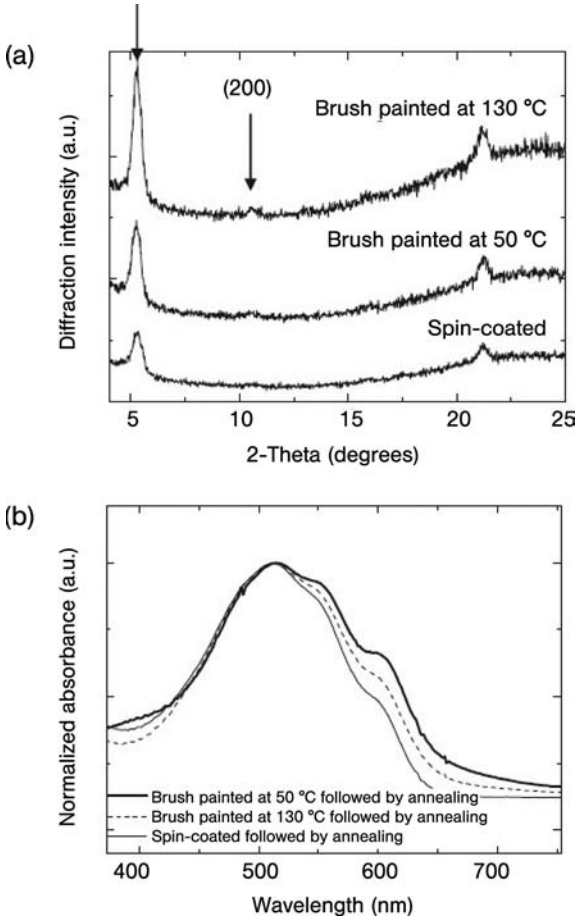

Figure 4.16 (a) XRD spectra and (b) UV–vis absorption spectra of photoactive layers prepared by spin coating and brush painting at 50 °C and 130 °C followed by annealing at 110 °C for 7 min. (Reproduced from Ref. [17], with permission).

charges within the interpenetrating networks and a reduced loss of charges by recombination.

4.6 Power Plastic

Figure 4.17 shows the 1992–2007 efficiency trend for plastic solar cells [18]. In general, polymer-based solar cells are approaching power conversion efficiencies >5%, still one fifth of the 15% average efficiency of commercial Si-based modules. The record efficiencies have been observed in disordered nanostructured

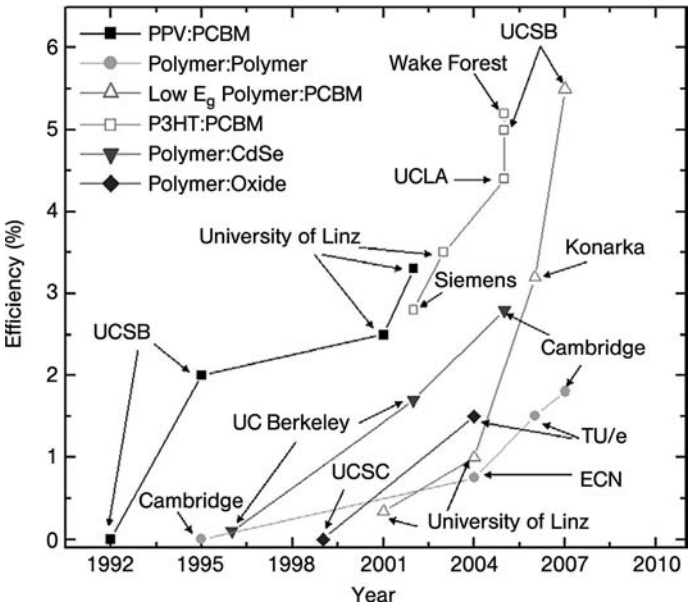

Figure 4.17 Reported efficiencies of various BHJ technologies over time. The references in chronological order are: PPV:PCBM, polymer:polymer, and polymer:CdSe, polymer:oxide, low E_g polymer:PCBM, and P3HT:PCBM. The abbreviations are: University of California, Santa Barbara (UCSB); University of California, Santa Cruz (UCSC); University of California, Berkeley (UC Berkeley); University of California, Los Angeles (UCLA); Technische Universiteit Eindhoven (TU/e).

heterojunctions but further gains are expected upon optimizing ordered nanostructure architectures.

Current challenges are [19]:

1. Creating an ordered nanostructure with the appropriate domain size (<10 nm) and dimensions (300–500 nm thick).
2. Developing small bandgap polymers with absorption edges as low as 1 eV, absorption coefficients larger than $10^5\,cm^{-1}$, and charge carrier mobilities higher than $10^{-4}\,cm^2\,V^{-1}\,s^{-1}$.
3. Minimizing energy loss at the donor–acceptor interface by tuning energy levels.

Progress on these basic points is necessary to achieve higher efficiencies. The commercial modules will also have to be stable in sunlight for at least ten years. Current performance is around 5% for cell stripes of 10 cm^2 surface (Figure 4.18).

High efficiency is not paramount in many of the applications envisioned for plastic cells. Customers care about total power (and lower cost); so if one needs more power from a plastic cell, it is enough to make the footprint longer.

In early 2006, portable battery chargers and square meter tent materials of Power Plastic (a trademark of Konarka Technologies) were delivered to the US Army and US Airforce, respectively. The US military has further contracted the company to build a series of camouflaged power-generating buildings.

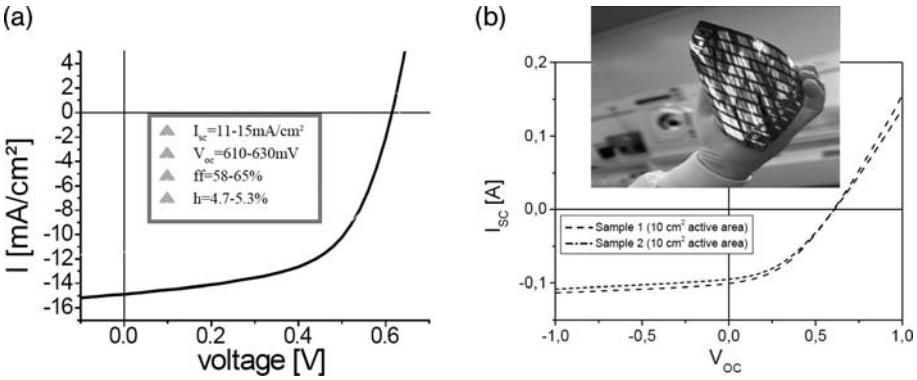

Figure 4.18 Efficiencies of the first commercial plastic solar cells are in the 5% regime (a) with an active area of a single stripe of 10 cm^2 (b). (Image courtesy of Konarka).

One crucial feature of the plastic solar cells is that Konarka can offer flexible plastic solar panels with printed patterns – such as bricks or camouflage, which clearly are a requirement for the military. More generally, it is the patterns, colors, and all the esthetic attributes that considerably *add value* to the Power Plastic, beyond the power it produces.

Indeed, the company, rather than bring end products to market itself, is partnering with companies and allowing these partners to integrate solar cells into their products in compelling ways, rather than trying to compete with solar panel makers on cost per watt. For example, the company has a partnership with Air Products to make windows that generate electricity using Konarka's solar films; and another with Sky Shades to commercialize power generating shades (Figure 4.19).

In Konarka's technology the photovoltaic polymer blend is printed between printed electrodes which are further sandwiched between the substrate and the transparent packaging material (Figure 4.20). The finished product is only 50–250 μm thick.

Figure 4.19 By integrating Power Plastic into fabric, shades generating electricity will be available commercially by the end of 2008. (Image courtesy of Sky Shades).

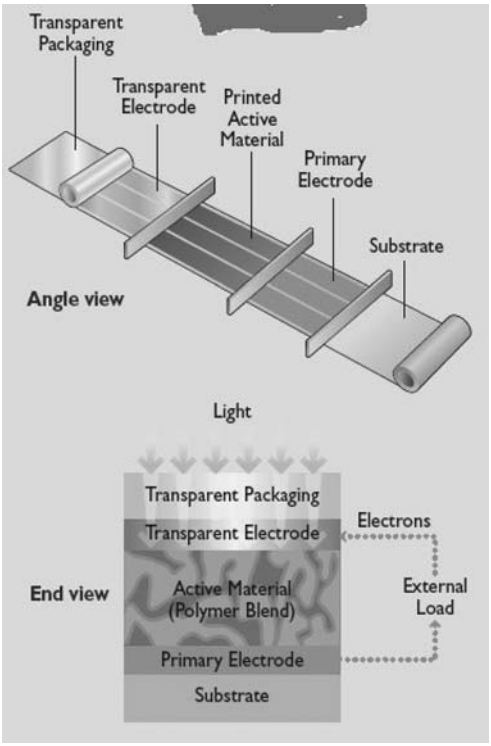

Figure 4.20 The structure of Power Plastic. (Image courtesy of Konarka).

The product advantages in terms of cost, form and versatility intrinsic to the technology are self-evident. The Power Plastic is inexpensive (five times less than traditional solar), lightweight (50 g m^{-2}) versatile (can be colored, patterned and cut-to-fit), and flexible (easily adapted to an application's form factor). Furthermore, the light weight and flexible nature of Power Plastic enable product design to evolve from tethered-to to designed-in and designed-around (Figure 4.21).

Among the first organic PV products there will probably be a solar-powered camping lantern, followed by tents that generate their own electricity, and trickle chargers (which charge the battery at the same rate that it is discharging) for portable

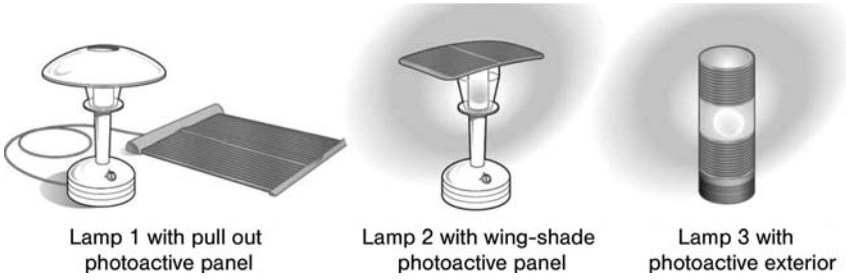

Figure 4.21 The evolution of design with Power Plastic. (Image courtesy of Konarka).

Figure 4.22 The ship currently navigates in Italy's seas using a hybrid motor (diesel + electric) with solar electricity being produced by either Si or organic (polymer with carbon nanotubes) photovoltaic thin films. (Photo courtesy: Michelangelo Calamai & Figli).

devices such as mobile phones and MP3 music players, awnings and canopies and powered smart cards [20].

Another related application will be solar sails. Such sails are already being explored worldwide and represent a potentially huge market (Figure 4.22). Once integrated in the fabric of the sail, the organic PV material is stabilized towards the harsh conditions of navigation in open sea and will provide ships with increasing levels of energy, well beyond the amount needed to power the navigation electronic devices.

For example, the ship shown in Figure 4.19. currently navigates Italy's seas using a hybrid motor (diesel + electric) with solar electricity being produced by both Si and organic (polymer with carbon nanotubes) photovoltaic thin films.[1)]

In conclusion, the field of organic photovoltaics is set to boom and the three most important aspects of successful device design: materials, device physics, and manufacturing technologies, are being addressed with increasing success [18]. Following large scale commercialization, that will start in 2008, the advantages in terms of system integration, reel-to-reel large scale manufacturing issues and production costs will open the route to a spectacular commercial success that will feed further R&D activities aimed at improving efficiency, eventually integrating the PV industry with a brand new family of products.

1) The ship is operated by Italy's textile company Figli di Michelangelo Calamai within the research project SIEP co-financed by the Tuscany Region and led by the University of Perugia's Department of Civil Engineering.

References

1 Tang, C.W. (1986) Two-layer organic photovoltaic cell. *Applied Physics Letters*, **48**, 183.

2 Sariciftci, N.S., Smilowitz, L., Heeger, A.J. and Wudl, F. (1992) Photoinduced electron transfer from a conducting polymer to buckminsterfullerene. *Science*, **258**, 1474.

3 Spanggaard, H. and Krebs, F.C. (2004) A brief history of the development of organic and polymeric photovoltaics. *Solar Energy Materials and Solar Cells*, **83**, 125.

4 Granstrom, M., Petritsch, K., Arias, A.C., Lux, A., Andersson, M.R. and Friend, R.H. (1998) Laminated fabrication of polymeric photovoltaic diodes. *Nature*, **395**, 257.

5 Yu, G., Gao, J., Hummelen, J.C., Wudl, F. and Heeger, A.J. (1995) Polymer Photovoltaic Cells: Enhanced Efficiencies via a Network of Internal Donor-Acceptor Heterojunctions. *Science*, **270**, 1789.

6 Coakley, K.M. and McGehee, M.D. (2004) Conjugated polymer photovoltaic cells. *Chemistry of Materials*, **16**, 4533.

7 Kim, Y., Cook, S., Tuladhar, S.M., Choulis, S.A., Nelson, J., Durrant, J.R., Bradley, D.D.C., Giles, M., McCulloch, I., Ha, C.S. and Ree, M. (2006) A strong regioregularity effect in self-organizing conjugated polymer films and high-efficiency polythiophene:fullerene solar cells. *Nature Materials*, **5**, 197.

8 Sun, S.-S., Zhang, C., Ledbetter, A., Choi, S., Seo, K. and Bonner, C.E., Jr (2007) Photovoltaic enhancement of organic solar cells by a bridged donor-acceptor block copolymer approach. *Applied Physics Letters*, **90**, 043117.

9 Padinger, F., Rittberger, R.S. and Sariciftci, N.S. (2003) Effects of postproduction treatment on plastic solar cells. *Advanced Functional Materials*, **13**, 85.

10 Peet, J., Kim, J.Y., Coates, N.E., Ma, W.L., Moses, D., Heeger, A.J. and Bazan, G.C. (2007) Efficiency enhancement in low-bandgap polymer solar cells by processing with alkane dithiols. *Nature Materials*, **6**, 497.

11 Deibel, C. http://blog.disorderedmatter.eu., March 2008.

12 Hadipour, A., de Boer, B. and Blom, P.W.M. (2008) Organic tandem and multi-junction solar cells. *Advanced Functional Materials*, **18**, 169.

13 Kim, J.Y., Lee, K., Coates, N.E., Moses, D., Nguyen, T.-Q., Dante, M. and Heeger, A.J. (2007) Efficient tandem polymer solar cells fabricated by all-solution processing. *Science*, **317**, 222.

14 Brabec, C.J., Sariciftci, N.S. and Hummelen, J.C. (2001) Plastic solar cells. *Advanced Functional Materials*, **11**, 15.

15 Hoth, C.N., Choulis, S.A., Schilinsky, P. and Brabec, C.J. (2007) High photovoltaic performance of inkjet printed polymer: fullerene blends. *Advanced Materials*, **19**, 3973.

16 Hoppe, H., Niggemann, M., Winder, C., Kraut, J., Hiesgen, R., Hinsch, A., Meissner, D. and Sariciftci, N.S. (2004) Nanoscale morphology of conjugated polymer/fullerene-based bulk-heterojunction solar cells. *Advanced Functional Materials*, **14**, 1005.

17 Kim, S.-S., Na, S.-I., Jo, J., Tae, G. and Kim, D.-Y. (2007) Efficient Polymer Solar Cells Fabricated by Simple Brush Painting. *Advanced Materials*, **19**, 4410.

18 Mayer, A.C., Scully, S.R., Hardina, B.E., Rowell, M.W. and McGehea, M.D. (2007) Polymer-based solar cells. *Materials Today*, **10**, 28.

19 Brabec, C., Dyakonov, V. and Scherf, U. (2008) *Organic Photovoltaics: Materials, Device Physics, and Manufacturing Technologies*, Wiley-VCH, Weinheim.

20 Graham-Rowe, D. (2007) Solar cells get flexible. *Nature Photon*, **1**, 433.

5
Organic–Inorganic Thin Films

5.1
Dye Cells: A Versatile Hybrid Technology

Leaves of plants are tiny factories in which sunlight converts carbon dioxide gas and water into carbohydrates and oxygen. They are not very efficient, however, but are very effective over a wide range of sunlight conditions. In spite of the low efficiency and the fact that the leaves must be replaced, the process has worked for hundreds of millions of years and forms the primary energy source for all life on earth.

Since the 1970s, attempts have been made to create a better solar cell based on this principle. There were early attempts to cover crystals of semiconductor titanium dioxide with a layer of chlorophyll. However, the electrons were reluctant to move through the layer of pigment, so the efficiency of the first solar cells sensitized in this way was about 0.01%. Then, in 1991, in Switzerland, scientists discovered that nanotechnology could overcome the problem [1].

Instead of using a single large titanium dioxide (titania) semiconductor crystal, they worked with a sponge of small particles, each about twenty nanometers in diameter, coated with an extremely thin layer of pigment. This method increased the effective surface area available for absorbing the light by a factor of one thousand – now the sunlight was very efficiently converted into an electric current.

The working principle of a dye-sensitized solar cell is shown in Figure 5.1 [2]. The system, for which a global efficiency of up to 11% has been reported, comprises a photosensitizer linked (usually, by –COOH, $-PO_3H_2$, or $-B(OH)_2$ functional groups) to the semiconductor surface, a solution containing a redox mediator, and a metallic counter electrode. The sensitizer is first excited by light absorption. The excited sensitizer then injects an electron, on the femto- to pico-second timescale, into the conduction band of the semiconductor. The oxidized sensitizer is reduced by a relay molecule, which then diffuses to discharge at the counter electrode which is a conductive glass. As a result, a photopotential is generated between the two electrodes under open-circuit conditions and a corresponding photocurrent can be obtained on closing the external circuit by use of an appropriate load.

A great number of photosensitizers of the Ru-oligopyridine family, which display metal-to-ligand charge-transfer excited states, have been employed. The most

Flexible Solar Cells. M. Pagliaro, G. Palmisano, and R. Ciriminna

ISBN: 978-3-527-32375-3

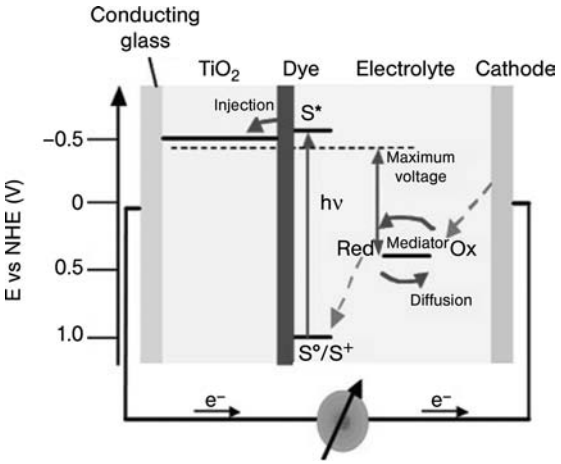

Figure 5.1 Operating scheme of a dye-sensitized nanocrystalline solar cell. The energy levels of the different phases are indicated. (Reproduced from Ref. [3], with permission).

efficient ones are those bearing two NCS- and two substituted bpy ligands, showing intense absorption bands in the visible region. A variety of solvents, of different viscosity, and redox mediators have been used, the most common being the I^{3-}/I^{-} couple in acetonitrile solution.

Invented in the early 1990s, dye-sensitized solar cells (DSC) entered the global market in 2003 with the first commercial modules based on this versatile hybrid (organic–inorganic) technology being installed in Australia.

With plastic solar cells, DSCs share the low weight, flexibility and the low cost of production due to roll-to-roll manufacturing of thin-film modules. Yet, their typical 7% efficiency in commercial modules is about twice the efficiency of polymeric modules; whereas their good performance in diffuse light conditions is a feature they have in common with inorganic thin film solar modules. Finally, dye cells work well in a wide range of lighting conditions and orientation and they are less sensitive to partial shadowing and low level illumination. All these attributes make them particularly well suited for architectonic applications. For example, colored DSC modules are excellent multifunctional building elements, capable of generating electricity either from outdoor daylight or indoors, while functioning as heat and noise insulators and weather protection materials (Figure 5.2) [4].

The Australian company Dyesol has pioneered the commercialization of DSCs and developed the technology in practically every aspect, including its engineering. A typical solar panel available from the company (Figure 5.3) is made of colored tiles (available in ochre, gray, green and blue colors) connected (in series or parallel) and sandwiched between two layers of glass, then further encapsulated in a UV-resistant polymer [5].

Dyesol manufactures the solar cells in the form of architectural panels for building facades and roofs. At Konarka Technologies, researchers are developing low-cost

Figure 5.2 Example of indoor building integration of transparent colored DSC at the Schott Iberica building in Barcelona (Spain). (Photo courtesy: Dr. I. B. Hagemann and Schott Iberica).

manufacturing processes to produce the cells on rolls of flexible plastic sheeting to be prepared in all sorts of sizes and shapes and applied to many kinds of surfaces.

In 2007, the US company G24 Innovations started roll-to-roll printing of DSC-based thin film solar modules in a factory based in Wales (UK) [6]. Its modules are less

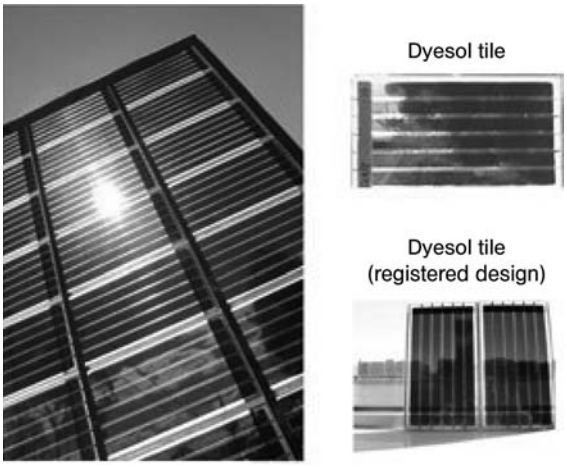

Figure 5.3 DSC Panels commercialized by Dyesol. (Photo courtesy: Dyesol).

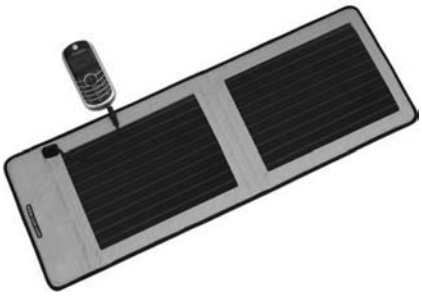

Figure 5.4 The *G10* charger commercialized by G24i. (Photo courtesy: G24 Innovations).

than 1 mm thick and the original production capacity of 25 MW in 2007 is planned to scale up to 200 MW in a few years, following market response to the initial commercialization. The first product is a solar charger series, working indoors and outdoors, compatible with mobile phones, laptops, audio players and digital cameras (Figure 5.4).

Many other companies worldwide are working in this field, including Mitsubishi, Dai Nippon, Peccell Technologies Sharp, Toshiba, IMRA-Aisin Seiki/Toyota and Sony in Japan, and Solaronix in Switzerland. Sony and Sharp, for example, have already developed highly efficient, proprietary DSC-based modules, already exhibited at international PV fairs and ready to be commercialized. Remarkably, these modules will be available either in the form of flexible solar panels or rigid and highly stable panels, much like the new CIS panels discussed in Chapter 3. In general, products envisaged by the producers cover a broad range from colorful decorative elements to electric power-producing glass tiles for facade integration in buildings.

In Israel, OrionSolar has developed inexpensive modules based on $15 \times 15\,cm^2$ dye cells, based on a low-cost method of depositing TiO_2 in a sponge-like array on top of flexible plastic sheets (Figure 5.5) [7].

The interest in this field of DSC is demonstrated by the large number of patents (>300 in 2005) and by the recently started organization of a series of conferences

Figure 5.5 Orionsolar dye cells have an additional advantage in that they are particularly suited to warmer climates. (Photo courtesy: OrionSolar).

dedicated specifically to the topic of industrialization of DSC (www.dyesol.com/conference).

5.2 DSC Working Principles

Contrary to conventional PV systems in which the same semiconductor absorbs light and works as a charge carrier, DSC are based on absorption and charge transfer from separate species. Hence, a dye "sensitizer" doping the semiconductor TiO_2, absorbs the light and then transfers an electron to the semiconductor conduction band (CB), through which electrons are led to an electrode working as charge collector [8].

The first example of high conversion efficiency DSC used a 10 μm thick, optically transparent film of TiO_2 particles of tens of nm in size, coated by a monolayer of a charge-transfer dye to sensitize the film for light harvesting. Remarkably, even this first cell had 7.1% efficiency and photocurrent density up to 12 mA cm^{-2} [1].

In addition, the performance of DSC is only slightly influenced by the temperature, in contrast with the other competing available technologies. Temperature variation in the 20–60 °C range has indeed practically no influence on the overall efficiency of the cell.

The working scheme is shown in Figure 5.1. DSC-based photovoltaics is a *kinetic phenomenon*. Indeed, once the electron is transferred into the CB, the thermodynamically preferred process is the back reaction with the oxidized sensitizer which would only produce thermal dissipation. For instance, with efficient ruthenium complexes, the forward injection process occurs in femtoseconds (10^{-20} s), whereas the back reaction of photoinjected CB electrons with the oxidized dye occurs in microseconds (Figure 5.6) [9].

Figure 5.7 shows the injection and recombination processes. Tailoring the semiconductor/sensitizer interface to minimize the back reaction is a major aim of current research. Such a recombination reaction is very sensitive to electron trap occupancy in the nanocrystalline TiO_2 with, for example, the recombination kinetics accelerating from milliseconds to picoseconds as an electrical bias is applied to the film to increase trap occupancy; hence this reaction may be critical in limiting device performance.

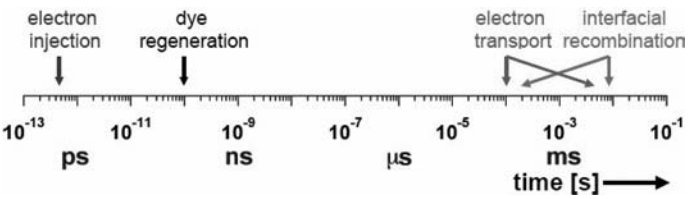

Figure 5.6 DSC photovoltaics is made possible by winning the dynamic competition between electron transport (that occurs in femtoseconds) and interfacial recombination (occurring in microseconds). (Reproduced from Ref. [10], with permission).

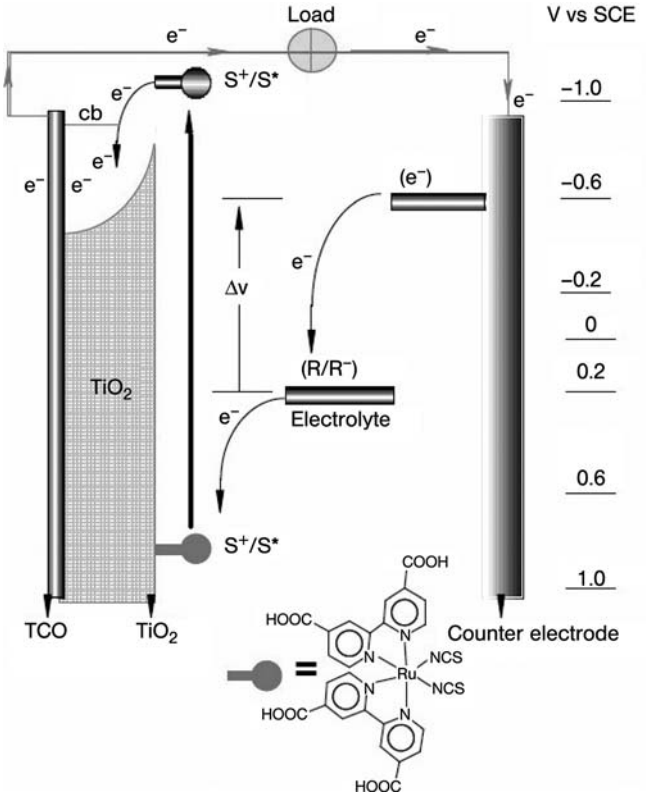

Figure 5.7 The injection and recombination processes at the surface of TiO_2 films in a typical DSC. (Reproduced from Ref. [8], with permission).

In addition to being a highly effective semiconductor, TiO_2 is also abundant, low cost, non-toxic and biocompatibile. Typically, nanocrystals of mesostructured TiO_2 in the anatase phase are prepared by sol–gel hydrothermal processing of a suitable titania precursor in the presence of a template such as Pluronic P123. The xerogel is isolated as a thin film supported on glass further covered by another conductive layer [11].

Mesoporosity ensures excellent penetration by the electrolyte into the inner porosity of the film's sol–gel cages, whereas a large surface roughness (roughness factors >1000) favors the penetration of light through hundreds of adsorbed dye monolayers. Annealing at 400–500 °C consolidates the mesoporous structure and frees the oxide from residual organic matter.

A typical film has the structure shown in Figure 5.8 and the properties listed in Table 5.1.

Using a lift-off technique, pre-sintered porous, composite layers comprising nanoparticles of TiO_2 up to tens of micrometers thick, are easily transferred to a second flexible substrate, and the original electrical properties of the transferred

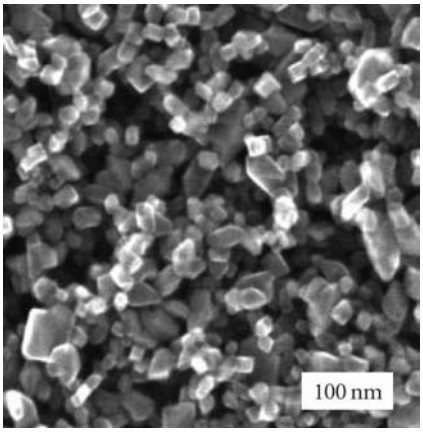

Figure 5.8 SEM picture of a nanocrystalline TiO_2 anatase film, used in dye-sensitized solar cells. (Reproduced from Ref. [12], with permission).

Table 5.1 Properties of common TiO_2 anatase films used in dye-sensitized solar cells.

Particle size (nm)	Film thickness (μm)	Porosity (%)	Average pore size (nm)
15–30	5–20	50–75	15

porous layers are maintained [13]. This avoids the need to use process temperatures of up to 500 °C, commonly used for sintering the TiO_2 nanoparticles, which typical flexible plastic substrates cannot withstand, and has opened the route to mass production of plastic solar cells based on the DSC technology.

A plastic substrate can also be used to afford flexible solar cells, whose efficiency is much improved by a method consisting of mechanical compression of a water-based TiO_2 paste to coat the film and prepare the TiO_2 photoelectrode without any heat treatment [14].

The resulting device (Figure 5.9) shows the highest light-to-electrical energy conversion efficiency based on plastic-substrate dye-sensitized solar cells, 7.4% under 100 mW cm^{-2} (1 sun) AM1.5 illumination. The first flexible DSC developed in the UK in 2003 had a remarkable 5.3% efficiency and was based upon dye sensitized nanocrystalline Al_2O_3-coated TiO_2 films and an I_2/NaI doped solid-state polymer electrolyte [15]. By changing the polymer electrolytes, the device current–voltage characteristics can be optimized to reach the highest efficiency (Figure 5.10) [16].

The University of Yokohama's spin-off Peccel Technologies in Japan is pursuing the development of plastic dye solar modules (Figure 5.11) using plastic titania electrodes. The company is currently developing new plastic sealers and expects to commercialize the first modules by 2010.

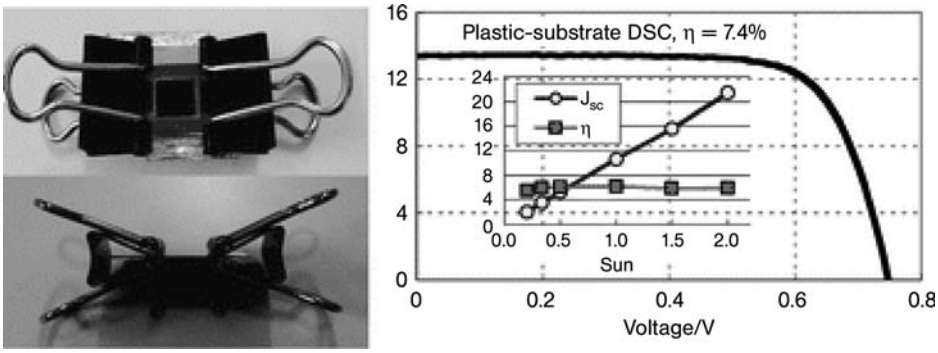

Figure 5.9 By simple pressing, a 7.4% flexible DSC can be easily obtained. (Reproduced from Ref. [14], with permission).

In general, any photoactive material can be fashioned in the form of an inverse opal leading to effects that transcend the sum of the parts and can be harnessed for practical purposes [17]. In this case the opal is a colloidal photonic crystal made of anatase TiO_2 and its role is to enhance light conversion efficiency in the red spectral range (600–750 nm), where the sensitizer is a poor absorber. The absorption enhancement arises from the position of the stop-band edges of the opal layer. Indeed, photons propagating through a photonic crystal present a very low group velocity, and this slow motion implies a higher probability of the photon being captured than in the disordered material.

Hence, simply coupling a conventional DSC to an inverse opal also made of titania results in an increase in the J_{SC} across the visible spectrum by about 26% relative to conventional dye solar cells made of a random collection of dye-sensitized anatase nanocrystallites with no photonic crystal lattice (Figure 5.12) [18].

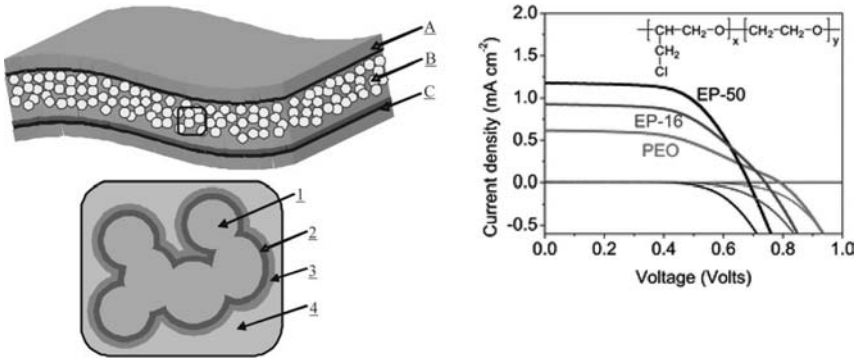

Figure 5.10 (a) The first flexible DSC was based upon nanocomposite film B sandwiched between ITO-coated (A) and Pt-coated ITO plastic (C) substrates. The nanocomposite film comprises four distinct structurally organised phases: (1) nanocrystalline TiO_2 film, (2) Al_2O_3 coating, (3) $Ru(L)_2(NCS)_2$ dye and (4) redox active polymer electrolyte interpenetrated in the film pores. (b) Using different polymer electrolytes, the device current–voltage characteristics can be optimized. (Reproduced from Ref. [16], with permission).

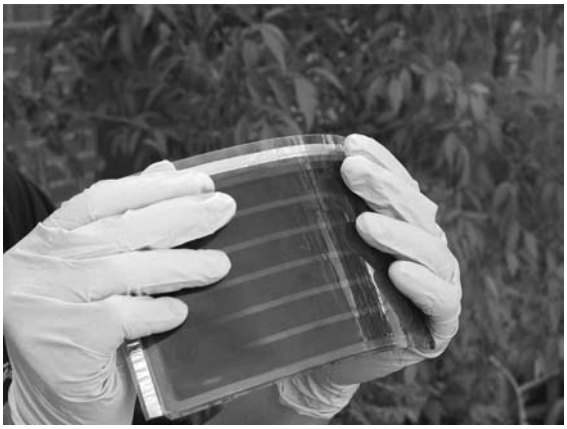

Figure 5.11 A flexible, plastic dye solar module manufactured by Peccell Technologies.

Once again, it is the bilayer *nanoarchitecture*, rather than enhanced light harvesting within the inverse opal structures, that is responsible for the bulk of the gain in incident photon-to-current conversion efficiency (IPCE) due to enhanced backscattering [19].

Detrapping of electrons from sub-band gaps to the CB is responsible for the electron transport [20]. The presence of traps in the film represent a major factor in limiting the efficiency of electron transportation, preventing their passage to the extracting electrode. Such traps are mostly present at the surface of TiO_2 rather than in the particle bulk or interparticle grain boundaries, as their number increases linearly with the exposed surface area [21].

As mentioned above, the redox couple in the electrolyte, most commonly iodide/triiodide, functions well because the electron transfer from nanocrystalline TiO_2 to I_3^- is much slower than that from a counter electrode [22]. The $I_2^{-\bullet}/I^-$ couple potential determines the thermodynamic driving force for the electron transfer from I^- to the oxidized dye. Indeed, the mechanism of electron transfer from TiO_2 to I_3^- is

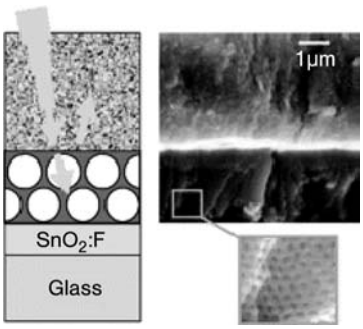

Figure 5.12 Coupling an inverse opal layer of titania to a conventional DSC also made of anatase results in 26% enhancement in the short circuit photocurrent. (Reproduced from Ref. [18], with permission).

preceded by a weak dissociative chemisorption of iodine on TiO_2:

$$I_3^- \leftrightarrows I_2 + I^- \tag{5.1}$$

$$I_2 + e^-_{(TiO_2)} \rightarrow I_2^{-\bullet} \tag{5.2}$$

Equation 5.1 has a very low equilibrium constant ($\sim 10^{-7}$ in acetonitrile), whereas the iodine radical is further reduced in a second electron transfer step:

$$I_2^{-\bullet} + e^-_{(TiO2)} \rightarrow 2I^- \tag{5.3}$$

Regeneration of the dye ground state involves reduction of the oxidized dye by iodide:

$$Ru(III) + 2I^- \rightarrow Ru(II) + I_2^{-\bullet} \tag{5.4}$$

Sensitizers are generally based on polypyridyl complexes of Ru with a $RuL_2(X)_2$ structure (Figure 5.13).

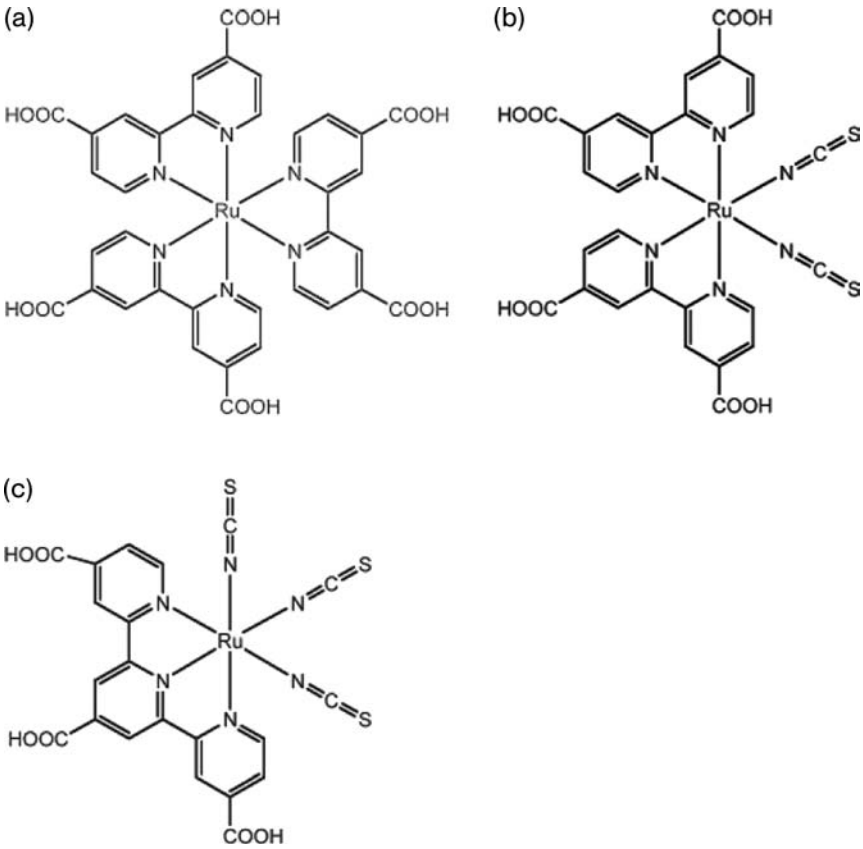

Figure 5.13 Structure of the ruthenium sensitizers (a) RuL_3, (b) *cis*-$RuL_2(NCS)_2$ and (c) $RuL'(NCS)_3$, where L = 2,2′-bipyridyl-4,4′-dicarboxylic acid and L′ = 2,2′,2″-terpyridyl-4,4′,4″-tricarboxylic acid. (Reproduced from Ref. [3], with permission).

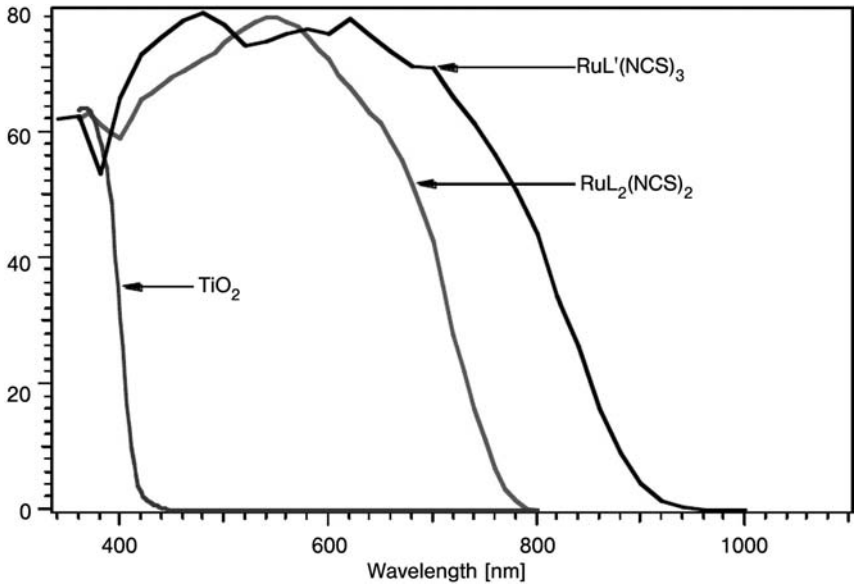

Figure 5.14 Incident photon to current efficiency obtained as the response of bare TiO_2 and TiO_2 sensitized by *cis*-$RuL_2(NCS)_2$ and $RuL'(NCS)_3$ (L = 2,2′-bipyridyl-4,4′-dicarboxylic acid and L′ = 2,2′,2″-terpyridyl-4,4′,4″-tricarboxylic acid). (Reproduced from Ref. [24], with permission).

The spectral response of these dyes is shown in Figure 5.14. The improvement of the IPCE in the visible range is clear with respect to bare TiO_2. The efficiency plateau is in both cases about 80%, and the response of $RuL'(NCS)_3$ has an extra 100 nm extension into the IR region.

An ideal sensitizer should absorb light below a threshold of about 900 nm. Carboxylate and phosphonate groups are needed in order to ensure grafting of the dye over the semiconductor surface, and thus fast electron injection into the conduction band of TiO_2 [23]. Fine tuning of the molecular orbitals by appropriate choice of the ligands eventually leads to a pronounced unit quantum yield for electron injection ϕ_{inj} and solar to power conversion of 10.4%, such as in the case of the $RuL'(NCS)_3$ dyes (Figure 5.14) [24].

The redox electrolyte regenerates the sensitizer, provided that the respective redox potentials are compatible. Sensitizer stability, moreover, is a key point for DSC, and 10^8 turnover cycles should be achievable theoretically without any significant modification. This last condition corresponds to about 20 years of exposure to natural light.

The light-harvesting efficiency (LHE), is related to the absorption length and to the thickness of the film through Beer–Lambert's law (Equation 5.5), whereas the IPCE is proportional to the quantum yield for electron injection ϕ_{inj} and the electron

$$LHE(\lambda) = 1 - 10^{-\alpha d} \tag{5.5}$$

collection efficiency η_{coll} (Equation 5.6):

$$IPCE(\lambda) = LHE(\lambda)\phi_{inj}\eta_{coll} \tag{5.6}$$

In which $\alpha = \sigma c$ is proportional to the optical cross section of the sensitizer σ and to its concentration c in the film. Clearly the LHE values depend strongly on the wavelength, approaching values over 90% near the absorption maxima of the dyes. Techniques to increase the absorption in the red and near-infrared spectrum can be applied. The most common consists in incorporating larger TiO_2 particles (100–300 nm) in the mesoporous film, also improving the absorption in the areas where the optical cross section of the sensitizer is small [25]. The use of mixtures of dyes is an attractive option to achieve panchromatic devices in which dyes absorbing in different spectral regions are blended without any negative interference [26].

5.3
A Roadmap for Dye Solar Cells

Dye sensitized cells are very tolerant to the effects of impurities because both light absorption and charge separation occur near the interface between two materials. The relative impurity tolerance and simplicity allows for easy, inexpensive scale-up to non-vacuum- and low-temperature-based high-volume manufacturing via continuous processes including screen-printing, spraying, pressing, or roll-to-roll production. Indeed, manufacture of the first industrial modules uses an automated "roll-to-roll" process transforming a lightweight roll of metal foil into a 45 kg half-mile of G24i's dye-sensitized thin film in less than three hours (Figure 5.15) [4].

This material is rugged, flexible, lightweight and generates electricity even indoors and in low light conditions. In place of liquid electrolyte, solid or quasi-solid hole conductors can be employed [27], but the reduction in efficiency currently precludes practical application.

The first, and still the most efficient electrolytes were liquid, so cell and module designs which prevented electrolyte leakage had to be developed to prevent evaporation. The stability and lifetime of DSC modules have thus reached appreciable values (Figure 5.16), and rapid improvements are being made.

Figure 5.15 Roll-to-roll production of the first PV modules results in a flexible, lightweight PV material suitable for largely different applications. (Photo courtesy of G24 Innovations).

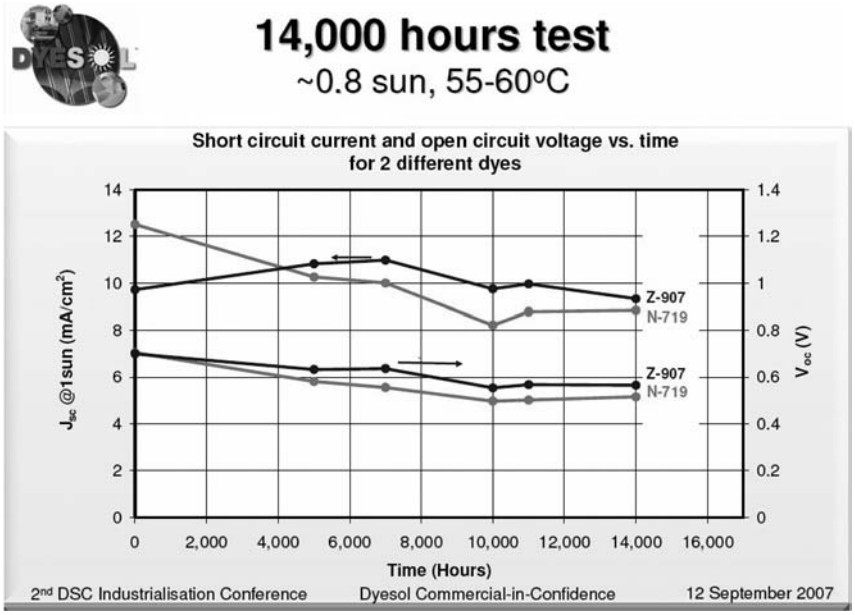

Figure 5.16 Stability of DSC-based solar modules has reached 22 years in Central Europe and 13 years in the warmer, Southern Europe. However, rapid improvements are being made. (Image courtesy of Dyesol).

A major advance is the recent solvent-free DSC based on an ionic liquid (IL) mixture of 1-ethyl-3 methylimidazolium tetracyanoborate and 1-propyl-3-methyl-imidazolium iodide as electrolyte and the ruthenium complex, Ru(2,2′-bipyridine-4,4′-dicarboxylic acid)(4,4′-bis(2-(4-tert-butyloxy-phenyl)ethenyl)-2,2′-bipyridine)$(NCS)_2$ as sensitizer [28]. The resulting cells show the record light-conversion efficiency of 7.6% under simulated sunlight conditions and are stable at 80 °C in the dark and under visible-light soaking at 60 °C for over a thousand hours, with a cell efficiency loss of only 10%, which points to the possibility of their use in outdoor applications in warm climates. The low viscosity of the binary IL helps to overcome mass-transfer challenges, whereas the inert anion counteracts the deleterious influence of the iodide anions. A short-circuit photocurrent density around 14 mA cm^{-2}, open circuit voltages of about 0.7 V and fill factors of 0.7 were obtained.

Such is the promise of ILs for future generation dye PV modules, that G24i, the first producer of these modules, entered into agreement with BASF to work on the selection of suitable ILs for their forthcoming products.

New high surface area electrodes have overcome both the recombination and the slow diffusion of the injected electron in the porous TiO_2 layer (Figure 5.17) [29].

The new electrode design involves a core shell configuration consisting of a conductive nanoporous matrix coated with standard wide band gap TiO_2 (Figure 5.17). In this "collector-shell electrode" the distance between the injection spot and the current collector decreases to several nanometers from the several micrometers

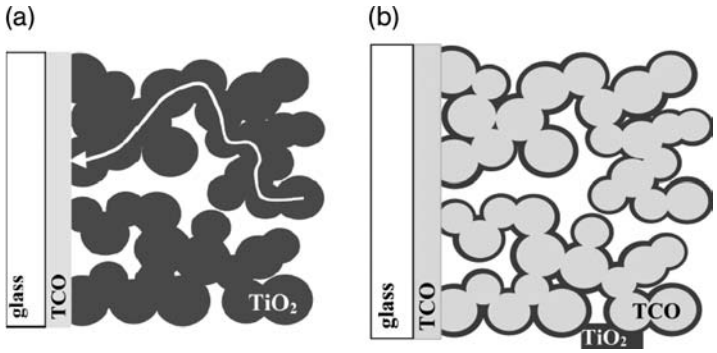

Figure 5.17 The new, efficient electrode for DSC is based on a conductive nanoporous core (b) rather than a semiconducting one (a) as in the standard design. (Reproduced from Ref. [22], with permission).

associated with the standard electrode. In other words, all electrons injected into the electrode, including those that are generated several micrometers away from the substrate, have now to travel a very short distance before reaching the current collector. This new design enables efficient charge separation and collection for thick nanoporous layers provided that its thickness is above 6 nm, when much higher V_{OC} (or photocurrent) values are reached (Figure 5.18).

In practice the results presented in Figure 5.18 reflect a change in the rate-determining factor of the recombination process, from surface reaction control in the thin films to a transport limited rate in the thick ones. The Israeli company Orion Solar uses this technology for producing its large dye modules equipped with 15 × 15 cm cells.

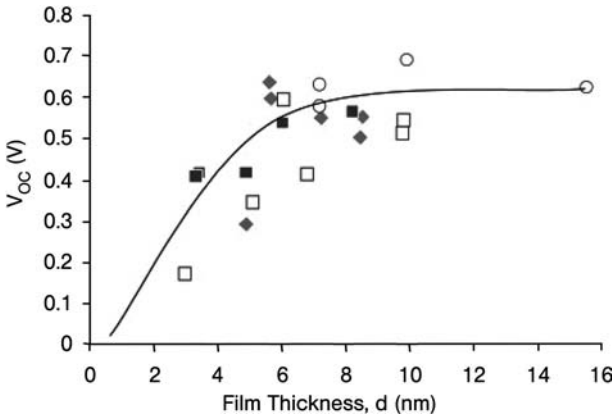

Figure 5.18 Correlation between the thickness of the TiO_2 layer and the open circuit photovoltage in the DSSC. The symbols represent sets of electrodes that were made by the different preparation methods. (Reproduced from Ref. [22], with permission).

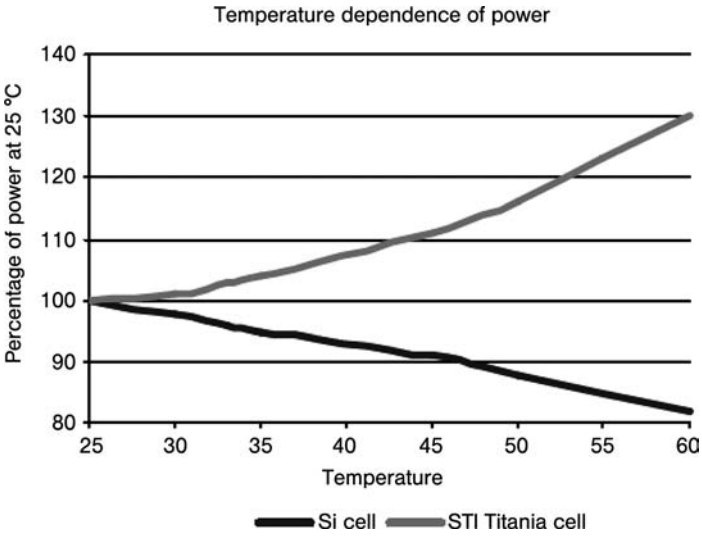

Figure 5.19 In contrast to Si-based modules, the performance of dye PV modules increases with temperature. (Reproduced from Ref. [30], with permission).

In addition to low cost (the materials are inexpensive and abundant: titania is widely used in toothpastes, sunscreen and white paint) and ease of production (see below), the unique advantages over Si-based cells lie in their transparency (for power windows), easy bifacial configuration (advantage for diffuse light) and versatility (the color can be varied by selection of the dye, including invisible PV-cells based on near-IR sensitizers). Furthermore, in contrast to Si-based modules, the performance of dye PV modules actually increases with temperature (Figure 5.19).

As a result, they outperform amorphous Si-based modules, despite their lower 5% efficiency. This was demonstrated, for example, during the 2005 Expo in Japan when the Toyota exhibition house was equipped with DSC modules consisting of wall-integrated $2.5 \times 2.5\,m^2$ solar panels (Figure 5.20). Monitoring of the energy produced revealed that the DSC modules give a faster output rise in the morning and a slower fall in the afternoon due to a different dependence on the solar insolation angle [31].

According to a recent report [32], stable 10% efficient modules are certainly within reach, with the energy-payback period being significantly shorter than other PV technologies. As evidence of chemical and thermal robustness, recent accelerated aging tests showed that $\geq$8%-efficient laboratory DSSCs retain 98% of their initial performance over 1000 h when subjected to thermal stress (80 °C) in the dark or when exposed to both thermal stress (60 °C) and continuous light-soaking over 1000 h. Outdoor tests (Toyota/Aisin) of first-generation DSSC modules have shown less than 15% degradation in four years. These results and others inspire investment in the technology, and several companies are working toward commercializing this technology.

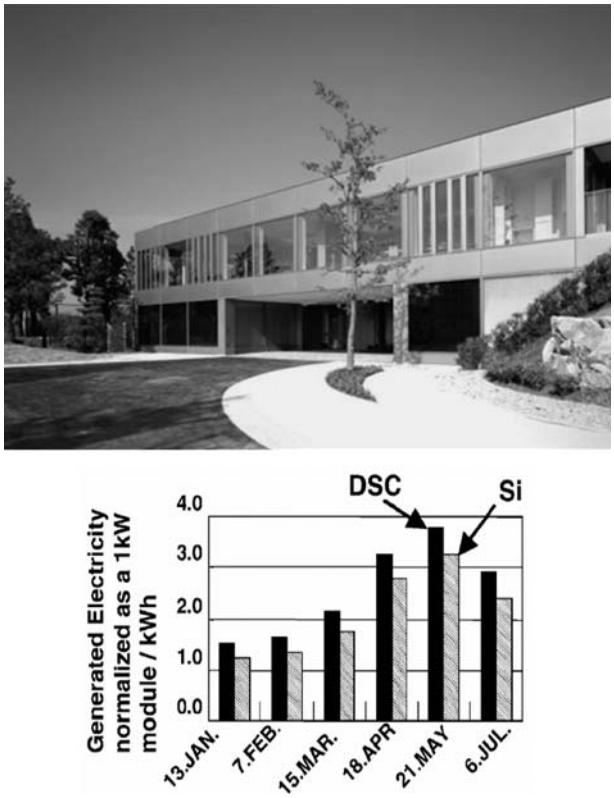

Figure 5.20 Toyota's exhibition house at Aichi 2005 Expo was equipped with two large, elegant DSC modules whose output outperformed that of an a-Si panel. (Reproduced from www.tytlabs.co.jp/english/news/tec/elech41_1_higuchi.pdf, with permission).

By 2015, it is expected that companies will attain 10% efficient modules that approach the criteria for solar module certification for thermal aging at 85 °C for 1000 h in the dark and for light-soaking in full sunlight for 1000 h at 60 °C. A realistic goal is that 20% efficient laboratory-sensitized solar cells will be achieved (Table 5.2).

Research on innovative dyes, for example, is expected to lead to considerable improvement in the cell's efficiency. Mitsubishi, a leading manufacturer of PV traditional modules, has developed a whole new series of undisclosed, high-efficient new dyes. Progressively, the company makes its proprietary newly developed dyes available to Japan's scientific community engaged in PV research. Among such dyes, in the early 2000s there was the first example of a metal-free, entirely organic dye, indoline (Figure 5.21).

In 2003 the new indoline dye was 8.00% efficient, whereas under the same conditions, the Ru-based dyes N3 and the N719 dye were 7.89 and 8.26% efficient, respectively [33]. At that time, this value was the highest obtained efficiency for dye-sensitized solar cells based on metal-free organic dyes without an antireflection layer.

Table 5.2 Performance characteristics for present and future PV dye-sensitized solar cells.

Parameter	Present status (2007)	Future goal (2015)
Champion device efficiency	11%	16%
Laboratory cell degradation	<5% after stress at 80 °C for 1000 h in dark or after light-soaking for 100 h at 1 sun at 60 °C	<5% after stress at 85 °C for 3000 h in the dark or after light-soaking for 3000 h at 1 sun at 60 °C
Module efficiency	5–7%	10%
Outdoor module degradation	<15% in 4 years	<15% in 10 years
Identification of key degradation mechanisms	degradation mechanisms are controversial	primary degradation mechanisms identified

(Reproduced from Ref. [34], with permission).

More recently, the Grätzel group has reported on a 15% tandem cell consisting of a DSC top cell and a Cu(In,Ga)Se bottom cell. By stacking the two cells an efficiency of 15% is obtained, which is roughly twice the value of each cell individually. ECN is investigating the possibility of replacing the electrolyte commonly used in DSC by a simple gold electrode.

Important advances have been made in DSC technology [34]. While the best laboratory cell efficiency of more than 11% established by the Grätzel group at EPFL (Switzerland) was not equalled by other groups, several advances in DSC module development have been presented. The Frauenhofer ISE (Freiburg, Germany) fabricated a 1 cm^2 laboratory solar cell with certified efficiency of 10.4%. They demonstrated sealed 30 cm by 30 cm modules containing six interconnected cells providing 0.8 A at 4.2 V. By improving the printing process, efficiencies of 5% are

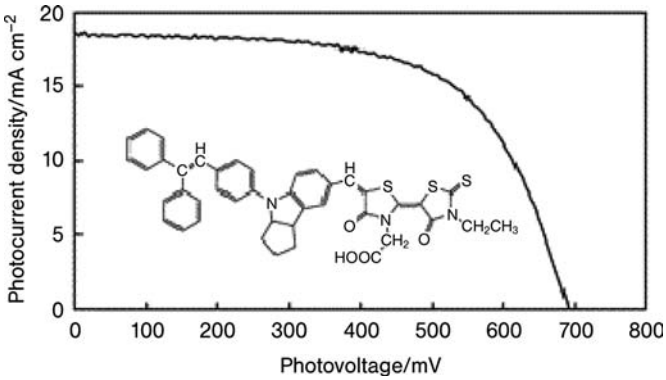

Figure 5.21 Photocurrent–voltage curve for the metal-free based DSC developed by Mitsubishi in the early 2000s. The company has developed a brand new series of dyes for DSC and is ready to enter mass production. (Reproduced from Ref. [33], with permission).

targeted for modules as large as 60 cm by 100 cm. ECN (Petten, Netherlands) demonstrated certified DSC efficiencies of 8.81% obtained on $2.5 \times 2.5\,cm^2$ cells. SHARP (Japan) presented a very nice 25 cm by 25 cm black DSC module with a thickness of 0.8 cm. The module consists of 43 cells providing a maximum power of 3 W, which corresponds to a remarkable power efficiency of 4.8%. Most of the other works reported on the fabrication of flexible solar cells use PET (CREST, Leicester, UK) or stainless steel substrates (HUT, Helsinki, Finland).

5.4
Building-Integrated PV with Colored Solar Cells

Due to its elegant colored and transparent aspect, the DSC technology is particularly well suited for being integrated into buildings. Sensitized solar cells operate optimally over a wide range of temperatures and their efficiency is relatively insensitive to the angle of incident light. The DSC is also particularly suited to indoor applications that require stability of voltage and power output over a wide range of low light conditions.

The range of applications is vast because the sensitizer can take on any color with a full range of transparencies. This allows for building-integrated windows, walls, and roofs of varying color and transparency that will simultaneously generate electricity, even in diffuse light or at relatively low light levels, in addition to whatever other function they serve.

The integrated module design comprises two sheets of conducting glass with the electrode deposited on one sheet and the counter-electrode deposited on the second sheet (Figure 5.22).

Such optionally transparent or translucent modules are hermetically sealed for ultra-long life and are suitable for high solar radiation. Indeed, the DSC is particularly suited to target markets in temperate and tropical climates, because of its good temperature stability and its excellent performance under indirect radiation, during cloudy conditions, and when temporarily or permanently partially shaded.

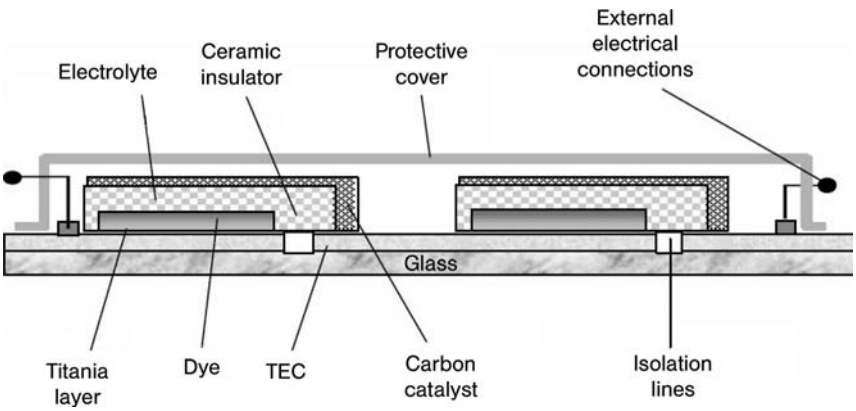

Figure 5.22 Integrated module design for a typical DSC module. (Image courtesty of Dyesol).

In general, the production of commercial cells is a straightforward nine-step process, easily scaled up. A transparent conducting oxide glass is coated by spreading out a given volume, of ~10 ml cm^{-2} of titanium dioxide commercial paste (Ti-Nanoxide T, for example) to give a layer of 8 µm.

Optimal sintering is carried out by heating the electrode to about 450 °C for about 30 min, to allow the titanium dioxide nanocrystals to "melt" partially together, and thus ensure electrical contact and mechanical adhesion on the glass. Slow cooling ensures that cracking of the glass is avoided. Then a sensitizer such as Ruthenium 535 dissolved in pure ethanol (20 mg of dye per 100 mL of solution) is used to impregnate the sintered electrode (either heated at ~70 °C when it will take only 1–2 h, or at room temperature when it will take about 5–10 h, depending on the actual titanium dioxide layer thickness).

The counter-electrode of the cells prdouced by Solaronix [35], for example, is made by depositing an invisible layer of platinum catalyst on a TCO glass. The electrodes are then sealed with an appropriate sealing material (Figure 5.23). Finally, electrolyte filling is done by adding a droplet onto one hole, and letting it soak in. After sealing the cells, testing of such a DSC, having silver painted contacts to ensure optimal electrical connections and to minimize serial resistance losses, yields a typical output voltage in the range of 0.6–0.7 V in full light (1000 W m^{-2}); and short-circuit current density between 8 and 12 mA cm^{-2} for a 8–10 µm thick fully impregnated electrode. The current remains constant under illumination.

A standard DSC ochre tile is designed to be isostrucutral to the façade (Figure 5.24). In other words, it replaces the traditional tiles and functions as a true building element. These tiles can be connected in series or parallel to produce 12 or 24 V solar

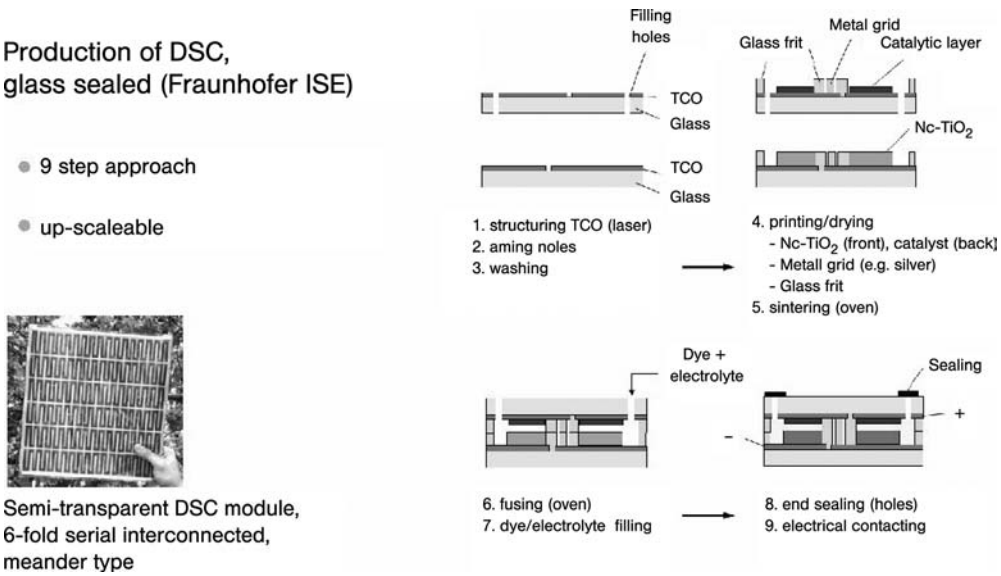

Figure 5.23 Cross-section of assembled dye solar cell showing sealing rim. (Image courtesy: Fraunhofer ISE).

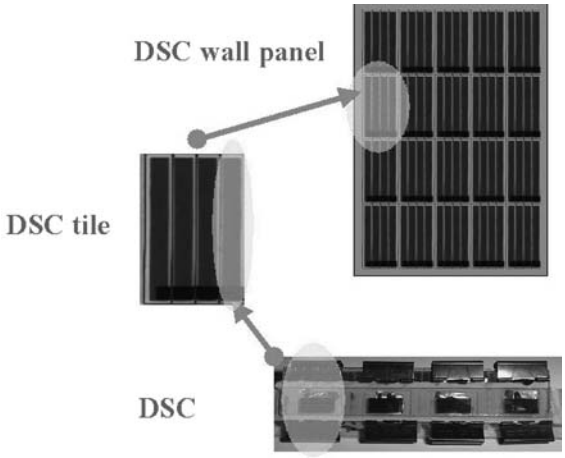

Figure 5.24 Solar wall panels are made of DSC tiles connected in series or in parallel and function as true building blocks. (Photo courtesy of Dyesol).

panels. The solar panel modules, of varying sizes to meet the existing market requirements, are rated initially at about 50 Wp m^{-2} for a typical panel of 600 × 900 mm^2. The rated power is expected to rise by 40% over the next few years as techniques are being developed to reduce voltage losses due to junction formation at the interfaces.

Solar wall panels are constructed in a laminated design, with the connected tiles sandwiched between two panes of glass, fully encapsulated in the UV-resistant transparent laminating polymer. The electrical interface can be typically via a short DC bus to a local area network for regulation and distribution or inversion to AC.

The world's first such integration occurred in Australia (home country of Dyesol) in 2003 as the research body CSIRO commissioned a DSC BIPV system for the CSIRO Energy Center, in Newcastle. Dyesol manufactured the solar wall panels to supply and install (Figure 5.25).

5.5 Personalizing Solar Power

Compared to all other PV technologies, DSC-based photovoltaics offers a unique versatility that architects and engineers will harness to renew the facades of existing buildings, as well as in the construction of new estate. In other words, it will enable a true personalization of solar power.

In wealthy countries, the building industry has become entirely customer-driven. Customer needs are identified locally, and then met by tailoring design and architecture to these needs. This means that the traditional PV industry with a bulk production of standard devices for the world market is of practically no use to this

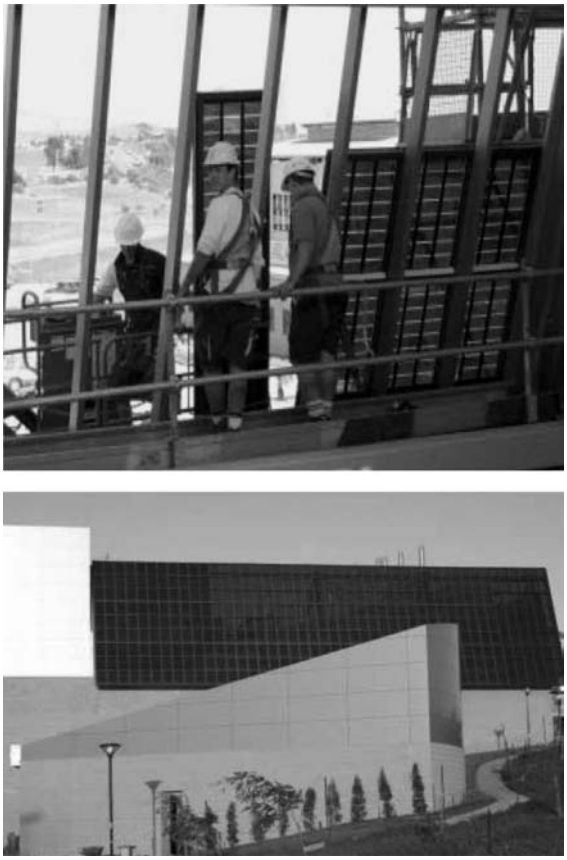

Figure 5.25 One of the facades of the new CSIRO Energy Centre, in Newcastle, Australia, was made with Dyesol's solar wall panels. (Photo courtesy of CSIRO and Dyesol).

large portion of the building industry. DSC modules offer a solution to this problem enabling the production of semi-finished products that can be adapted to individual building situations [36]. (Figure 5.26).

DSC modules offer flexibility, light weight, transparency, power performance under low light conditions and do not suffer power losses on heating during hot days. For DSC on glass substrates, one should note that glass is among the preferred materials for today's building. DSC can be integrated into modified standard glass facades and processes that are familiar in the glass industry such as screen printing will be widely used.

Eventually, once marketed, plastic dye solar cells will provide building component manufacturers with flexible, thin and lightweight PV foil that allows a seamless integration with building materials of various architectural shapes, thus realizing not only the total and esthetic merger between PV and architecture, but also a cost effective PV integration.

Figure 5.26 Built in 2005, this house in Australia uses the DSC-based Living Building Panel from Dyesol. (Photo courtesy: Dyesol).

In general, as stated by Hagemann [4], we are evolving from the old, serial PV product development scheme to one in which basic and applied research are carried out together using information fed back from manufacturing, marketing and social evaluation of technology (Figure 5.27).

Therefore, the value added chain becomes one in which design and marketing enter the chain from the very beginning of the product development, enriching the value of the product with unique features such as printing decorative elements (Figure 5.28).

This is what Germany's Fraunhofer Institute is currently doing by interviewing architects in the field of building-integrated PV and transferring requirements to the production of two prototypes for facade integration. Glass modules with 4–5% efficiency over the total area are likely to reach the market in 2009 following demonstration on a few square meters [36].

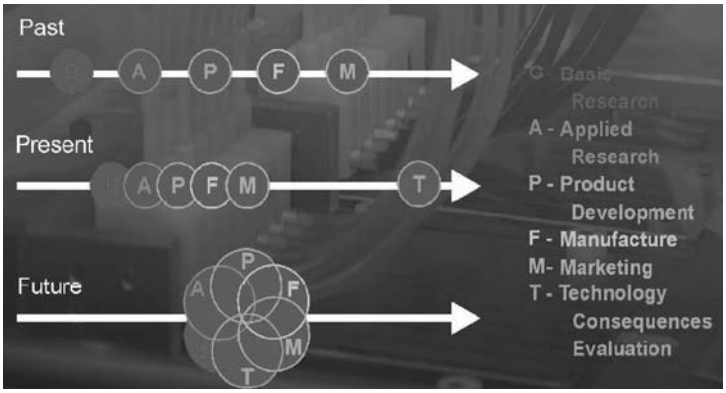

Figure 5.27 PV product development is evolving from an older, serial approach to one in which basic and applied research are performed using information fed back from marketing and societal acceptance of the technology. (Source: Ingo W. Hagemann).

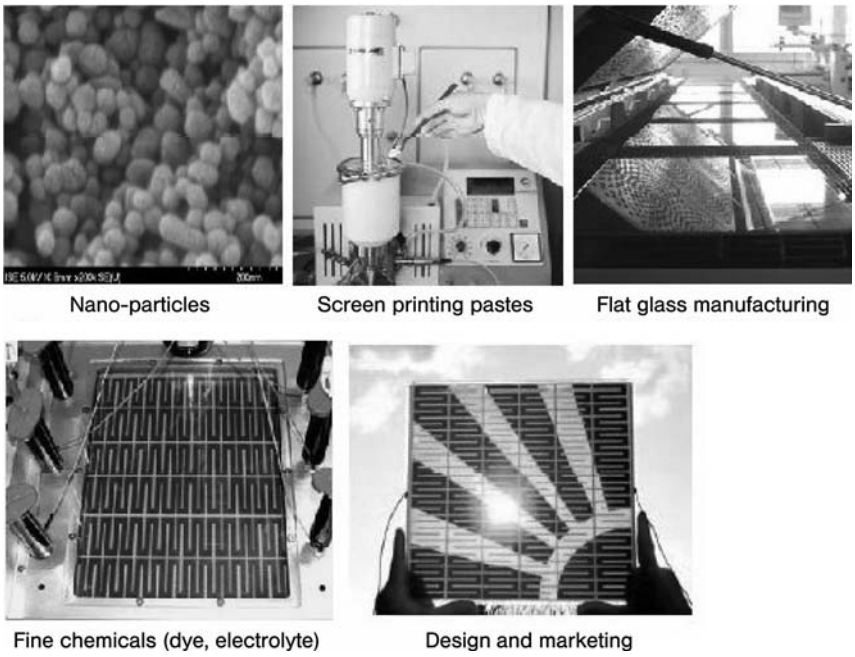

Figure 5.28 Marketing and design enter the value chain of dye solar modules production since the early development of the commercial products. (Photo courtesy: Fraunhofer ISE).

References

1 O'Regan, B. and Grätzel, M. (1991) A low-cost, high-efficiency solar cell based on dye-sensitized colloidal TiO_2 films. *Nature*, **353**, 737.

2 Balzani, V., Credi, A. and Venturi, M. (2008) Photochemical Conversion of Solar Energy. *ChemSusChem*, **1**, 26.

3 Grätzel, M. (2005) Solar conversion by dye-sensitized photovoltaic cells. *Inorganic Chemistry*, **44**, 6841.

4 Hagemann, I.B.(11–13 September 2007) New perspectives for building integrated photovoltaics, Proceedings of the 2nd International Conference on the Industrialisation of DSC, St Gallen, Switzerland (DSC-IC 2007).

5 See the company's website at: http://www.dyesol.com.

6 See the company's website at: http://g24i.com.

7 See the company's website at: http://www.orionsolar.net.

8 Peter, L.M. (2007) Dye-sensitized nanocrystalline solar cells. *Physical Chemistry Chemical Physics*, **9**, 2630.

9 Nakade, S., Kubo, W., Saito, Y., Kanzaki, T., Kitamura, T., Wada, Y. and Yanagida, S. (2003) Influence of measurement conditions on electron diffusion in nanoporous TiO_2 films: effects of bias light and dye adsorption. *Journal of Physical Chemistry B*, **107**, 14244.

10 Nazeeruddin, M.K.(May 29 2006) Dye Sensitized Solar Cells, Presentation at the International Summer School 2006, Krutyn (Poland).

11 Ito, S., Zakeeruddin, S.M., Humphry-Baker, R., Liska, P., Charvet, R., Comte, P., Nazeeruddin, M.K., Péchy, P., Takata, M., Miura, H., Uchida, S. and Grätzel, M. (2006) High-efficiency organic-dye sensitized solar cells controlled by nanocrystalline-TiO_2 electrode thickness. *Advanced Materials*, **18**, 1202.

12 Lenzmann, F.O. and Kroon, J.M. (2007) Recent advances in dye-sensitized solar cells. *Advances Optoelectronics*, 65073.

13 Dürr, M., Schmid, A., Obermaier, M., Rosselli, S., Yasuda, A. and Nelles, G. (2005) Low-temperature fabrication of dye-sensitized solar cells by transfer of composite porous layers. *Nature Materials*, **4**, 607.

14 Yamaguchi, T., Tobe, N., Matsumoto, D. and Arakawa, H. (2007) Highly efficient plastic substrate dye-sensitized solar cells using a compression method for preparation of TiO_2 photoelectrodes. *Chemical Communications*, 4767.

15 Haque, S.A., Palomares, E., Upadhyaya, H.M., Otley, L., Potter, R.J., Holmesc, A.B. and Durrant, J.R. (2003) Flexible dye sensitised nanocrystalline semiconductor solar cells. *Chemical Communications*, 3008.

16 Upadhyaya, H.M., Hirata, N., Haque, S.A., de Paoli, M.-A. and Durrant, J.R. (2006) Kinetic competition in flexible dye sensitised solar cells employing a series of polymer electrolytes. *Chemical Communications*, 877.

17 Ozin, G.A. and Arsenault, A.C. (2005) *Nanochemistry*, RSC Publishing, Cambridge. 360.

18 Nishimura, S., Abrams, N., Lewis, B.A., Halaoui, L.I., Mallouk, T.E., Benkstein, K.D., van de Lagemaat, J. and Frank, A.J. (2003) Standing Wave Enhancement of Red Absorbance and Photocurrent in Dye-Sensitized Titanium Dioxide Photoelectrodes Coupled to Photonic Crystals. *Journal of the American Chemical Society*, **125**, 6306.

19 Halaoui, L.I., Abrams, N.M. and Mallouk, T.E. (2005) Increasing the Conversion Efficiency of Dye-Sensitized TiO2 Photoelectrochemical Cells by Coupling to Photonic Crystals. *Journal of Physical Chemistry B*, **109**, 6334.

20 Bisquert, J. (2004) Chemical diffusion coefficient of electrons in nanostructured semiconductor electrodes and dye-sensitized solar cells. *Journal of Physical Chemistry B*, **108**, 2323.

21 Kopidakis, N., Neale, N.R., Zhu, K., van de Lagemaat, J. and Frank, A.J. (2005) Spatial location of transport-limiting traps in TiO_2 nanoparticle films in dye-sensitized solar cells. *Applied Physics Letters*, **87**, 202106.

22 Peter, L.M. (2007) Characterization and modeling of dye-sensitized solar cells. *Journal of Physical Chemistry C*, **111**, 6601.

23 Greijer Agrell, H., Lindgren, J. and Hagfeldt, A., (2004) Coordinative interactions in a dye-sensitized solar cell. *Journal of Photochemistry and Photobiology A: Chemistry*, **164**, 23.

24 Nazeeruddin, M.K., Pechy, P., Renouard, T., Zakeeruddin, S.M., Humphry-Baker, R., Comte, P., Liska, P., Cevey, L., Costa, E., Shklover, V., Spiccia, L., Deacon, G.B., Bignozzi, C.A. and Grätzel, M. (2001) Engineering of efficient panchromatic sensitizers for nanocrystalline TiO_2-based solar cells. *Journal of the American Chemical Society*, **123**, 1613.

25 Tomita, T. (2007) (Sony Co.), US Patent 7,312,507.

26 Cid, J.-J., Yum, J.-H., Jang, S.-R., Nazeeruddin, M.K., Martínez-Ferrero, E., Palomares, E., Ko, J., Grätzel, M. and Torres, T. (2007) Molecular co-sensitization for efficient panchromatic dye-sensitized solar cells. *Angewandte Chemie-International Edition*, **46**, 8358.

27 Li, B., Wang, L., Kang, B., Wang, P. and Qiu, Y. (2006) Review of recent progress in solid-state dye-sensitized solar cells. *Solar Energy Materials and Solar Cells*, **90**, 549.

28 Kuang, D., Klein, C., Zhang, Z., Ito, S., Moser, J.-E., Zakeeruddin, S.M. and Grätzel, M. (2007) Stable, high-efficiency

ionic-liquid-based mesoscopic dye-sensitized solar cells. *Small*, **3**, 2094.

29 Chappel, S., Grinis, L., Ofir, A. and Zaban, A. (2005) Extending the Current Collector into the Nanoporous Matrix of Dye Sensitized Electrodes. *Journal of Physical Chemistry B*, **109**, 1643.

30 Dyesol, DSC Solar Technology for the New Millenium, (2006). http://www.sta.com.au/downloads/DSC%20Booklet.pdf.

31 R&D Review of Toyota CRDL Vol.41 No.1. Available at: http://www.tytlabs.co.jp/english/news/tec/etech41_1_higuchi.pdf.

32 Matson, R.(June 2007) *Sensitized Solar Cells*, NREL/MP-520-41739Management Report.

33 Horiuchi, T., Miura, H., Sumioka, K. and Uchida, S. (2004) High Efficiency of Dye-Sensitized Solar Cells Based on Metal-Free Indoline Dyes. *Journal of the American Chemical Society*, **126**, 12218.

34 Nüesch, F.(4–8, September 2006) Organic and hybrid solar cells, 21st European Photovoltaic Solar Energy Conference and Exhibition Dresden.

35 http://www.solaronix.ch/technology/dyesolarcells/.

36 Hinsch, A., Putyra, P., Würfel, U., Brandt, H., Skupien, K., Drewitz, A., Einsele, F., Gerhard, D., Gores, H., Hemming, S., Himmler, S., Khelashvili, G., Nasmudinova, G., Opara-Krasovec, U., Rau, U., Sensfuß, S., Walter, J. and Wasserscheid, P. (7 September 2007) Developments towards low-cost Dye Solar Modules, 22nd European Photovoltaic Solar Energy Conference and Exhibition, Milano.

6
Emerging Technologies

6.1
The Solar Paradox

The only source of power that we have enough supply for is solar energy. We simply do not have enough wind, wave, geothermal, nuclear or biomass in our resources to cut our CO_2 levels and to create enough energy for only twice the amount required to feed every human by 2050 [1]. On the other hand, solar power generation will be a meaningful tool in limiting climate risks only when it can compete with other electricity sources on cost in developing countries, where even a small additional marginal cost can deter people and businesses (even the most prosperous of them) from switching to renewable energy options.

A power flow of 120 000 TW (terawatt) showers the Earth as photons from the sun reach the atmosphere and then land and sea. Covering just 0.16% of the Earth's surface with modest 10%-efficient PV systems would provide 20 TW of power, nearly twice the world consumption rate of fossil energy [2]. In other words, approximately 1/10 000 of the sunlight reaching the Earth would be sufficient to supply the whole world with energy. However, solar power is diffuse (about 170 W m^{-2}) and intermittent, so conversion into useful forms of energy should involve concentration and storage.

As seen in Chapter 1, our understanding of the photosynthetic processes in plants is rapidly advancing and, one day, these chemical processes will be mastered by industry to produce hydrogen, an excellent chemical fuel, especially suited to power fuel cells which in their turn produce large amounts of power with 80% efficiency (compare with the 20% efficiency of the internal combustion engine).

The grand challenges for today's chemists are thus twofold: (i) to create an artificial photosynthetic process for artificial conversion of solar energy into fuel and (ii) to invent new solar cells capable of achieving photovoltaic conversion at high efficiency [4]. Then, civilization will continue based on the sun's energy, as clearly foreseen by Giacomo Ciamician one hundred years ago (Figure 6.1), in his famous *The Photochemistry of the Future* lecture delivered in New York in 1912 [5].

Flexible Solar Cells. M. Pagliaro, G. Palmisano, and R. Ciriminna

ISBN: 978-3-527-32375-3

Figure 6.1 "Our black and nervous civilization based on coal, – foresaw chemist G. Ciamician as early as 1912 – shall be followed by a quieter civilization based on the utilization of solar energy." (Reproduced from Ref. [3], with permission).

> *So far human civilization has made use almost exclusively of fossil solar energy. Would it not be advantageous to make a better use of radiant energy?... Solar energy is not evenly distributed over the surface of the earth. There are privileged regions, and others that are less favored by the climate. The former ones would be the prosperous ones if we should become able to utilize the energy of the sun. The tropical countries would be conquered by civilization which would in this manner return to its birth-place... If our black and nervous civilization, based on coal, shall be followed by a quieter civilization based on the utilization of solar energy, that will not be harmful to the progress and to human happiness.*

Photovoltaics, on the other hand, *already*, on its own, has the potential to replace nuclear power on the required timescale, even in northern countries such as the U K. For example, the UK currently generates 12 GW (gigawatts) of electricity from nuclear power stations, around one sixth of the country's total electricity output. This is the same amount of pollution-free energy electricity that Germany will generate through photovoltaics by 2012 if it continues to expand its solar energy programme at its present rate [6].

The UK has a similar sunshine profile to Germany and could produce 12 GW of solar electricity by 2023 if production is expanded by 40% per year, less than the world increase of 57% in 2004.

The most common first-generation PV cells consist of single-crystalline silicon, have efficiencies around 15–17%, a lifetime of about 30 years and a cost for grid-connected

electricity of about 0.20–0.80 $/kWh. In particular, typical costs of 20–40 cents/kWh for low latitudes with solar insolation of 2500 kWh/m^2/year; 30–50 cents/kWh for 1500 kWh/m^2/year (typical of Southern Europe); and 50–80 cents for 1000 kWh/m^2/year (higher latitudes) [7].

These costs should to be compared to electric grid supplies from fossil fuels, which vary between 0.03 (off-peak, developed country) and 0.80 $/kWh (rural electrification). The energy payback time of a solar cell is thus of the order of 2–4 years and in its lifetime a cell may produce electricity with a value of around 10 times its cost of production [8]. Total world cumulated installed capacity of PV amounted to an estimated 7.7 GW in 2007. Solar electricity is already cost-competitive with fossil and nuclear electricity if externalities are taken into consideration.

Yet, paradoxically, the greatest growth in emissions of carbon dioxide, the principal greenhouse gas linked to recent global warming [9], is coming from China's rapidly growing use of coal to power the very industrial economy that is also producing solar panels to sell overseas.

For example, one of such companies successfully went public on the New York Stock Exchange, immediately after its foundation in 2001 and, today, Suntech Power Holdings (Figure 6.2) has risen to be the world's fifth-largest maker of solar cells, after the market leaders Sharp of Japan, Q-Cells of Germany, Kyocera of Japan and BP Solar of the UK [10].

The company's modules are 15.5–16.5% efficient, at the top of the industry's percentage of solar energy converted into electricity. The industry average is 15%. Suntech is piloting a new line yielding 18%, and is targeting 20% by 2008 [11]. Yet, the company's key markets are Germany, Japan and Spain, which subsidize renewable energy, whereas China accounted for just 10% of its 2006 sales of $599 million. In practice, local reduction in CO_2 emissions through solar power in the western world are based on coal-fired production of silicon cells in Shanghai's outskirts.

Since early 2007, a Chinese law requires power plants and factories to generate at least 10% of their power from renewable sources by 2010, but there is little hope that

Figure 6.2 Workers handle solar cells to produce solar panels in the factory run by Suntech Power in Wuxi, China. (Photo courtesy: AP).

solar power generation will be a meaningful tool in limiting climate risks if its cost is not reduced to compete with other electricity sources in developing countries.

Critics of energy from solar panels argue that just to avert less than one-tenth of the anticipated growth in coal burning by 2050, would require 200 of the "Million Solar Roof" initiatives launched by California's Government [12]. Yet, credible solar grand plans aimed at huge scale electricity generation from sun radiation actually do exist, based entirely on existing PV technologies assuming incremental improvements in the efficiency of current solar cells (Chapter 7).

Such incremental improvements are being reported with increasing frequency. For instance, recent efforts to address the issue of solar cell efficiency include a breakthrough from Sanyo in June this year which saw the company break its own record for the world's highest energy conversion efficiency in practical size crystalline silicon-type solar cells by demonstrating an efficiency of 22%. More recently, Global Warming Solutions announced the development of new solar energy conversion technology based on a special coating that can be applied to existing solar cells.

Similarly, different types of thin film solar cells have been recently developed and will soon be incorporated into existing thin film solar cells to increase the efficiency [13]. V-shaped organic cells increase solar cell efficiency by 52% by enhancing the chance for the light to be absorbed. Instead of the planar configuration of most organic solar cells in which when the light hits, there is only one chance to bounce, the V-shape creates an environment in which the light can bounce around.

However, limiting the PV research to these sets of PV technologies may be risky for two reasons: First, flat-plate modules are limited to efficiencies not exceeding 25%. Secondly, the PV industry would miss opportunities afforded by radical changes in technology [14].

The final step in developing affordable solar cell technologies with a cost below 0.5 €/Wp is to develop disruptive, beyond-evolutionary, scientific breakthroughs. Rather than first-generation fabrication of high-quality, low-defect, single-crystal PV devices that have high efficiencies approaching the limiting efficiencies for single-bandgap devices but use energy- and time-intensive techniques, third-generation approaches to photovoltaics aim to use thin-film, second-generation deposition methods [15]. The concept is to do this with only a small increase in areal costs and hence reduce the cost per Wp.

Also, in common with thin-film technologies, these will use materials that are both nontoxic and not limited in abundance. Thus, these third-generation technologies will be compatible with large-scale implementation of PVs.

6.2 Quantum Well Solar Cells

In recent years, worldwide solar cell manufacturing has been increasing by 47% each year. The rapid PV market expansion has led to a silicon feed-stock shortage, so cells based on a different material system and production technology such as the

strain-balanced quantum well solar cell (SB-QWSC) are important in order to maintain this expansion.

The first generation of these new quantum well photovoltaic cells operate at a 27% efficiency, which is approximately twice the efficiency of the current Si-based PV cells and close to the single junction cell efficiency record of 27.8%. Furthermore, they are based on technologies similar to those used for the amplifiers in mobile phones, so the ability to manufacture them on a large scale is already in place.

Indeed, the SB-QWSC is made from GaAs-based alloys (GaAsP/GaInAs) and was introduced as a way to extend the spectral range of high efficiency GaAs cells, using the quantum well (QW) technology which underpins modern communication devices such as the laser, LED and the amplifier in mobile phones [16].

Furthermore, relatively inexpensive optics such as mirrors or lenses focus sunlight from a broad collection area onto a much smaller area of active semiconductor PV cell material.This reduces the area of the expensive PV cell by about 1/500 leading to a major price reduction. Indeed, the PV semiconductor material dominates the costs of such solar PV systems, and reducing the amount of PV material required to capture a given amount of sunlight leads to substantially lower system cost and cost per watt of output.

The QWs give the cell a wider spectral range without introducing crystal dislocations (the alloy compositions and well and barrier thicknesses are adjusted to minimize the formation of dislocations.). Both features give the SB-QWSC a number of advantages in concentrator applications over the expensive tandem or triple junction GaAs-based cells which were designed for use in space.

The absence of dislocations means the SB-QWSC will have a longer device lifetime than the highest efficiency version of the multi-junction cell. At the same efficiency a SB-QWSC will outperform a conventional tandem cell because it does not require a tunnel junction to connect the cells. The wider spectral range of the QW cell results in significantly more electrical energy being harvested over a year due to the seasonal and daily spectral variation of the sunlight.

Overall, the advantages of these "third generation" cells based on GaAs and other III–V semiconductor materials over commonly used Si-based cells for flat panel PV are shown in Table 6.1.

The band-gap of the SB-QWSC represented in Figure 6.3) consists of a p–i–n diode with an i-region containing a number (up to 65) of approximately 7 nm wide QWs of compressively strained $In_xGa_{1-x}As$ inserted into tensile strained $GaAs_{1-y}P_y$ barrier regions. The crystal structure, Figure 6.4, is grown epitaxially with the same lattice constant as the substrate, yielding a critical thickness well above 1 μm.

When the SB-QWSC is incorporated in a tandem cell, the wider spectral range leads to higher cell efficiency. This enhancement is such that in a place like Madrid, where there is a guaranteed price for PV electricity fed into the grid, the energy savings are as large as the system capital cost over the anticipated 25 year lifetime.

The SB-QWSC also exhibits a phenomenon known as photon recycling when operating at high concentration. When a mirror, known as a distributed Bragg reflector (DBR) is grown under the quantum wells, some of these lost photons are

Table 6.1 Competitive advantages of SB-QWPV (Adapted from Quantasol's web site).

Feature	Benefit	Technical Details
Tuneable spectral properties	Higher overall efficiency	The spectral response of an SB-QWPV cell can be tuned to maximize the conversion efficiency over a wide range of radiation spectra simply by varying the composition and thickness of the III–V semiconductor nanolayers in the active region of the solar cell. Therefore: (i) SB-QWPVs can be engineered to maximize the efficiency of a single-junction cell under the most typical solar spectra; (b) SB-QWPVs provide a very effective solution to significantly enhance the efficiency of multi-junction cells over the current commercial solutions (like GaInP/GaAs or GaInP/GaAs/Ge.
No crystal defects	Best available structural stability, improved reliability and operating life.	The structural stability of an SB-QWPV cell is ensured by having oppositely stressed quantum wells and barriers which prevent any extended crystal defects from nucleating and propagating into the active region of the cell. Compared to a SB-QWPV, any bulk material having the same optimum light absorption-edge, cannot sustain the build-up of elastic energy due to the mismatch with respect to the crystal substrate. This means that plastic relaxation inevitably occurs somewhere in the heterostructures. No matter how low the number of extended defects, like dislocations, that can reach the active region, their negative impact on the dark current (opposite to the photocurrent) of the cell is inevitably significant. Moreover dislocations can accelerate the degradation of the device and thereby shorten its lifetime.
Photon recycling	Higher conversion efficiency than competing cells.	At the typical operating point under solar concentration (>200×), SB-QWPVs are "radiatively limited" that is, any lossy non-radiative carrier recombination becomes negligible. This effect, called "photon recycling," can be exploited by designing the cell in such a way that the radiation generated by the inevitable carrier recombination is partially recycled back into the active region of the device, thus reducing the dark current (enhancing the open-circuit voltage). Tandem cells based on SB-QWPVs and designed to take full advantage of photon recycling (by means of radiative coupling between the sub-cells).

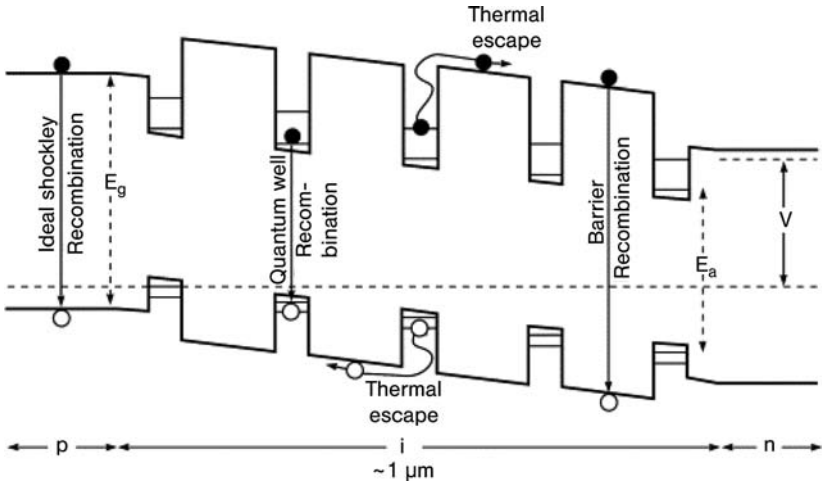

Figure 6.3 Schematic of a SB-QWSC with compressively strained $In_xGa_{1-x}As$ wells and tensile strained $GaAs_{1-y}P_y$ barriers higher than the bulk GaAs in p and n regions. (Reproduced from Ref. [16], with permission).

reflected back into the QWs. Here they are absorbed like the incident sunlight, add to the current and enhance the efficiency. The maximum efficiency gain which might be achieved is around 4%, which is similar to that discussed above, that is, giving savings similar to the system cost in a sunny location with a guaranteed price for PV electricity.

The use of deeper QWs, different DBRs and transparent substrates to maximize the effect in both single-junction and tandem cells is being investigated, and will lead to the first PV products of the company QuantaSol, established in the UK to commercialize solar modules based on these innovative cells (Figure 6.5).

The company plans to manufacture single and multi-junction concentrator solar cells with efficiency levels of up to 40%, providing the first cells for use in

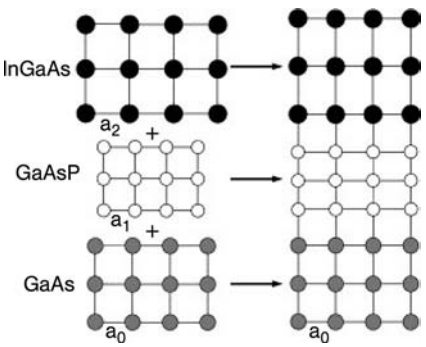

Figure 6.4 Schematic of the crystal structure of the strain-balanced quantum well solar cell. (Reproduced from Ref. [16], with permission).

Figure 6.5 Formed in 2006, the UK-based Quantasol company is ready to commercialize the QW solar cells developed at London's Imperial College physics department.

concentrating PV (CPV) systems for the fast growing utility-scale solar power generation market. Currently the firm, in which in 2007 the investment company Imperial Innovations Group invested £1.35 million reaching a 24% stake, is producing prototypes of its quantum well cells.

6.3 Nanostructured Solar Cells

Nanotechnology has opened up new and promising possibilities to reduce the cost of PV cells and modules for bulk power generation as well as to improve the cell conversion efficiency. For example, most recently, a solar cell measuring 10 cm by 10 cm was created by a nanochemistry approach with efficiency similar to that of conventional, silicon-based cells, but with much cheaper production costs. This will boost the technique's usefulness in producing commercial amounts of solar power [17].

Metallic wires made of platinum nanorods (Figure 6.6), synthesized in solution via a surfactant-template processing of a Pt(II) salt, are mounted on conductive glass and can form the basis of solar cells with efficiency similar to that of conventional, silicon-based cells. The technique reduces the amount of platinum needed by a factor of 40 and greatly enhances efficiency in comparison to linked arrays of very small cells, in which the sunlight hitting the space between the cells is not converted to electricity.

Similarly, the recent discovery [18] of a perfect crystalline structure made of InAs is one of the breakthroughs needed to develop third-generation solar modules. Indeed, a cell made with this new material will be capable of converting up to 30% of the solar energy into electricity [19]. Being a perfect crystalline structure, it also absorbs all incident light and thus may soon become a high performing, low cost solar cell. The solar cell production costs can be lowered because it needs less expensive semiconducting silicon in the process due to the use of nanotechnology. At the same time, the solar cell will exploit the reduced loss of energy due to the shorter distance of energy transportation in the cell (Short distance from electron–hole pair generation to the n/p junction).

Other potential advantages of the SunFlake solar cell design include:

- n/p junctions in perfect single crystals on a non-lattice matched substrate
- only small amounts of expensive solar grade material is used in the nanostructures, none in the substrate. SunFlake is developing a new generation of solar cells based on a novel shape of semiconductor nanostructures (NanoFlakes).

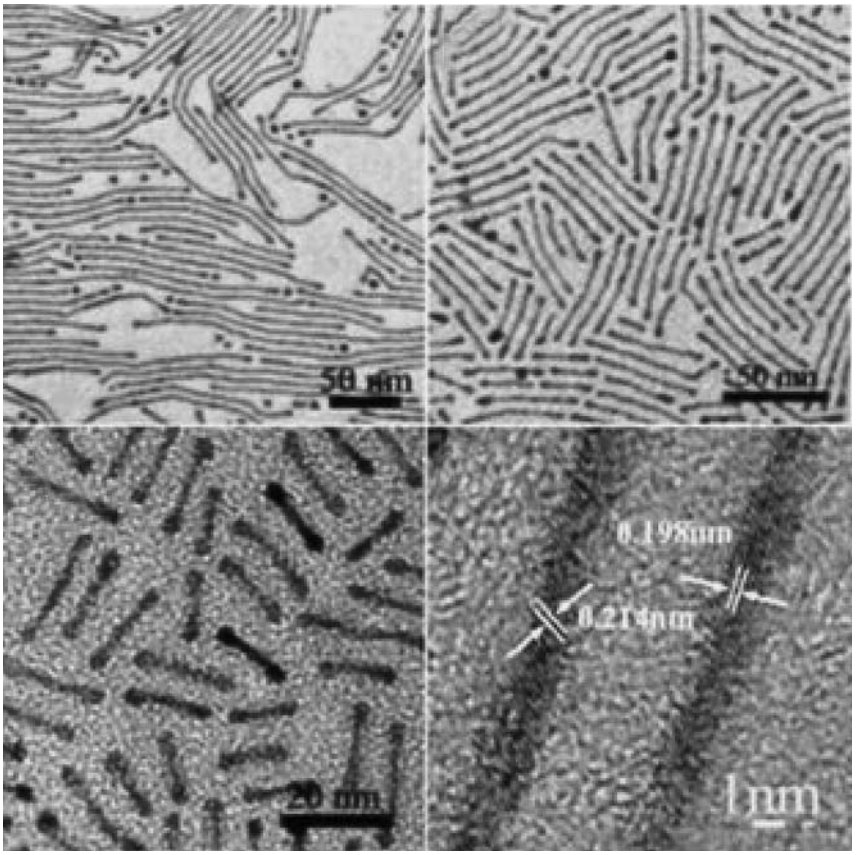

Figure 6.6 Platinum nanorods similar to these made of iron–platinum, enable production of $10 \times 10\,cm^2$ solar cells with 40% reduction in the amount of platinum needed. (Image courtesy of Angewandte Chemie, with permission).

A limited company SunFlake was founded in order to start production of solar cells based on the new technology.

The patented nanostructures [20] can eliminate the need for a lattice-matched substrate as well as the need for a clean solar grade substrate. The only roles of the carrier substrate are to allow the growth of the nanostructures and – when the solar cell is operating – act as a contact to the light absorbing nanostructures.

The surface of the material consists of extremely tiny crystals of InAs grown by molecular beam epitaxy (Figure 6.7), which provide a huge surface area in which sunlight can be caught. With increasing growth times the epitaxial vapor–solid InAs growth on the high-energy surfaces causes them to continue upward and outward, thereby increasing the nanoplate width, eventually reaching an average width at the nanoplate base of 350 nm for 45 min growth, and 500 nm in 60 min.

Under the growth conditions used, arsenic-terminated surfaces created on the two sides of the nanorod crystal are high-energy surfaces with a significantly higher

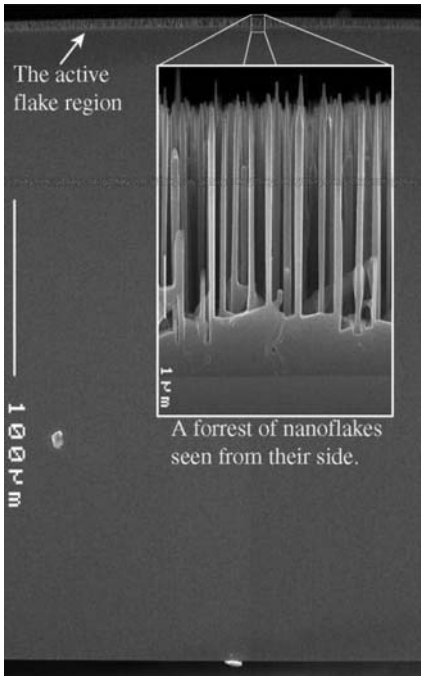

Figure 6.7 A forest of InAs nanoflakes seen from their side. (Reproduced from Ref. [18], with permission).

incorporation coefficient. As a consequence, InAs growth now takes place almost *only on these high-energy surfaces* causing the two-dimensional crystal shape (Figure 6.8). After 45–60 min, depending on the growth conditions used, the nanoplates have a triangular shape with high-energy surfaces.

Using a similar approach, light-absorbing nanowires made of photovoltaic GaAs were recently grown on thin silicon (Figure 6.9), carbon and flexible polyester film.

The nanowires grow upward from the substrate, creating a surface that is able to absorb more sunlight than a flat surface. It is theoretically possible to achieve 40% efficiency, given the superior ability of such materials in absorbing energy from sunlight and the light-trapping nature of the nanowire structures.

The aim is to produce flexible, affordable solar cells composed of Group III–V nanowires that, within five years, will achieve a conversion efficiency of 20% and, in the longer term, 40%. Cost is reduced with nanowires as far lower amounts of active material are used due to the intrinsically enhanced way in which the nanostructure absorbs light and extracts electrons freed by the light.

In conventional solar cells made of slabs of crystalline material, greater thickness means better light absorption, but it also means that it is more difficult for electrons to escape. This forced trade-off is overcome with nanowires. Each nanowire is 10–100 nm wide and up to 5 µm long. Their length maximizes absorption, but their nanoscale width permits a much freer movement and collection of electrons. The

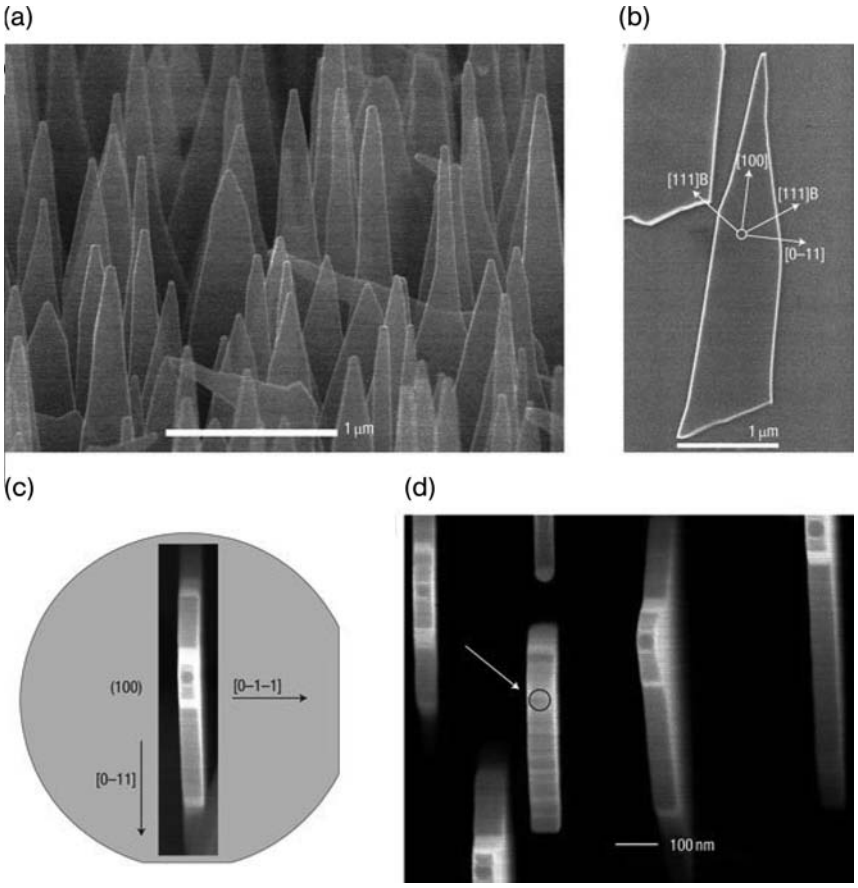

Figure 6.8 (a) A forest of InAs nanoplates grown perpendicular from the surface of a (1 0 0) GaAs substrate. (b) A single InAs plate transferred to a SiO_2 surface. (c,d) SEM images taken directly from above. The orientation of the nanoplates on a (1 0 0) substrate is shown in (c), the depicted nanoplate having a thickness of 60 nm. The plate thickness is determined by the diameter of the Au catalyst particle as indicated by the circle in (d). (Reproduced from Ref. [18], with permission).

direction in which the light is absorbed is essentially perpendicular to that in which the electricity is collected and so the dilemma is overcome.

A similar approach makes use of nanowires containing multiple layers of Group III–V materials, such as gallium arsenide, indium gallium phosphide, aluminum gallium arsenide, and gallium arsenide phosphide. It creates tandem or multi-junction solar cells that can absorb a greater range of the light spectrum compared to silicon [21]. In conventional crystalline solar cells, Group III–V materials have much higher efficiencies than silicon, but the great cost of these materials has limited their use.

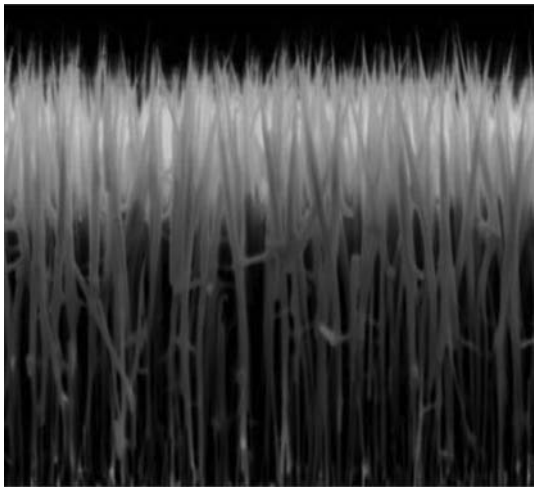

Figure 6.9 A forest of GaAs nanowires growing on a silicon substrate. (Reproduced from Ref. [21], with permission).

In addition to reducing costs by using less active material, there is also a reduction in the cost of the substrate that the nanowires are grown on by using more plentiful and relatively cheaper silicon, glass and polymer films, thus opening the route to inexpensive roll-to-roll manufacturing.

Another free-standing nanostructure holding promise in the fabrication of flexible photovoltaic "fabrics" is a "mat" composed of dense arrays of GaAs nanowires that has been recently grown on the surfaces of a single-walled carbon nanotube (SWNT) covalently functionalized with poly(ethylene imine) (PEI). The process yielded the first macroscopic samples in which nanoparticles are uniformly dispersed in high density throughout the nanotube substrate. This was accomplished by passing an aqueous solution of PEI-SWNTs through a 0.2 μm pore diameter polycarbonate ultrafiltration membrane. The resulting PEI-SWNT mat exhibits excellent mechanical properties, being highly flexible and capable of being bent and folded without cracking. In addition, well-defined Au nanoparticles can be introduced within this film through reduction of $HAuCl_4$ solutions, leading to controllable size distribution and loading density of Au nanoparticles within the nanotube mats.

The resulting materials are thin, flexible, electrically conducting, and transparent electrodes that are superior to conventional transparent conducting oxides (Figure 6.10) and show great promise as photoactive materials for future flexible solar cells [22].

The simple method for the production of carbon nanotube thin films containing Au nanoparticles uses SWNT functionalized with highly branched PEI ($M_n = 10$ kDa) whose high aqueous solubility (180 mg L^{-1}), allows the formation of homogeneous thin films by vacuum filtration. Films are subsequently functionalized with Au nanoparticle clusters by *in situ* reduction of $HAuCl_4$ under mild conditions in the absence of additional reducing agents (Figure 6.11).

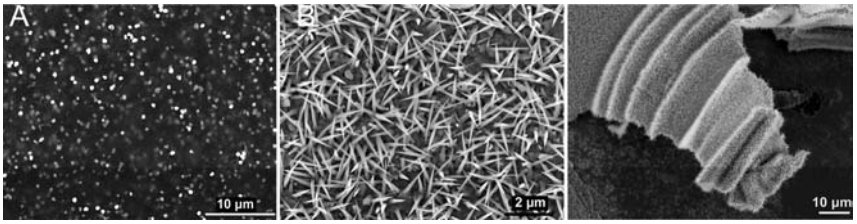

Figure 6.10 SEM images of Au nanoparticles embedded within a PEI-SWNT film (A); GaAs nanowires grown from the nanotube film (B); and a torn section of a similar nanowire-containing film, showing flexibility of the film (C). (Reproduced from Ref. [22], with permission).

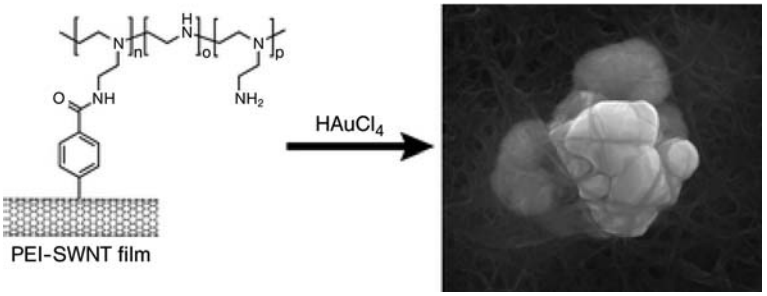

Figure 6.11 This nanochemistry process results in the formation of seed particles for doped nanotubes growth on the surface of a conducting, highly flexible substrate. (Reproduced from Ref. [22], with permission).

6.4 Graphene Solar Cells

Graphene – discovered only in 2004 – a flat, one-atom thick sheet of carbon can be used as ultra-thin transparent conductive film for window electrodes in solar cells [23]. Such conductive, transparent, and ultrathin graphene films obtained from exfoliated graphite oxide, followed by thermal reduction, have a thickness of about 10 nm and exhibit a high conductivity, comparable to that of polycrystalline graphite, and a transparency of more than 70% over 1000–3000 nm. The graphene films can also be prepared via bottom-up construction of extremely large PAHs, nanographene molecules, followed by thermal fusion. To demonstrate how the transparent graphene films are potential window electrodes for optoelectronics a dye sensitized solid solar cell using the graphene film as anode and gold as cathode was fabricated (Figure 6.12).

The efficiency of these non-optimized DSC is lower than traditional titania coating-based solar cells, but there is large room for improvement of the device performance

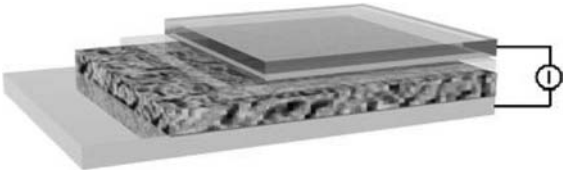

Figure 6.12 Illustration of solar cell based on graphene electrodes. Shown is the dye-sensitized solar cell using graphene film as electrode, the four layers from bottom to top are gold, dye-sensitized heterojunction, compact titanium dioxide, and graphene film. (Image courtesy: Max Planck Institute for Polymer Research).

by, for example, further increasing the conductivity of the graphene films via the use of large graphene sheets.

In general, however, the excellent properties of the as-obtained graphene film including high conductivity, good transparency in both the visible and near infrared regions, ultra-smooth surface with tunable wettability, and high chemical and thermal stabilities, render the graphene-based electrodes suitable as a very practicable option for future solar cells. Furthermore, simple processing enables inexpensive and large-scale industrial manufacturing, another reason why the concept of using graphene electrodes is emerging as a very promising option for future optoelectronic devices.

By the same token, free-standing graphene layers using the bandgap engineering approach recently developed [24], may well have opened the route to a new generation of carbon-based PV cells. Indeed, a significant 0.26 eV gap has been recently introduced into the electronic band structure. This carbon allotrope was first fabricated in 2004 by simple epitaxial graphene growth of its two-dimensional crystal on a silicon carbide substrate.

Graphene is a densely packed single layer of carbon atoms, arranged in a hexagonal pattern like a honeycomb, that forms a two-dimensional sheet. Electrons can move ballistically through graphene, even at room temperature, which means they can fly through the sheet like photons through a vacuum, undergoing none of the collisions with atoms that generate heat and limit the speed and size of silicon-based devices.

The 0.26 eV gap is created when the graphene lattice's symmetry is broken (indicated by alternating red and blue carbon atoms, in Figure 6.13a and b) as a result of the interaction between the graphene and the substrate. Broken symmetry separates the bands of the sublattices at K and K′ in momentum space (Figure 6.13c) and opens a gap between the graphene's valence and conduction bands.

The interaction between graphene and the substrate needs to be strong enough that a band-gap will be opened up but not so strong as to lose the important properties of graphene. By selecting the right substrate, therefore, this effect opens the route to the band-gap engineering of graphene, as different substrates have different potentials, and the strength of the interaction between the graphene and the substrate leads to different band-gap sizes.

Incidentally, graphene-based cells would eliminate the problem of indium scarcity that may affect development of thin film photovoltaics (Chapter 3). Indium is

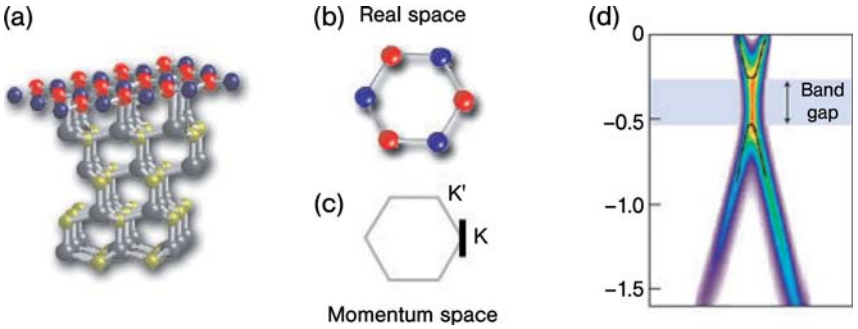

Figure 6.13 Substrate SiC (a) breaks the symmetry and separates the bands of the sublattices at K and K′ in momentum space (c) and opens a gap between the graphene's valence and conduction bands, as shown in the ARPES intensity map (d) representing the black line (c). The band gap raises the possibility of using graphene in photovoltaics. (Image courtesy: University of Berkeley).

expensive and scarce and demand is increasing. From the depressed levels of $60/kg in 2002, indium prices rose to over $1000/kg during the summer of 2007. Recently, prices have fallen back to $400–$500/kg. However, the cost of indium may soon be irrelevant because geologists report that the earth's supply of this element could be exhausted within just a few years.

6.5 Nanorectennas

The current photovoltaic technologies rely on the quantum nature of light and semiconductors which are fundamentally limited by the band-gap energies. A revolutionary new approach suggested by Bailey in 1972 revolves around the wave nature of light [25].

The idea was that broadband rectifying antennas could be used for solar to DC conversion. These *rectennas* would not have the fundamental limitation of semiconductor band-gap limiting their conversion efficiencies. Rectennas for solar conversion would have dimensions of the order of the wavelengths of solar radiation which falls mostly in the sub-micron range. The challenges in actually achieving the objectives are many.

The antenna concept relies on the fact that solar radiation is electromagnetic in nature. In other words, the waves are oscillating electric and magnetic fields propagating from the sun to the earth. Incoming light waves oscillate electrons in an antenna tuned to the wavelength of light – hence the devices have to be of the order of a few hundred nanometers. The broadband incoherent nature of the solar spectrum also requires a wide range of antenna sizes to match all the wavelengths and the need to arrange two directions of polarization.

New, highly-efficient, solar cells use aligned multi-walled carbon nanotube (MWCNT) arrays, grown on a metal substrate (Figure 6.14) using a plasma-enhanced

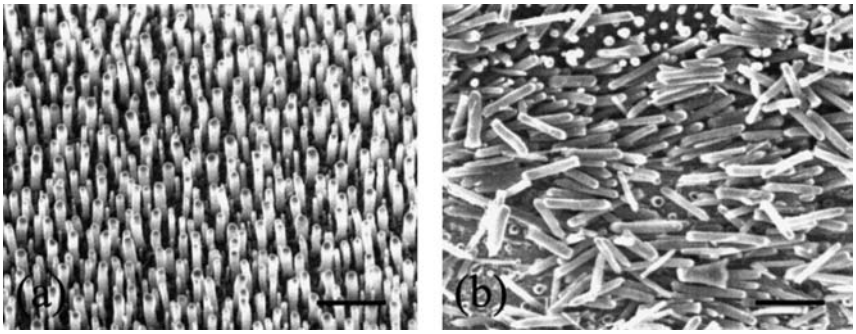

Figure 6.14 Aligned (a) and scratched (b) random arrays of MWCNTs. Each nanotube is a metallic rod of about 50 nm in diameter and about 200 to 1000 nm in length. Therefore, one can view the interaction of these arrays with the electromagnetic radiation as that of an array of dipole antennas. Scale bars, 1 μm. (Reproduced from Ref. [27], with permission).

chemical vapor deposition (PECVD) process, as optical rectennas, receiving and transmitting light at ultraviolet, visible and infrared frequencies [26]. In addition, the cell comprises a semiconductor, acting as a rectifier, having the optical antenna at one and attached to a substrate at the other end; and a metal layer surrounding the rectifier, wherein the optical antenna accepts energy and converts the energy from AC to DC along the rectifier.

The bottom-up fabrication procedure takes advantage of nanomaterial synthesis, and is carried out by a scalable layer-by-layer technique compatible with large-scale industrial production. A typical energy conversion device made using a bottom-up procedure is shown in Figure 6.15.

A semiconducting thin film 710 (such as, p^+-Si) is deposited onto a conductive substrate 705 (such as, Al), and standard procedures are carried out to form an ohmic contact. A catalytic material 715, such as Ni is deposited onto the semiconducting film 710 using magnetron sputtering.

New nanochemistry strategies for the chemical synthesis of nanotubes developed in the early 2000s are crucial to manufacturing the solar rectennas. Indeed, the desired length and diameter of the carbon nanotubes (CNTs) are achieved by accurate chemical control of the growth parameters [27]. The deposition thickness of the catalytic material 715 has a direct effect on the average diameter of the aligned CNTs.

Clean aligned CNT 715 arrays with Ni particles on top can then be grown using a DC glow discharge plasma in an atmosphere of NH_3 and C_2H_2, as shown in step 740. A growth time of about 1–2 min, yields CNTs of 1000 nm or less. The morphology of the CNTs including length, diameters, straightness and so on, can be finely tuned by the other growth parameters such as plasma intensity and etching time, temperature and total growth time.

In this configuration, at the bottom of each individual CNT, a nanoscale CNT–semiconductor (Sc) tunnel junction is formed which rectifies the AC current excited within each antenna into a DC current at optical frequencies. The characteristics of

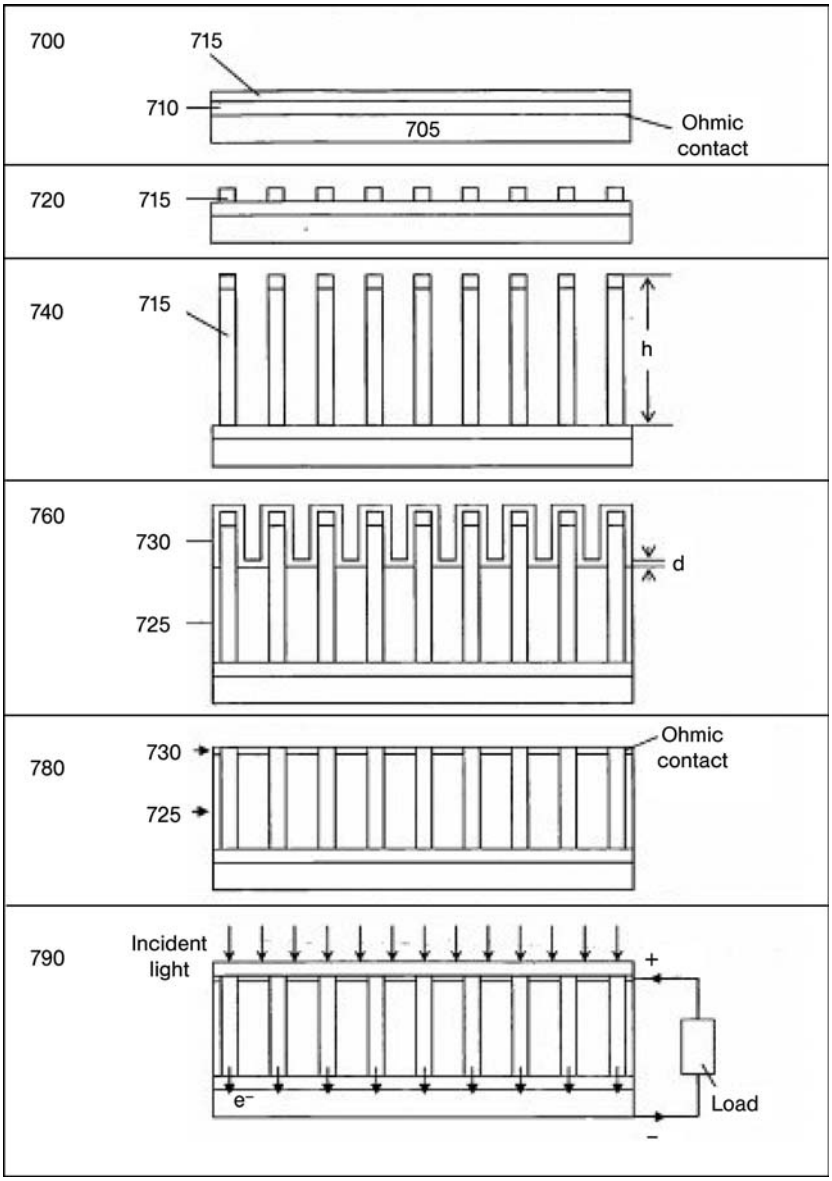

Figure 6.15 A typical energy conversion device based on nanoantennas is made using a bottom-up procedure. See text for details. (Reproduced from Ref. [26], with permission).

the CNT–Sc tunnel junction resemble a conventional metal–semiconductor tunnel junction due to the intrinsic metallic property of the MWCNTs. The CNTs should have an average diameter of less than about 70 nm for a significant quantum mechanical tunneling effect to dominate the thermoionic emission.

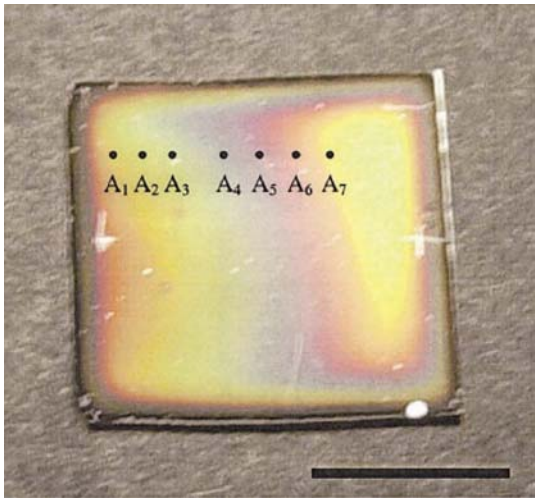

Figure 6.16 Antenna length effect. Interference colors from the random array of MWCNTs. A1–A7 are the selected positions where the length and optical measurements were carried out. Scale bar, 1 cm. (Reproduced from Ref. [27], with permission). This nanotechnology invention resolves the biggest problem in achieving the antenna solar energy conversion (ASEC) concept, namely the ability to rectify electromagnetic waves in the high frequency range of visible and IR radiation. Although infrared rays create an alternating current in the nanoantenna, the frequency of the current switches back and forth ten thousand billion times a second, much too fast for electrical appliances, which operate on currents that oscillate only 60 times a second.

A highly transparent passivation layer 725 (a silicone elastomer, for example) is then spin-coated in between the CNTs, as shown in step 760, up to a height h of $\lambda/4n - d$ or $\lambda/2n - d$ (50 nm–500 nm for visible and near-infrared), where λ is the wavelength of incident light in vacuum and n is the refractive index of the passivation material 725. The spin-coating can be performed by varying the viscosity of the polymer solution and the spin rate. After baking (usually at <200 °C), a thin film (thickness $d \ll \lambda/4n$ or $\lambda/2n$) of transparent conductive material 730 (such as ITO or ZnO) is deposited on top of the passivation layer 725 and the exposed part of the CNTs 715 by e-beam evaporation or sputtering, as shown in step 760.

The CNTs grow sufficiently long ($>\lambda/4n$ or $\lambda/2n$, respectively) so that, by carefully polishing the surface at this stage, the protruding CNT tips will be broken up and removed together with the conductive materials coated on the tips, exposing the CNT cross-sections, as shown in step 780. The cross-sections tend to be automatically closed or partially closed through the collapse of the CNT walls near the open end.

The CNT–transparent conductive material contacts are ohmic. An additional thin layer of the same passivation material 725 may be again spin-coated on top to provide a uniform dielectric medium surrounding the CNT antennas and protecting them from outside attack. A configuration where all the CNT rectennas as individual

current sources are connected in parallel is thus achieved and the rectified DC currents will add up to a much higher magnitude accompanied by a substantially reduced total internal resistance of the rectennas 715.

The two conductive layers can be connected across an external load such as DC electrodes, as shown in step 790. The so-established single-wavelength energy conversion device, when the incident light is polarized in the direction of CNT alignment, will convert the photon energy into DC electricity at an efficiency greater than about 90%.

The other fundamental characteristic of an antenna is its resonant response behavior as a function of the radiation wavelength. This results from the condition that the induced current oscillations must fit into the antenna length. A general equation describing the scattering maxima from a random array of dipole antennas (with vanishing current at each end) is:

$$L = m(\lambda/2)\, f(\theta, n), \tag{6.1}$$

where $f(\theta, n) = 1$ for a single, simple diode, and $f(\theta, n) = (n^2 - \sin^2\theta)^{-1/2}$ in the limit of the very dense array (thin film limit), where the average interantenna distance $D < \lambda$, $f(\theta, n)$ is equal to about 1, and is only weakly dependent on the angle θ. Similar behavior is expected for the random array of MWCNTs.

Computer simulations of the electromagnetic response from a random dipole antenna array yield reflection curves for various antenna lengths, as shown in Figure 6.17b. Both experimental (Figure 6.17a) and theoretical (Figure 6.17b) results follow closely the ideal dipole antenna condition, and thus demonstrate that MWCNTs can act as light antennas. Indeed, in Figure 6.18 the positions of

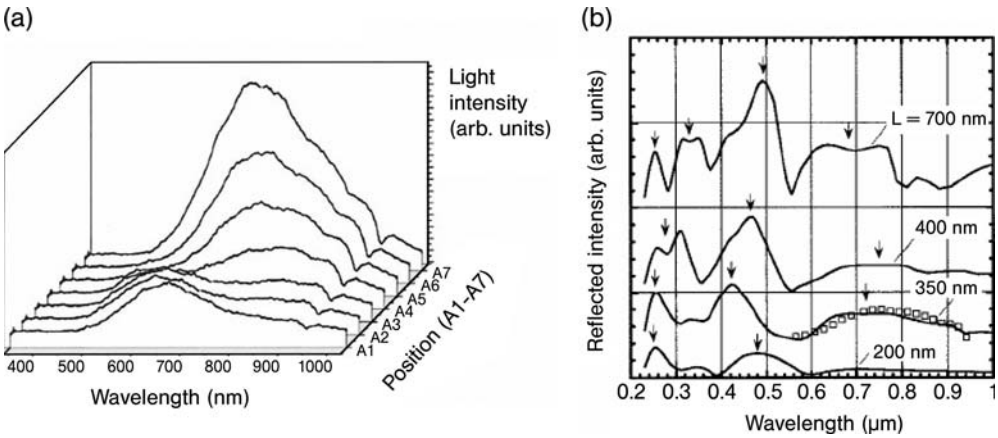

Figure 6.17 (a) Experimental reflection curves for various antenna lengths. (b) Computer simulated reflection curves for the various antenna lengths. Comparison between an experimental curve (for position A_5), shown as squares, and the corresponding calculated response is shown in (b). (Reproduced from Ref. [27], with permission).

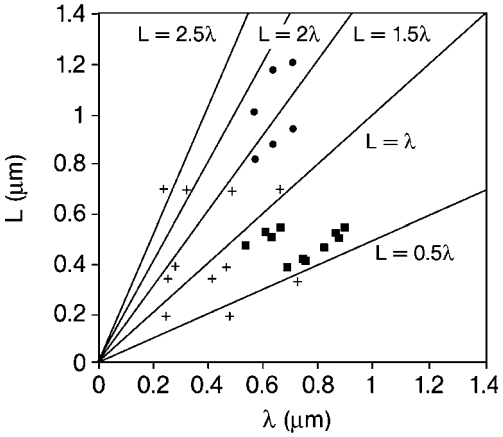

Figure 6.18 Positions of the various reflected intensity maxima versus the corresponding average antenna length, *L*. The measured results are represented as solid circles and squares. Crosses mark the positions of the distinct maxima of the theoretical curves (indicated by arrows in Figure 6.17.The solid lines represent the ideal dipole antenna condition (Equation 6.1, with $f = 1$) for different m. (Reproduced from Ref. [27], with permission).

the various reflected intensity maxima are plotted versus the corresponding average antenna length L. The solid lines represent the ideal dipole antenna condition (Equation 6.1, with $f = 1$) for different m.

This study also estimates the quality of the nanotube antennas. Figure 6.17b shows a comparison between one of the experimental curves of Figure 6.17a (for position A_5) shown as squares, and the corresponding calculated response. This comparison shows that the calculation, which assumed infinite conductivity of the metallic antenna, reproduces well the measured line width of the peak. The antenna length effect can be tuned by controlling the nanotube length, and to some extent the array density during the growth process, making the devices frequency selective. Once the engineering problems of scale are solved, the door to abundant solar electricity will be open.

Cells such as these will soon be deployed on flexible films. Indeed, another similar method for developing cheap solar energy technology that could be imprinted on flexible materials and still draw energy from the sun after it has set has been developed recently [28]. The technology uses a special manufacturing process to stamp tiny square spirals, or "nanoantennas" of gold onto a sheet of plastic. Each square contains roughly 260 million antennas. This INL-patented manufacturing process demonstrates that nanoscale features can be produced on a larger scale. The manufacturing process stamps tiny square spirals of conducting metal onto a sheet of plastic. Each interlocking spiral nanoantenna is as wide as 1/25 the diameter of a human hair (Figure 6.19). The length scales for the antennas are of the order of the wavelength of the solar radiation (Table 6.2), namely with lengths of less than a micron to a few microns while the width at its broadest point is in the sub-micron down to the nanometer range.

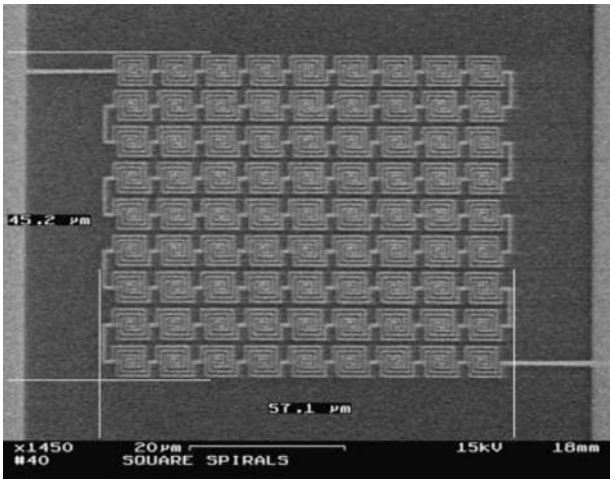

Figure 6.19 An array of nanoantennas, printed in gold and imaged with a scanning electron microscope. The deposited wire is roughly a thousand atoms thick. A flexible panel of interconnected nanoantennas may one day replace heavy, expensive solar panels. (Photo courtesy: Idaho National Laboratory).

The nanoantennas absorb energy in the infrared part of the spectrum, just outside the range of what is visible to the eye. Since the sun radiates a lot of infrared energy, some of which is soaked up by the earth and later released as radiation for hours after sunset, the nanoantennas can take in energy from both sunlight and the earth's heat, with higher efficiency than conventional solar cells. The team estimates individual nanoantennas can absorb close to 80% of the available energy. Double-sided panels could absorb a broad spectrum of energy from the sun during the day using one side of the panel, while the other side might be designed to take in the narrow frequency of energy produced from the earth's radiated heat. The team estimates individual nanoantennas can absorb close to 80% of the available energy.

The INL team envisions the antennas might one day be produced like foil or plastic wrap on roll-to-roll machinery. So far, they have demonstrated the imprinting process with six-inch circular stamps, each holding more than 10 million antennas. The circuits themselves can be made of a number of different conducting metals, and the nanoantennas can be printed on thin, flexible materials like polyethylene, a

Table 6.2 Length and time scales of electromagnetic radiation.

Frequency (Hz)	Wavelength in vacuum (m)	Time period (s)	Regime/source
10^{9}	3×10^{-1}	1×10^{-9}	Microwave
10^{11}	3×10^{-3}	1×10^{-11}	Millimeter wave
10^{12}	3×10^{-4}	1×10^{-12}	Far infrared
10^{14}	3×10^{-6}	1×10^{-14}	Infrared
10^{15}	3×10^{-7}	1×10^{-15}	Ultraviolet

Figure 6.20 INL researcher Steven Novack holds a plastic sheet of nanoantenna arrays, created by embossing the antenna structure and depositing a conductive metal in the pattern. (Photo courtesy: Idaho National Laboratory).

plastic that is commonly used in bags and plastic wrap. In fact, the team first printed antennas on plastic bags used to deliver the Wall Street Journal, because they had just the right thickness (Figure 6.20).

References

1 Lewis, N.S. (2007) Toward Cost-Effective Solar Energy Use. *Science*, **315**, 798.

2 Key World Energy Statistics 2007, International Energy Agency, Paris, 2007. Available at: http://www.iea.org/textbase/nppdf/free/2007/key_stats_2007.pdf.

3 Albini, A. and Fagnoni, M. (2008) 1908: Giacomo Ciamician and the Concept of Green Chemistry. *ChemSusChem*, **1** (1), 63.

4 Balzani, V., Credi, A. and Venturi, M. (2008) Photochemical Conversion of Solar Energy. *ChemSusChem*, **1** (1), 26.

5 Ciamician, G. (1912) The Photochemistry of the Future. *Science*, **36**, 385.

6 Barnham, K.W.J., Mazzer, M. and Clive, B. (2006) Resolving the energy crisis: nuclear or photovoltaics? *Nature Materials*, **5**, 161.

7 Worldwatch Institute, Washington, DC , (2007) Renewables 2007- Global Status Report, available at: http://www.worldwatch.org/files/pdf/renewables2007.pdf.

8 US Department of Energy Office of Science , Basic Research Needs for Solar Energy Utilization, (2005) available at: http://www.er.doe.gov/bes/reports/files/SEU_rpt.pdf.

9 Hoffert, M.I., Caldeira, K., Jain, A.K., Haites, E.F., Harvey, L.D.D., Potter, S.D., Schlesinger, M.E., Schneider, S.H., Watts, R.G., Wigley, T.M.L. and Wuebbles, D.J. (1998) Energy Implications of Future Stabilization of Atmospheric CO_2 Content. *Nature*, **395**, 881.

10 McDonald, J. (April 23 2007) Solar power pays off for Chinese entrepreneur, The Associated Press.

11 Kho, J. (6 January 2006) Solar Power, the Chinese Way. *Red Herring*. www.redherring.com/home/15061

12 Pacala, S. and Socolow, R. (2004) Stabilization Wedges: Solving the Climate Problem for the Next 50 Years with Current Technologies. *Science*, **305**, 968.

13 Rim, S.-B., Zhao, S., Scully, S.R., McGehee, M.D. and Peumans, P. (2007) An effective light trapping configuration for thin-film solar cells. *Applied Physics Letters*, **91**, 243501.

14 Goswami, D.Y., Vijayaraghavan, S., Lu, S. and Tamm, G. (2004) New and emerging developments in solar energy. *Solar Energy*, **76**, 33.

15 Green, M.A. (2003) *Third Generation Photovoltaics: Ultra-High Efficiency at Low Cost*, Springer-Verlag, Berlin.

16 Mazzer, M., Barnham, K.W.J., Ballard, I.M., Bessiere, A., Ioannides, A., Johnson, D.C., Lynch, M.C., Tibbits, T.N.D., Roberts, J.S., Hill, G. and Calder, C. (2006) Progress in quantum well solar cells. *Thin Solid Films*, **511–512**, 76.

17 Sandler, G.(October 16 2007) Bar Ilan University makes solar cells 10× bigger thanks to Nanotechnology, Israel-Times.com.

18 Aagesen, M., Johnson, E., Sørensen, C.B., Mariager, S.O., Feidenhans, R., Spiecker, E., Nygård, J. and Lindelof, P.E. (2007) Molecular beam epitaxy growth of free-standing plane-parallel InAs nanoplates. *Nature Nanotechnology*, **2** (2008) 761–764.

19 The company has chosen not to go public with the SunFlake PV details since we are still in the early research and development phase. M. Aagsen, personal communication (to M.P.), January 14, 2008.

20 University of Copenhagen. Martin Aagsen (2008) An optical device WO/2008/067824. US patent application 60868826.

21 Chen, C., Shehata, S., Fradin, C., Couteau, C., Weihs, G. and LaPierre, R.R. (2007) Self-directed growth of AlGaAs core-shell nanowires for visible light applications. *Nano Letters*, **7**, 2584.

22 Lawson, G., Gonzaga, F., Huang, J., de Silveira, G., Brook, M.A. and Adronov, A. (2008) Au–Carbon Nanotube Composites From Self-Reduction Of Au^{3+} Upon Poly (Ethylene Imine) Functionalized SWNT Thin Films. *Journal of Materials Chemistry*, **14** (2008) 1694.

23 Wang, X., Zhi, L. and Müllen, K. (2008) Transparent, Conductive Graphene Electrodes for Dye-Sensitized Solar Cells. *Nano Letters*, **8**, 323.

24 Zhou, S.Y., Gweon, G.-H., Fedorov, A.V., First, P.N., de Heer, W.A., Lee, D.-H., Guinea, F., Castro Neto, A.H. and Lanzara, A., (2007) Substrate-induced bandgap opening in epitaxial graphene. *Nature Materials*, **11**, 916.

25 Bailey, R.L. (1972) *Journal of Engineering for Power*, **94** (1972) 73.

26 Ren, Z., Kempa, K. and Wang, Y. (2007) Solar cells using arrays of optical rectennas, US Patent 20070240757.

27 Wang, Y., Kempa, K., Kimball, B., Carlson, J.B., Benham, G., Li, W.Z., Kempa, T., Rybczynski, J., Herczynski, A. and Ren, Z.F. (2004) Receiving and transmitting light-like radio waves: Antenna effect in arrays of aligned carbon nanotubes. *Applied Physics Letters*, **85**, 2606.

28 See the Idaho National Laboratory Feature Story Archive at: http://www.inl.gov/featurestories/2007-12-17.shtml.

7
Helionomics

7.1
Oil Peak Meets Climate Change

The world simply runs on oil and natural gas, and even if it is debated whether oil production will peak in the 2030s or before [1], the high and increasing hydrocarbon prices of the century's first decade are already posing serious threats to the world economy. The oil market is an unreliable one, historically influenced by politics and characterized by sequences of oil scarcity and overproduction. Figure 7.1 clearly shows that besides the 1973 crisis – incidentally, when the first solar panels were installed in New York City – we had to wait until 2005 to see the price of oil exceed 25 $/barrel. Yet, global demand for oil currently rises at some 2% annually [2] and, in March 2008, the price of oil reached the historic level of 104 $/barrel.

Now, according to one industry's view [1], these variations are more related to economics and politics than to geology and technology. Yet, a simple look at the evolution of global production (Figure 7.2) reveals a clear trend: discovery reached a peak in the mid 1960s, since when it has been falling despite a worldwide search, always aimed at the biggest prospects; despite improved geological knowledge and great technological progress and despite favorable tax treatment of exploration costs. Given these facts, as put by Leggett [3], there is no reason to expect this trend to change direction.

On a smaller scale, what happened in the US reveals a direct economic consequence of oil's peak production. In 1956 Hubbert predicted that the US production would peak in 1971. Indeed, the peak of production occurred, with astonishing precision, in 1971 (Figure 7.3; the peak of discovery was in 1930) and today the United States is the most depleted country, now importing more than 60% of its needs on rising trends.

The economic consequence of the peak is that the EROI (the energy return on energy invested) in the US has dwindled from 100 joules for every joule invested in the 1930s to today's 15 J [4]. Studies on net energy suggest that we need an EROI of at least 5 to run civilization, because the energy to make the machines, mitigate environmental damage, feed and house the workers and so on must be included [5].

Flexible Solar Cells. M. Pagliaro, G. Palmisano, and R. Ciriminna

ISBN: 978-3-527-32375-3

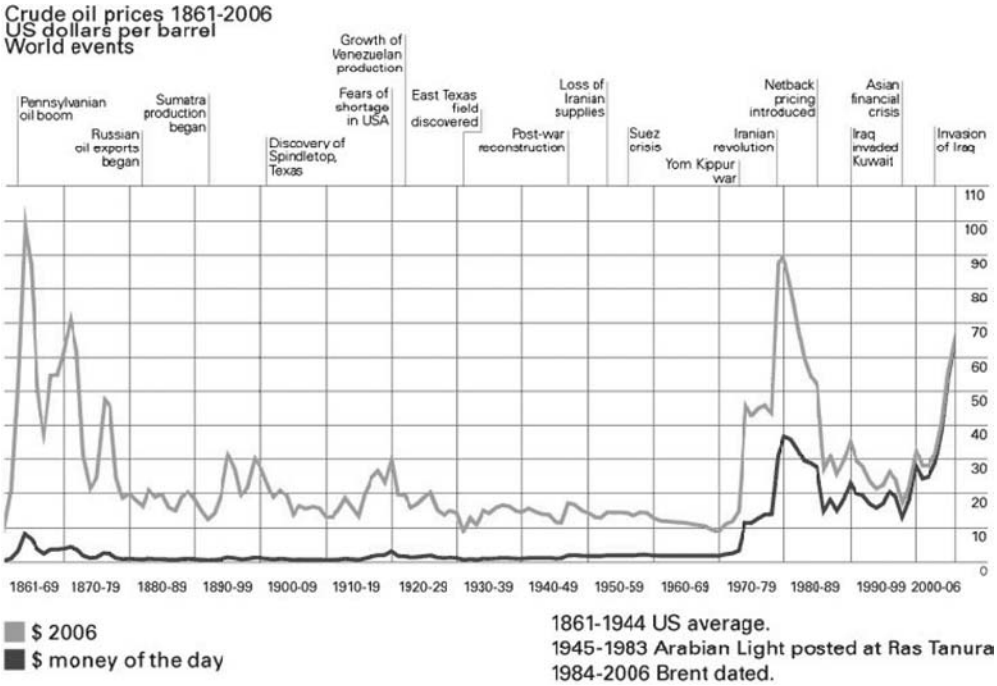

Figure 7.1 Crude oil prices 1861–2006. (Source: BP).

For example, when the EROI for oil was at least 100 to 1 most of the current infrastructure in advanced countries was built.

In the meanwhile, the energy transition from wood to coal and later from coal to oil has caused an explosion in carbon emissions with concomitant accumulation of CO_2

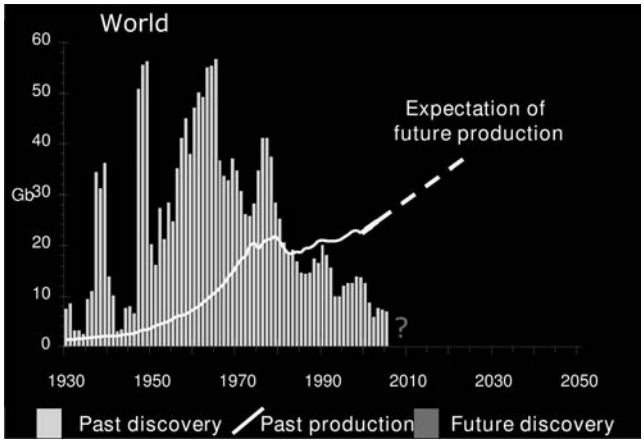

Figure 7.2 Global oil's past discovery and production. (Reproduced from Ref. [36], with permission).

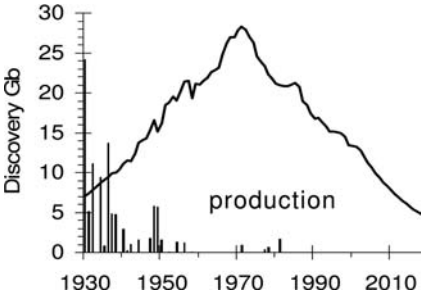

Figure 7.3 US oil's past discovery and production. (Reproduced from Ref. [37], with permission).

in the atmosphere up to today's 350 ppm, the global impact of which in terms of temperature increase (Figure 7.4) is causing climate change due to the greenhouse effect.

Such environmental change has already significantly impaired the health of people, and the economics and ecosystems at local, regional and global levels. Today, however, "the environmental frontier is closed" [6], and the need to restrain carbon emissions adds to the political and social pressure to accelerate the transition to renewable energy sources.

Overall, the combined effect of these trends is forcing society globally to switch from fossil fuels to renewable fuels. The era of renewable energy, and of the solar energy economy – a true helionomics – has arrived.

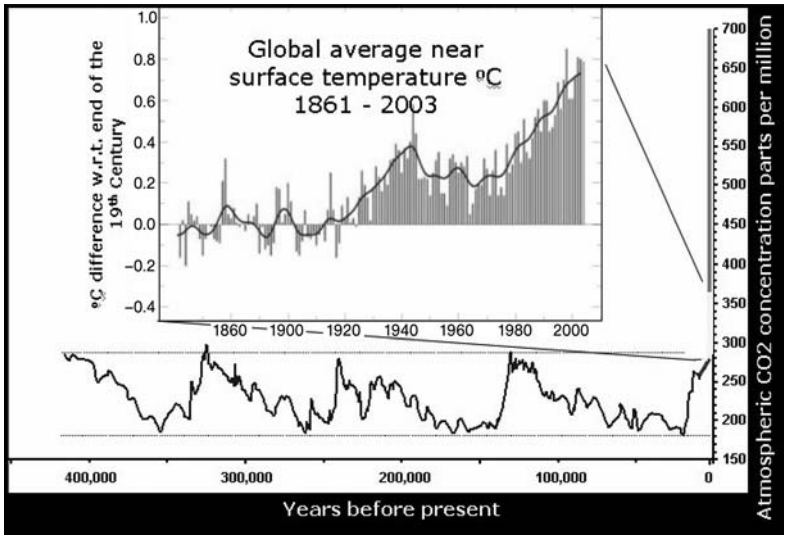

Figure 7.4 Trends of CO_2 atmospheric concentration. The insert shows the 1861–2003 trend together with the measured temperature rise. (Source: IPCC, United Nations, 2006).

7.2
Solar Energy. Rewarding People, Rewarding Capital Markets

In contrast to fossil fuel deposits that are a concentrated source of high-quality energy, commonly extracted with power densities of 10^2 or 10^3 W m^{-2} of coal or hydrocarbon fields, biomass energy production has densities well below 1 W m^{-2}, while densities of electricity produced by water and wind are commonly below 10 W m^{-2}. Among renewable energy (RE) sources only photovoltaic generation, can deliver a power density – the rate of energy production per unit of the earth's area – larger than 20 W m^{-2} of peak power (Figure 7.5).

Future energy systems must be designed and deployed with environmental constraints that were absent from the minds of the inventors of the steam engine and internal combustion engines. PV energy has the intrinsic versatility to meet both intensive production needs (through a concentrated approach, see Section 7.6) and localized, distributing energy demand through onsite installed modules.

In the past three decades computers and telephones have become decentralized and wireless. Solar energy will do the same for the energy industry, using similar semiconductor technologies. In other words, photovoltaics, distributed on a small scale instead of with today's industrial-size electricity grids, will begin to unravel the economies of scale that Edison's electricity transmission created over the last century [8].

As the price of solar electricity approaches that of fossil energy, developing nations will adopt distributed solar generation, as they did with mobile phones increasingly replacing fixed-line phones. Hence, in the place of large fossil fuel power stations and a national electric grid, both fixed infrastructures with large costs, these nations will develop distributed generation. Similarly, in wealthy nations, where electricity costs are rapidly rising, citizens and companies can benefit greatly from solar energy.

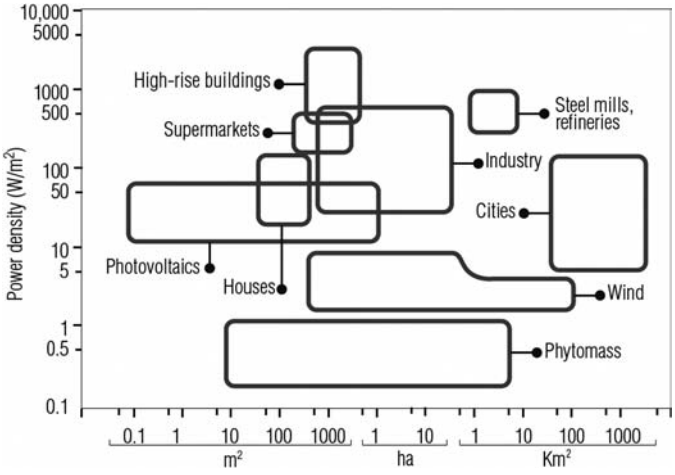

Figure 7.5 Power densities for fossil and renewable fuels. (Reproduced from ref. [7], with permission).

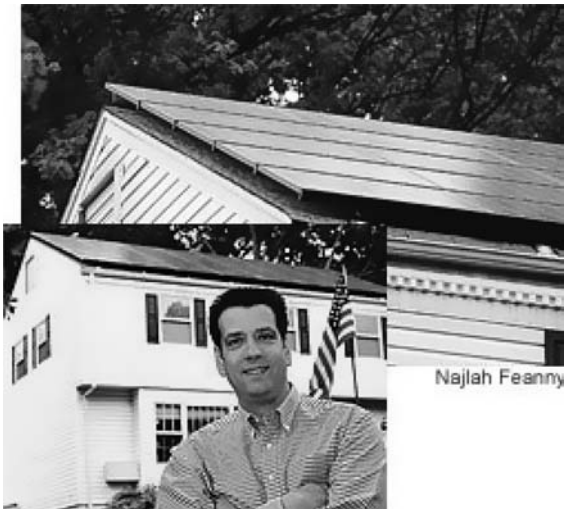

Figure 7.6 Frank Corradi and his roof-mounted solar panels in Cedar Grove, N.J. (Reproduced with permission from ref. [38]).

Indeed, solar energy typically incurs a high upfront cost, but sees extremely low ongoing costs. This means that a low cost of finance amortized over the life of the equipment/capital investment can vastly enhance the economics of renewable energy.

For example, as late as in 2005, in the US it was enough to cover the roof of a four-bedroom colonial home in a suburban New Jersey city with solar panels (Figure 7.6) to quit paying $140 a month in electric bills, and start earning about $170 in cash roughly every six weeks under a state program that rewards developers of clean energy. In this typical case, the $50 000 cost was covered more than two-thirds by various incentives funded by alternative-energy surcharges on utilities bills. Today in the US, incentives such as these are available in all the Union's states, up from just four in 1999 [9].

A typical suburban home needs a 2.5 to 3 kW system, costing from $19 000 to $22 500, including installation costs. With an electricity bill of, say $1000 a year, most people would consider the installation cost too high to justify the savings. That is why incentives were established, which are generally financed by surcharges on electricity bills.

Despite opposition from traditional energy companies arguing that the initiative would place an extra burden on non-solar customers whose surcharges would support installations, California adopted the "Million Solar Roofs" bill on August 2006 to build a million solar roofs in the next ten years.

Almost everywhere in Europe and in many US States, homeowner power generators can finance the cost of buying and installing solar modules by borrowing against future earnings from selling home-produced energy. Local laws in fact enable home generators to sell their electricity back to the local utility through a net metering clause that enables a homeowner to sell excess power back to the utility, and to draw

power from the utility at times when the solar panels are not generating enough electricity.

Investors raised large profits from the huge growth of the PV market. For example The PPVX index[1)] has boomed +151.6% in 2007. Yet, this is only a start, as the traditional exceedingly low return on capital invested (ROI), ranging from 1/10 to 1/25 of revenue/capital invested, is multiplying by a factor of 10. As soon as this ratio becomes more rewarding "the capital will flow; the talent will follow and every one else will follow the most investment-worthy and solidly financed" [10].

Indeed, a number of venture capital funds have largely financed new companies operating in second and third generation photovoltaics. Even the United Arab Emirates invests large capital in solar energy. The country accesses some of the largest oil and gas reserves in the world yet its Government opted for a large investment funding administered by a 100 million US$ fund called Masdar.

With booming consumer interest, strong public support in terms of legislation and incentives, and growing market demand worldwide, enormous opportunity exists for those who want to work in the photovoltaic industry. In Germany only, it created 235 000 jobs in 2006 only, 20 000 more than expected [11].

Overall, the industry has the potential to create more than 2 million jobs worldwide by 2020. Jobs are becoming available for installers, sales people, mechanical engineers, manufacturing personnel, research and development scientists and engineers, marketing and finance personnel. Opportunities in the solar industry are advertised through online job sites, solar training organizations and publications, and professional organizations. Important periodicals such as *Solar Today* and *Photon International* provide good links to educational and volunteer opportunities.

Highly paid jobs are available in the research and development of new products such as solar modules, inverters and mounting hardware [12]. The sector needs a diverse and qualified workforce ranging from technicians, close to the customers, who install and maintain the PV systems to expert semiconductor specialists working in high-tech solar cell factories. Installers need to earn certification of their skills. Indeed, contrary to alternate current, direct current generated by solar panels kills a man at voltage >50 V through the deadly Joule effect.

7.3 Zero Emissions, Lean Production

Since its publication in 1979, the pragmatic quality management theory of management thinker Philip B. Crosby has been implemented by all sort of manufacturing

1) The PPVX is a weighted index calculated weekly on a euro base from Aug. 1, 2001 when it began at 1000 points. As recently as January 2008, its market capitalization totalled €58.6bn and included 30 stocks listed on the market in different countries. To be included in the PPVX, more than 50% of a company's sales in the previous year must have come through PV products or services.

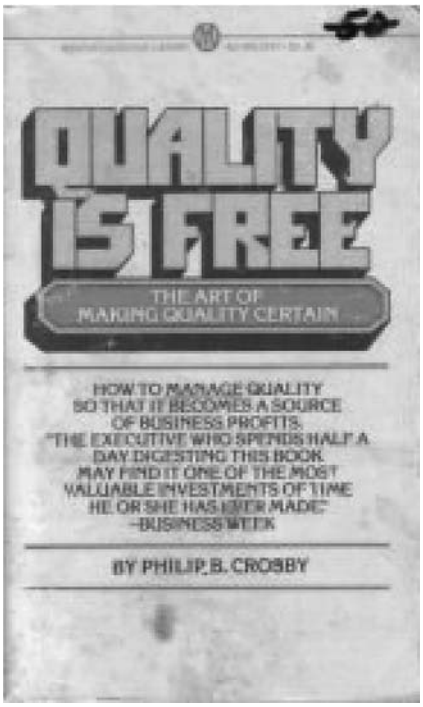

Figure 7.7 Zero defects is the true standard of quality. And the cost of doing things wrong amounts to up to 40% of sales. (Image courtesy).

and service companies worldwide. The book [13] showed managers everywhere that doing things wrong makes costs skyrocket (Figure 7.7).

Having defined quality as "conformance to the work requirements," Crosby showed that doing things right the first time not only adds nothing to the cost of a product or service, but actually it is the only way to avoid wasting a sum between 25 and 40% of sales. Quality is a source of profits, and not of cost. Zero defects is the only acceptable quality standard for any performance, and quality is achieved through systematic prevention of wrong work.

Now, every organization consumes materials and energy and emits waste in the form of spent materials and degraded energy (heat). The yearly value of energy and material waste is generally omitted from the bottom line as it is transferred as "externality" to the environment and to society. For example, only 2–3% of the electricity going through an incandescent light bulb is converted into light, and all the rest is wasted as heat. In other words, we burn coal or hydrocarbons, converting some 30% of their chemical energy into electricity and producing large amounts of pollutants. Then, after wasting another 5% of this high-value energy through transportation in the grid, we convert 98% of it into heat, and the rest into light!

Not only the global sustainability crisis makes it impossible to go ahead with similar practices, but also organizations of all sizes and purpose have an enormous

economic opportunity to eliminate this waste and cut related costs, thereby freeing the financial resources that are lost via such inefficient energy usage.

Zero emissions is the quality standard in managing environmental material and energy resources. Solar electricity, silently obtained from sunlight conversion, is a source of profits for organizations, as it reduces the cost of fossil energy and makes every solar-powered company an energy supplier.

Indeed, another major difference between today's and tomorrow's electricity grid is that the former is supplied with large amounts of energy from a few large (500 to 3000 MW) generating power plants whereas, in a solar society, the grid will be fed with delocalized energy production, close to the point of use, by citizens and organizations alike, operating plants typically ranging from 1 kW to 5 MW in capacity (Figure 7.8).

This reverses the "push" scheme in which customers are invited to consume increasing amounts of energy, into a "pull," customer-driven system, in which customers pull the energy required for their needs leaving the rest available for other customers.

This requires public management of the distribution network, as happened in the German city of Schönau (population 2500) where citizens purchased the grid and ended the use of nuclear energy bought from reactors in nearby Switzerland.Today, Schönau's Electricity Works (or EWS) delivers green electricity to 31 000 customers throughout Germany, up from 1070 customers in the late 1990s. Most of EWS's electricity mix is old hydroelectricity from plants in the region, but it is increasing its supply of solar electricity by encouraging residents to install solar power systems. The

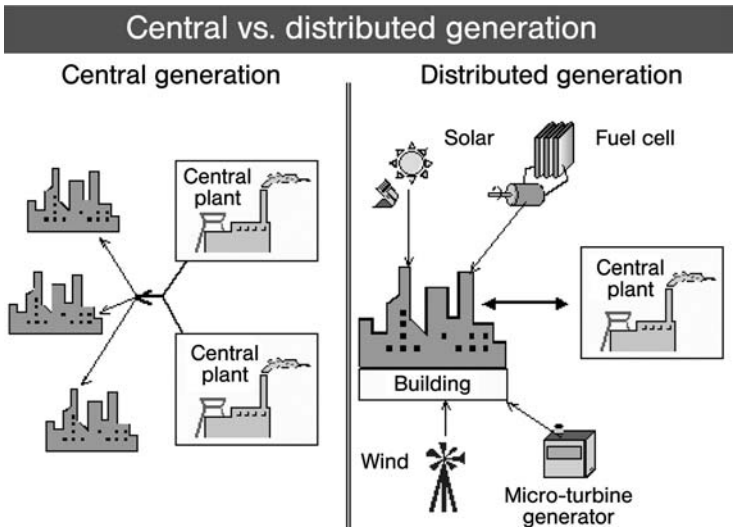

Figure 7.8 Distributed energy resources are autonomous generating, storage, and load control technologies that are typically located at customer premises and operated for the customer's benefit.

Figure 7.9 This plant in the Austrian town of Güssing makes fuel from wood. It uses steam to separate carbon and hydrogen from scrap lumber, then recombines the molecules to make a form of natural gas. (Photo courtesy: International Herald Tribune/Bianca Otero).

feed-in tariff for solar energy has been prescribed by law since 1991, but the EWS pays *more* in order to promote this technology.

Again, there is a full analogy with the evolution of manufacturing that has transformed itself from mass production of standard goods and services "pushed" to customers through massive advertising, into a "pull" system, the so-called "lean" production, in which only what is required from the customer is produced, with no waste and no warehousing [14].

Tomorrow's solar energy society will work as towns such as Güssing in Austria already do. This town of 4000 people is now building Rindler, a € 50 million solar plant, adding its output of renewable energy to the 22 MWh of power a year, including an 8 MW surplus that is sold to the national grid, obtained from organic waste (scrap lumber, Figure 7.9) [15]. Sales of excess power generate about € 4.7 million in annual revenue and a €500 000 profit that is ploughed back into alternative energy projects, while the city has reduced carbon dioxide emissions by 93% from 1995 levels and has energy costs some 30% lower than in the rest of the country .

7.4
The Solar Energy Market

By many measures, solar power is miniscule. The entire sector produced only 4 GW from cells/modules in 2007, compared to global installed electricity capacity of over 4000 GW. In the same year, the installed base of solar power systems was only 0.06% of global electricity consumption [16].

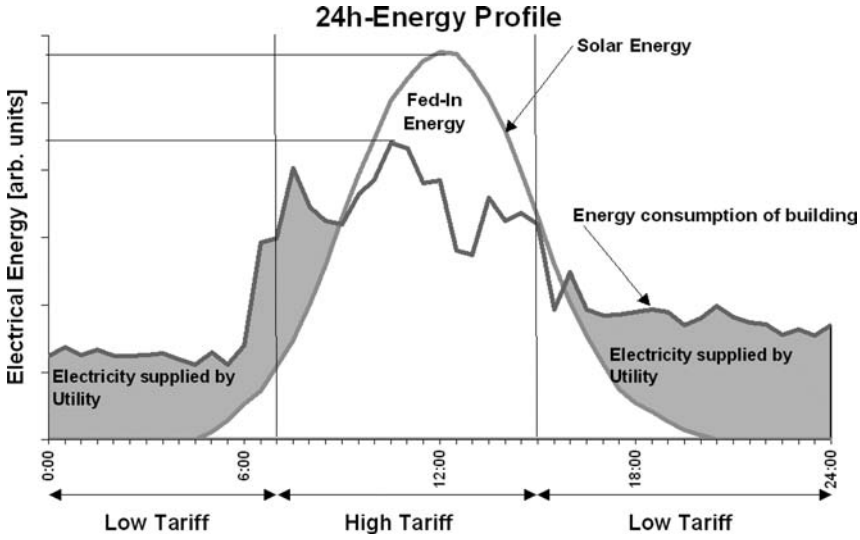

Figure 7.10 Correlation between daily PV power production and energy consumption of an office building (in Spain) shows that PV energy is competitive with fossil electricity during peak hours when the cost of electricity is considerably higher. (Reproduced from Ref. [18], with permission).

The commercial relevance of PV electricity, however, is *already* pronounced. In fact, even a relatively modest level of solar electricity production threatens to disproportionately affect the profitability of established electricity producers, because electricity from photovoltaic systems is generally produced during peaks in daily demand, when the marginal costs of electricity production are highest (Figure 7.10). Moreover, with solar radiation, a clear temporal and seasonal assignment is possible for the assessment of electric energy output and thus of its cost.

Solar energy produces maximum output at the time of high demand (over a 24 h period) and thus it has greater value to both the utility and the customer as it fits with daily load peaks where summer air conditioning is required and can pass surplus power back to the grid during the day, while drawing on the grid at night.

Periods of peak load are the most expensive time because the utility has to have that capacity available. This approach maximizes the value, while minimizing the cost of solar energy. For example, during the heat wave that affected Europe in July 2006, peak prices paid at the European electricity exchange (EEX) spot market exceeded the PV feed-in tariff paid in Germany. This will happen more frequently in future as the feed-in tariff system (surplus electricity buy-back program) decreases, meaning that the occasions when PV electricity is a cost-effective form of generation, even without support mechanisms, will become more common.

The direction of PV module prices is dependent on the manufacturer product line in question, the region and, in some cases, the module types themselves. Prices in

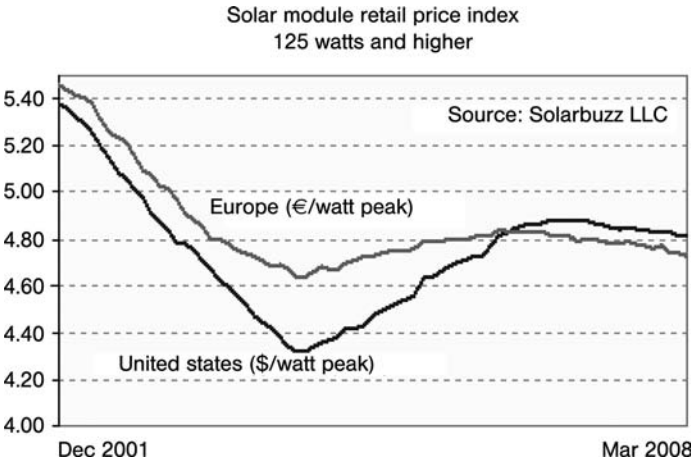

Figure 7.11 Solar module retail price index as of March 2008. (Source: Solarbuzz.com).

2007 showed an unchanged market picture with low overall price activity with a balanced ratio of price increases to decreases (Figure 7.11).

The PV industry is rapidly evolving into an advanced, customer-driven sector in which products are tailored to the customer's needs. For example, the German Solar Industry Association has reported that despite the fact that more than 50% of the solar cells installed in PV systems in Germany are imported, 70% of the added value stays within the German economy [18].

Government subsidies from renewable energy laws in Germany and Japan have been at the basis of the development of the photovoltaic technology for the last 10 years. Consequently, today the world's second and third economic powers lead the global market, either in terms of share or technology. The solar PV industry produced 2.5 GW in 2006, up 40% from 1.8 GW in 2005. Production was expected to reach 3.5–3.8 GW in 2007.

The top four global producers in 2007 of solar modules were Suntech in China, Sharp and Kyocera in Japan, and Q-Cells in Germany. (Table 7.1) [19] Together with Sanyo (Japan) these five accounted for almost half of the global production. The highest ranked US company was First Solar, ranked eighth globally. Investment in new solar PV manufacturing facilities was strong in Europe, Japan, China, Taiwan, and the United States, with many new ventures reported. Notably, China production (370 MW) significantly surpassed the United States (200 MW) for the first time in 2006. Taiwan was also fast catching the United States, with 180 MW produced in 2006, double the 2005 level.

Sharp and Kyocera have major cell manufacturing facilities in Japan, even if Japanese production in 2007 dropped from 46% to 39% share, to the benefit of Chinese cell manufacturer Suntech, today the world's largest manufacturer, followed by Sharp itself and Q-Cells.

Table 7.1 PV production (MW) by top ten companies (Source: Earth Policy Institute, 2007).

Company	2006	First half of 2007
Sharp (Japan)	434	225
Q-Cells (Germany)	253	160
Suntech (China)	158	145
Kyocera (Japan)	180	108
Sanyo (Japan)	155	87
Motech (Taiwan)	102	85
Deutsche Solar/Shell (United States, Germany)	86	66
First Solar (United States)	60	61
Mitsubishi (Japan)	111	55
SunPower (Philippines)	63	54

Source: Prometheus Institute, "Asian Cell Producers Swamping the Boat: A Look at the First Half of 2007," *PVNews*, September 2007, *26*(9), 6–8.

Capitalizing on the polysilicon supply crunch, First Solar in the United States moved into the top 15 global manufacturers in 2006 by producing 60 MW of CdTe thin-film PV, triple its production in 2005. In the first half of 2007, First Solar leapt onto the top ten list, moving up five places to number eight as the fastest-growing PV manufacturing company in the world.

The solar PV industry also saw a boom in silicon production facilities around the world, responding to silicon feedstock shortages of recent years. Solar PV manufacturers were signing long-term contracts to ensure a growing supply, and silicon manufacturers are consistently announcing plans to build new plants. By the end of 2007, more than 70 silicon manufacturing facilities were being constructed or planned.

Germany, Japan, the United States, and Spain are the top four markets. In a future outlook, Navigant forecasts for the photovoltaics world market 2010 say that Germany will remain the solar power champion with a market share of 36%, followed by the USA (15%) and Japan (12%). Spain takes up place 4 with 8% market share, then China (6%) and India (4%). Italy, France and Greece together achieve 7% (Figure 7.12).

With a combined market capitalization of over $140 billion today, annual production growing to 20 GW by 2011 and 8% profit margin expansion in the next four years, solar power is the fastest-growing industry of significant size in the world, with a spectacular average *annual* growth rate around 30% for the last five years. Global industry revenues were $10.6bn in 2006, while capital investment through the PV business chain totalled $2.8bn. The industry raised over $4bn in equity and debt financing, up from $1.8bn the previous year.

An estimated $71 billion was invested in new renewable energy capacity worldwide in 2007, up from $55 billion in 2006 and $40 billion in 2005 (Figure 7.13) [20]. Almost all of the increase was due to increased investment in solar PV and wind power. Technology shares of the $71 billion annual investment were wind power (47%), and solar PV (30%). A number of companies have announced intentions to scale up manufacturing with 1000 MW "mega" production plants [21].

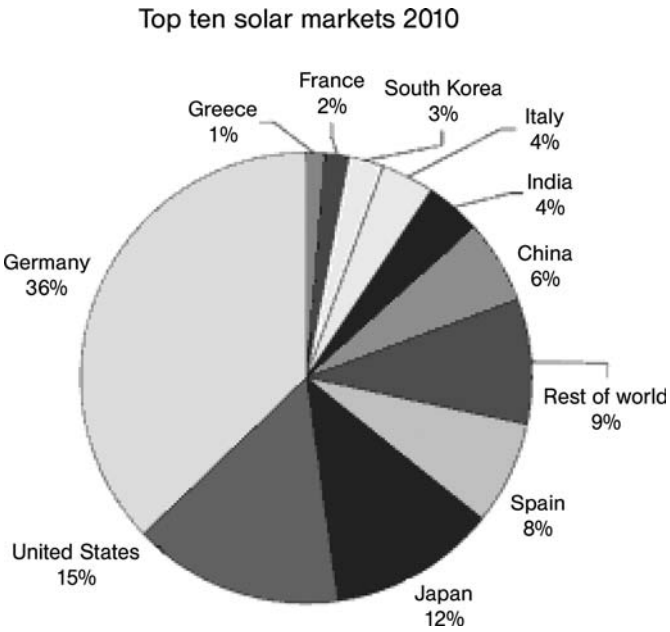

Figure 7.12 Pie chart in megawatts manufactured in 2003 with the main producers. Navigant forecast for the photovoltaics world market 2010: Germany will remain the solar power champion with a market share of 36%, followed by the USA (15%) and Japan (12%). Spain takes up place 4 with 8% market share, then China (6%) and India (4%). Italy, France and Greece together achieve 7%. (Data and graph: Navigant Consulting).

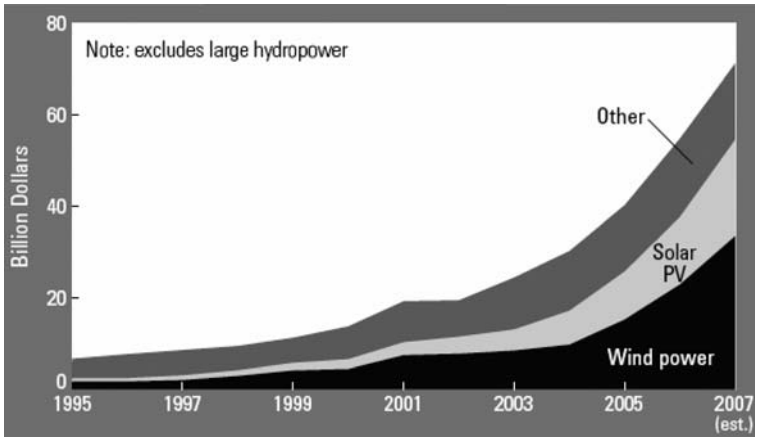

Figure 7.13 Annual investment in new renewable energy capacity, 1995–2007. (Source: Worldwatch Institute).

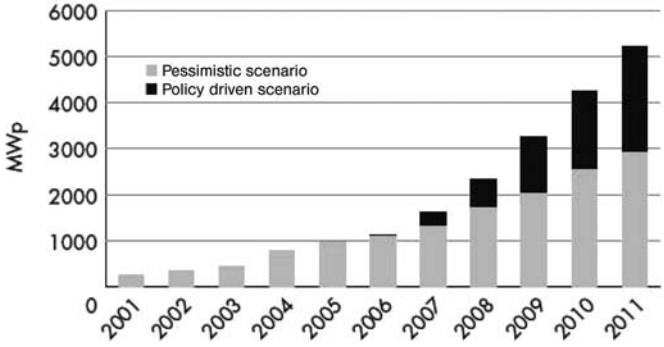

Figure 7.14 Global PV installations. The dark bar shows the chances of an active promotion policy for PV. (Source: EPIA).

Looking at the future prospects for the PV industry, three scenarios for the next five year period (2007–2011), yield a range of annual worldwide industry revenues of between $18.6bn and $31.5bn by 2011 [22].

Figure 7.14 displays the 2001–2011 evolution forecast for PV installed in Europe. The feed-in tariff system (surplus electricity buy-back program) which began in Germany and is now spreading to neighboring countries, including Spain and Italy, caused further expansion in demand for traditional and thin-film solar cells in the whole of Europe. This was also due to their outstanding temperature characteristics.

Solar energy has the highest annual growth rate and this is predicted for the whole decade 2010–2020. If this holds true, photovoltaic electricity will reach 35 GWp production from the bare 0.26 GWp production of 2001. Indeed, early in 2007 the European Union set the ambitious target of a 20% rise in renewable energy consumption in the EU member states by 2020.

7.5
PV Technology Trend

Wafer-based crystalline silicon has dominated the photovoltaic industry since the dawn of the solar PV era. It is widely available, has a convincing track-record in reliability and its physical characteristics are well understood.

Research targets for wafer-based crystalline silicon technology are a reduced specific consumption (g/Wp) of silicon and materials in the final module, so new and improved silicon feedstock and wafer (or wafer equivalent) manufacturing technologies, with careful consideration of cost and quality aspects are to be developed. An increase of 1% in efficiency alone is able to reduce the costs per Wp by 5–7%.

Wafers are becoming thinner and larger. For example, wafers have decreased in thickness from 400 µm in 1990 to 200 µm in 2006 and have increased in area from 100 to 240 cm^2; modules have increased in efficiency from about 10% in 1990 to typically 15% today, with the best performers above 17%.

From 2013 to 2020 wafers should reach a thickness below 120 µm and from 2020 even below 100 µm. Si consumption from 2020 is targeted to be lower than 2 g/Wp. Targets for module efficiency are: until 2010, above 17%; from 2013 to 2020, above 20% and from the beginning of 2020, above 25%.

Recent industrial estimates suggest that the cost of silicon contributes 4/5 (2 € per Wp) to the overall unit cost of solar electricity, whereas the module production process contributes only 1/5 (0.4 €).

Even reducing the latter figure to a minimum, the silicon production cost cannot be further reduced as it basically requires reduction of silica in an arc furnace followed by further purification to obtain high purity silicon, equivalent to the electronic grade silicon used in computers. Hence, even today, to satisfy the average 3 kWh need of a typical family, one needs 14 m^2 of solar modules of 15% efficiency, which cost about 18 000 € (VAT excluded).

Thin film PV clearly is the technology for the future as it has already reduced the unit cost of solar electricity to the 1 $ per watt, as in the case of Nanosolar's CIGS-based technology. The other least expensive modules today are thin films made of cadmium telluride. Current modules have 10% efficiency and an installed system cost of about $4 per watt.

Low cost and high-volume production of thin film PV modules is achievable and little difference in cost between the different thin-film technologies is expected in the long term (Figure 7.15).

Recent months have seen a sharp increase in new activity in the field of thin-film PV. There are now over 80 companies active in thin film technology [23]. At present,

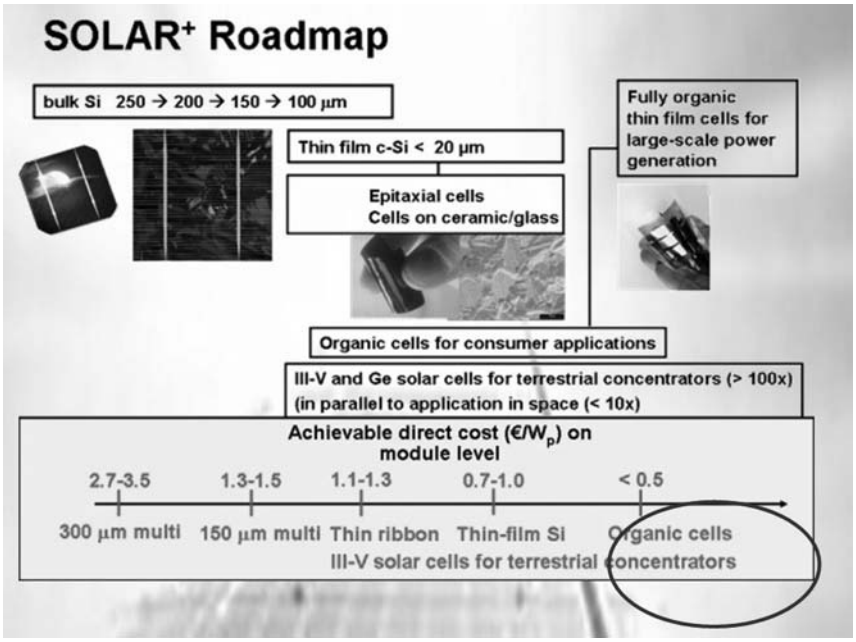

Figure 7.15 Roadmap for PV technologies and price. (Source: IMEC).

the market share of thin film PV within total PV production is below 10% (about 6–8% in 2006), but might grow to 20% by 2010 and beyond 30% in the long term. Thin film gained acceptance as a "mainstream" technology during 2006/2007, due partly to manufacturing maturity and lower production costs, and partly to its advantage in terms of silicon feedstock (it requires just one-hundredth as much silicon as conventional cells).

Beyond the United States and Europe, at least a dozen manufacturers in China, Taiwan, India, Japan, and South Africa are planning to expand thin film production in the near future. Sharp of Japan announced plans in late 2007 to complete a new 1 GW thin film production plant by 2010, bringing its total thin film capacity to 1.2 GW by then.

New applications for thin film solar cells that differ from those for crystalline solar cells continue to evolve and a broad range of new applications can be anticipated, including windows and wall surfaces of homes and buildings. For example, they are being adopted as architectural materials that offer outstanding design characteristics, including "see-through" types for use in curtain walls that allow natural light to shine through, and illuminating solar panels with integrated LEDs that generate electricity during the day and provide illumination at night (Figure 7.16).

Taking account of the increase in production facility sizes, improvements in module efficiency and differences in the calculation methods used by the PV

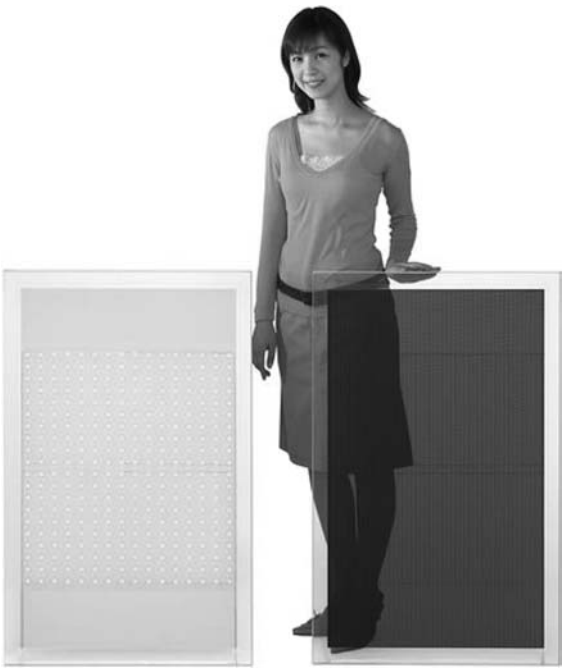

Figure 7.16 Lumiwall is a transparent solar panel that also includes a high-brightness LCD light. The idea is, obviously, to stick one onto your roof for use as a skylight during the day, then switch it on to light your home at night.

industry, in 2010, the total manufacturing costs will most likely be in the range 1–1.5 €/Wp. Further cost reduction to below 0.75 €/Wp in 2020 and 0.5 €/Wp by 2030 may be reached if intensive research and development is carried out.

For example, to provide electricity at 6 cents per kWh by 2020, cadmium telluride modules would have to convert electricity with 14% efficiency, and systems would have to be installed at $1.20 per watt of capacity. Progress is clearly needed, but the technology is advancing quickly; commercial efficiencies have risen from 9 to 10% in the past 12 months.

The challenges facing thin films are to be found mainly in the realm of up-scaling production capacity. The global production capacity of thin films is expected to reach 1 GW_p/year in 2010 and 2 GW_p/year in 2012. It is being installed mainly in Japan, the USA and Europe.

As thin film PV modules have broadly similar structures and the key steps in their production resemble one another, research and development effort directed at one technology can be applied to another, synergically accelerating progress.

Europe already has excellent thin film research and development infrastructure and a number of thin film factories. In Japan, Sharp has increased the capacity of its production system for 10% efficient modules based on a-Si thin film solar cells at its Katsuragi plant in Japan from the current level of 15 MW per year to 160 MW per year by the end of 2008.

7.6 Grand Solar Plans

As mentioned above, a massive switch to PV energy would have major implications for the next energy transition due to its relatively low power density. In order to energize the high power densities of existing residential, industrial and transportation infrastructures inherited from the fossil-fueled era, a solar-based society would have to concentrate diffuse flows to bridge these large power density gaps. This means that a solar-based system will require a profound spatial restructuring with major environmental and socioeconomic consequences [24].

Yet, solar energy technologies have the flexibility to address global power supply needs, without major changes in lifestyle. For example, in 2007 Europe's first commercial solar power concentrating plant opened near the Spanish city of Seville (Figure 7.17). It produces 11 MW of electricity, enough to power 6000 homes. Once fully developed the plant will generate the same amount of power that is used by Seville's population of 600 000. The plant currently operates 624 heliostats (large movable mirrors). These concentrate the sun's rays at the top of a 115 m tower where a heat receiver is located. The receiver converts sunlight into steam, which drives turbines that produce electricity.

Similarly, a vast project for energy, water and climate security in Europe, the Middle East and North Africa is currently under scrutiny (Figure 7.18) [25]. The project would require an investment of €45bn until 2050, and yield annual savings of up to €10bn.

Figure 7.17 In March 2007 Europe's first commercial solar power concentrating plant, known as PS10, opened near the Spanish city of Seville. (Photo courtesy of Wikipedia.)

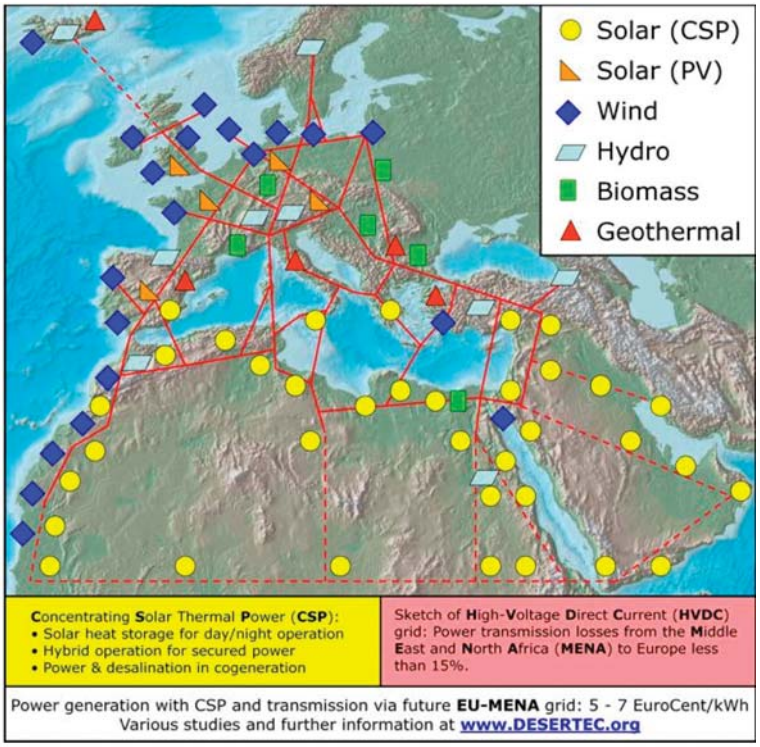

Figure 7.18 The grid with a EU-MENA-connection: Sketch of possible infrastructure for a sustainable supply of power to Europe from Africa and the Middle East. (Photo Courtesy of Desertec.com)

Another project was recently advanced for the US for which a massive switch from coal, oil, natural gas and nuclear power plants to solar power plants could supply 69% of the US electricity and 35% of its total energy by 2050, relying on existing technology and incremental improvements to it. The scheme would require $420bn in subsidies over 40 years [26].

A vast area of photovoltaic cells would have to be erected in the Southwest. Large solar concentrator power plants would also be built. A new DC power transmission backbone would deliver solar electricity across the country. But $420bn in subsidies from 2011 to 2050 would be required to fund the infrastructure and make it cost-competitive.

Remarkably, in the plan by 2050, photovoltaic technology would provide almost 3000 GW of power, requiring some 30 000 square miles of photovoltaic arrays. Once again, the main progress required, is to raise module efficiency to 14%. Although the efficiencies of commercial modules will never reach those of solar cells in the laboratory, cadmium telluride cells at the National Renewable Energy Laboratory are now up to 16.5% and rising. At least one manufacturer, First Solar in Perrysburg, Ohio, increased module efficiency from 6 to 10% from 2005 to 2007 and is aiming for 11.5% by 2010.

A simple idea is to utilize the immense solar power of North Africa's deserts and make them an inexhaustible source of clean energy to sell to European countries. In the scenario developed by German scientists it will be possible to cut emissions of CO_2 from electricity generation by 70% and phase out nuclear power at the same time.

In this case, the most suitable solar power technology for providing secure power output is solar thermal power plants based on concentrating solar thermal power (CSP, Figure 7.19). They use mirrors to concentrate sunlight and create heat, which is used to raise steam to drive steam turbines and electricity generators. Excess heat

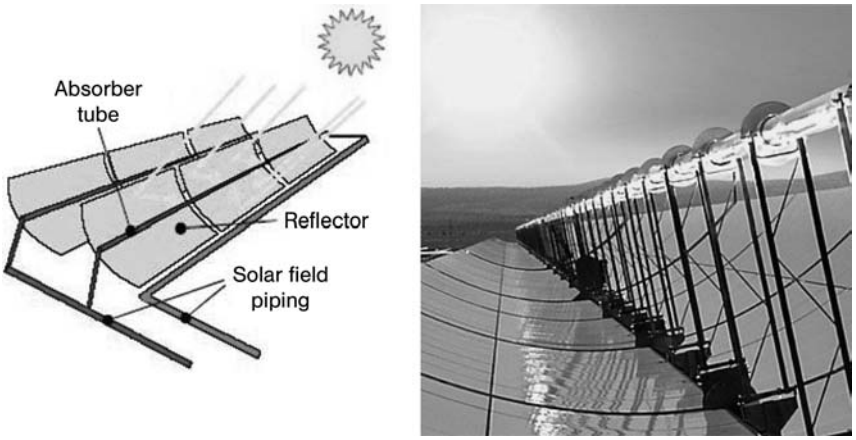

Figure 7.19 Sketch of a parabolic trough collector (A simplified alternative to a parabolic trough concentrator is the linear Fresnel mirror reflector.).

from additional collectors can be stored in tanks of molten salt and used to power steam turbines during the night or when there is a peak in demand.

Power from deserts, as a supplement to European sources of renewable energy, can speed up the process of cutting European emissions of CO_2 and can help to increase the security of European energy supplies. At the same time, it can provide jobs, earnings, drinking water and an improved infrastructure for people in the Middle East and North Africa (MENA).

Satellite-based studies have shown that, using less than 0.3% of the entire desert areas of the MENA region, solar thermal power plants can generate enough electricity and desalinated seawater to supply current demands there and in Europe, and anticipated future increases in those demands. Harnessing the winds in Morocco and on land around the Red Sea would generate additional supplies of electricity.

Using high voltage direct current (HVDC) transmission lines, loss of power during transmission can be limited to only about 3% per 1000 km. The high solar radiation in the deserts MENA (twice that in Southern Europe), outweighs by far the 10–15% transmission losses between Africa and Europe. The grid will have enough balancing power capacity to compensate fluctuating power sources and unforeseeable failures of power lines or power plants.

In this scenario, by 2050, between 10 and 25% of Europe's electricity may be clean power that is imported from sunny deserts, with domestic renewables comprising about 65% of European supplies, while solar imports from MENA provide a further 17% (Figure 7.20).

Finally, one approach does not exclude the other. Developing large distant plants, capable of generating vast amounts of electricity, we shall also focus on distributed generation: small-scale plants situated in local communities like Seville's PS10, and solar panels on home and office roof-tops. In this way, we shall have a mix of

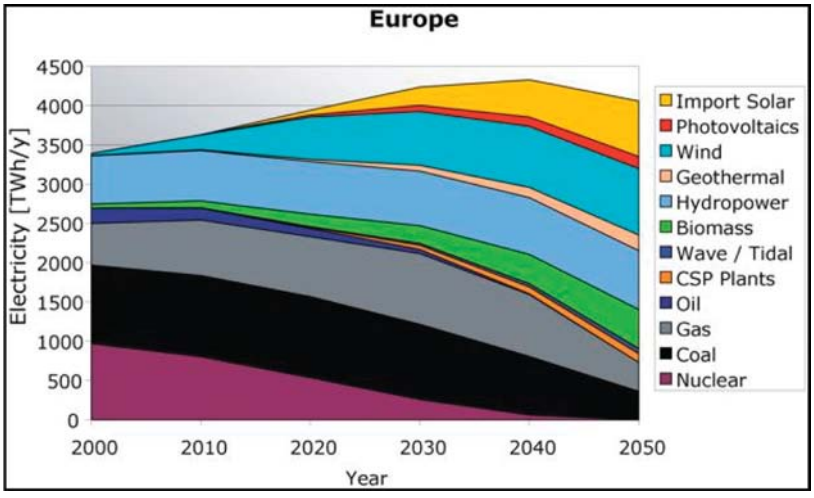

Figure 7.20 In the solar grand plan devised by TREC, by 2050 Europe's dependence on fossil fuel would be terminated. (Source. TREC, 2008).

medium-size plants and distributed generation. This will diversify a country's energy supply, making grids, cities, and communities more resilient in times of crisis.

7.7
A New Manhattan Project?

Polls on energy and global warming in rich countries consistently find that the public is more concerned about rising energy prices than about global warming [27]. In poor countries, people are concerned with primary needs such as food, heat and housing and practically no attention is paid to topics such as global warming and pollution.

As no change can take place without people's involvement, to effectively counter global warming and rising oil costs we need to reduce the cost of clean energy below the price of dirty energy as quickly as possible, including in the process giant developing economies such as China, India and Africa.

Hence, as suggested by Nordhuas and Shellenberger [28], rather than pollution-oriented environmental lobbying from environmentalists, we need to prioritize research and development investments in clean energy technology, focusing on technological innovation and economic opportunity.

Physicists discovered nuclear fission in 1938. Einstein had derived the $E = mc^2$ equation in 1935. Six years later the US Government started the formal Manhattan project to make atomic weapons. The first atomic bomb exploded near Alamogordo, in the New Mexico desert, on July 16, 1945 (the Trinity test). Only seven years to go from detecting an isotope of barium produced by neutron bombardment of uranium in a Berlin laboratory, to full technical control of the process on such a sophisticated detail that on August 6, 1945, the city of Hiroshima disappeared, along with its inhabitants.

The contrast with photovoltaics is striking. Discovered in 1954, silicon-based photovoltaic panels had a 6% efficiency. The first commercial solar panels installed in New York City in 1975 had efficiency around 7%.

Today, 54 years later, the best commercial silicon panels reach a 22% efficiency and those actually commercialized are 15% efficient (on average).[2)] This rather mediocre performance is well rendered by an experience factor of 0.19 (price falling 19% every doubling in cumulative production over the past 30 years) which should be compared to the 0.32 factor of semiconductor memories. The responsibility for this lies with the Governments of developed countries.

Plots in Figure 7.21 show that in order to reach a unit price of 1$/W we should wait for cumulative production to reach 10^5 MW. The relation between cumulative

2) Available from San Jose-based SunPower Corporation, the 22% efficient SPR-315 solar panel carries a rated power output of 315 W, rather than the conventional 160 W, requiring less than half the surface of traditional panels and only 15 solar panels to feed a typical 4 kW (AC rating)solar system.

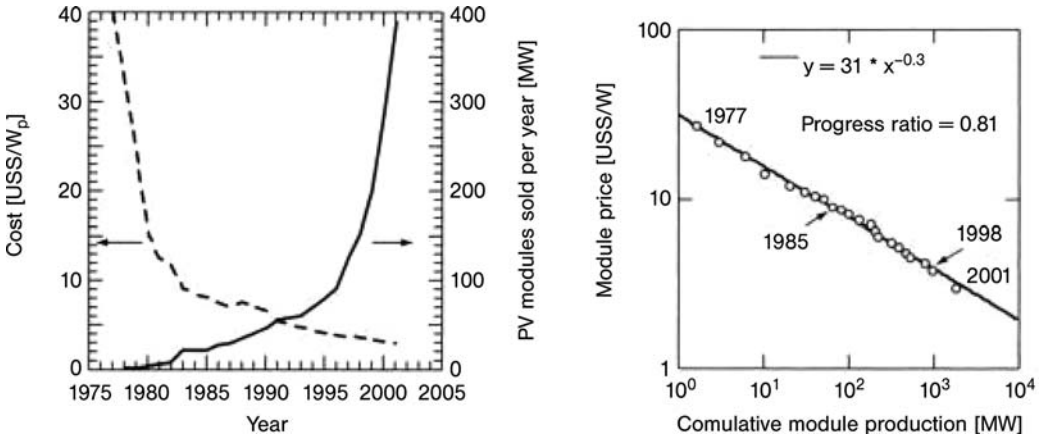

Figure 7.21 Trend of cost per watt for solar cells and volume of production experience curve for PV between 1973 and 1998. The experience factor is $1-2^{-E}$. (Reproduced from Ref. [24], with permission).

production $M(t)$ of PV modules in MW_p and price $p(t)$ in \$/W is described by an experience curve in which E is called the experience exponent [29] .

$$\frac{p(t)}{p_o} = \left(\frac{M(t)}{M_o}\right)^{-E}$$

Indeed, no big, long-term investments have been made in clean energy. The roughly \$33bn invested each year on supporting clean-energy technological deployment is dwarfed by the existing subsidies for fossil fuels worldwide that are estimated at \$150bn to \$250bn each year [30].

PV research in fact did not benefit from being directed by a giant such as Robert Oppenheimer and a team made up of some of the brightest scientists ever who worked together focusing on a single project of historic importance [31].

A similar attempt has not even been made, because Governments actually earn large amounts of money from oil every year. Most of the world's oil is extracted by US, European, Japanese and Chinese companies abroad. Such companies generally earn a large share (30–50%) of the generated revenues, thereby enriching their countries, where taxes are paid, and providing well paid jobs. After that, governments earn further money through heavy taxation on petrol which normally accounts for more than 68% of the price at the pump. The blue portion of the bar in Figure 7.22 shows how much of the end price goes to oil producers, the yellow is what goes to refineries, and the red indicates the amount attributable to government taxes [32].

Clearly, the large differences are not due to differences in crude prices, but to widely varying levels of taxation in the major consuming nations. Tax levels can range from relatively low in the USA to very high in many European countries. In the UK, for example, the government receives substantially more from taxation than OPEC gets from the sale of its oil.

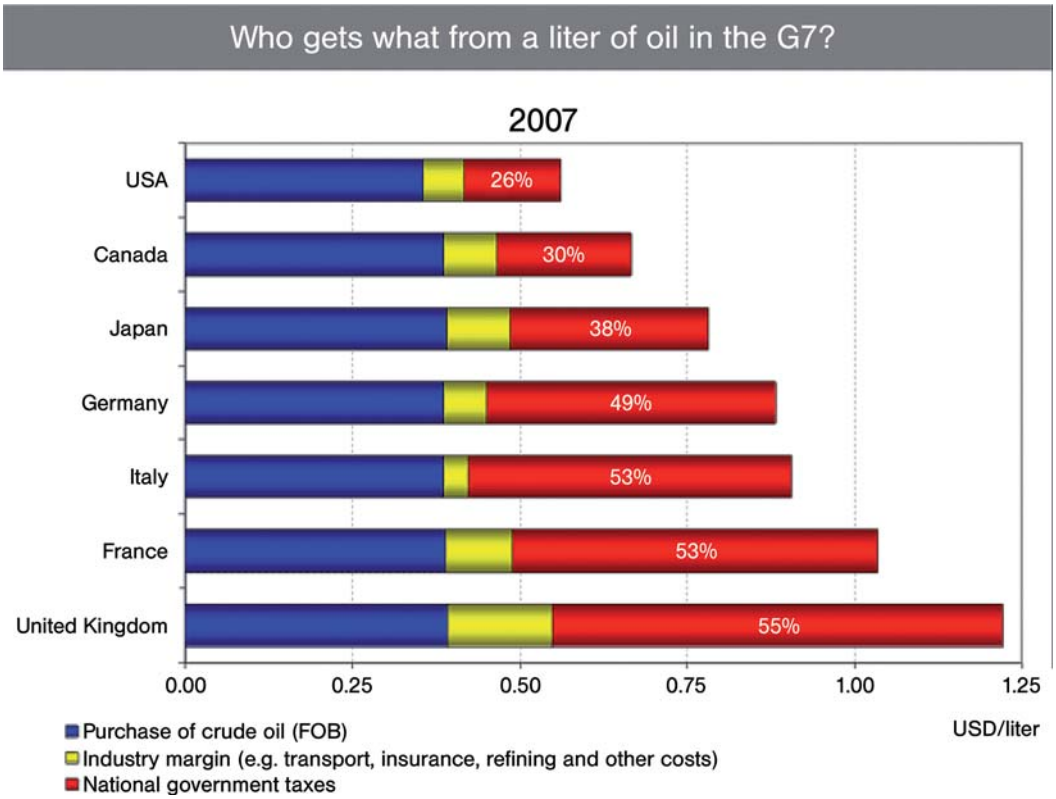

Figure 7.22 Who gets what from a liter of oil in the G7 countries. (Source: Opec).

Why, then, change this situation? One may think that environmental pressure with growth in emissions from fossil fuels tripled to an annual average of 3.4% in 2001–2006 [33], may be a good reason. But in practice nothing much has been done beyond verbal commitment before the recent surge in the price of oil.

Italy, for example, claims to be at the forefront among the countries who are implementing the Kyoto protocol but instead of reducing its CO_2 emissions from the 1990 level, the country's emissions actually rose by 20%.

Solar power is a practical alternative and the greatest obstacles to implementing a solar energy system have been the lack of public awareness and of large, long-term investments in research and development.

The 1973 oil and 1979 energy crises resulted in incentive programs such as the Federal Photovoltaic Utilization Program in the USA and the Sunshine Program in Japan. Research facilities were established such as the Solar Energy Research Institute (now NREL) in the USA, the New Energy and Industrial Technology Development Organization (NEDO) in Japan, and the Fraunhofer Institute for Solar Energy Systems in Germany.

Today, dwindling oil reserves and increasing prices along with climate change are causing a massive shift to renewable energy and to solar energy in particular.

Strategic, long-term investments are finally being established along with a number of public–private partnerships, while training programs are created and international collaboration is strengthened.

To accelerate this process, we urgently need to invest heavily in solar energy following the example of public policy leadership by Japan and Germany that in the early 2000s enabled a multi-billion dollar global market by creating an investable regulatory framework for solar electricity technology.

Furthermore, as shown by initiatives such as the United Arab Emirates Masdar (a first 250 million USD fund already operative, Figure 7.23) [34], Islamic finance will play a crucial role in this evolution. There are two major reasons for this: First, the leadership of these countries is aware that their current fortune is dependent on dwindling oil reserves, and thus that they need now to invest part of their fortunes in

Figure 7.23 Initiatives such as Abu Dhabi's Masdar with its Future Energy Company (ADFEC) are a consequence of Islamic finance principles and will play a crucial role in advancing the large scale adoption of solar energy. (Image courtesy: Masdar).

alternative energy sources to benefit tomorrow from such investments. Given the enormous surplus that is being accumulated in Islamic hydrocarbon countries at current oil prices, and the evident crisis of traditional, Western finance, recent studies suggest that Islamic finance will indeed become predominant within the next decade [35]. Second, the principles of Islamic finance rooted in the Sharia code encourage investments that are largely beneficial to mankind – such as those in solar energy – and forbid investments in companies such as banks or insurance (that borrow money on interest or keep their surplus in an interest bearing account).

Together, Western public and Islamic financial investments will lead us into the solar era of abundant, cheap and clean solar energy, saving the world from the perils of global warming and creating at the same time a large, wealthy new industry that will drive economic growth for decades to come.

References

1 Maugeri, L. (2006) *The Age of Oil: The Mythology, History, and Future of the World's Most Controversial Resource*, Praeger Publishers, Westport CT.

2 According to International Energy Agency demand will rise by an average of 2.2 million barrels a day in 2008, compared with the 1.5 million barrel rise seen in 2007. See at: http://www.iea.org/.

3 Leggett, J. (2005) *The Empty Tank*, Random House, New York.

4 Hall, C., Tharakan, P., Hallock, J., Cleveland, C. and Jefferson, M. (2003) Hydrocarbons and the Evolution of Human Culture. *Nature*, **426**, 318.

5 Hall, C.,(June 2004) The Myth of Sustainable Development: Personal Reflections on Energy, its Relation to Neoclassical Econimics, and Stanely Jevons. *Journal of Energy Resources Technology*, **126**, 85–89.

6 Cleveland, C. *et al*. (2006) *Science*, **312**, 1746.

7 Smil, V. (2006) 21st century energy: Some sobering thoughts. *OECD Observer*, **258/59**, 22.

8 Bradford, T. (2006) *Solar Revolution The Economic Transformation of the Global Energy Industry*, MIT Press, Boston.

9 Pereira, J.(June 3rd 2005) Solar Power Heats Up. *The Wall Street Journal*, A list of states and incentives is at www.dsireusa.org.

10 Rocheisen, M. (2005) Nanotechnology to the rescue of capital efficiency. *Photon International Magazine*, **7**, 29.

11 Data from the German Ministry for the Environment: See at: http://www.bmu.de/english/current_press_releases/pm/40791.php.

12 Black, A."How to Find Your Dream Job In Solar" for the Solar Living Institute. See also at: http://www.ongrid.net/papers/DreamJobInSolarSP2007slides.pdf.

13 Crosby, P.B. (1979) *Quality is Free*, McGraw-Hill, New York.

14 Seddon, J. (2005) *Freedom From Command and Control*, Productivity Press, New York.

15 Tirone, J. (August 28 2007) 'Dead-end' Austrian town blossoms with green energy. *International Herald Tribune*.

16 The True cost of solar power, Photon Consulting Report, (September 2007).

17 Hoffmann, W. (September 28th 2004) A Vision for PV Technology up to 2030 and beyond – An industry view, Brussels. http://ec.europa.eu/research/energy/pdf/1105_hoffmann_en.pdf.

18 Photovoltaics in Germany: Market and Industry Development. Available at: http://www.solarkorea.or.kr/board/

download.asp?board_id=info_b8&IDX=6&FILE_INDEX=0.

19 See the Earth Policy Institute data at: http://www.earth-policy.org/Indicators/Solar/2007_data.htm#table6.

20 REN21. 2008. "Renewables 2007 Global Status Report" (Paris: REN21 Secretariat and Washington, DC: Worldwatch Institute).

21 M., Fawer, *Solar Energy 2007 – The industry continoues to boom*, Bank Sarasin & Co. Ltd, available on request from the company: http://www.sarasin.ch

22 See the statistics section at: www.solarbuzz.com.

23 *The Thin-film Future*, Munich (Germany), June 11, 2008. http://www.solarplaza.com/event/thethinfilmfuture/The_Thin-Film_Future_-_Shortcut_to_Grid-Parity.html.

24 Cleveland, C.J. (January 7 2008) Energy transitions past and future. *The Encycoplaedia of Earth*, available at: http://www.eoearth.org/article/Energy_transitions_past_and_future.

25 The Trans-Mediterranean Renewable Energy Cooperation. (TREC) has developed the concept: http://www.trecers.net/.

26 Zweibel, K., Mason, J. and Fthenakis, V. (January 2008) A Solar Grand Plan. *Scientific American*, 64.

27 Navin, J. Energy Attitudes, American Environics, Report available at: http://www.americanenvironics.com/PDF/EnergyAttitudesSummer2007.pdf.

28 Nordhuas, T. and Shellenberger, M. (2007) *Break Through: From The Death of Environmentalism to the Politics of Possibility*, Houghton Mifflin, New York.

29 Hegedus, S.S. and Luque, A. (2003) Status, Trends, Challenges and the Bright Future of Solar Electricity from Photovoltaics, in *Handbook of Photovoltaics Science and Engineering* (eds A. Luque and S.S. Hegedus), John Wiley & Sons, New York.

30 The Stern Review on the Economics of Climate Change. Available at: http://www.hm-treasury.gov.uk/independent_reviews/stern_review_economics_climate_change/sternreview_index.cfm.

31 Kelly, C. (ed.) (2007) *The Manhattan Project: The Birth of the Atomic Bomb in the Words of Its Creators, Eyewitnesses and Historians*, Black Dog & Leventhal Publishers, New York.

32 Organization of the Petroleum Exporting Countries. From the 2007 report "Who gets what from imported oil" available at URL: http://www.opec.org/home/PowerPoint/Taxation/taxation.htm.

33 BP Statistical Review of World Energy 2007. Report available at: http://www.bp.com/productlanding.do?categoryId=6848&contentId=7033471.

34 In April 2006, the major hydrocarbon-producing nation UAE launched Masdar, a global cooperative platform for open engagement in the search for solutions to energy security, climate change and sustainable human development. http://www.masdaruae.com.

35 Napoleoni, L. (2008) *Rogue Economics: Capitalism's New Reality*, Seven Stories Press, New York.

36 Leggett, J., http://www.soilassociation.org/Web/SA/saweb.nsf/cfff6730b881e40e80256a6a002a765c/902f12def991d13a80256f9c005e300e/$FILE/conference_leggett.pps

37 Leggett, J., http://www.soilassociation.org/Web/SA/saweb.nsf/cfff6730b881e40e80256a6a002a765c/902f12def991d13a80256f9c005e300e/$FILE/conference_leggett.pps

38 Wsj.com (The Wall Street Journal, June 3, 2005).

A list of companies commercializing new PV technologies *(Flexible Solar Cells, Wiley-VCH, 2008. Periodically updated on the book's website: qualitas1998.net/flexible_solar_cells)*

Copper Indium Diselenide and Copper Indium Sulfur CIS Modules

Würth Solar (Schwäbisch Hall, Germany)
www.wuerth-solar.de

Avancis (Torgau, Germany)
www.avancis.de

Schüco (Bielefeld, Germany)
www.schueco.com

Sulfurcell Solartechnik (Berlin, Germany)
www.sulfurcell.de

Copper Indium Gallium Diselenide CIGS Modules

Nanosolar (San Jose, CA; USA)
www.nanosolar.com

Honda Soltec (Kumamoto, Japan)
http://world.honda.com/HondaSoltec

Global Solar (Tucson, AZ; USA)
www.globalsolar.com

HelioVolt (Austin, TX; USA)
www.heliovolt.net

Cadmium Telluride Modules

First Solar (Tempe, AZ; USA)
www.firstsolar.com

Arendi (Lainate, Milano; Italy)
www.arendi.eu

a-Si Modules

Flexcell (Yverdon-les-Bains, Switzerland)
www.flexcell.com

Solar Integrated (Los Angeles, USA)
www.solarintegrated.com

United Solar Ovonic (Auburn Hills, MI; USA)
www.uni-solar.com

Sharp Solar (Katsuragi, Japan)
http://sharp-world.com/solar

Schott Solar (Alzenau, Germany)
www.schott.com

Biohaus PV Handels (Paderborn, Germany)
www.biohaus.de

Flexible Solar Cells. M. Pagliaro, G. Palmisano, and R. Ciriminna

ISBN: 978-3-527-32375-3

Kaneka (Toyooka, Japan)
www.pv.kaneka.co.jp

Applied Materials (Santa Clara, CA; USA)
www.appliedmaterials.com

Suntech (Shanghai, China)
www.suntech-power.com

DSC Modules

G24 Innovations (Cardiff, UK)
www.g24i.com

Dyesol (Queanbeyan, Australia)
www.dyesol.com

Aisin Seki (Aichi, Japan)
www.aisin.com

Fraunhofer ISE (Freiburg, Germany)
www.ise.fhg.de

Sharp, Toshiba, DAI Nippon and Peccel Technologies (Toin University of Yokohama, Japan),
Prof. Tsutomu Miyasaka, Department of Biomedical Engineering

Solaronix (Aubonne, Switzerland).
www.solaronix.com

Polymeric Modules

Konarka (Lowell, MA; USA)
www.konarka.com

Third Generation PV Modules

QuantaSol (Richmond, Surrey; UK)
www.quantasol.com

SunFlake (Copenhagen, Denmark)
www.sunflake.dk

Index

Flexible Solar Cells. M. Pagliaro, G. Palmisano, and R. Ciriminna

ISBN: 978-3-527-32375-3